UNIVERSIDADE ESTADUAL DE CAMPINAS

Faculdade de Engenharia de Alimentos

FERNANDA LUISA LÜDTKE

"DEVELOPMENT AND CHARACTERIZATION OF BETA-CAROTENE LOADED NANOSTRUCTURED LIPID CARRIERS"

"DESENVOLVIMENTO E CARACTERIZAÇÃO DE CARREADORES LIPÍDICOS NANOESTRUTURADOS PARA INCORPORAÇÃO DE BETA-CAROTENO"

CAMPINAS, SP.

2021.

FERNANDA LUISA LÜDTKE

"DEVELOPMENT AND CHARACTERIZATION OF BETA-CAROTENE LOADED NANOSTRUCTURED LIPID CARRIERS"

“DESENVOLVIMENTO E CARACTERIZAÇÃO DE CARREADORES LIPÍDICOS NANOESTRUTURADOS PARA INCORPORAÇÃO DE BETA-CAROTENO”

Thesis presented to the Faculty of Food Engineering of the University of Campinas in partial fulfillment of the requirements for the degree of Doctor in Food Technology

Tese apresentada à Faculdade de Engenharia de Alimentos da Universidade Estadual de Campinas como parte dos requisitos exigidos para a obtenção do título de Doutora em Tecnologia de Alimentos

Orientadora: Profa. Dra. Ana Paula Badan Ribeiro
Coorientador: Prof. Dr. António Augusto Vicente

Este exemplar corresponde à versão final da tese defendida pela aluna Fernanda Luisa Lüdtke e orientada pela Profa. Dra. Ana Paula Badan Ribeiro.

Campinas, SP.
2021.

Agência(s) de fomento e número(s) de processo(s):CAPES - Código de Financiamento 001; FAPESP, 2018/03172-0 e 2019/05176-6.

Ficha catalográfica
Universidade Estadual de Campinas
Biblioteca da Faculdade de Engenharia de Alimentos
Claudia Aparecida Romano - CRB 8/5816

L966d

Lüdtke, Fernanda Luisa, 1990-
Desenvolvimento e caracterização de carreadores lipídicos nanoestruturados para incorporação de beta-caroteno / Fernanda Luisa Lüdtke. – Campinas, SP : [s.n.], 2021.

Orientador: Ana Paula Badan Ribeiro.
Coorientador: António Augusto Vicente.
Tese (doutorado) – Universidade Estadual de Campinas, Faculdade de Engenharia de Alimentos.

1. Nanopartículas lipídicas. 2. Lipídeos. 3. Compostos bioativos. 4. Estabilidade. 5. Biodisponibilidade. I. Ribeiro, Ana Paula Badan. II. Vicente, António Augusto. III. Universidade Estadual de Campinas. Faculdade de Engenharia de Alimentos. IV. Título.

Informações para Biblioteca Digital

Título em outro idioma: Development and characterization of beta-carotene loaded nanostructured lipid carriers
Palavras-chave em inglês:
Lipid nanoparticles
Lipids
Bioactive compounds
Stability
Bioavailability
Área de concentração: Tecnologia de Alimentos
Titulação: Doutora em Tecnologia de Alimentos
Banca examinadora:
Ana Paula Badan Ribeiro [Orientador]
Ana Sílvia Prata
Guilherme José Máximo
Katia Sivieri
Severino Matias de Alencar
Data de defesa: 16-12-2021
Programa de Pós-Graduação: Tecnologia de Alimentos

Identificação e informações acadêmicas do(a) aluno(a)
- ORCID do autor: 0000-0002-0221-5633
- Currículo Lattes do autor: http://lattes.cnpq.br/2395604657263833

COMISSÃO EXAMINADORA

Profa. Dra. Ana Paula Badan Ribeiro – Presidente da Comissão Examinadora
Faculdade de Engenharia de Alimentos (FEA)
Universidade Estadual de Campinas (UNICAMP), Campinas, SP

Profa. Dra. Ana Sílvia Prata – Membro titular
Faculdade de Engenharia de Alimentos (FEA)
Universidade Estadual de Campinas (UNICAMP), Campinas, SP

Prof. Dr. Guilherme José Máximo – Membro titular
Faculdade de Engenharia de Alimentos (FEA)
Universidade Estadual de Campinas (UNICAMP), Campinas, SP

Profa. Dra. Kátia Sivieri – Membro titular
Faculdade de Ciências Farmacêuticas
Universidade Estadual Paulista "Júlio Mesquita Filho" (UNESP), Araraquara, SP

Prof. Dr. Severino Matias de Alencar – Membro titular
Escola Superior de Agricultura Luiz de Queiroz (ESALQ)
Universidade Estadual de São Paulo (USP), Piracicaba, SP

A Ata da defesa, assinada pelos membros da Comissão Examinadora, consta no SIGA/Sistema de Fluxo de Tese e na Secretaria do Programa da Unidade.

Dedico esta tese a todas as pessoas que, avessas à obscuridade e ao negacionismo que estamos experienciando, perseveram na busca de conhecimentos à luz da ciência.

“O correr da vida embrulha tudo.
A vida é assim: esquenta e esfria,
aperta e daí afrouxa,
sossega e depois desinquieta.
O que ela quer da gente é coragem”

(Guimarães Rosa)

“Be less curious about people and more curious about ideas”
(Marie Curie)

“Trabalhar com você deve ser tanto produtivo quanto prazeroso”
(Délia Rodriguez-Amaya)

AGRADECIMENTOS

Agradeço à Universidade Estadual de Campinas e à Faculdade de Engenharia de Alimentos pela oportunidade em realizar este trabalho, assim como ao seu corpo docente e funcionários pelo valioso apoio durante esses anos de pós-graduação. Me sinto honrada em ter na minha formação uma universidade de incontestável excelência.

Ao Laboratório de óleos e gorduras por toda a infraestrutura disponibilizada, pela formação contínua e aplicada, por todo o conhecimento e por todas as possibilidades, agradeço.

À Coordenação de Aperfeiçoamento de Pessoal de Nível Superior - Brasil (CAPES) - Código de Financiamento 001, pela concessão da bolsa de doutorado e pelo suporte financeiro.

À Fundação de Amparo à Pesquisa do Estado de São Paulo (Fapesp) pelo apoio financeiro através do projeto de auxílio à pesquisa (Processo n° 2016/11261-8), pela concessão das bolsas de doutorado regular no país (Processo n° 2018/03172-0) e de estágio e pesquisa no exterior (Processo n° 2019/05176-6).

À Universidade do Minho e ao Centro de Engenharia Biológica pela oportunidade da realização de investigações em uma instituição de notória qualidade.

Ao Renato Grimaldi, por ter me aberto as portas, não apenas do LOG, mas também do mundo de óleos e gorduras. Pela amizade, pelos conselhos e incentivos. Pelo vigor e competência, que tomarei como referência para minha jornada profissional. Pelo exemplo de profissional ímpar que és e por teu coração altruísta, agradeço.

À minha querida orientadora Profa. Ana Paula Badan Ribeiro, por tudo e por tanto. Afortunadamente encontrei em ti muito além de uma orientadora, uma amiga. Pelas palavras sempre bondosas e cuidadosas. Pelo exemplo de benevolência e de genuinidade. Por me inspirar a olhar ao próximo com cuidado, respeito e dignidade. Por acreditar em mim e constantemente buscar me incentivar. Pela autonomia com que permitiu me aventurar no mundo da pesquisa e além-fronteiras, agradeço.

Ao Prof. António Augusto Vicente, pela disponibilidade de coorientação e pela oportunidade de estar inserida em um grupo de pesquisa excelente. Por todos os aprendizados, por vossa liderança e humanidade que cativa a todos; e por vossa generosidade e alegria, que são contagiantes, agradeço

À Ana Cristina Pinheiro, agradeço imenso toda a atenção, disponibilidade e aprendizagens. Tu me inspiraste muito pela maneira com que conduzes a vida profissional e as relações interpessoais, obrigada por seres exemplo Cris!

Aos professores Lisandro Pavie Cardoso e Marcus Bruno Forte, por todas as contribuições, carregadas de muita energia e boa vontade em auxiliar na execução deste trabalho.

À comissão avaliadora, pela disponibilidade de leitura da tese, pela contribuição ao trabalho através de valiosas sugestões e correções.

À Marcella Stahl, minha B1, companheira de doutorado, de sala, da vida. Obrigada por partilhar esse desafio tão árduo, com sutileza e alegria. Tua leveza e dedicação muito trouxeram a este trabalho e à minha vida, serei para sempre grata!

Aos alunos de iniciação científica que muito contribuíram para este trabalho: Alan Avila, Barbara Zaia e Bruno Brito. Obrigada pela colaboração, por compartilhar comigo vossas experiências e por todos os momentos de amizade e descontração.

Ao Jean-Michel Fernandes por toda a paciência e amparo com o DIVGIS, pela amizade e pelo ânimo, agradeço imenso. À Raquel Filipa Gonçalves, por todo auxílio com as partículas, pelos cafés pós almoço e por amenizar a angústia de incertezas do período pandêmico, agradeço. À Joana Martins, pelo auxílio com os ensaios de viabilidade celular e pela imensa contribuição a este trabalho, agradeço. Ao Paulo Berni, não apenas pelos aprendizados com os carotenoides, mas para a vida. Obrigada por todo auxílio na execução deste trabalho! À Ana Loureiro, por me propiciar bons sorrisos aquando da obtenção das nanopartículas, a culminar numa valiosa experiência, agradeço.

À Bianca Wopereis e Juliana Hashimoto, por todo o auxílio com os equipamentos, sugestões para o trabalho e boa vontade em colaboração com a execução das análises, agradeço.

Aos alunos e funcionários do LOG pelos momentos vividos, repletos de importantes ensinamentos. Agradeço, de forma muito carinhosa, à Rosana e à Dona Dalva, que desde cedo, animavam os meus dias.

Ao Luís Marangoni, meu amigo Fapesp, pelo entusiasmo e apoio; À Natani Amaro, pela amizade sincera, por nossas conversas nostálgicas e por todo o incentivo; À Ana Paula Barbante, pelos feriados e finais de semana no lab, pelas caronas, por todo cuidado e amor para conosco. Nossos almoços, junções, viagens, e momentos compartilhados juntamente com a Marcella, foram fortaleza durante o período de doutorado.

À Larissa Grimaldi, pela amizade, pelo carinho, por todo o apoio e torcida. Por sempre estar bem disposta e pronta para acorrer, mesmo que a distância, agradeço.

As amigas que a FEA trouxe à minha vida: Ana Gabriela Anthero, Carol Maloper, Fernanda Procópio, Klycia Fidelis, Laura Suemitsu, Mariana Carvalhal, Maria Isabel Neves e Monique Strieder, pelos almoços de domingo, pelas viagens, pelos mates e cucas, pelos encontros na

pracinha...pelo fortalecimento e crescimento em conjunto, pelo apoio mútuo, por todo amor e amizade compartilhados, agradeço.

Aos LIPinhos, malta que fez meus dias na terrinha *bué* de especiais, pelo acolhimento, pelo excelente ambiente de trabalho, pelas aulas recorrentes de “PT-PT”, por nossos lanches, sempre muito alegres. Por compartilharem seus conhecimentos de forma aberta e irrestrita. Por todos os momentos, agradeço imenso.

Ao Jorge Vieira, pela amizade tão dedicada, por todos os sorrisos que me arrancastes, por nossos momentos extra lab e pelo apoio incondicional; À Zlatina Genisheva, pelo exemplo de coragem e serenidade, e por toda a amizade; Ao Luís Loureiro pela alegria contagiante, pela amizade e por ter me recebido de forma muito especial desde o primeiro dia no LIP; Ao João Araújo, por toda atenção, carinho e musicalidade que trouxestes à minha vida; À Cristiane Andrade, pelo exemplo de dedicação à pesquisa, pela preocupação e doação; Ao Rui Rodrigues, meu amigo trans (montano), pela agradável companhia, pelas aulas de cultura portuguesa e por todo o incentivo; À Zita Avelar, por compartilhar seu lugar, seu dia-a-dia e seus conhecimentos; À Maria José Costa por embelezar meus dias na terrinha, agradeço.

Aos Micelos, por todos os vinhos e os momentos compartilhados em terras ibéricas.

Aos meus amigos paraisenses, pela alegria do reencontro e pela simplicidade de nossos momentos, agradeço.

Ao Danrlei de Menezes e à Luiza Adorna, pela amizade, carinho e entusiasmo, recíprocos e verdadeiros, agradeço.

À Katherine Romero, pelos sorrisos e desabafos, pelos açaís na feirinha entremeados às atividades laboratoriais, pela preocupação e amizade, agradeço.

Aos meus companheiros de casa, das Repúblicas Muralha do Norte e Minions, em especial ao George Araújo e à Selma Regina Olla, pelas conversas infindas, tão necessárias e reconfortantes, por tornarem a vida em Campinas mais alegre e completa, agradeço.

Ao Felipe Franzen, por tudo nesta década de amizade, pelo convívio agradável, pela alegria na simplicidade e por dividir seu lar comigo, sou imensamente grata!

À Lilian Lissner, pela amizade forte e ao mesmo tempo leve, por todo o incentivo, alegria e companhia constante, agradeço.

À Melina Holzschuh, pelo carinho, reciprocidade, e pela certeza de uma amizade duradoura e atemporal, agradeço.

À Ana Karoliny, pela simplicidade de uma amizade tão verdadeira e genuína, e a toda família Souza de Indaiatuba, que me acolheram como uma filha e foram o refúgio para quando a saudade insistia em apertar. Agradeço toda a afeição, o cuidado e o apoio.

As famílias Lüdtke e Lovato, pela hospitalidade e amorosidade, pelos momentos sempre regados de muita comida e muitas risadas, pelo valor inestimável que a união em família representa. À minha família metropolitana, pela acolhida entre as idas e vindas. Agradeço de forma carinhosa e saudosa, meus avós Arno e Rosa, e meus tios Moacir, Nilson e Zaira, que, durante esse período, deixaram este plano, e muito me acompanham na memória e nos seus exemplos.

Aos meus afilhados Bento, Guilherme, Isabella, Maria Luiza e Otto, pelo amor genuíno, pelos momentos de alegria e pelas descobertas.

Às minhas irmãs, Lívia e Rosiele, pelo carinho, amor e apoio constante. Aos meus cunhados e sobrinhos pelos momentos alegres em família. Agradeço pela receptividade, pelo encorajamento e por vibrarem comigo!

Ao Thiago Tolfo, por todo amor, zelo e afeto que me dedicas. Por trazer à minha vida, além de um vocabulário mais vasto, a leveza de uma companhia segura... Pelas vírgulas, crases, acentos, *et al*... Por diariamente relembrar minha força, me incentivar à persistência. Por sempre estar, ainda que a um oceano de distância a nos separar, agradeço. Obrigada à família Tolfo, pelo acolhimento, pelo estímulo e pelos momentos compartilhados.

Aos meus pais, Almiro e Rosângela, pela humildade e humanidade, no ser e no viver, por compreenderem os meus voos e serem terra firme para os meus regressos. Por não limitarem minhas escolhas, por me incentivarem a seguir oportunidades que sequer lhe foram disponibilizadas, por, mesmo que com o mínimo de estudos, fomentarem em mim a importância da educação. Esse trabalho só foi possível porque vocês são meus pilares.

Muitos foram os caminhos percorridos até a entrega deste documento. Muitas renúncias, abdicações e esperas. Muitos aprendizados, conhecimentos e experiências. Agradeço imensamente a todas as pessoas que estiveram comigo, sob diversas formas, durante este período, e muito acresceram à realização deste trabalho e ao meu crescimento pessoal. Muito Obrigada!

RESUMO

Os carreadores lipídicos nanoestruturados (CLN) foram desenvolvidos como um sistema para a incorporação e entrega de compostos bioativos lipossolúveis, que devido à instabilidade química e baixa solubilidade em água, apresentam baixa biodisponibilidade. Compostos por lipídios que apresentam alto e baixo ponto de fusão, os CLN exibem várias vantagens potenciais que podem ser exploradas através da escolha dos materiais utilizados em sua composição. O objetivo deste trabalho foi obter CLN para incorporação de β-caroteno a partir de matérias-primas lipídicas comumente utilizadas na indústria de óleos e gorduras. Com este propósito, o trabalho foi dividido em quatro etapas. A primeira etapa consistiu na otimização das condições de processo da homogeneização a alta pressão (HAP) e avaliação do desempenho de emulsificantes sintéticos e naturais para obtenção dos CLN. Os emulsificantes lecitina de soja modificada enzimaticamente (LS), monooleato de sorbitana etoxilado (Tween 80) e isolado proteico do soro de leite (WPI), e a pressão de 700 bar e 2 ciclos de homogeneização foram definidos como componentes de formulação e condições de processo, efetivos e otimizados, para a obtenção de CLN nas demais etapas do trabalho. A segunda etapa esteve relacionada à obtenção, caracterização e estudo de estabilidade de CLN a partir de diferentes sistemas lipídicos compostos por óleo de soja totalmente hidrogenado (OSTH) e óleo de girassol alto oleico (OGAO). Sistemas lipídicos compostos por OSTH:OGAO em diferentes proporções foram caracterizados em macroescala em termos de composição, propriedades físicas e de cristalização, e partir dessa avaliação definiu-se os sistemas 80:20, 60:40, 40:60 e 20:80 OSTH: OGAO (m/m), para obtenção dos CLN. Dentre os sistemas lipídicos considerados, o sistema 60:40 OSTH: OGAO (m/m) proporcionou a obtenção de nanopartículas estáveis e com características de cristalinidade adequadas para incorporação do composto bioativo lipofílico de interesse na etapa subsequente. A terceira etapa esteve direcionada à avaliação do potencial de CLN para a incorporação de compostos bioativos lipofílicos. Nesse sentido, os CLN, obtidos com três distintos emulsificantes (LS, Tween 80 e WPI), foram avaliados quanto à eficiência de incorporação e capacidade de carga dos CLN, bem como a avaliação da estabilidade física, cristalina e polimórfica das nanoestruturas com incorporação de β-caroteno. Os carreadores obtidos utilizando LS e Tween 80 apresentaram maior eficiência de incorporação de β-caroteno, sendo assim selecionados para o estudo da digestibilidade *in vitro* na etapa subsequente. Na quarta etapa, foram realizados estudos relacionados à digestibilidade dinâmica *in vitro*, bioacessibilidade do composto bioativo incorporado e citotoxicidade de CLN e dos componentes utilizados em sua composição. Os CLN obtidos com Tween 80 apresentaram maior estabilidade durante a passagem pelo TGI e proporcionaram maior proteção e entrega do composto bioativo. A viabilidade celular, encontrada após os ensaios

de citotoxicidade indicou que ambos os CLN não apresentaram efeito tóxico nas concentrações testadas (1- 25 μg.ml^{-1}). A utilização de OSTH e OGAO como matrizes lipídicas proporcionou a obtenção de CLN com elevada estabilidade cristalina, boa capacidade de carga e proteção do composto bioativo incorporado, biocompatíveis e com custo viável para aplicação em alimentos.

Palavras-chave: Nanopartículas lipídicas, matrizes lipídicas, compostos bioativos, estabilidade, biodisponibilidade.

ABSTRACT

Nanostructured lipid carriers (NLC) were developed as a system for entrapment and delivery of liposoluble bioactive compounds, which due to their chemical instability and low water solubility, have low bioavailability. Composed of lipids that have high and low melting points, CLN exhibit several potential advantages that can be exploited through the choice of materials used in their composition. Thus, the objective of this work was to obtain β-carotene loaded NLC, through lipid matrices commonly used in the oil and fat industry. For this purpose, the work was divided into four stages. The first step consisted of optimizing the process conditions of high pressure homogenization (HPH) and evaluating the performance of synthetic and natural emulsifiers to obtain NLC. Enzymatically modified soy lecithin (SL), ethoxylated sorbitan monooleate (Tween 80) and whey protein isolate (WPI), the pressure of 700 bar and 2 homogenization cycles were defined as effective and optmized process conditions and components for obtaining NLC in subsequent stages of the work. The second stage was related to the obtainment, characterization, and stability study of NLC from different lipid systems composed of fully hydrogenated soybean oil (FHSO) and high oleic sunflower oil (HOSO). The lipid systems were characterized in macroscale in terms of composition, physical and crystallization properties, and from this, FHSO: HOSO (w/w) 80:20, 60:40, 40:60 and 20:80 lipid systems were defined to obtain NLC. Among the lipid systems considered, the 60:40 FHSO: HOSO (w/w) system provided the obtainment of stable particles with adequate crystallinity characteristics for entrapment of the lipophilic bioactive compound of interest. So, in the third step, the potential of NLC for entrapment of lipophilic bioactive compounds was evaluated. In this sense, β-carotene loaded NLC obtained with three different emulsifiers (SL, Tween 80 and WPI), were evaluated for the entrapment efficiency and loading capacity, as well as the evaluation of physical stability, crystalline and polymorphic stability. NLC obtained using SL and Tween 80, showed greater potential for of β-carotene entrapment, being thus selected for the study of *in vitro* digestibility in the subsequent step. In the fourth step studies related to behavior of NLC during *in vitro* dynamic digestibility, β-carotene bioaccessibility and cytotoxicity of NLC and the components used in its composition were carried out. The NLC obtained with Tween 80 showed greater stability during the passage through the TGI and provided greater protection and delivery of β-carotene. The cell viability found after cytotoxicity assays indicated that both NLC do not present toxic effect at the tested concentrations (1- 25 $\mu g.ml^{-1}$). The use of FHSO and HOSO as lipid matrices provided the obtainment of NLC with high crystal stability, good load capacity and protection of the incorporated bioactive compound, which are biocompatible and presents a viable cost for application in foods.

Keywords: Lipid nanoparticles, lipid matrices, bioactive compounds, stability, bioavailability.

SUMÁRIO

CAPÍTULO I

INTRODUÇÃO GERAL

1. INTRODUÇÃO GERAL

Apesar do conhecimento do papel crítico que os compostos bioativos desempenham na saúde humana, a deficiência ou a insuficiência de alguns nutrientes ainda prevalece na população de alguns países, tanto em desenvolvimento, quanto desenvolvidos. A deficiência de nutrientes pode ocorrer por vários fatores, incluindo baixos níveis dietéticos, baixa biodisponibilidade ou a necessidade do consumo de maiores quantidades. Para tal, uma série de estratégias vem sendo desenvolvidas para combater as deficiências de nutrientes na dieta humana, dentre estas, a fortificação de alimentos com compostos bioativos, uma vez que muitos destes não podem ser sintetizados em níveis suficientemente elevados pelo corpo humano (MOHAMMADI; ASSADPOUR; JAFARI, 2019; PASCOVICHE *et al*., 2019; TAN; MCCLEMENTS, 2021).

O β-caroteno, principal precursor da vitamina A, é um composto vital para a saúde humana (DONHOWE; KONG, 2014; TAN; MCCLEMENTS, 2021). O consumo deste composto bioativo em quantidades suficientes promove alguns benefícios à saúde, incluindo atividade antioxidante e prevenção de certas doenças crônicas, como câncer, doenças cardiovasculares e degeneração macular relacionada à idade (PEZESHKI *et al*., 2019). No entanto, a fortificação de alimentos através da incorporação de compostos bioativos lipossolúveis, como o β-caroteno, é limitada devido à sua baixa solubilidade em água e suscetibilidade à oxidação (REZAEI; FATHI; JAFARI, 2019).

Devido a sua alta hidrofobicidade e tendência para formar cristais, a dispersibilidade e biodisponibilidade do β-caroteno em alimentos de base aquosa é muito baixa (PEZESHKI *et al*., 2019). O carreamento destes compostos em alimentos consiste então em um desafio quanto aos requisitos de estabilidade às condições de processamento, que podem ser superados com abordagens nanotecnológicas (HUANG; YU; RU, 2010). Dessa forma, a incorporação destes compostos em sistemas de entrega em nanoescala se mostra promissora, a fim de melhorar a dispersibilidade em alimentos de base aquosa, protegê-los contra as ações de pró-oxidantes, aumentando assim a sua biodisponibilidade (REZAEI; FATHI; JAFARI, 2019).

A biodisponibilidade de um composto bioativo, ou seja, a proporção de um nutriente ou composto ingerido que pode ser absorvido e estar disponível na circulação sistêmica para utilização em várias funções vitais (CARBONELL-CAPELLA *et al*., 2014) é dependente, entre outros fatores, de vários fenômenos físico-químicos que ocorrem durante sua passagem pelo trato gastrointestinal (TGI), incluindo a liberação do composto da matriz alimentar, solubilização dentro de micelas mistas, transformação em uma forma ativa, transporte para o epitélio intestinal e captação pelas células (MCCLEMENTS *et al*., 2015).

Uma vez que a liberação e solubilização de compostos bioativos lipossolúveis está intimamente relacionada à digestão de lipídios (SALVIA-TRUJILLO *et al*., 2013), sistemas de entrega em nanoescala baseados em lipídios têm atraído considerável interesse, devido ao seu potencial para aumentar a estabilidade e biodisponibilidade oral de compostos bioativos, preservando suas características nutricionais, aumentando sua dispersibilidade em água e protegendo o composto da degradação química (KATOUZIAN *et al*., 2017; MCCLEMENTS; XIAO, 2014; PINHEIRO *et al*., 2017; SOLEIMANIAN *et al*., 2018).

Dentre os sistemas de entrega em nanoescala baseados em lipídios, os carreadores lipídicos nanoestruturados (CLN) têm se mostrado como sistemas promissores para o carreamento e proteção de compostos bioativos lipossolúveis, como o β-caroteno, promovendo o aumento da biodisponibilidade e da estabilidade, bem como a liberação direcionada e controlada destes compostos em seus locais de ação (ZHENG *et al*., 2013; PEZESHKI *et al*., 2019). Matrizes lipídicas com diferentes pontos de fusão são utilizadas para sua obtenção, fazendo com que a cristalização ocorra de uma forma menos ordenada, permitindo assim uma maior incorporação de compostos bioativos (ATTAMA; MOMOH; BUILDERS, 2012; PINTO *et al*., 2014; PYO *et al*., 2017).

Fatores como a proporção e a composição da fase lipídica, o tamanho de partícula e as propriedades interfaciais têm um efeito pronunciado sobre a digestão lipídica e a biodisponibilidade de compostos bioativos lipofílicos (SALVIA-TRUJILLO *et al*., 2017b; TAN; MCCLEMENTS, 2021). Assim, a matriz lipídica e o emulsificante utilizados para obtenção de CLN desempenham papéis críticos no destino biológico do β-caroteno incorporado a estas nanoestruturas, uma vez que afetam, dentre outros fatores, as propriedades físico-químicas dos CLN obtidos, a taxa e a extensão da digestibilidade lipídica, e consequentemente a biodisponibilidade dos compostos (TAMJIDI *et al*., 2013; LIN *et al*., 2018).

Uma vez que a liberação e a absorção de compostos bioativos lipofílicos, como o β-caroteno, podem ser concebidas de forma racional com base na compreensão da lipólise digestiva (WILDE; CHU, 2011; CARRIÈRE, 2016), a realização de ensaios de digestibilidade *in vitro* é uma ferramenta para determinação da bioacessibilidade e biodisponibilidade destes compostos, e a influência da composição de CLN sobre sua estabilidade durante a passagem pelo TGI. Estes ensaios podem ser realizados através de sistemas estáticos ou dinâmicos. Em comparação com os modelos estáticos, os modelos dinâmicos de digestibilidade *in vitro* são considerados mais adequados para fornecer uma melhor previsão do destino biológico dos sistemas de entrega, devido à simulação mais eficaz dos atributos bioquímicos, biomecânicos e temporais que ocorrem *in vivo* (LIN *et al*., 2018).

Além disso, quando um novo composto ou ingrediente é utilizado para obtenção de CLN, é necessário avaliar sua possível toxicidade contra as células intestinais, pois o intestino delgado é o órgão-alvo do consumo oral de CLN (JAFARI; MCCLEMENTS, 2017). A

linhagem celular de adenocarcinoma do cólon humano - Caco-2- é utilizada para os estudos de citotoxicidade e permeabilidade dos compostos bioativos incorporados aos nanocarreadores, e corresponde a um dos principais modelos de absorção intestinal utilizados para o estudo das características de transporte e permeabilidade de compostos bioativos. Esta técnica fornece dados importantes relacionados principalmente à dose limite a ser ingerida e a bioacessibilidade dos compostos bioativos, permitindo, dessa forma, um estudo mais completo desde o momento da ingestão até a absorção intestinal dos carreadores lipídicos nanoestruturados com incorporação de β-caroteno. Assim sendo, o desenvolvimento de sistemas de entrega que proporcionem a maior funcionalidade e segurança de compostos bioativos nutracêuticos pode criar oportunidades para aplicação de tecnologias, como a nanotecnologia, de forma mais ampla na indústria de alimentos (GONÇALVES *et al*., 2018).

1.1 Objetivos

O objetivo geral deste trabalho foi a obtenção de carreadores lipídicos nanoestruturados (CLN) a partir de matrizes lipídicas convencionais (óleo de girassol alto oleico e óleo de soja totalmente hidrogenado), através do método de homogeneização a alta pressão (HAP), para a incorporação e a proteção de β-caroteno, visando alta estabilidade cristalina, elevada biocompatibilidade e custo viável. Para que este objetivo fosse alcançado, fez-se necessário alcançar os seguintes objetivos específicos:

- Avaliar as condições gerais de processo para a obtenção de CLN, com respeito à pressão de homogeneização e número de ciclos;
- Avaliar o efeito de emulsificantes específicos sobre as propriedades gerais dos CLN obtidos;
- Avaliar a estabilidade física de CLN obtidos a partir de diferentes sistemas lipídicos;
- Estabelecer o efeito particular do tamanho de cadeia dos ácidos graxos e do teor de ácidos graxos insaturados de sistemas lipídicos sobre as propriedades de morfologia, ultraestrutura, polimorfismo, cristalinidade e estabilidade dos CLN obtidos;
- Avaliar o potencial de estruturas CLN para a incorporação de compostos bioativos lipofílicos;
- Avaliar a digestibilidade dos nanocarreadores, a bioacessibilidade do β-caroteno incorporado às nanoestruturas e o perfil de liberação de ácidos graxos, através de um sistema dinâmico de digestibilidade *in vitro*;
- Avaliar a citotoxicidade do β-caroteno incorporado às nanoestruturas, das estruturas CLN, bem como dos principais componentes utilizados para sua obtenção.

1.2 Estrutura da tese

A apresentação deste trabalho foi organizada em capítulos, conforme descrito a seguir.

Capítulo I**:** *Introdução geral*

Neste capítulo são apresentados a introdução geral, os objetivos, geral e específicos do estudo, bem como a estrutura em que a tese está organizada.

Capítulo II**:** *Revisão bibliográfica*

Neste capítulo são abordados aspectos teóricos acerca do uso de CLN como uma estratégia para o aumento da bioacessibilidade de β-caroteno, considerando a revisão bibliográfica da literatura mais recente e relevante sobre o tema deste estudo.

Os capítulos III, IV, V, VI e VII são relacionados às etapas de desenvolvimento deste estudo, apresentadas na Figura 1. A descrição de cada etapa, bem como do capítulo referente, está relatada a seguir.

A Etapa I teve como objetivo estabelecer o conhecimento necessário quanto aos parâmetros gerais de obtenção de CLN, referentes à avaliação da efetividade de emulsificantes (sintéticos e naturais) utilizados na indústria de alimentos na otimização das condições de processo da homogeneização a alta pressão (HAP) (pressão de homogeneização e número de ciclos). Para isto utilizou-se um sistema lipídico modelo constituído por trioleína (TO) e triestearina (TS) na proporção 40:60 (TS: TO m/m). Os CLN foram obtidos através da HAP a quente, com condições de processo definidas através de um planejamento fatorial completo 2^2. Ao final desta etapa, foram selecionados os emulsificantes lecitina de soja modificada enzimaticamente (LS), monooleato de sorbitana etoxilado (Tween 80) e isolado proteico do soro de leite (WPI), a pressão de homogeneização 700 bar e 2 ciclos de homogeneização, como os componentes de formulação e as condições de processo efetivas e otimizadas para a obtenção de CLN em nanoescala. Os resultados deste estudo compõem o Capítulo III: "*Performance of natural and synthetic emulsifiers in the optimization of high pressure homogenization conditions to produce nanostructured lipid carriers"*.

Para a Etapa II, preconizou-se o uso de matrizes lipídicas convencionais da indústria de alimentos, para, dessa forma, diminuir o custo de obtenção de CLN, bem como para proporcionar novos usos para fontes lipídicas comumente utilizadas para obtenção de produtos alimentícios. As matrizes lipídicas selecionadas foram o óleo de soja totalmente hidrogenado (OSTH) e o óleo de girassol alto oleico (OGAO). A escolha do OSTH, como matriz lipídica de alto ponto de fusão ocorreu devido ao fato da alta disponibilidade desta matéria-prima no país, maior produtor mundial de soja, e em virtude de sua composição majoritária em ácido esteárico, ácido graxo saturado que apresenta efeito aterogênico neutro no organismo humano.

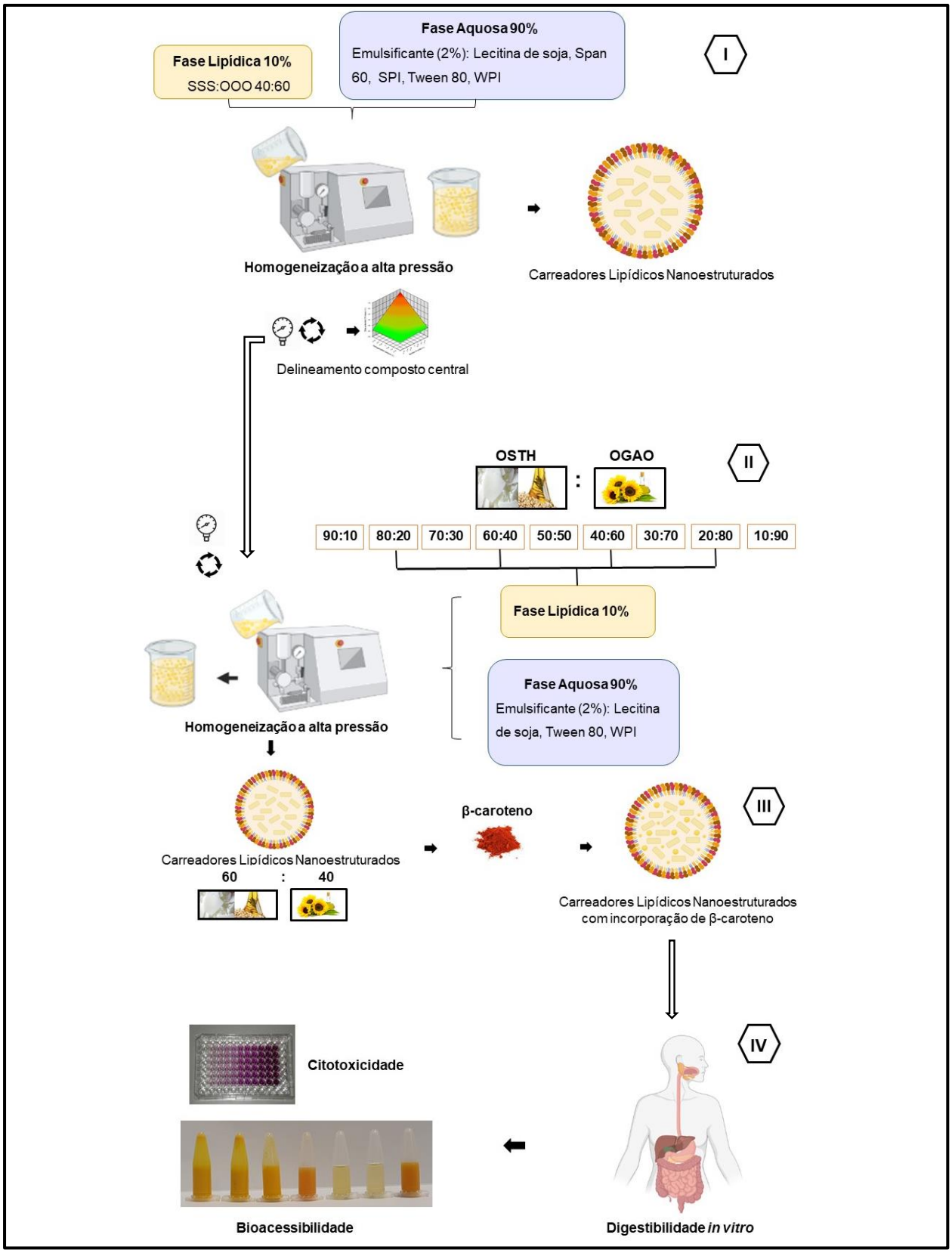

Figura 1: Etapas de desenvolvimento do estudo. **Etapa I**: Desempenho de emulsificantes e otimização das condições de processo para a obtenção de CLN. **Etapa II**: Obtenção de CLN utilizando OSTH e OGAO como matrizes lipídicas. **Etapa III**: Incorporação de β-caroteno aos CLN. **Etapa IV**: Estudo da digestibilidade *in vitro* e citotoxicidade de CLN.

O OGAO foi escolhido como matriz lipídica de menor ponto de fusão devido principalmente ao seu alto conteúdo de ácido oleico, o que lhe confere elevada estabilidade oxidativa.

Inicialmente, foram obtidos sistemas lipídicos compostos por OSTH:OGAO (m/m) nas proporções - 90:10, 80:20, 70:30, 60:40, 50:50, 40:60, 30:70, 20:80 e 10:90; e caracterizados quanto a composição, propriedades físicas e de cristalização. A partir desta caracterização, definiu-se os sistemas lipídicos 80:20, 60:40, 40:60 e 20:80 OSTH: OGAO (m/m), para a obtenção dos CLN. Os resultados deste estudo compõem o Capítulo IV**:** *"Lipid systems based on fully hydrogenated soybean oil and high oleic sunflower oil to obtain nanostructured lipid carriers: composition, physical properties, and crystallization parameters"*.

Sequencialmente, ainda na Etapa II do projeto, os CLN foram obtidos utilizando-se as condições de processo e emulsificantes definidos na Etapa I (700bar e 2 ciclos de homogeneização); e caracterizados quanto às propriedades gerais de distribuição de tamanho de partícula, estrutura, estabilidade física, comportamento térmico, cristalinidade e polimorfismo, considerando-se os efeitos de composição da fase lipídica relativos ao grau de insaturação dos sistemas lipídicos utilizados. Ao final desta etapa selecionou-se o sistema lipídico 60:40 OSTH:OGAO (m/m) como matriz lipídica para obtenção de CLN com incorporação de β-caroteno na Etapa III, em virtude deste sistema proporcionar a obtenção de partículas estáveis durante os 60 dias de armazenamento e com características de cristalinidade adequadas para incorporação do composto bioativo lipofílico de interesse. Os resultados deste estudo compõem o Capítulo V: "*High oleic sunflower oil and fully hydrogenated soybean oil nanostructured lipid carriers: development and characterization"*.

A Etapa III esteve direcionada à avaliação do potencial de CLN selecionados na Etapa II, quanto à incorporação de compostos bioativos lipofílicos. Nesse sentido, os CLN, obtidos com três distintos emulsificantes (LS, Tween 80 e WPI), foram avaliados quanto à eficiência de incorporação, capacidade de carga, estabilidade física, cristalina e polimórfica das nanoestruturas com incorporação de β-caroteno. Dessa forma, os carreadores obtidos utilizando LS e Tween 80 como emulsificantes foram selecionados para o estudo da digestibilidade *in vitro* na etapa IV. Os resultados deste estudo compõem o Capítulo VI: "*Development and characterization of fully hydrogenated soybean oil and high oleic sunflower oil β-carotene loaded nanostructured lipid carriers"*.

A Etapa IV foi realizada no Laboratório de Indústria e Processos (LIP) da Universidade do Minho (UMinho) em Braga/Portugal, durante o período de Bolsa de Estágio e Pesquisa no Exterior-BEPE (Processo FAPESP 2019/05176-6) sob supervisão do Prof. Dr. António Augusto Vicente. Nesta etapa foram realizados ensaios relacionados à digestibilidade *in vitro* dinâmica, bioacessibilidade do composto incorporado às estruturas, ao perfil de liberação de ácidos graxos e a citotoxicidade dos CLN e dos componentes utilizados em sua composição. Esse período no exterior teve a duração de 16 meses e possibilitou, dentre outros

fatores, a complementaridade das etapas de projeto realizadas no Brasil, fornecendo informações pertinentes relativas ao comportamento de nanopartículas lipídicas durante a passagem pelo TGI, à toxicidade de nanoestruturas e, por conseguinte, à aplicação de nanoestruturas lipídicas em alimentos. Os resultados deste estudo compõem o Capítulo VII**:** "*Fully hydrogenated soybean oil and high oleic sunflower oil β-carotene loaded nanostructured lipid carriers: citotoxicity and bioaccessibility"*.

Capítulo VIII: *Discussão geral*

Neste capítulo, através de uma abordagem geral considerando as distintas etapas executadas, são apresentadas as discussões acerca dos principais resultados obtidos a partir do desenvolvimento deste estudo.

Capítulo IX: *Conclusões gerais*

Neste capítulo são relatadas as principais conclusões obtidas a partir dos resultados e discussões deste estudo.

Capítulo X: *Sugestões para trabalhos futuros*
Capítulo XI: *Referências bibliográficas*
Capítulo XII: *Anexos*

CAPÍTULO II

REVISÃO BIBLIOGRÁFICA

2. REVISÃO BIBLIOGRÁFICA

2.1 Nanopartículas e alimentos

Segundo o National Nanotechnology Initiative (NNI), a nanotecnologia pode ser definida como: i) pesquisa e desenvolvimento tecnológico nos níveis atômico, molecular ou macromolecular; ii) criação e utilização de estruturas, dispositivos e sistemas com novas propriedades e funções, devido às dimensões reduzidas; iii) capacidade de controle e manipulação em escala atômica (NNI, 2014).

De maneira geral, a nanotecnologia é considerada a aplicação dos princípios científicos e de engenharia para desenvolvimento e utilização de materiais de dimensões nanométricas, envolvendo a criação e manipulação da matéria orgânica e inorgânica em nanoescala (NNI, 2014). Os materiais resultantes apresentam propriedades físicas e químicas significativamente diferentes das propriedades dos materiais em macroescala, constituídos pela mesma substância (DUNCAN, 2011).

As propriedades físico-químicas (tais como a cor, solubilidade, viscosidade, difusividade, a resistência do material e toxicidade) e biológicas das estruturas e sistemas em nanoescala são substancialmente diferentes do que as estruturas em macro e microescala (NEETHIRAJAN; JAYAS, 2011). Partículas em macroescala são mais influenciadas pela inércia e gravidade do que por forças interparticulares; partículas menores que 10 µm geralmente apresentam interações interparticulares proporcionais à força gravitacional; nas partículas em escala nanométrica as forças interparticulares são menores e a interação ocorre a nível atômico e molecular (LI *et al*., 2004). Essa interação individual entre átomos e moléculas oferece novas e originais aplicações funcionais (NEETHIRAJAN; JAYAS, 2011).

A aplicação da nanotecnologia em alimentos é recente em comparação com a área biomédica e as indústrias de tecnologia de informação, nas quais a nanotecnologia já é utilizada na fabricação de materiais. No entanto, já existem inúmeras oportunidades que podem ser exploradas, como a elaboração de produtos com características funcionais e nutracêuticas, o desenvolvimento de processos e as embalagens inteligentes (ASSIS *et al.*, 2012).

A nanotecnologia representa um campo científico e tecnológico multidisciplinar em amplo desenvolvimento. A redução do tamanho de materiais em escala nanométrica modifica as propriedades físico-químicas e biológicas, resultando em novas aplicações. O pequeno tamanho das partículas em combinação com a grande área de superfície confere às nanopartículas características únicas e enorme potencial para aplicação na produção e processamento de alimentos (CHAU; WU; YEN, 2007). No campo da ciência de alimentos, o controle dos componentes em nanoescala pode levar à modificação de diversas características fundamentais, como textura e atributos sensoriais em geral, além da

processabilidade e estabilidade durante a vida de prateleira, além do desenvolvimento de sistemas para liberação de compostos bioativos (HUANG; YU; RU, 2010; MORARU *et al.*, 2003).

Há muitos benefícios potenciais derivados da aplicação da nanotecnologia em toda a cadeia de produção de alimentos: desenvolvimento de equipamentos de fabricação de alimentos mais leves e precisos, técnicas de processamento de alimentos mais baratas e eficientes, sistemas de distribuição de nutrientes, desenvolvimento de ingredientes alimentares e aditivos nanométricos, vida de prateleira de produtos alimentícios através do desenvolvimento de embalagens inovadoras ativas e inteligentes, reduções no desperdício de alimentos, bem como uma melhor qualidade e uma oferta de alimentos mais segura (HANDFORD *et al.*, 2014).

O termo nanoalimento (*nanofood*) descreve alimentos que foram cultivados, produzidos, processados ou embalados utilizando-se técnicas ou instrumentos nanotecnológicos, ou para os quais nanomateriais manufaturados tenham sido adicionados (CHAU; WU; YEN, 2007; HANDFORD *et al.*, 2014).

As estratégias de uso da nanotecnologia na indústria de alimentos apresentam-se bastante diferenciadas, uma vez que o processamento de alimentos consiste em uma abordagem multi-tecnológica, envolvendo grande variedade de matérias-primas, requerimentos de biossegurança, além de processos tecnológicos bem estabelecidos. As principais áreas da produção de alimentos que podem obter grandes benefícios pelo uso da nanotecnologia referem-se ao desenvolvimento de novos alimentos funcionais e de novos ingredientes. Entretanto, as questões regulatórias, aceitação pública e viabilidade econômica dos *nanofoods* demandam a utilização preferencial de matérias-primas naturais (CERQUEIRA *et al.*, 2014; LIVNEY, 2015).

Sistemas de nano-entrega apresentam grandes perspectivas para a nanotecnologia na área alimentícia, assim como nas áreas farmacêutica e cosmética. Em geral esses sistemas podem ser divididos em dois grupos: sistemas baseados em polímeros e baseados em lipídios (SAWANT; DODIYA, 2008). A obtenção de nanopartículas utilizando polímeros apresenta certas limitações relacionadas principalmente a questões de não biodegradabilidade e citotoxicidade de alguns polímeros, uso de solventes orgânicos e agentes de reticulação em sua preparação, baixa disponibilidade de biopolímeros e falta de técnicas de produção em larga escala (CHEN *et al.*, 2010; MÜLLER; MÄDER; GOHLA, 2000; RAWAL; PATEL, 2018; WEISS *et al.*, 2008).

Essas limitações foram transpostas pelo desenvolvimento de nanopartículas lipídicas (NL) que comparadas às nanopartículas poliméricas, apresentam vantagens potenciais para o sistema de nano-entrega de compostos, tais como elevada tolerância devido à utilização de lipídios fisiológicos e produção em larga escala (MÜLLER *et al.*, 1996).

Estabilidade física e química, capacidade de produção a baixo custo, ausência de solventes orgânicos na obtenção, possibilidade de esterilização, são alguns dos benefícios suplementares oferecidos pelas NL (RAWAL; PATEL, 2018). Como os lipídios fazem parte da nutrição humana e são parte integrante de muitos processos fisiológicos e bioquímicos, os sistemas nanoparticulados à base de lipídios são considerados um dos meios mais seguros, mais biocompatíveis, versáteis e acessíveis para entrega de compostos (ATTAMA; MOMOH; BUILDERS, 2012).

Além disso, o mecanismo de transporte dessas nanopartículas no TGI apresenta diferenças. A interação das nanopartículas com a barreira intestinal pode indicar a aplicação das mesmas para o transporte de determinados compostos. Enquanto as nanopartículas poliméricas são mais eficientes no transporte e entrega de peptídeos/proteínas, NL são mais eficientes para carrear compostos de baixa solubilidade em meio aquoso (BELOQUI; DES RIEUX; PRÉAT, 2016).

As NL têm sido reconhecidas como sistemas ideais para incorporação de compostos funcionais ou bioativos, em termos de seguridade toxicológica, escalabilidade e desempenho tecnológico, justificando uma série de estudos recentes no tema (ADITYA; KO, 2015). Em comparação aos sistemas de encapsulamento convencionais, os sistemas lipídicos apresentam como vantagem a possibilidade de produção com ingredientes naturais em escala industrial, grande diferenciação das propriedades físico-químicas das NL obtidas, além da capacidade de retenção de compostos de solubilidade bastante variável (YOON; PARK; YOON, 2013).

2.2 Nanopartículas lipídicas

O estudo das NL teve início na década de 90, com o desenvolvimento de nanopartículas lipídicas sólidas (NLS) como um sistema transportador coloidal alternativo para a entrega controlada de compostos (MÜLLER *et al.*, 1996). As NL integraram a alta biodisponibilidade e biocompatibilidade de emulsões, a permeabilidade da membrana de lipossomas, diferentes modificações químicas e liberação controlada de nanopartículas poliméricas; ao mesmo tempo em que minimizaram desvantagens destes sistemas de entrega tradicional como a utilização de solventes orgânicos, baixa inclusão de compostos e problemas de produção em larga escala (MEHNERT; MÄDER, 2012; MÜLLER; MÄDER; GOHLA, 2000).

A primeira geração de NL (NLS) foi produzida somente com lipídios sólidos e tensoativos e, é baseada no conceito da substituição do centro aquoso de emulsões por lipídios sólidos (SEVERINO; SANTANA; SOUTO, 2012). As NLS podem ser produzidas a partir de uma única matriz lipídica sólida, a exemplo de triacilgliceróis (TAG) de alto ponto de

fusão (PF), ou mediante o uso de uma mistura de classes lipídicas (TAMJIDI *et al.*, 2013). Em alguns casos, as NLS produzidas a partir de matrizes lipídicas de alta pureza podem se cristalizar de forma muito ordenada, o que permite menor espaço para incorporação de compostos, resultando em problemas de estabilidade durante a expulsão do componente encapsulado (YOON; PARK; YOON, 2013). O processo completo de cristalização ou recristalização dos lipídios reduz a solubilidade do composto incorporado na estrutura das NL, levando em alguns casos a expulsão desse composto, especialmente quando a concentração na formulação é muito alta. A maioria dos compostos tem maior solubilidade em lípidios no estado líquido do que em lipídios sólidos (MÜLLER; RADTKE; WISSING, 2002).

O uso de NLS como carreador lipídico apresenta algumas desvantagens como: menor espaço livre para acomodar os compostos bioativos em sua estrutura; liberação das moléculas bioativas durante o armazenamento; instabilidade física e química devido à tendência de a matriz lipídica sólida recristalizar durante o armazenamento; suscetibilidade à agregação de partículas; transições polimórficas (PYO; MÜLLER; KECK, 2017).

Diversos estudos relataram que as NLS, nanoemulsões que consistem em um núcleo de lipídios sólidos, forneceram maior proteção a compostos bioativos do que nanoemulsões obtidas apenas com lipídios líquidos (NIK; LANGMAID; WRIGHT, 2012), o que foi atribuído a uma difusão reduzida entre o núcleo lipídico e a fase aquosa (SALVIA-TRUJILLO *et al.*, 2019). No entanto, dependendo do estado cristalino da matriz lipídica utilizada para obtenção de NLS, poderá ocorrer uma expulsão do composto bioativo incorporado a estrutura promovendo assim sua degradação (WEISS *et al.*, 2008). Matrizes lipídicas de alto PF podem se cristalizar em uma estrutura altamente compacta, ocasionando assim a degradação de carotenoides (QIAN *et al.*, 2013).

Com o intuito de contornar possíveis limitações associadas às NLS, foi desenvolvida uma segunda geração de NL denominada de carreadores lipídicos nanoestruturados (CLN) (YOON; PARK; YOON, 2013). A Figura 2 apresenta os principais componentes de formulação de CLN e NLS. A obtenção de CLN é realizada utilizando-se sistemas lipídicos sólidos, líquidos e emulsificantes. Esta segunda geração surgiu com o intuito de produzir uma matriz lipídica menos estruturada em relação à cristalinidade,capaz de obter melhor eficiência de encapsulação e evitar a liberação dos compostos incorporados durante a estocagem (SERRA *et al.*, 2008; SOUTO; SANTANA; PINHO, 2011). As misturas lipídicas utilizadas, no entanto, devem apresentar PF superior à temperatura corporal. Como resultado das imperfeições na estrutura cristalina dos CLN, a capacidade de encapsulação das partículas pode ser aumentada, minimizando a liberação do composto ativo durante o período de armazenamento (YOON; PARK; YOON, 2013).

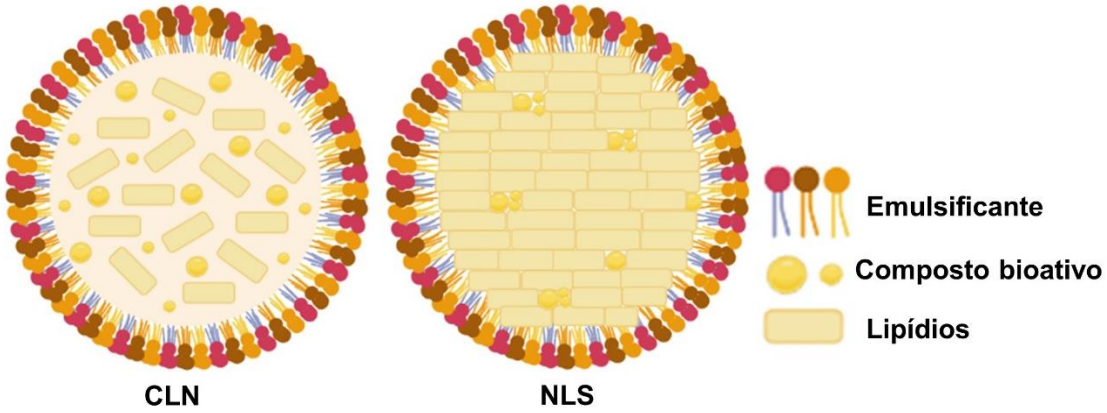

Figura 2: Principais componentes de formulação de CLN e NLS. Fonte: autoral, adaptado de Rostamabadi *et al*. (2019), criado com *Biorender.*

2.3 Carreadores Lipídicos Nanoestruturados

Os CLN consistem em uma matriz lipídica sólida desordenada, obtida através da mistura de lipídios de maior e de menor PF, e uma fase aquosa contendo um agente tensoativo ou uma mistura de agentes tensoativos (PARDEIKE; HOMMOSS; MÜLLER, 2009). O objetivo da formulação de CLN é produzir partículas em que a fração lipídica líquida seja incorporada a uma matriz lipídica sólida, o que conduz a uma maior capacidade de carga (CC) e entrega controlada de compostos solubilizados no óleo e simultaneamente encapsulados pelo lipídio sólido (VARSHOSAZ; ESKANDARI; TABAKHIAN, 2010).

Os CLN podem combinar as vantagens de diferentes sistemas de entrega coloidal e superar algumas de suas desvantagens (baixa CC, perda de ingredientes bioativos por expulsão durante o armazenamento, agregação de partículas e instabilidade durante o armazenamento) (MOHAMMADI; ASSADPOUR; JAFARI, 2019). A redução na expulsão de compostos no caso de CLN é atribuída ao fato de que os lipídios puros tendem a sofrer mudanças polimórficas e recristalizar em um estado de fusão menos estável e mais tarde, para um polimorfo mais estável (RAWAL; PATEL, 2018). Para isso a mistura lipídica utilizada para obtenção dos CLN deve apresentar menor velocidade das transições polimórficas, bem como menor grau de cristalinidade, propriedades associadas à existência de domínios lipídicos líquidos no centro das partículas (TAMJIDI *et al.*, 2013).

Em geral, imperfeições dos cristais podem ser aumentadas pelo uso de misturas de TAG ou acilgliceróis compostos por diferentes ácidos graxos (AG), no que se refere ao tamanho de cadeia e grau de saturação. A incompatibilidade estrutural dos elementos lipídicos para composição dos CLN pode, portanto, ser promovida pelo uso de fontes lipídicas com características físico-químicas distintas, a exemplo de TAG de alto PF e óleos vegetais líquidos (MÜLLER; RADTKE; WISSING, 2002).

A aplicação de CLN em alimentos apresenta algumas vantagens como: alta eficiência de incorporação (EI) por proporcionar maior espaço para a acomodação de compostos bioativos; alta estabilidade físico-química; obtidos por método simples, de custo viável e com possibilidade de fabricação em grande escala; fornece um perfil de liberação controlada devido a matriz lipídica sólida; apresenta capacidade de encapsular uma ampla gama de compostos bioativos tanto de natureza hidrofílica, quanto hidrofóbica; liberação prolongada de compostos bioativos; proteção dos compostos incorporados contra as condições de degradação externa; obtidos a partir de ingredientes biodegradáveis e naturais com baixo nível de toxicidade, entre outras (AKHAVAN *et al.*, 2018; MOHAMMADI; ASSADPOUR; JAFARI, 2019).

2.4 Composição de CLN

Os componentes essenciais para a obtenção de CLN constam da fase lipídica, emulsificantes e água. Neste caso, o percentual de lipídios na formulação pode ser superior a 95% (m/m) e o percentual do composto bioativo incorporado, com relação à formulação total, é próximo de 5% (m/m) (PURI *et al.*, 2009; TAMJIDI *et al.*, 2013). A formulação de CLN ideal para aplicação em produtos alimentares deve preconizar a seleção adequada de lipídios e emulsificantes aprovados como que se enquadram na categoria GRAS - *Generally Recognized as Safe*, ou com status regulatório aprovado para elaboração de sistemas transportadores de compostos bioativos destinados à administração oral ou parenteral (MOHAMMADI; ASSADPOUR; JAFARI, 2019; SERRA *et al.*, 2008).

O conteúdo, a composição da fase lipídica e o tipo de emulsificante utilizados para obtenção de CLN influenciam suas propriedades físico-químicas, como tamanho e distribuição de partículas, carga superficial, estabilidade física, CC, EI, bem como a taxa e a extensão da digestão lipídica no TGI. A escolha racional dos materiais para a composição de CLN pode, portanto, maximizar o potencial que estas nanoestruturas apresentam para o carreamento, proteção, entrega e aumento da bioacessibilidade de compostos bioativos lipofílicos como o β-caroteno (BC). A otimização da combinação entre lipídios e emulsificantes, bem como do método utilizado para obtenção permite a obtenção de CLN com propriedades físico-químicas eficientes (ASHKAR; SOSNIK; DAVIDOVICH-PINHAS, 2021).

2.4.1 Lipídios

Óleos e gorduras comestíveis são nutrientes essenciais da dieta humana, apresentando papel vital mediante o fornecimento de AG essenciais e energia. Em adição às qualidades nutricionais, os óleos e gorduras provêm consistência e características de fusão específicas aos produtos que os contém, atuam como meio de transferência de calor

durante o processo de fritura e como carreadores de vitaminas lipossolúveis e aroma (YOUNG, 1985). Quimicamente óleos e gorduras são substâncias insolúveis em água (hidrofóbicas), de origem animal ou vegetal, formados predominantemente por ésteres de TAG, produtos resultantes da esterificação entre o glicerol e AG (MORETTO; FETT, 1998). Óleos e gorduras naturais consistem de misturas multi- componentes de TAG, e pequenas quantidades de lipídios polares(ou minoritários), como diacilgliceróis (DAG), monoacilgliceróis (MAG), ácidos graxos livres (AGL), fosfolipídios, glicolipídios e esteróis.

TAG são constituídos por três AG combinados a três carbonos de uma molécula de glicerol por meio de ligações ésteres. Cada AG pode ocupar diferentes posições na molécula (*sn-1*, *sn-2* ou *sn-3*), possibilitando uma grande diversidade de combinações. Entretanto, a distribuição dos AG nos TAG naturais não é randômica. O padrão taxonômico dos óleos e gorduras de obedece à distribuição *1,3-random-2-random*, com os ácidos graxos saturados (AGS) localizados quase exclusivamente nas posições *sn-1* e *sn-3* e os ácidos graxos insaturados (AGI) preferencialmente na posição *sn-2* dos TAG (O'BRIEN, 2008).

Grande parte do comportamento dos lipídios depende das características da cadeia alquila dos AG presentes, como por exemplo a presença de saturação ou insaturação, configuração *cis* ou *trans*, tamanho de cadeia e número de carbonos par ou ímpar. AGS são menos reativos e apresentam PF superior em relação ao AG correspondente de mesmo tamanho de cadeia com uma ou mais duplas ligações. A presença de cadeias longas e saturadas aumenta o PF dos TAG , em razão de sua conformação linear, acarretando maior interação das moléculas e, consequentemente, permitindo melhor empacotamento das cadeias de AG (SCRIMGEOUR, 2005).

A composição triacilglicerólica e distribuição regioespecífica determinam as propriedades físicas dos óleos e gorduras, afetando a estrutura, estabilidade, sabor, aroma, qualidade de estocagem, características sensoriais e visuais dos alimentos, além de seu valor nutritivo (O'BRIEN, 2008); e originam uma notável diversidade na estrutura polimórfica e, consequentemente, complexos perfis de cristalização (RIBEIRO *et al.*, 2009).

As matrizes lipídicas são os principais ingredientes das NL, influenciando diretamente na sua CC, estabilidade e liberação de compostos incorporados à estrutura (KATOUZIAN *et al.*, 2017; SHAH *et al.*, 2015). As características físico-químicas dos lipídios utilizados para a obtenção de sistemas de entrega à base de emulsões impactam diretamente sua digestibilidade, e consequentemente a bioacessibilidade dos compostos bioativos lipofílicos que são solubilizados dentro das gotas de óleo (SALVIA-TRUJILLO *et al.*, 2017b).

A seleção de matrizes lipídicas apropriadas para o desenvolvimento de CLN deve considerar os seguintes aspectos: i) a solubilidade do princípio encapsulado na fase lipídica, a eficiência de encapsulação e viabilidade de uso nas NL obtidas; ii) estabilidade da fase

lipídica à processos de oxidação química e enzimática; iii) emprego de componentes lipídicos biodegradáveis, e com perfil toxicológico aceitável (KATOUZIAN *et al.*, 2017; TAMJIDI *et al.*, 2013).

A porcentagem de lipídio líquido na matriz lipídica para obtenção de CLN influencia propriedades físicas, como o TP, o início do processo de cristalização e a temperatura de fusão, além de produzir partículas com menor cristalinidade, promovendo maior espaço para incorporação de compostos bioativos (ZHENG *et al.*, 2013). As características dos AG que compõem as matrizes lipídicas de maior e menor PF utilizadas para obtenção de CLN podem promover a formação de uma fase lipídica mais viscosa, o que pode levar ao aumento da tensão superficial e consequentemente à formação de partículas maiores (PINTO; DE BARROS; FONSECA, 2018). Nesse sentido, deve-se considerar e escolha de uma proporção racional entre os lipídios de maior e de menor PF para compor os CLN (KATOUZIAN *et al.*, 2017). Para obtenção de CLN, os constituintes lipídicos de alto e baixo PF devem apresentar configuração espacial bastante diferenciada. Isto significa que a fase lipídica líquida não deve ser incorporada à fase lipídica sólida, e que os cristais não devem ser solubilizados pela fase líquida. Adicionalmente, uma condição essencial para garantir a estabilidade dos CLN é que os constituintes lipídicos de alto e baixo PF apresentem miscibilidade completa nas concentrações de uso (DOKTOROVOVÁ *et al.*, 2010).

Vários estudos que consideraram o desenvolvimento de CLN a partir de sistemas lipídicos com diferentes proporções de fontes de maior e menor PF já foram reportados na literatura. How, Rasedee e Abbasalipourkabir (2013), por exemplo, caracterizaram CLN formulados com azeite de oliva e óleo de palma hidrogenado em diferentes proporções, obtidos utilizando Tween 80 como emulsificante. Os autores relataram que as características físico-químicas dos CLN foram independentes da proporção da matriz lipídica de menor PF no sistema lipídico. Em geral o aumento na proporção de azeite de oliva proporcionou o aumento do Potencial Zeta (PZ) e na polidispersidade dos CLN, sendo que os CLN obtidos com maior conteúdo de azeite de oliva apresentaram maior TP dentre os CLN avaliados. Oliveira *et al*. (2016) caracterizaram CLN com incorporação de BC obtidos a partir de triestearina e óleo de girassol alto oleico (OGAO) em diferentes proporções, e encontraram que a composição lipídica não alterou o TP dos CLN obtidos. Os termogramas obtidos pela análise de calorimetria diferencial de varredura (DSC) demonstraram que o OGAO gerou um distúrbio na ordem dos cristais, uma vez que nanopartículas com matriz lipídica menos organizada foram produzidas. Os autores encontraram ainda que, embora a degradação total do BC tenha sido semelhante para todos os sistemas, a análise colorimétrica demonstrou que a degradação do BC encapsulado foi menor para nanopartículas com alto teor de OGAO. Pan, Tikekar e Nitin (2016) avaliaram CLN preparados através de sistemas lipídicos com distintas proporções de trioctanoato de glicerilo (lipídio de menor PF) e eicosano (lipídio de maior PF),

e LS de alto PF (Phospholipon® 80 H) como emulsificante. Os autores reportaram que a porcentagem de lipídio de menor PF não influenciou significativamente ($p<0,05$) o TP dos CLN obtidos. No entanto, verificou-se um aumento na quantidade de BC carregado nos CLN proporcional ao conteúdo de lipídios de menor PF. Babazadeh, Ghanbarzadeh e Hamishehkar (2017) realizaram a obtenção de CLN utilizando fontes lipídicas de maior (ácido láurico, ácido esteárico, e manteiga de cacau) e de menor PF (glicerol, miglyol 812, óleo de milho e oleico ácido) combinadas em diferentes proporções, a partir de distintos emulsificantes (Poloxamer 407, Tween 80 e Tween 20). Os autores relataram que as dimensões e a morfologia dos CLN obtidos foram influenciadas pela concentração da fase lipídica de menor PF. O aumento no teor do lipídio de menor PF em até 30% produziu partículas esféricas com superfícies lisas e menores dimensões. Pinto, Barros e Fonseca (2018) desenvolveram CLN a partir de óleos vegetais (girassol, amêndoa doce, coco e azeite de oliva) como matrizes lipídicas de menor PF e ácido mirístico (C14:0) como matriz lipídica de maior PF, em diferentes proporções, utilizando quatro distintos emulsificantes (Tween 80, Span 60, Span 80 e Poloxamer 188). Neste estudo verificou-se que embora o TP dos CLN tenha diminuído com o aumento da porcentagem de óleos vegetais, algumas exceções foram observadas, indicando que além da proporção da matriz lipídica de menor PF, sua composição em AG influenciou o TP dos CLN obtidos. Pezeshki *et al*. (2019) avaliaram CLN com incorporação de BC obtidos utilizando octanoato de octilo e Precirol como matrizes lipídica de maior e menor PF, respectivamente, em diferentes proporções; e Poloxamer 407 como emulsificante em diferentes concentrações (1%, 2%, 3% e 4% m/v). Em todas as concentrações de emulsificante, verificou-se que o aumento do grau de insaturação do sistema lipídico também foi acompanhado de aumento no TP dos CLN obtidos. Rohmah *et al*. (2020) obtiveram CLN com incorporação de BC, utilizando estearina e oleína de palma como matrizes lipídicas e Tween 80 como emulsificante através da sonicação. O aumento da proporção do lipídio de maior PF resultou no aumento do TP. Yang *et al*. (2020) avaliaram a obtenção de CLN com incorporação de BC através da homogeneização a alta pressão (HAP) utilizando monoestearato de glicerila (GMS) e TAG de cadeia média (TCM) em diferentes proporções como matrizes lipídicas, e Tween 80 como emulsificante. Os autores encontraram que o aumento adicional na proporção de lipídio de maior PF para lipídio de menor PF, não foi benéfico na redução do TP e do índice de polidispersidade (IP) e no aumento da estabilidade do sistema. Um estudo realizado por Queirós *et al*. (2021) avaliou a influência do grau de insaturação de diferentes sistemas lipídicos compostos por gordura do leite totalmente hidrogenada, gordura do leite anidra e OGAO sobre as características de CLN obtidos através da HAP. Neste estudo, o isolado proteico do soro de leite (WPI) e o Caseinato de Sódio foram utilizados como emulsificantes. Os autores relataram que o aumento no grau de insaturação do sistema lipídico utilizado para obtenção de CLN promoveu o aumento significativo no TP.

Os resultados encontrados nos diversos estudos reforçam a importância da escolha racional das matrizes lipídicas de maior e menor PF para compor os CLN. O conhecimento das propriedades físicas e de cristalização das matrizes lipídicas utilizadas para obtenção dos CLN é importante para otimizar sua formação, estabilidade e atuação funcional (KHARAT; MCCLEMENTS, 2019). Dessa forma, a caracterização completa da matriz lipídica e de sistemas lipídicos formados por diferentes proporções destas matrizes, é essencial para a formulação de CLN com características de cristalinidade adequadas para a incorporação de compostos bioativos. Além disso, conhecer o comportamento de matrizes lipídicas em macroescala é primordial para o entendimento de seu comportamento em nanoescala, permitindo assim definir as proporções mais adequadas de lipídios de maior e menor PF para compor os CLN.

Os TCM e o ácido oleico são os componentes de baixo PF mais utilizados no desenvolvimento de CLN (JANNIN; MUSAKHANIAN; MARCHAUD, 2008; JOSEPH; BUNJES, 2012). Os TCM são obtidos através da modificação (hidrólise/esterificação) e fracionamento de óleos naturais como óleo de palma, por exemplo. Apresentam grau alimentar (reconhecido como *GRAS*), são digeridos mais rapidamente que TAG de cadeia longa e apresentam elevada estabilidade oxidativa (PORTER; TREVASKIS; CHARMAN, 2007); porém apresentam custo elevado (TAMJIDI *et al.*, 2013). O ácido oleico - ácido cis-9- octadecenóico – C18:1 (9) – é um constituinte da grande maioria dos óleos e gorduras comestíveis. Apresenta efeito benéfico à saúde bem documentado e estabelecido, e menor susceptibilidade à oxidação quando comparado aos ácidos linoleico e linolênico (SCRIMGEOUR, 2005).

Os componentes lipídicos sólidos empregados na preparação de CLN constam principalmente de TAG, AG, MAG, DAG e ceras. Os ácidos mirístico, palmítico e esteárico, especialmente, são compatíveis com a composição lipídica dos tecidos animais, e em consequência, têm sido utilizados como matriz lipídica preferencial para o preparo de NL (ELTAYEB *et al.*, 2013). Tanto o ácido esteárico quanto a triestearina, ou misturas lipídicas ricas nestes componentes, representam matérias-primas de grande utilização para composição de NL. O ácido esteárico, em particular, consiste em um AG endógeno de cadeia longa, e representa um componente importante em óleos e gorduras naturais e modificados. Possui ponto de fusão de aproximadamente 70°C e é considerado neutro com respeito ao impacto no perfil de lipoproteínas plasmáticas (ELTAYEB *et al.*, 2013; MENSINK, 2005; SEVERINO *et al.*, 2011; WANG *et al.*, 2014).

2.4.1.1 Óleo de Girassol Alto Oleico (OGAO)

Os óleos vegetais apresentam alto potencial como matrizes lipídicas de menor PF para a formulação de CLN, possibilitando a obtenção de nanoestruturas a partir de fontes naturais, com menor custo e presença de antioxidantes naturais em sua composição. No entanto, como muitos óleos vegetais apresentam alto grau de insaturação e alta viscosidade, podem comprometer a obtenção dos CLN, em termos de instabilidade oxidativa, inconvenientes relacionados ao rompimento das gotículas durante a redução de tamanho e baixa EI de compostos bioativos (LIU; WU, 2010; NGUYEN *et al.*, 2012; TAMJIDI *et al.*, 2013). Assim sendo, a escolha do óleo vegetal para obtenção de CLN deve considerar suas características físico-químicas e sua resistência aos processos oxidativos. Outro fator muito importante a ser considerado ao se utilizar óleos vegetais para a obtenção de CLN é a avaliação dos atributos de qualidade desta matéria-prima, uma vez que esta é dependente de fatores edafoclimáticos no cultivo, manuseio durante o pré-processamento, refino e armazenamento.

Óleos provenientes de fontes vegetais, como o de soja, de milho e girassol, por exemplo, são grandes candidatos para uso como matriz lipídica de menor PF visando a obtenção de CLN para uso como aditivo alimentar (MOHAMMADI; ASSADPOUR; JAFARI, 2019). A modificação genética do girassol convencional para a variedade alto oleico conferiu a este óleo estabilidade oxidativa dez vezes superior em comparação aos óleos de soja, canola e ao próprio óleo de girassol de composição regular, sendo dessa forma considerado uma matéria-prima premium para a obtenção de CLN (GUNSTONE, 2011; O'BRIEN, 2008).

O OGAO foi desenvolvido por pesquisadores russos a partir da mutagênese química e cruzamentos seletivos do girassol (*Helianthus annus*), visando a obtenção de uma variedade de semente estável às condições climáticas, e, portanto, com alto teor de ácido oleico (O'BRIEN, 2008). A composição típica do OGAO é representada por 3-5% de ácido palmítico, 2-6% de ácido esteárico, 75 a 88% de ácido oleico e menos de 1% de ácido linolênico. Adicionalmente, a distribuição regioespecífica do OGAO mostra-se diferenciada, com elevada proporção de ácido linoleico na posição *sn-2*, propriedade que também justifica sua característica de alta estabilidade ao processo de oxidação (GROMPONE, 2005; O'BRIEN, 2008). Essas características têm direcionado o OGAO à obtenção de produtos de máxima segurança toxicológica e biodegradabilidade; justificando seu alto potencial de aplicação em alimentos, cosméticos e fármacos, atribuindo seu direcionamento como fonte lipídica líquida de alta qualidade para a obtenção de CLN (GUNSTONE, 2011).

2.4.1.2 Óleo de soja totalmente hidrogenado (OSTH)

TAG puros e suas misturas comerciais podem ser utilizados com sucesso na obtenção de NL. Contudo, o uso de TAG na forma purificada mostra-se geralmente inviável economicamente quando se considera a escala e possibilidade de aplicação em sistemas alimentícios. Uma opção de alto potencial como matriz lipídica de alto PF para obtenção de CLN consiste nos óleos ou gorduras totalmente hidrogenados, também conhecidos como *hardfats* (SANTOS *et al.*, 2019). Essa abordagem de aplicação em NL, ainda pouco explorada, apresenta diferenciais de produção, aplicação e estabilidade (DAN, 2016; TAMJIDI *et al.*, 2013).

O processo de hidrogenação total de óleos vegetais promove a adição de hidrogênio às duplas ligações dos AGI através de reação catalítica, clivando-as; promovendo assim a conversão de AGI em AGS. Este processo, é considerado de baixo custo relativo, representa uma alternativa de uso para as plantas industriais anteriormente utilizadas para o processo de hidrogenação parcial, e permite a obtenção de bases lipídicas de alto PF, compostas por TAG trissaturados, a partir de óleos vegetais de uso convencional (RIBEIRO *et al.*, 2009; RIBEIRO; BASSO; KIECKBUSCH, 2013; WASSELL; YOUNG, 2007). Teores expressivos de ácido esteárico nos *hardfats*, a exemplo do óleo de soja totalmente hidrogenado (OSTH), mostram-se favoráveis ao uso destes componentes em NL, devido ao efeito aterogênico neutro associado a este AG, que não apresenta efeito adverso sobre o risco de doenças cardiovasculares (VALENZUELA; DELPLANQUE; TAVELLA, 2011).

Os *hardfats* têm sido objeto de estudos recentes voltados aos processos de modificação lipídica. Sua composição em AG e em TAG representam fatores importantes na determinação do efeito modulador dos processos de cristalização em fases lipídicas contínuas. *Hardfats* específicos, provenientes de uma determinada fonte oleosa, apresentam perfil triacilglicerólico único e diferenciado, embora sejam compostos, em sua totalidade, por TAG trissaturados (RIBEIRO; BASSO; KIECKBUSCH, 2013).

O OSTH é obtido após a hidrogenação total do óleo de soja. A composição em AG do óleo de soja é influenciada pela genética da semente e pelas condições climáticas de cultivo; apesar disso, o óleo de soja é constituído essencialmente pelo ácido oleico (C18:1) (22%), ácido linoleico (C18:2) (53%) e ácido linolênico (C18:3) (8%). Após a hidrogenação deste óleo, o AG predominante é o ácido esteárico (C18:0) (87,22%), seguido pelo ácido palmítico (C16:0) (10,57%) (OLIVEIRA; RIBEIRO; KIECKBUSCH, 2015; RIBEIRO; BASSO; KIECKBUSCH, 2013).

2.4.2 Emulsificantes

Os emulsificantes são moléculas anfifílicas que consistem em uma cabeça hidrofílica e uma cauda hidrofóbica, e executam dois papéis fundamentais na formação de CLN: facilitam a dispersão do lipídio fundido em uma fase aquosa durante a etapa de emulsificação; e estabilizam as nanopartículas após a fase de resfriamento das emulsões (RAWAL; PATEL, 2018).

A escolha dos emulsificantes e suas concentrações específicas apresentam grande impacto na qualidade das dispersões de CLN, pois estes se caracterizam por uma função fundamental, que consiste no controle do processo de cristalização da fase lipídica. Devido às pequenas dimensões das nanoemulsões, o número de moléculas lipídicas que interagem com os diferentes grupos funcionais dos emulsificantes é grande o suficiente para que estes tenham ação como moduladores de cristalização. Além disso, o emulsificante pode modificar a cinética de cristalização e o hábito polimórfico natural das matérias-primas lipídicas utilizadas, minimizando problemas de recristalização e desestabilização de CLN durante estocagem e aplicação (WEISS *et al.*, 2008).

Os diferentes processos para obtenção de NL exigem misturas e concentrações específicas de emulsificantes, incorporados à fase lipídica ou aquosa. A concentração ótima de emulsificantes na formulação mostra-se dependente da matriz lipídica utilizada para composição das nanopartículas. A quantidade utilizada deve ser suficiente para que uma camada protetora da fase lipídica seja formada após a constituição das partículas. Consequentemente, testes preliminares considerando os materiais lipídicos utilizados na obtenção de NL, emulsificantes de composição e suas concentrações, bem como a avaliação do método de produção, são fundamentais para as características de funcionalidade, qualidade e aplicabilidade dos sistemas lipídicos nanoparticulados (HELGASON *et al.*, 2009; MEHNERT; MÄDER, 2012).

As características estruturais (peso molecular e número e localização dos grupos hidrofóbicos e hidrofílicos) afetam fortemente a habilidade de um emulsificante reduzir a tensão superficial entre a fase oleosa e a fase aquosa (MCCLEMENTS; JAFARI, 2018). A solubilidade e a dispersão de um emulsificante influenciam diretamente seu desempenho em emulsões. A formação de emulsões normalmente requer que o emulsificante apresente boa solubilidade em água e se disperse facilmente na fase aquosa, ao invés da oleosa. No entanto, no caso dos fosfolipídios a dispersão é facilitada na fase oleosa (MCCLEMENTS; JAFARI, 2018; MEYERS, 2006). O balanço hidrofílico-lipofílico (BHL) é normalmente utilizado para descrever características de solubilidade e dispersão de emulsificantes. Definido como a razão entre a porcentagem em massa de grupos hidrofílicos e a porcentagem em massa de grupos hidrofóbicos presentes na molécula, o BHL de um emulsificante pode variar de 0

(lipofílico) a 20 (hidrofílico). Emulsificantes com valores baixos (2-6) de BHL normalmente se dispersam na fase oleosa, enquanto emulsificantes com valores superiores (BHL=8-18) se dispersam na fase aquosa (MEYERS, 2006).

Emulsificantes sintéticos considerados em estudos diversos relacionados à obtenção de NL para uso em aplicações alimentícias incluem ésteres de poliglicerói s, ésteres de sorbitana, polissorbatos, MAG e DAG. Dentre estes, destacam-se o monooleato de sorbitana etoxilado (Tween 80) e o monoestearato de sorbitana (Span 60), pelas características gerais de segurança toxicológica para uso em alimentos, obtenção a partir de fontes renováveis e alta estabilidade conferida às nanoestruturas lipídicas (ADITYA *et al.*, 2013; CARVALHO *et al.*, 2013; CHOI; ADITYA; KO, 2014; DORA *et al.*, 2012; LIU; WANG; XIA, 2012; LOBATO *et al.*, 2013; PATEL; SAN MARTIN-GONZALEZ, 2012; SHANGGUAN *et al.*, 2014).

Como o número de emulsificantes aprovados para uso alimentar é limitado, um dos principais desafios a serem transpostos na obtenção de CLN é o desenvolvimento das nanoestruturas a partir de emulsificantes naturais (KATOUZIAN *et al.*, 2017; OLIVEIRA; FURTADO; CUNHA, 2019). Entre as principais tendências, destaca-se o uso de emulsificantes extraídos de fontes vegetais, como a lecitina e os isolados proteicos, por exemplo, e de fontes animais, como as proteínas provenientes do leite. As lecitinas são consideradas tensoativos neutros, encontrados naturalmente em fontes vegetais como a soja, canola, e animais, como o ovo e consideradas como *GRAS.* Devido à sua ampla disponibilidade, são considerados emulsificantes de baixo custo com potencial para uso na obtenção de CLN (KATOUZIAN *et al.*, 2017; MCCLEMENTS, 2015; MOHAMMADI; ASSADPOUR; JAFARI, 2019).

Embora a maior parte dos emulsificantes utilizados para a obtenção de CLN sejam emulsificantes de baixo peso molecular, macromoléculas como as proteínas são ingredientes naturais e biocompatíveis que têm sido utilizados na estabilização de NL (MOHAMMADI; ASSADPOUR; JAFARI, 2019). Proteínas do soro do leite são consideradas como emulsificantes naturais devido à sua capacidade de alterar as propriedades da interface das gotas de óleo dispersas, aumentando sua estabilidade frente aos processos de cremeação (HU; MCCLEMENTS; DECKER, 2003). As proteínas do soro de leite são muito utilizadas como emulsificantes/estabilizantes (GUZEY; MCCLEMENTS, 2006), além de possuírem alto valor nutricional e serem consideradas seguras (GRAS) (CHEN; REMONDETTO; SUBIRADE, 2006). O WPI é um dos ingredientes mais utilizados na indústria de alimentos para a obtenção de emulsões óleo em água. O WPI é composto por duas frações principais, a β-lactoglobulina e a α-lactoalbumina que juntas representam cerca de 70% das proteínas encontradas no soro de leite (CHATTERTON *et al.*, 2006). O isolado proteico de soja (SPI), um subproduto da extração do óleo de soja, é um constituinte natural e de baixo custo em produtos comerciais

(WANG *et al.*, 2019). O uso do isolados proteicos como agentes emulsificantes apresenta as seguintes vantagens: são ingredientes funcionais e nutricionais, comercialmente e abundantemente disponíveis; além de emulsificar, promovem a estabilização estérica; não necessitam de modificação química para melhoria das propriedades de superfície das partículas e são compatíveis com a HAP (LIU; TANG, 2014).

De forma geral a efetividade de emulsificantes para obtenção de CLN está relacionada a dois fatores principais: a velocidade em que o emulsificante recobre a partícula e a interação entre a molécula emulsificante e a fase lipídica dispersa. Idealmente, o processo de obtenção de CLN deve proporcionar o aumento contínuo do número de gotas e o recobrimento imediato destas gotas pelas moléculas de emulsificantes utilizadas para a estabilização das partículas. Portanto, a seleção do emulsificante adequado para a obtenção de CLN deve considerar dentre outros fatores as características físico-químicas e estruturais, o método utilizado para a obtenção, a compatibilidade com a fase lipídica e com o composto bioativo a ser incorporado, bem como a estabilidade destes emulsificantes frente às condições do TGI.

2.5 Obtenção de CLN

A obtenção de CLN é um processo complexo que envolve o aquecimento da matriz lipídica acima do seu PF e sua recristalização através de um resfriamento rápido (ATTAMA; MOMOH; BUILDERS, 2012; KHOSA; REDDI; SAHA, 2018). De forma geral a síntese de CLN relaciona-se a variações das seguintes abordagens tecnológicas: i) criação de uma nanoemulsão óleo-em-água como precursora das etapas posteriores; ii) subsequente solidificação da fase lipídica dispersa (SHARMA *et al.*, 2011).

As nanoemulsões podem ser obtidas por distintos métodos. Em geral, os métodos de obtenção de nanoemulsões são classificados em métodos de alta ou de baixa energia (ACOSTA, 2009; LEONG *et al.*, 2009). Os métodos de alta energia utilizam dispositivos mecânicos que geram forças mecânicas que rompem e homogeneízam a fase óleo/água (O/A) e a imobilizam numa gotícula de óleo (LEONG *et al.*, 2009); enquanto nos métodos de baixa energia ocorre a formação espontânea de gotículas de óleo pelo sistema óleo/água/emulsificante (O/A/E), quando condições ambientais são alteradas (pH, força iônica, temperatura) (FREITAS; MERKLE; GANDER, 2005; YIN *et al.*, 2009).

Em geral os métodos de alta energia apresentam facilidade de transposição de escala, possibilitam a produção em larga escala e o uso de uma ampla variedade de óleos e emulsificantes para a obtenção da nanoemulsão. Os métodos de baixa energia, apesar de muitas vezes serem mais eficazes que os métodos de alta energia, apresentam dificuldade de transposição de escala, limitação no uso de certos óleos e emulsificantes (como proteínas

e polissacarídeos) para formação da nanoemulsão, além de se tornar necessário o uso de maiores quantidades de emulsificantes sintéticos, o que pode limitar seu uso em aplicações alimentares. Os métodos de alta energia já utilizados na obtenção de NL são a HAP, microfluidização e ultrassonicação. Os métodos de baixa energia utilizados são a emulsificação espontânea, inversão de fases e difusão/evaporação do solvente (MCCLEMENTS; RAO, 2011). Preferencialmente a obtenção de CLN é realizada por métodos de alta energia devido à facilidade de transposição de escala (OLIVEIRA *et al.*, 2016).

2.5.1 Homogeneização a alta pressão (HAP)

A HAP é o método mais utilizado para a obtenção de partículas em escala nanométrica na indústria alimentícia (SCHUBERT; ENGEL, 2004). Duas diferentes abordagens da HAP, denominadas homogeneização a quente e homogeneização a frio, podem ser utilizadas para a produção de NLS e CLN. Em ambos os casos, uma etapa preparatória envolve a incorporação do composto a ser encapsulado na matriz lipídica, por dissolução ou dispersão do mesmo na fase lipídica (MEHNERT; MÄDER, 2012).

O método HAP a quente é o mais utilizado para a obtenção de NL (TAMJIDI *et al.*, 2013). A Figura 3 apresenta o esquema de obtenção de CLN através da HAP a quente. No processo a quente, a matriz lipídica é completamente fundida, a temperatura acima do seu PF, o composto ativo é incorporado; em seguida esta fase é emulsionada em uma fase aquosa, com o uso de agitação mecânica, obtendo-se assim uma pré-emulsão (SOUTO; SANTANA; PINHO, 2011). Nesta etapa devem ser obtidas partículas com dimensões de poucos micrômetros, pois a qualidade desta pré-emulsão está diretamente relacionada com a qualidade final das NL (MEHNERT; MÄDER, 2012). Em seguida, a pré-emulsão é alimentada para a válvula de entrada do HAP, a temperaturas entre 70 e 90°C; um pistão admite a emulsão dentro de uma câmara e em seguida, obriga a passagem desta, por uma válvula estreita geralmente inferior a 30µm (SOUTO; SANTANA; PINHO, 2011). Nessa válvula são aplicadas forças destrutivas intensas (cisalhamento, turbulência e cavitação), que promovem o rompimento destas partículas em escala nanométrica (MCCLEMENTS; RAO, 2011), resultando em uma nanoemulsão do tipo óleo/água, que ao ser resfriada promoverá a cristalização da matriz lipídica e assim, a obtenção das NL (JAFARI; HE; BHANDARI, 2007).

A etapa de homogeneização pode ser realizada em diferentes ciclos e pressões; em geral, de 1 a 5 ciclos, sob 500-1500 bar são suficientes (JAFARI; HE; BHANDARI, 2007). O tamanho das nanopartículas obtidas usualmente diminui com o aumento da pressão, com o número de passagens da emulsão pelo HAP (número de ciclos) e com o aumento da temperatura. Um ciclo corresponde ao tempo necessário para a completa transferência de determinado volume de amostra pelo equipamento; o número de ciclos depende da

formulação e da viscosidade da emulsão a ser bombeada (MCCLEMENTS; RAO, 2011). A aplicação de pressão de homogeneização excessiva, no entanto, pode promover o aumento no TP, pois quanto maior a pressão mais intensa a colisão entre as partículas resultando na aglomeração destas partículas, aumento no TP e menor estabilidade do sistema transportador (CHU *et al.*, 2007).

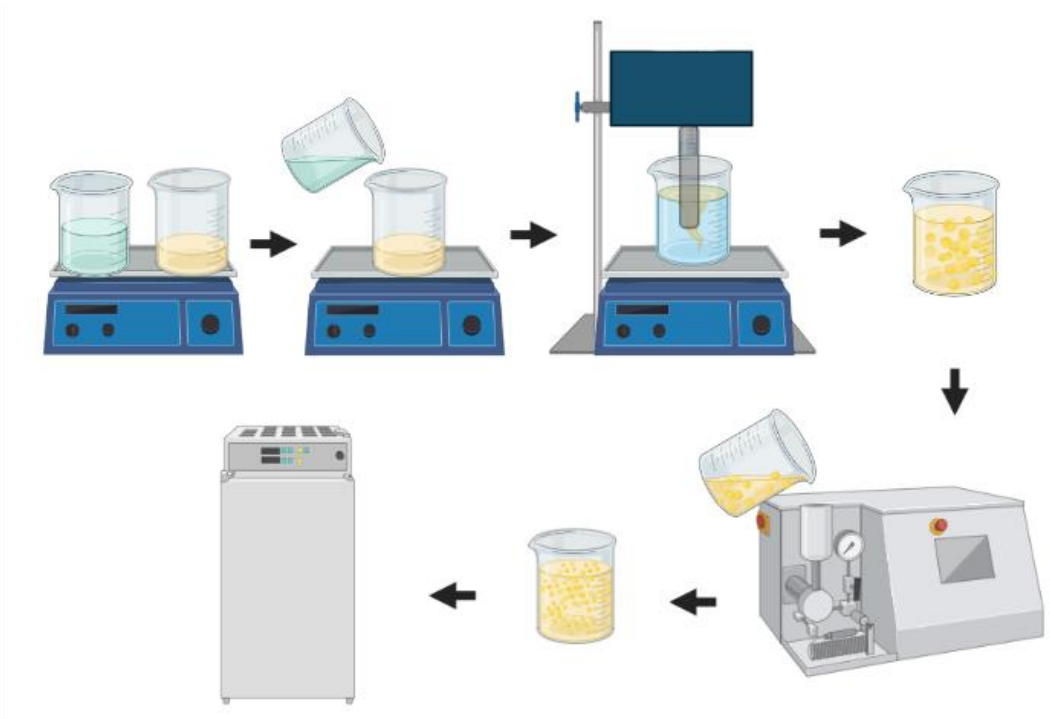

Figura 3: Esquema de obtenção de CLN através da HAP a quente. Fonte: autoral, criado com *Biorender.*

A HAP a quente apresenta muitas vantagens, como a facilidade de transposição de escala, a ausência de solventes orgânicos e o menor tempo de produção comparado a outros métodos de obtenção (PARDEIKE; HOMMOSS; MÜLLER, 2009). O aumento da temperatura promove a redução da viscosidade da fase interna e por isso resulta em menor TP. Porém, o uso de altas temperaturas pode promover a degradação de compostos ativos labéis; a redução da capacidade emulsificante de compostos que possuam baixo ponto de ebulição e com isso aumentar a instabilidade das nanopartículas (TAMJIDI *et al.*, 2013). Portanto, o controle da temperatura deve ser compatível com a estabilidade do composto ativo que está sendo adicionado (JAFARI; HE; BHANDARI, 2007).

Nesse sentido, os CLN podem ser obtidos através da HAP a frio, que considera o uso de temperaturas mais baixas durante o procedimento para obtenção de NL. Neste método, após a incorporação do composto bioativo na mistura lipídica líquida, a mistura é resfriada rapidamente, com nitrogênio líquido por exemplo. Subsequentemente, a mistura

lipídica é moída para formar micropartículas, por um moinho de esferas por exemplo, monitorando-se a temperatura, para que esta não ultrapasse a temperatura de fusão do lipídio com menor PF. As micropartículas são então dispersas em uma solução fria contendo o emulsionante e homogeneizadas para obtenção dos CLN (SHAH *et al.*, 2015; TAMJIDI *et al.*, 2013).

Este método promove a redução da degradação térmica dos componentes bioativos, além de maior incorporação dos compostos e a distribuição homogênea deste na estrutura. O processo de cristalização é controlável e o resfriamento rápido pode levar a formação da estrutura cristalina desejada (TAMJIDI *et al.*, 2013). Porém, quando comparadas a outros métodos como a HAP a quente, as partículas obtidas apresentam maior tamanho e uma ampla distribuição deste (MEHNERT & MADER, 2012) e, portanto, não apresentam a mesma funcionalidade em termos de velocidade de dissolução durante a mastigação e a digestão (WEISS *et al.*, 2008).

2.5.2 Microfluidização

O princípio deste método é similar a HAP, na medida em que envolve alta pressão para promover a passagem da emulsão pelos canais do microfluidizador, para facilitar o rompimento da gota. No entanto a concepção dos canais por onde a emulsão circula é diferente. Enquanto no HAP a emulsão circula por apenas um canal, neste método há uma divisão da emulsão que flui em um canal de duas correntes, passando cada uma por um canal fino e em seguida dirigidas para uma câmara de interação em que forças destrutivas são aplicadas para romper a gota. Assim como na técnica de HAP, o tamanho da gotícula tende a diminuir com o aumento da pressão e do número de ciclos. No entanto, a viscosidade da pré-emulsão deve estar em uma faixa que facilite a passagem pelo equipamento e posterior rompimento das gotas em escala nanométrica (MCCLEMENTS; RAO, 2011).

2.5.3 Ultrassonicação

Homogeneizadores de ultrassom utilizam ondas ultrassônicas de alta intensidade para criar as forças destrutivas intensas necessárias para o rompimento das fases de óleo e água em gotas muito pequenas (LEONG *et al.*, 2009). A energia é fornecida por sondas que contêm cristais de quartzo piezoelétricos que se expandem e se contraem em resposta a uma tensão elétrica alternada. A ponta da sonda é colocada dentro da emulsão a ser homogeneizada, gerando intensas vibrações mecânicas que conduzem ao efeito de cavitação, rompendo a gotícula em escala nanométrica. Para que a homogeneização seja eficiente é necessário garantir que a emulsão passe o tempo suficiente na região onde ocorre o rompimento da gota (sonda). O tamanho da gotícula diminui com o aumento da intensidade

das ondas aplicadas, assim como com o aumento do tempo de contato da emulsão com a sonda (MCCLEMENTS; RAO, 2011).

2.5.4 Emulsificação Espontânea

Neste método, uma emulsão ou uma nanoemulsão é formada espontaneamente quando dois líquidos são misturados. Na prática, este método pode ser realizado de diversas maneiras: variando-se a composição das duas fases; alterando-se as condições ambientais (por exemplo, temperatura, pH e força iônica); e/ou as condições da homogeneização das fases da emulsão (por exemplo, ordem de adição dos componentes, velocidade de agitação, taxa de adição) (MCCLEMENTS; RAO, 2011).

Uma série de mecanismos físico-químicos tem sido propostos para explicar a emulsificação espontânea. O mecanismo que melhor elucida essa emulsificação é a ação do agente emulsificante, que é parcialmente miscível nas duas fases da emulsão (oleosa e aquosa). Quando essas duas fases são colocadas em contato, parte deste agente migra de uma fase para a outra, promovendo um aumento da área da interface óleo/água, uma turbulência interfacial e a formação espontânea das gotas (MCCLEMENTS; RAO, 2011). Portanto, o principal objetivo nesse método, é alterar as condições para que o emulsificante possa promover a formação das gotas em escala nanométrica.

2.5.5 Inversão de Fases

Esse método baseia-se na inversão de fases de uma emulsão, por exemplo, a partir de uma emulsão O/A obter-se uma emulsão água em óleo (A/O) (e vice-versa), através da modificação de alguma condição como a temperatura ou a composição das fases da emulsão (MCCLEMENTS; RAO, 2011). A mudança na temperatura modifica propriedades físico-químicas dos agentes surfactantes não iônicos, como a solubilidade relativa e a geometria molecular, promovendo a inversão das fases (ANTON; BENOIT; SAULNIER, 2008). A inversão de fases pode ocorrer também pela modificação da composição das fases da emulsão, como a adição de sal, por exemplo, que promove a mudança na curva ótima do agente surfactante e assim a inversão das fases (MCCLEMENTS; RAO, 2011).

2.5.6 Difusão, Emulsificação e Evaporação do Solvente

A fase lipídica de uma emulsão pode ser composta por lipídios de maior e menor PF, compostos bioativos lipofílicos ou uma mistura destes. Quando a fase lipídica contém algum material cristalino, há dificuldade na formação da emulsão; para facilitar a dissolução desses materiais lipídicos são utilizados solventes hidro, lipo ou anfifílicos (HORN; RIEGER, 2001). Os lipídios e compostos bioativos são dissolvidos em um solvente orgânico com baixo

PF (cloreto de metileno, por exemplo), e posteriormente são homogeneizados com a fase aquosa, que contêm água e o emulsificante hidrofílico (TAMJIDI *et al.*, 2013). Após a homogeneização as gotículas contêm uma mistura de lipídio e solvente orgânico. O solvente orgânico precisa ser removido para que ocorra a redução do tamanho da gota e obtenha-se assim, as nanopartículas (MCCLEMENTS; RAO, 2011).

A remoção do solvente pode ocorrer quando a solução é colocada em contato com a água, ocorrendo a difusão deste para a fase aquosa ou pela evaporação deste sobre baixa pressão. Em casos em que a difusão não remova totalmente o solvente, pode-se promover a evaporação para remover o solvente remanescente (MCCLEMENTS; RAO, 2011). A remoção do solvente é fundamental para que se obtenha as NL nas concentrações desejadas, e principalmente que estas não contenham resíduos do solvente empregado (TAMJIDI *et al.*, 2013).

A grande vantagem deste método é a minimização da exposição térmica da amostra, preservando a integridade do composto bioativo (TAMJIDI *et al*., 2013); utilizando solventes adequados quanto a miscibilidade em água, PF, enquadrados na categoria *GRAS* (MCCLEMENTS; RAO, 2011). Segundo Tamjidi *et al*. (2013), as NL obtidas apresentam TP entre 30 e 100nm e IP estreito, dependendo da carga lipídica, do tipo de solvente e emulsificante utilizados e de condições do processo.

2.6 Propriedades físico-químicas de CLN

As características das nanopartículas (estrutura, dimensão, composição, entre outras) influenciam as suas propriedades físico-químicas e o seu desempenho funcional, como por exemplo, propriedades óticas, reológicas, estabilidade, destino biológico e taxa de entrega (KHOSA; REDDI; SAHA, 2018; MCCLEMENTS, 2013). A caracterização de CLN, no entanto, é uma tarefa bastanta desafiadora devido as suas dimensões reduzidas e a complexidade do sistema, formado por lipídios, emulsificantes e compostos bioativos (MEHNERT; MÄDER, 2012). As principais propriedades físico-químicas apresentadas pelos CLN são o tamanho e a distribuição de partículas, a carga superficial, a morfologia e as propriedades estruturais, térmicas e de cristalização.

2.6.1 Tamanho de Partícula e Índice de Polidispersidade

O TP e a distribuição do TP, conhecida como IP são as características mais importantes para caracterização das NL, pois regem a estabilidade física, a solubilidade e o desempenho biológico (ANTON; BENOIT; SAULNIER, 2008), bem como a taxa de liberação, a turbideze a estabilidade química destas (TAMJIDI *et al*., 2013). O TP confirma se as dimensões desejadas foram obtidas mediante o uso de formulações e processos

específicos e principalmente, se estas dimensões são mantidas durante armazenamento ou processamento posterior. Esta propriedade pode ser correlacionada com a composição da matriz lipídica utilizada para obtenção das NL; com a sua estabilidade físico-química; e permite ainda, obter informações complementares sobre a morfologia das NL (BUNJES, 2004).

O controle das dimensões das NL é essencial, uma vez que este parâmetro influencia suas propriedades físico-químicas, funcionalidade e potencial de aplicação (MCCLEMENTS; RAO, 2011; TAMJIDI *et al.*, 2013). Segundo Martini e Herrera (2008), a determinação de alterações no TP durante o armazenamento das NL, é considerada como o melhor parâmetro para estimar a estabilidade física destas.

Uma vez que os CLN apresentam dimensões na faixa entre 10 e 1000nm, a técnica mais adequada para analisar o TP é o espalhamento dinâmico de luz (DLS). O mecanismo de medida desta técnica, baseia-se na oscilação da intensidade de luz espalhada pelo movimento das partículas e permite além de avaliar o TP, a homogeneidade destas através da polidispersidade (IP) (LAKSHMI; KUMAR, 2010).

Instrumentos baseados neste princípio (DLS) medem as flutuações aleatórias na intensidade da luz espalhada pelas partículas em suspensão coloidal quando mudam de posição devido ao movimento browniano. A frequência das flutuações de intensidade depende da taxa em que as partículas mudam de posição e, portanto, seu tamanho: as partículas menores se movem mais rapidamente do que as maiores e, portanto, apresentam flutuações de intensidades mais rápidas. A amostra é analisada registrando-se as flutuações de intensidade da onda espalhada em um determinado ângulo de espalhamento e, então, as flutuações são convertidas em distribuição de TP através de um modelo matemático (MCCLEMENTS; MCCLEMENTS, 2016).

O IP indica o quanto as NL estão polidispersas, ou seja, a sua distribuição de tamanho. Esse índice tem um efeito importante sobre a estabilidade física das NL e deve ser o mais baixo possível para que a NL apresente longa estabilidade física. Valores de IP entre 0,1 a 0,25 mostram uma estreita distribuição de tamanho, indicando que as NL apresentam TP similares; enquanto que valores de IP maiores que 0,5 indicam uma distribuição muito ampla e a instabilidade do sistema, podendo ocasionar a aglomeração das NL (LAKSHMI; KUMAR, 2010). Tanto o TP, quanto o IP, podem ser determinados por Espectroscopia de Correlação de Fótons (PCS), através da técnica de DLS, que fornece além desses parâmetros, a medida PZ (SEVERINO; SANTANA; SOUTO, 2012).

2.6.2 Potencial zeta

NL são sistemas heterogêneos e termodinamicamente instáveis e, portanto,

apresentam uma tendência significativa de perder a estabilidade física durante o armazenamento (HUANG *et al.*, 2008). O PZ é uma medida da carga da superfície das partículas, e pode ser considerado um indicativo da estabilidade física do sistema durante o armazenamento, uma vez que determina sua interação com outras espécies carregadas em seu ambiente como moléculas, superfícies ou partículas (MCCLEMENTS, 2007; MOHAMMADI; ASSADPOUR; JAFARI, 2019).

O PZ é definido como o parâmetro característico para a carga das NL; é uma medida do potencial elétrico na superfície hidrodinâmica de corte em torno das partículas coloidais (ROBLES *et al.*, 2008). É uma medida indireta da estabilidade físicas das NL, e influencia a cinética de liberação dos compostos e o destino biológico das NL (TAMJIDI *et al.*, 2013). Esta análise permite também a determinação das interações das NL com os diferentes compostos de inclusão, principalmente durante o período de estocagem (BUNJES, 2004).

Os instrumentos mais utilizados para determinação de PZ em NL, baseiam-se na medida da velocidade e direção em que as partículas se movimentam quando um campo elétrico bem definido é aplicado (MCCLEMENTS, 2007). A amostra diluída é acondicionada em uma célula de medição que contém um par de eletrodos. O campo elétrico é então aplicado fazendo com que as partículas carregadas se movam em direção ao eletrodo com carga oposta a uma velocidade que depende da magnitude de sua carga e da viscosidade do líquido circundante. O instrumento calcula a mobilidade eletroforética a partir de medições da velocidade da partícula e, em seguida, através de um software, converte as informações obtidas em valores de PZ. O movimento das partículas na célula de medição pode ser realizado por várias técnicas, sendo a de *laser light scattering* a mais comum (MCCLEMENTS; MCCLEMENTS, 2016).

No estudo de NL, a determinação do PZ tem sido principalmente empregada para informações sobre a estabilidade de formulações durante a estocagem ou instabilidade das NL quando da interação com eletrólitos, permitindo importantes ajustes de formulação (BUNJES, 2004). O uso de distintos emulsificantes para estabilização de CLN normalmente resulta em PZ distintos, devido à composição destes emulsificantes e a interação específica com as fases lipídica/aquosa. Os CLN estabilizados com emulsificantes iônicos, devem apresentar valores superiores a |30Mv| para serem considerados estáveis. No entanto, quando se utiliza emulsificantes não iônicos para a estabilização de CLN, os valores de PZ são inferiores, uma vez que, nestes casos, a estabilidade é conferida pelo impedimento estérico resultante da estrutura complexa destes emulsificantes (MCCLEMENTS; RAO, 2011).

2.6.3 Morfologia e Ultraestrutura

Além do tamanho, da dispersidade e da composição das partículas, a morfologia

é uma característica importante de sistemas lipídicos nanoestruturados, visto que fornece informações importantes acerca do estado físico e de propriedades como a EI de compostos bioativos. A forma das partículas mostra-se bastante variável e pode influenciar a CC e as propriedades de liberação dos compostos bioativos incorporados aos CLN. As partículas esféricas apresentam menor área superficial e portanto são estabilizadas com quantidades menores de emulsificantes. Além disso apresentam via de difusão mais longa e menor contato com o meio aquoso, proporcionando dessa forma a liberação controlada e lenta dos compostos incorporados. O formato esférico proporciona ainda, o contato mínimo com o líquido circundante, conferindo assim maior estabilidade aos compostos incorporados a estrutura (BUNJES, 2004; SHAH *et al.*, 2015). As NL não esféricas apresentam grande área específica, vias de difusão curtas e uma camada lipídica menos espessa (MEHNERT; MÄDER, 2012).

Por apresentarem menor área específica, as NL esféricas requerem menor quantidade de emulsificante (BUNJES, 2004); enquanto que para a obtenção e estabilização de NL não esféricas, são requeridas maiores quantidades de emulsificante (TAMJIDI *et al*., 2013). Entretanto, NL anisométricas podem apresentar vantagens quando os compostos de inclusão incorporam-se à camada de emulsificantes (BUNJES, 2004).

A morfologia e organização espacial das nanopartículas desempenha um papel importante na determinação de suas propriedades funcionais e, portanto, é fundamental o uso de métodos adequados para determinar esses parâmetros (MCCLEMENTS; MCCLEMENTS, 2016). Vários métodos de microscopia estão disponíveis para caracterizar a morfologia ou a organização das nanopartículas, sendo as mais comuns a microscopia óptica, eletrônica ou de varredura (MURPHY; DAVIDSON, 2012).

Os métodos de microscopia apresentam vantagens e desvantagens para aplicações específicas. A microscopia óptica é o método mais simples e barato, porém é indicada apenas para fornecer informações sobre a localização, movimento ou agregação de nanopartículas, ao invés da estrutura de nanopartículas individuais. Devido às limitações mecânicas dos componentes do microscópio e o movimento browniano das nanopartículas (MCCLEMENTS; MCCLEMENTS, 2016), a microscopia de luz ótica não consegue examinar com exatidão partículas menores que 500nm (KLANG *et al.*, 2012). Assim, a microscopia óptica de luz polarizada pode ser utilizada para distinguir nanopartículas opticamente anisotrópicas de um fundo isotrópico (MCCLEMENTS; MCCLEMENTS, 2016).

Para determinação da morfologia e ultraestrutura de NL são necessárias técnicas avançadas de microscopia. Assim, técnicas como microscopia eletrônica de varredura (MEV), microscopia de transmissão eletrônica (MTE) e microscopia de força atômica (MFA) são frequentemente utilizadas para fornecer informações com respeito ao TP, distribuição do tamanho, morfologia, topografia da superfície e estrutura interna de NL(TAMJIDI *et al.*, 2013).

Dentre as técnicas microscópicas, a microscopia eletrônica é a mais adequada para caracterizar a microestrutura e organização das nanopartículas, devido principalmente à sua capacidade de detectar elementos estruturais através de feixes de elétrons (resolução aproximadamente 1nm), que são muito pequenos para serem visualizados através de ondas de luz em microscópios ópticos (MCCLEMENTS; MCCLEMENTS, 2016).

2.6.4 Cristalinidade e Polimorfismo

A cristalização de gorduras é um parâmetro crítico associado à estrutura e propriedades de grande parte dos alimentos. A estabilidade de muitos produtos processados é consideravelmente influenciada por mudanças no estado físico das gorduras e alterações nos processos de cristalização (TORO-VAZQUEZ *et al.*, 2005). O aspecto mais importante das propriedades físicas de óleos e gorduras está relacionado às mudanças de fase sólido-líquido e líquido-sólido; fusão e cristalização, respectivamente (TAN; CHE MAN, 2002).

O processo de cristalização refere-se à ordenação espontânea de um sistema lipídico, caracterizado por restrição total ou parcial de movimento ocasionada a partir de interações químicas ou físicas entre as moléculas triacilglicerólicas. Diferenças nas formas cristalinas resultam de diferentes empacotamentos moleculares. Um cristal, portanto, consiste de moléculas arranjadas em um padrão fixo conhecido como reticulado. Seu alto grau de complexidade molecular permite que um mesmo conjunto de TAG empacote-se em diversas estruturas diferentes e relativamente estáveis (SATO, 2001).

O processo de cristalização inclui a nucleação e crescimento dos cristais (BOISTELLE, 1988). Um núcleo é o menor cristal que pode existir em uma solução a determinada temperatura e concentração e sua formação requer a organização das moléculas em um reticulado cristalino de tamanho crítico, a partir da superação de uma barreira energética (LAWLER; DIMICK, 2008; METIN; HARTEL, 2005). Quandoos núcleos formados atingem as dimensões favoráveis, estes elementos tornam-se cristalitos (FOUBERT; VAN DE WALLE; DEWETTINCK, 2007). O crescimento de cristais envolve a difusão dos TAG da solução através de uma camada estagnada junto à interface e a incorporação dos mesmos dentro da rede cristalina (cristalitos) pré-existente. Estes mecanismos dependem do grau de super-resfriamento, da taxa de difusão molecular para a superfície do cristal e do tempo necessário para as moléculas dos TAG se encaixarem na rede cristalina em crescimento (MARANGONI, 2005).

Em gorduras, os cristais são sólidos com átomos arranjados em um padrão tridimensional periódico. Uma célula é a unidade de repetição que compõe a estrutura integral de um determinado cristal. Uma sub-célula, por sua vez, é a menor estrutura periódica existente na unidade real da célula, sendo definida como o modo de empacotamento transversal das cadeias alifáticas nos TAG . As formas polimórficas de

uma gordura são identificadas com base em sua estrutura de sub-célula (BOISTELLE, 1988).

Nos lipídios predominam três tipos específicos de sub-células, referentes aos polimorfos α, β' e β, segundo a atual nomenclatura polimórfica. A forma α é metaestável, com empacotamento de cadeia hexagonal; a forma β' possui estabilidade intermediária e empacotamento perpendicular ortorrômbico, enquanto a forma β possui maior estabilidade e empacotamento paralelo triclínico. A temperatura de fusão aumenta com o aumento da estabilidade (α→β'→ β), como resultado das diferenças de densidade do empacotamento molecular (MARTINI; AWAD; MARANGONI, 2006).

TAG cristalizam-se inicialmente nas formas α e β', embora a forma β seja a mais estável. Este fenômeno relaciona-se ao fato de que a forma β possui maior energia livre de ativação para nucleação. A transformação polimórfica é um processo irreversível da forma menos estável para a mais estável (transformação de fase monotrópica), dependendo da temperatura e tempo envolvidos. A temperatura constante, as formas α e β' podem transformar-se, como função do tempo, na forma β através dos mecanismos líquido-sólido ou sólido-sólido (HIMAWAN; STAROV; STAPLEY, 2006). A velocidade de transformação é menor quanto maior o grau de heterogeneidade dos TAG (SATO, 2001).

As características polimórficas dos TAG tornam complexo o estudo das propriedades térmicas e estruturais das gorduras. O comportamento térmico reflete, portanto, as propriedades gerais de funcionalidade e aplicabilidade de lipídios, e mostra-se dependente dos perfis de TAG nos óleos e gorduras comestíveis (RIBEIRO *et al.*, 2009).

Para uma aplicação industrial das NL é necessário controlar o polimorfismo, pois a estrutura polimórfica tem influência direta na eficiência de encapsulação e na expulsão do ativo durante o processo de estocagem (SOUTO; MEHNERT; MÜLLER, 2006). A incorporação do composto ativo na estrutura CLN depende diretamente da velocidade de resfriamento do lipídio e da sua composição, pois estes fatores ditam a organização tridimensional que a matriz lipídica adquire durante a solidificação. Quando a velocidade de resfriamento é lenta, as cadeias hidrocarbonadas dos lipídios podem rearranjar-se numa forma mais ordenada e estável; já quando a velocidade de resfriamento é elevada, a solidificação da matriz ocorre também rapidamente, rearranjando-se numa forma polimórfica mais instável (FREITAS; MÜLLER, 1999).

Em relação à composição lipídica, as matrizes com um conteúdo elevado de DAG (>50%) cristalizam-se na forma polimórfica metaestável β' que se caracteriza por alguma imperfeição na sua estrutura tridimensional (WINDBERGS; STRACHAN; KLEINEBUDDE, 2009). As matrizes lipídicas formadas por TAG esterificados com um único tipo de AG, cristalizam-se, normalmente, no polimorfo mais estável β, que se caracteriza por um grau de organização elevado (JENNING; GOHLA, 2000).

A estabilidade termodinâmica das NL e o seu grau de empacotamento lipídico aumentam, enquanto a incorporação do princípio ativo diminui na seguinte ordem: forma polimórfica α, forma polimórfica β', forma polimórfica β. Em regra, as moléculas lipídicas apresentam maior mobilidade quando se encontram em configurações termodinamicamente mais instáveis, como, por exemplo, a forma polimórfica α. Por esta razão, estas configurações apresentam um grau de empacotamento lipídico menor, sendo maior a sua capacidade para incorporar os princípios ativos (FREITAS; MÜLLER, 1999). Portanto, para a preparação de NL com elevada CC, em particular quando se pretende incorporar ativos hidrofílicos, o lipídio deverá cristalizar, preferencialmente, em formas polimórficas mais instáveis (BUMMER, 2004; MULLER; KECK, 2004).

Durante a estocagem das NL, o rearranjo da rede cristalina pode ocorrer para o estado de maior estabilidade (α→ β'→β) promovendo a instabilidade da dispersão coloidal (HELGASON *et al.*, 2009). Essas alterações polimórficas e o comportamento de fusão da fase dispersa das NL governam a forma dos cristais, a morfologia das partículas, a taxa de liberação dos compostos bioativos, CC e índice de cristalinidade de NL, e também indicam a máxima temperatura na qual as NL permanecem sólidas (TAMJIDI *et al.*, 2013).

A ocorrência de transformações polimórficas é acompanhada por alterações na forma das partículas, designadamente das formas esféricas (α) para as formas achatadas (β) (BUNJES; KOCH; WESTESEN, 2003). Além disso, segundo Tamjidi *et al*. (2013) como o estado físico do composto bioativo, nas fases aquosa e lipídica regula a sua biodisponibilidade e a eficácia da liberação controlada, as transições polimórficas são geralmente associadas à expulsão de uma fração do componente incorporado.

O problema associado às modificações lipídicas não é sempre resolvido com a manipulação das formas α, β e β'. A complexidade do sistema aumenta devido às subespécies polimórficas e às interações do lipídio com os agentes tensoativos. Para preparar NL com CC elevada utilizando formas polimórficas instáveis, é necessário o desenvolvimento de estratégias que previnam a transformação das formas instáveis para as formas mais estáveis, durante o armazenamento (BUNJES; UNRUH, 2007). A eficácia dos sistemas lipídicos nanoestruturados, é, portanto, determinada pelas modificações da rede cristalina característica de um conjunto específico de TAG (HELGASON *et al.*, 2009).

O grau de cristalinidade de lipídios e as transições polimórficas podem ser avaliados através da difração de Raios-X (DRX). A DRX é uma das ferramentas mais adequadas para medir o arranjo espacial das moléculas dentro de um material e pode, portanto, fornecer informações valiosas sobre seu estado físico (líquido, cristalino ou amorfo) e forma polimórfica (HARTEL, 2013). As formas polimórficas exibem picos característicos, sendo que a forma α exibe um único pico em 4,15 Å, a forma β' é caracterizada por duas linhas de difração uma em 3,8 Å e outra em 4,2 Å e a forma β está relacionada a uma linha

de intensidade relativamente alta em 4,6 Å e picos de baixa intensidade em 3,6 e 3,8 Å (MARANGONI; ROUSSEAU, 2002).

2.6.5 Propriedades térmicas

A análise de DSC é uma das ferramentas mais comumente utilizadas para fornecer informações sobre o estado físico das nanopartículas. Baseia-se na medida das mudanças de entalpia (calor liberado ou absorvido) quando uma amostra é submetida a uma varredura de temperatura controlada (QIAN *et al.*, 2012; SHUKAT; BOURGAUX; RELKIN, 2012). A análise de DSC é útil para entender o comportamento de misturas entre lipídios de menor e maior PF, fornecendo informações relevantes sobre o comportamento térmico de sistemas lipídicos (HAN *et al.*, 2008).

Normalmente os CLN apresentam comportamento térmico distinto das matrizes lipídicas quando avaliadas em macroescala, portanto é importante considerar a avaliação das propriedades térmicas das matrizes lipídicas utilizadas para obtenção de CLN (MEHNERT; MÄDER, 2012). A escolha do sistema lipídico para compor os CLN para incorporação de compostos bioativos deve considerar o comportamento térmico dos sistemas lipídicos à temperatura corporal (37°C).

Na caracterização de CLN, o DSC fornece informações relacionadas ao estado físico e grau de cristalinidade, através do comportamento térmico na fusão. Essa técnica permite avaliar os principais parâmetros dos processos utilizados para a obtenção de CLN, uma vez que a matriz lipídica é aquecida e posteriormente resfriada para a formação de CLN (SOUZA *et al.*, 2012).

Embora os instrumentos de DSC sejam capazes de medir com muita precisão os eventos endotérmicos que ocorrem em uma matriz lipídica, não possibilitam informar com precisão a causa desses eventos térmicos. Para tal, é preciso considerar técnicas instrumentais complementares como a DRX, que fornece informações precisas sobre o hábito polimórfico e a ocorrência de transições polimórficas (KHOSA; REDDI; SAHA, 2018).

2.7 Incorporação de compostos bioativos em CLN

Os bioativos em alimentos são divididos em compostos bioativos e células vivas bioativas (probióticos). Os compostos bioativos lipofílicos mais importantes em alimentos e que precisam ser carreados são os carotenoides, tocoferóis, fitoesteróis e vitaminas lipossolúveis (MCCLEMENTS; LI, 2010). A adição direta de compostos bioativos em produtos de base aquosa e administração oral é dificultada, devido a sua baixa solubilidade em água resultando em uma reduzida absorção oral e baixa biodisponibilidade nos tecidos-alvo (MOHAMMADI; ASSADPOUR; JAFARI, 2019).

Normalmente produtos alimentícios com quantidades consideráveis de lipídios digestíveis são frequentemente utilizados para encapsular e entregar compostos bioativos lipossolúveis. Após a digestão esses produtos formam micelas mistas que podem solubilizar e transportar os compostos até o local de absorção no corpo humano (TAN; MCCLEMENTS, 2021).

A baixa biodisponibilidade de compostos bioativos que apresentam efeito benéfico à saúde pode ser superada através da incorporação destes compostos em sistemas de entrega como os CLN (KHARE; VASISHT, 2014; WEISS *et al.*, 2009). A utilização de nanoestruturas mostra-se uma alternativa promissora e diferenciada para o carreamento e proteção de carotenoides em sistemas alimentícios (MOZAFARI *et al.*, 2006; WEISS; TAKHISTOV; MCCLEMENTS, 2006). Os CLN podem ser utilizados como carreadores deste composto lipofílico em produtos alimentares a base de água, protegendo-o contra a degradação física e química, e aumentando assim sua biodisponibilidade (HENTSCHEL *et al.*, 2008; LIU; WU, 2010).

Diversos estudos vêm sendo direcionados ao desenvolvimento e aplicação de sistemas lipídicos nanoestruturados contendo carotenoides como componentes bioativos. Hentschel *et al*. (2008) aplicaram CLN contendo BC em bebidas funcionais. Helgason *et al*. (2009) avaliaram o impacto das propriedades dos emulsificantes sobre a estabilidade de BC incorporado às estruturas NLS e CLN. Liu e Wu (2010) estudaram o desenvolvimento de CLN compostas por tripalmitina e óleo de milho, para inclusão de luteína. Mitri *et al*. (2011) obtiveram NLS e CLN para incorporação de luteína em formulação contendo 9% de lipídios. Com objetivo de preparação de CLN para aplicação em bebidas funcionais, Zhang *et al*. (2013) utilizaram a gordura do leite anidra para incorporação de carotenoides. Hejri *et al*. (2013) obtiveram CLN com incorporação de BC a partir de ácido palmítico e óleo de milho. Tamjidi *et al*. (2014) desenvolveram CLN com incorporação de astaxantina utilizando ácido oleico e behenato de glicerila como matrizes lipídicas. Okonogi e Riangjanapatee (2015) utilizaram cera de laranja e óleo do farelo de arroz para a obtenção de CLN com incorporação de licopeno. Oliveira *et al*. (2016) avaliaram o efeito do aumento da proporção de OGAO em detrimento a triesterarina sobre a incorporação de BC em nanoestruturas (CLN e NLS).Pan, Tikekar e Nitin (2016) desenvolveram CLN a partir trioctanoato de glicerila e eicosano, para incorporação de BC. Zardini *et al*. (2018) estudaram a incorporação de licopeno em CLN obtidos utilizando monoesterato e diestearato de glicerol e TCM como matrizes lipídicas. Pezeshki *et al*. (2019) desenvolveram CLN com incorporação de BC, a partir de Precirol ATO5 e octanoato de octila. Rohmah *et al*. (2020) utilizando estearina e oleína de palma, desenvolveram CLN para incorporação de BC. Yang *et al*. (2020) obtiveram CLN com incorporação de BC a partir de GMS e TCM.

2.7.1 β-caroteno

O BC é um pigmento natural que pertence ao grupo dos carotenoides, um dos grupos mais importante de pigmentos naturais, devido à sua ampla distribuição, diversidade estrutural e numerosas funções (CHE MAN; TAN, 2003). Compreendem um grupo diverso de compostos lipofílicos que estão presentes em presentes em plantas, microorganismos fotossintetizantes e alguns fungos que participam dos processos de captação de luz necessários à fotossíntese, conferem fotoproteção e possuem atividade antioxidante (KOPEC; FAILLA, 2018).

As bandas de absorção na região dos 400 a 500nm conferem aos carotenoides sua coloração amarelada característica (TAIZ; ZEIGER, 2017), entre o amarelo e o vermelho. Além de ser utilizado como um corante natural pela indústria alimentar, o BC é um substância bioativa, pois apresenta atividade antioxidante e atividade pró-vitamínica A, trazendo assim efeitos benéficos à saúde (KAMAL-ELDIN, 2005) como diminuição do risco de doenças cardiovasculares e prevenção de alguns tipos de câncer (CHE MAN; TAN, 2003).

Após a absorção, nas células intestinais o BC (pró-vitamina A) é convertido a retinol (vitamina A), que é a forma biologicamente ativa (TAN; MCCLEMENTS, 2021). Estruturalmente, o retinol é composto por um anel beta-ionona ligada a uma cadeia isopropenóide, que também é referida como grupo retinil, enquanto o BC consiste em dois grupos retinil conectados por meio de suas cadeias isopropenóides. A estrutura do retinil apresenta uma região densa de elétrons que podem reduzir o estresse oxidativo, ao reagirem com radicais livres (SAUVANT *et al.*, 2012). Essa alta reatividade química, torna a vitamina A suscetível a degradação oxidativa e/ou isomerização quando exposta a luz, calor, metais e oxidantes. Por esta razão, são necessárias estratégias para protegê-la da degradação nos alimentos, durante sua produção, armazenamento e consumo (TAN; MCCLEMENTS, 2021).

O aproveitamento de carotenoides na íntegra pode ser prejudicado pela oxidação que por sua vez, pode ser acelerada por fatores como luz, temperatura, pH e presença de formas reativas de oxigênio. Esses diferentes fatores podem causar perda de bioatividade e qualidade (perda de cor e rancidez) em produtos alimentares fortificados com esses compostos (DAVIDOV-PARDO; GUMUS; MCCLEMENTS, 2016). Devido à sua capacidade antioxidante, carotenoides são compostos suscetíveis à oxidação, o que os torna relativamente instáveis quando utilizados como aditivos em sistemas alimentícios em resultado da susceptibilidade à luz, oxigênio e aos processos auto oxidativos. São adicionalmente caracterizados por baixa solubilidade em água, o que afeta sua biodisponibilidade. Consequentemente, a dispersão de carotenoides em alimentos

processados pode resultar em rápida degradação. Um desafio adicional para incorporação de carotenoides em alimentos decorre de seu alto PF, associado a seu estado cristalino a temperatura corporal e de estocagem (QIAN *et al.*, 2012; RIBEIRO; AX; SCHUBERT, 2003). Portanto estratégias inovadoras são necessárias para fortalecer alimentos e bebidas de base aquosa (SAUVANT *et al.*, 2012).

Três etapas são necessárias para a absorção de carotenoides no corpo humano: (i) a liberação da matriz alimentar, (ii) a incorporação na fase lipídica (durante o processamento de alimentos ou durante a digestão) e (iii) a digestão completa da fase lipídica em que os carotenoides estão solubilizados. De forma geral, quanto mais rápida e completa for a digestibilidade lipídica, maior será a bioacessibilidade dos carotenoides (SALVIA-TRUJILLO *et al*., 2017b). A absorção do BC incorporado a sistemas de entrega a base de lipídios apresenta algumas diferenças quando comparada a absorção do BC proveniente de fontes vegetais. Essa distinção ocorre principalmente devido a diferenças no estado do BC entre sistemas de entrega a base de lipídios e plantas. Geralmente, o BC na maioria das plantas está presente na forma de cristais dentro das células vegetais, enquanto o BC incorporado aos sistemas de entrega à base de lipídios é solubilizado no núcleo lipofílico. A incorporação e solubilização do BC em sistemas de entrega a base de lipídios protege o composto da ação enzimática e iônica, e de alteração do pH no TGI (LIN *et al.*, 2018).

2.8 Métodos para avaliação da EI e CC

Um sistema de entrega baseado em nanopartículas deve apresentar uma série de características para ser considerado adequado para a incorporação de compostos bioativos. Dentre estas características, destacam-se elevada CC e EI. Definida como a capacidade que o sistema de entrega apresenta para acomodar os compostos bioativos em sua estrutura, a CC normalmente é calculada levando em consideração a quantidade de composto bioativo incorporado em relação à quantidade de material lipídico utilizado (MOHAMMADI; ASSADPOUR; JAFARI, 2019). A CC indica a capacidade que a matriz lipídica utilizada na formulação possui para carregar o composto ativo desejado até o sítio de adsorção (NGUYEN *et al.*, 2012).

Este parâmetro mostra-se predominantemente influenciado pelo hábito polimórfico preferencial do sistema lipídico utilizado, pelas propriedades dos ingredientes utilizados para a obtenção do carreador, como natureza química, peso molecular e polaridade; pelas propriedades dos compostos bioativos incorporados às estruturas como hidrofobicidade ou hidrofilicidade, polaridade, nível de sensibilidade ao pH, temperatura, luz e oxigênio; pela solubilidade do composto encapsulado na matriz lipídica no estado líquido; pelas condições utilizadas para a obtenção de nanopartículas e pelas interações do sistema

de entrega com o alimento em que foi adicionado (MCCLEMENTS; MCCLEMENTS, 2016; MÜLLER; MÄDER; GOHLA, 2000; TAMJIDI *et al.*, 2013). A CC pode variar de 0 (baixa) a 100% (alta), sendo que a obtenção de CLN com alto valor de CC apresenta vantagens em termos de redução de custos e impactos em alimentos, necessitando-se assim uma menor quantidade de NL para a entrega do composto (TAMJIDI *et al*., 2013).

A estabilidade química de compostos bioativos incorporados aos CLN é determinada através da EI durante o armazenamento (MOHAMMADI; ASSADPOUR; JAFARI, 2019). Definida como a porcentagem de ingrediente ativo adicionado a um sistema que é realmente incorporado nas nanopartículas transportadoras, ao invés de no fluido circundante (MCCLEMENTS; MCCLEMENTS, 2016; SHARMA *et al.*, 2011), a EI é um dos principais fatores para avaliar a capacidade dos sistemas de entrega para retenção de compostos bioativos em sua estrutura (BABAZADEH; GHANBARZADEH; HAMISHEHKAR, 2017). A EI indica, ainda, o quanto deste composto permanece incorporado às estruturas CLN durante e após o armazenamento (SHARMA *et al.*, 2011).

A EI de CLN depende dos componentes de formulação e método de obtenção utilizado. Os componentes de formulação influenciam a solubilidade do composto na fase lipídica, a cristalinidade das NL, a viscosidade da fase contínua e assim, o coeficiente de difusão do composto; influenciando assim as propriedades de liberação do composto (TAMJIDI *et al*., 2013).

A quantidade de composto ativo dentro e fora de nanopartículas em um sistema de entrega só pode ser verificado após as nanopartículas serem separadas do ambiente circundante. Numerosas abordagens estão disponíveis para isolar nanopartículas da matriz circundante, diálise, filtração, separação gravitacional, centrifugação, entre outras. A concentração do composto bioativo presente nas nanopartículas pode ser medida utilizando ferramentas analíticas apropriadas, como cromatografia, eletroforese ou espectroscopia (MCCLEMENTS; MCCLEMENTS, 2016). A Tabela 1 apresenta as abordagens consideradas em diferentes estudos que consideraram a extração e quantificação do BC e outros carotenoides incorporados a estruturas CLN, para a determinação da EI, da CC e em alguns casos, da degradação do composto bioativo.

A maior parte dos estudos considera a extração e quantificação do BC incorporado às estruturas CLN através do uso de solventes orgânicos com posterior leitura da absorbância em espectrofotômetro, conforme verificado na Tabela 1. Alguns estudos consideram métodos que realizam a separação dos CLN do ambiente circundante através da filtração ou pela ação de uma força centrífuga. Alguns autores, no entanto, relataram dificuldades na separação do BC incorporado às estruturas CLN do BC livre. Oliveira *et al*. (2016) por exemplo, relataram dificuldades em separar o composto incorporado às estruturas CLN e moléculas de BC livre, uma vez que as nanopartículas precipitaram juntamente com os cristais de BC. Devido a isto,

os autores consideraram a degradação da cor das dispersões contendo CLN, como uma medida indireta do BC livre, considerando que as partículas carregadas com o composto não alteraram a cor das dispersões.

A escolha do método adequado para a extração e quantificação de carotenoides deve considerar, portanto, o protocolo que permita a extração mais fidedigna possível. Nesse sentido, a realização de estudos prévios considerando metodologias distintas pode permitir a otimização da separação tanto de CLN do ambiente circundante, quanto do BC incorporado e do BC livre na dispersão.

Tabela 1: CLN com incorporação de carotenoides obtidos a partir de diferentes matrizes lipídicas, emulsificantes e métodos de obtenção.

Composto Bioativo	Matrizes lipídicas	Emulsificantes	Método de Obtenção	TP e PZ	Métodos de extração e quantificação de BC	EI, CC ou degradação do BC	Referência
BC	Óleo de girassol Monoestearato de propilenoglicol (PGMS)	Tween 80	HAP	TP ~ 300nm PZ não reportado	A extração de BC foi realizada com n-hexano. Um banho ultrassônico foi usado para acelerar a extração. A concentração total foi medida em espectrofotômetro a 450 nm.	A degradação do BC foi inferior em CLN com adição de tocoferol.	(HENTSCHEL *et al.*, 2008)
Luteína	Precirol ATO5 Óleo de milho	Precirol e Myverol	Ultrassom	TP entre 139 e 234 nm PZ ~ -36mV	250 µl da dispersão aquosa de CLN foi misturada com 750 µL de hexano por 30 min em um tubo de microcentrífuga através de um Disruptor-Vertex.	EI ~ 85%	(LIU; WU, 2010)
BC	Ácido palmítico e óleo de milho	Tween 20	Difusão do solvente	TP entre 8 e 15 nm PZ não reportado	Uma certa quantidade da dispersão contendo os CLN foi dissolvido em acetona (1:1, v/v) e submetida a leitura da absorbância a 459 nm realizada em espectrofotômetro.	A formulação otimizada apresentou baixa degradação de BC (0–3%)	(HEJRI *et al.*, 2013)
Astaxantina	Ácido oleico e behenato de glicerila	Tween 80 Lecitina	Emulsificação por fusão e ultrassom	TP entre 86,8 e 138,3 nm PZ entre -21,9 e – 34,6 mV	0,5 mL da dispersão contendo os CLN com incorporação de astaxantina foi misturada com 1 mL de metanol em um tubo de vidro de 5 mL. Em seguida, 2 mL de diclorometano foram adicionados e o tubo foi agitado em vórtex por 40 s. Após 5 min de descanso, a mistura se separou em duas fases distintas, e então, a fase orgânica inferior colorida foi coletada por uma pipeta, diluída com diclorometano e, em seguida, o conteúdo de astaxantina foi determinado utilizando espectrômetro a 484 nm.	A estabilidade máxima da astaxantina (degradação próxima a 20% após 25 dias) foi observada na formulação otimizada.	(TAMJIDI *et al.*, 2014)
Licopeno	Cera de laranja e óleo do farelo de arroz	Eumulgin®SG	HAP	TP entre 150 e 160nm PZ ~ -74mV	Um volume de 10 mL da dispersão contendo os CLN foi diluída com 40 mL de água bidestilada. As amostras foram centrifugadas a 15.000 rpm por 30 min e a quantidade de licopeno no sobrenadante foi determinada utilizando espectrofotômetro a 475 nm.	EI ~ 100%	(OKONOGI; RIANGJANAPATEE, 2015)
BC	Tristearina e Óleo de girassol alto oleico	Tween 80	Deslocamento do solvente	TP ~500nm PZ não reportado	MI: 1mL da dispersão contendo os CLN foi misturado a 4 mL de etanol absoluto (4,0 mL) e aquecida a 80 ° C durante 30 min. Em seguida, 3mL de hexano (3,0 mL) foi adicionado. Após a separação de fases, a fase de hexano contendo o BC extraído foi removida e diluída novamente com hexano até um volume conhecido. O conteúdo de BC foi determinado a partir da absorbância a 450 nm em espectrofotômetro. MII: A degradação do β-caroteno livre foi monitorada por colorimetria.	MI: Os autores não foram capazes de determinar separadamente as moléculas de BC incorporadas nos CLN e livres no meio. MII: A degradação do BC diminuiu com o aumento de OGAO.	(OLIVEIRA *et al.*, 2016)

BC	Trioctanoato de glicerila e eicosano	Lecitina de alto ponto de fusão (Phospholipon® 80 H)	Homogeneização de alto cisalhamento e ultrassom	TP entre 200 e 350 nm PZ não reportado	Os CLN foram passados por um filtro de fibra oca com um tamanho de poro de 0,2 µm. A formulação concentrada (200 µL) foi misturada com 1 mL de THF e a mistura foi centrifugada a 14000 g por 10 min. O sobrenadante (1 mL) foi colocado em uma cubeta e a absorbância foi medida a 450 nm em espectrofotômetro.	CC entre 30 e 70%	(PAN; TIKEKAR; NITIN, 2016)
Astaxantina	Precirol® ATO5 e óleo de girassol	Tween 80 e Poloxamer 407	Homogeneização a quente	TP entre 57 e 60nm PZ entre -23,7 e -25,5 mV	1mL da suspensão contendo os CLN foi dissolvido em 5 mL de uma solução etanol/diclorometano (60/40 v/v %). As amostras foram centrifugadas (10.000 rpm por 5 min) e as concentrações de astaxantina foram determinadas em espectrofotômetro	EI ~ 90%	RODRIGUEZ-RUIZ *et al.*, 2018)
Licopeno	Monoesterato e diestearato de glicerol e TCM	Tween 80 e Lecitina	Homogeneização de alto cisalhamento e ultrassom	TP entre 74,93 e 183,40 nm PZ entre -5,78 e -15,87mV	0,3 ml da suspensão contendo os CLN foi misturada e agitada com 10 ml de hexano, e então centrifugada por 3 min a 2000 rpm. A fase superior contendo o licopeno livre em hexano foi separada e a quantidade do composto determinada por espectrofotometria a 472 nm.	CC entre 4,54 e 5,52% EI entre 64,79 e 78,89%	(ZARDINI *et al.*, 2018)
BC	Óleo de milho e ácido palmítico	Tween 80	Difusão de solvente	TP entre 111 e 218nm PZ não reportado	A dispersão de CLN foi dissolvida em acetona (1:1 v/v) e a absorbância foi medida a 455 nm em espectrofotômetro.	Degradação do BC entre 2.12 e 4.51% na formulação otimizada	(HEJRI *et al.*, 2019)
BC	Precirol ATO5 e octanoato de octila	Poloxamer 407	Homogeneização de alto cisalhamento	TP entre 88 e 108nm PZ não reportado	1mL da formulação foi adicionado a 2 mL de clorofórmio e a mistura foi agitada vigorosamente por 10 min. A absorbância da fase orgânica contendo BC foi determinada a 25 ° C a 453 nm através de espectrofotômetro.	EI: 97,7% na formulação otimizada	(PEZESHKI *et al.*, 2019)
BC	Estearina e oleína de palma	Tween 80	Sonicação	TP: 166 nm PZ: -26,9 mV	2 mL dos CLN contendo BC foram centrifugados a 14.500g por 30 min a 25 C. A fase aquosa foi separada da fase lipídica, e a quantidade de BC foi determinada através um espectrofotômetro em um comprimento de onda de 454 nm.	EI: 91,2% na formulação otimizada	(ROHMAH *et al.*, 2020)
BC	Monoestearato de glicerol (GMS) e TCM	Tween 80	HAP	TP entre 120 e 300 nm PZ não reportado	Uma mistura de 100 µL da dispersão contendo os CLN e 3 mL de hexano foram agitados em vórtex por 1 min e centrifugados a 2500 × g por 2 min. A fase orgânica superior foi coletada, e repetiu-se a extração por mais duas vezes. A fase orgânica foi filtrada usando uma membrana de 0,22 µm e submetida a análise de HPLC.	EI: 95.64% na formulação otimizada	(YANG *et al.*, 2020)
BC	Ácido esteárico e esqualeno	Fosfatidilcolina de soja hidrogenada	Ultrassonicação	TP entre 222,8 e 812 nm PZ ~ -43mV	Amostras de CLN foram suspensas em etanol e levadas ao banho de ultra-som por 5 min, filtradas através de membranas de celulose acetato (0,45 µm). O conteúdo de BC foi determinado em espectrofotômetro a 448 nm.	CC ~ 0,23 EI ~ 24%	(MARETTI *et al.*, 2021)

2.9 Digestibilidade de nanoestruturas lipídicas

A digestão humana é um processo complexo em que dois processos principais ocorrem simultaneamente: transformações mecânicas que reduzem o tamanho das partículas de alimentos, e transformações enzimáticas em que macromoléculas são hidrolisadas em constituintes menores que são absorvidos pela corrente sanguínea (GUERRA *et al.*, 2012). A maior função do TGI humano é digerir, através de um processo de dissolução e decomposição, alimentos em formas moleculares que possam ser absorvidas, ou seja, que sejam capazes de atravessar o epitélio intestinal (MARTINS *et al.*, 2015).

Assim sendo, antes da liberação do composto bioativo, as nanoestruturas passam por uma série de processos físico-químicos e fisiológicos complexos à medida que passam pelas diferentes regiões do TGI. Dentre esses processos estão (i) as mudanças consecutivas no pH do meio, o que pode alterar a carga elétrica das nanoestruturas e consequentemente, sua composição, estrutura e interações; (ii) variações no tipo e na concentração de íons, que podem impactar as interações eletrostáticas na nanoestrutura por meio de triagem eletrostática ou efeitos de ligação; (iii) presença de componentes tensoativos (fosfolipídios e sais biliares, por exemplo), que podem levar à mudanças na composição interfacial das nanoestruturas; (iv) presença de enzimas capazes de digerir os componentes da nanoestruturas, como lipídios (lipases) e fosfolipídios (fosfolipases); (v) temperatura, que pode causar mudanças no estado físico, conformação molecular ou interações de componentes específicos, impactando a digestibilidade de nanoestruturas; (vi) perfil de fluxo/força que, além de misturar os diversos componentes, pode levar ao rompimento da estrutura do sistema de entrega (PINHEIRO *et al.*, 2017)**.**

Em alimentos fortificados, os compostos bioativos lipossolúveis são normalmente dissolvidos em uma matriz lipídica, seja incorporados em partículas (micro ou nano) ou na forma livre; portanto o destino destes compostos no TGI está altamente correlacionado com o processo de digestão lipídica (TAN; MCCLEMENTS, 2021). A compreensão da digestibilidade lipídica é fundamental para a determinação da biodisponibilidade de compostos bioativos incorporados às estruturas CLN, pois normalmente, deve-se ter um conteúdo lipídico suficiente para a formação de micelas mistas em número suficiente para solubilizar os compostos. Além disso, também é importante que haja uma digestão completa dos lipídios, caso contrário, os compostos ficarão presos na fase oleosa não digerida, reduzindo assim a biodisponibilidade (SALVIA-TRUJILLO *et al.*, 2013).

O comprimento da cadeia dos AG que compõem o TAG influencia a digestibilidade lipídica. AG de cadeia média, normalmente apresentam uma formação de AGL mais rápida e em quantidades superiores, do que AG de cadeia longa (SALVIA-TRUJILLO *et al.*, 2013). Isto pode ser atribuído ao fato de os AG de cadeia média migrarem mais facilmente/rapidamente

para a fase aquosa, enquanto os ácidos de cadeia longa tendem a se acumular na interface óleo-água, apresentando, dessa forma, um processo de digestibilidade mais lento (ABREU-MARTINS *et al.*, 2020).

A composição da matriz lipídica utilizada influência também o comprimento de cadeia e o grau de insaturação dos AGL e MAG produzidos durante a digestão lipídica, afetando, assim, a taxa de digestibilidade lipídica e a capacidade de solubilização das micelas mistas formadas (TAN; MCCLEMENTS, 2021). De acordo com a sua dispersibilidade na fase aquosa, os AGL formados durante o processo de digestão permanecem na superfície das gotículas de óleo ou migram para a fase aquosa (fluidos gastrointestinais). Essa dispersibilidade dos AGL formados influencia diretamente a digestão lipídica, uma vez que se não forem removidos da superfície das gotículas de óleo, irão inibir o processo de digestibilidade lipídica e consequentemente a liberação e solubilização dos compostos incorporados às matrizes lipídicas (LI; HU; MCCLEMENTS, 2011; TAN; MCCLEMENTS, 2021).

O estado físico das matrizes lipídicas utilizadas para obtenção de CLN exerce forte influência sobre a taxa e a extensão da digestão lipídica. Estudos realizados por Bonnaire *et al*. (2008) e Nik, Langmaid e Wright (2012) relataram que a taxa e a extensão da digestão lipídica foram superiores em partículas líquidas do que em partículas sólidas. Os autores apresentaram duas razões para isto ter ocorrido. Em primeiro lugar, a matriz lipídica de menor PF pode oferecer mais moléculas de TAG móveis e fluidas na interface, o que aumenta a capacidade de ligação da lipase ao seu sítio ativo. Em segundo lugar, a cristalização dos TAG na forma polimórfica mais densa (β) pode ter contribuído para a menor acessibilidade da lipase.

A digestão de lipídios envolve fenômenos coloidais e reações enzimáticas que ocorrem na interface das gotículas (WILDE; CHU, 2011). De forma geral, a taxa da digestão de lipídios é determinada pela área de superfície de lipídios expostos às enzimas digestivas, bem pela capacidade dessas enzimas se aderirem à superfície óleo/água e acessar as moléculas de TAG (FU *et al.*, 2019).

A digestão e a absorção progressiva de alimentos no corpo humano ocorrem à medida que estes se movem através da boca, estômago, intestino delgado e colón, e são submetidos a uma série de processos físicos (forças mecânicas), químicos (alterações de pH e de composição) e bioquímicos (atividade enzimática) (TAN; MCCLEMENTS, 2021).

A primeira etapa da digestão acontece na cavidade oral. Embora muitos alimentos permaneçam pouco tempo (segundos a minutos), dependendo da composição do alimento, esta região do TGI pode ter forte influência sobre o processo digestivo subsequente (TAN; MCCLEMENTS, 2021). As forças mecânicas geradas durante a mastigação podem ajudar a decompor e homogeneizar alimentos líquidos, semi-líquidos e sólidos. Além disso, a secreção

de saliva na cavidade oral, cujos constituintes como água, enzimas, proteínas, minerais e mucina, podem provocar alterações no pH, força iônica, temperatura, estrutura e reologia dos alimentos (TAN *et al.*, 2020). Portanto, mesmo nessa fase inicial da digestão, o tamanho inicial e características interfaciais de nanoestruturas podem ser alterados (MARTINS *et al.*, 2015).

Após serem engolidas e passarem pelo esôfago, as nanoestruturas chegam até a câmara gástrica, permanecendo por um período que pode variar de 30 minutos a 4horas, dependendo de sua composição (TAN; MCCLEMENTS, 2021). As nanoestruturas ingeridas são então misturadas com fluidos gástricos e enzimas como as lipases gástricas, que iniciam o processo de digestão de lipídios. As nanoestruturas são expostas a um meio altamente ácido (pH 1-3) e a movimentos peristálticos (KONG; SINGH, 2010). O comportamento de sistemas de entrega à base de emulsão, como os CLN, na cavidade gástrica, depende do tamanho e das propriedades interfaciais das gotículas de óleo que estes contêm (TAN; MCCLEMENTS, 2021). As condições gástricas, como pH, força iônica e enzimas digestivas, podem promover alterações nas propriedades interfaciais e no tamanho das nanoestruturas ingeridas, deixando perdem a escala nanométrica durante a passagem por esta cavidade (MCCLEMENTS; XIAO, 2014).

A maior parte dos sistemas de entrega à base de lipídios não libera o BC incorporado às estruturas na boca e no estômago, enquanto na digestão de vegetais este é o primeiro passo da absorção deste bioativo (LIN *et al.*, 2018), visto que o processo de lipólise, hidrólise de lipídios, tem início na cavidade gástrica, onde ao redor de 10-30% de TAG são hidrolisados, dependendo do tamanho da gotícula de lipídios. A digestão dos lipídios no estômago pela lipase gástrica é realizada na superfície das gotículas de óleo, de maneira semelhante a lipase pancreática (TAN; MCCLEMENTS, 2021).

Durante a digestão no estômago e no intestino delgado, os TAG são reorganizados fisicamente e processados enzimaticamente liberando um MAG e dois AGL (CARRIÈRE, 2016). As lipases pancreáticas apresentam estéreo-especificidade *sn-1* e *sn-3*, portanto durante a lipólise, normalmente um MAG s*n*-2 permanece não digerido (ABREU-MARTINS *et al*., 2020). No entanto, a lipase gástrica é *sn-3* estéreo-específica. Devido as condições extremas encontradas nesta cavidade (como pH entre 1 e 3), a digestão lipídica na fase gástrica pode reduzir a biodisponibilidade de compostos lipossolúveis, uma vez que os libera da matriz lipídica deixando em contato com o meio (TAN; MCCLEMENTS, 2021).

O processo de esvaziamento gástrico, empurra então o quimo através do esfíncter do piloro para o intestino delgado, local onde ocorre a maior parte da absorção dos compostos bioativos (MARTINS *et al*., 2015). O intestino delgado é dividido em três segmentos: um curto, que recebe secreções de digestão do pâncreas e do fígado- o duodeno, e dois mais longos, o jejuno e íleo. As principais funções do intestino delgado na digestão são a quebra de macromoléculas e a absorção de água e nutrientes (GUERRA *et al*., 2012). Nesse

compartimento, os macronutrientes que passaram de forma intacta pelo estômago, podem ser digeridos, promovendo a liberação de compostos aprisionados em suas estruturas (TAN; MCCLEMENTS, 2021).

No duodeno as nanoestruturas são misturadas com sais biliares, fosfolipídios, pancreatina, colipase e bicarbonato de sódio, e o pH da mistura se eleva a valores próximos da neutralidade (POWELL *et al.*, 2010). Enzimas, como a lipase pancreática, atuam para hidrolisar os constituintes dos alimentos, e a bile, produzida no fígado, desempenha um papel específico na digestão de lipídios, emulsificando-os e assim, promovendo a atividade da lipase pancreática (GUERRA *et al*., 2012). A digestão nos fluidos intestinais é misturada e empurrada através do intestino delgado devido a forças peristálticas geradas pelas paredes intestinais (TAN; MCCLEMENTS, 2021).

Uma série de etapas está envolvida na digestão de lipídios no intestino delgado. Primeiramente, as forças peristálticas geradas pelas paredes intestinais podem levar ao rompimento das gotículas de óleo, aumentando a área superficial e assim, a exposição dos lipídios à lipase pancreática, promovendo a digestão lipídica (POWELL *et al.*, 2010; TAN; MCCLEMENTS, 2021). Porém em alguns casos, as condições do intestino delgado podem promover a coalescência ou floculação das gotículas, diminuindo assim a digestão. Em segundo lugar, os sais biliares presentes nos fluidos do intestino delgado, podem se adsorver as superfícies dos lipídios e deslocar substâncias tensoativas, como os emulsificantes utilizados para estabilizar a emulsão (TAN; MCCLEMENTS, 2021). Em terceiro, complexos de lipase/colipase pancreática se adsorvem as superfícies das gotículas de óleo e catalisam a conversão de TAG em AGL e MAG (POWEL *et al*., 2010). Quarto, a presença de íons e sais biliares nos fluidos intestinais pode facilitar a digestão lipídica, ao remover AGL (principalmente de cadeia longa) aderidos na superfície das gotículas lipídicas. O íon Ca^{+2} promove a precipitação dos AGL, enquanto os sais biliares fazem isso solubilizando os AGL dentro de micelas mistas. Quinto, uma pequena quantidade de cálcio é crucial para otimizar a atividade da lipase pancreática (TAN; MCCLEMENTS, 2021).

A digestão dos lipídios no intestino delgado promove a liberação de produtos como MAG e AGL, que por sua vez, juntamente com sais biliares e fosfolipídios contribuem para a formação de micelas mistas no intestino delgado. Os compostos bioativos, como o BC, que estão solubilizados na fase lipídica são então transferidos para as micelas mistas que os transportam até as células epiteliais do intestino delgado (PALMERO *et al.*, 2014; TAN; MCCLEMENTS, 2021). A formação de micelas mistas ocorre na mesma taxa que a digestão lipídica (SALVIA-TRUJILLO *et al*., 2017a).

A nanoestrutura das micelas mistas formadas dentro dos fluidos intestinais afeta sua capacidade de solubilizar os compostos bioativos (MCCLEMENTS; LI; XIAO, 2015). As dimensões dos domínios hidrofóbicos dentro das micelas mistas dependem da composição

da matriz lipídica presente originalmente no alimento. Esses domínios devem ser grandes o suficiente para incorporar o composto em seu interior, caso contrário, estes compostos não serão solubilizados. A natureza da matriz alimentar pode também influenciar a estrutura e o comportamento de micelas mistas no intestino delgado, influenciando assim a biodisponibilidade de compostos bioativos (TAN; MCCLEMENTS, 2021), conforme descrito a seguir no item 2.9.1.

As micelas mistas carregadas de compostos bioativos passam pelo lúmen do intestino e pela camada de muco antes de atingir as paredes das células intestinais, onde serão absorvidas. A camada de muco atua como uma membrana semipermeável que regula esse processo de transporte. A permeação das partículas através da camada de muco depende do tamanho dos poros (<500nm), da hidrofobicidade e da carga superficial (TAN; MCCLEMENTS, 2021). Depois de passar pela camada de muco, os compostos bioativos alcançam as células do epitélio intestinal em que podem ser absorvidos através de diferentes processos (MCCLEMENTS *et al*., 2015). Após sua absorção, a maior parte das vitaminas lipossolúveis são incorporadas em quilomícrons com TAG e colesterol nas células epiteliais e depois liberadas no sistema linfático (TAN; MCCLEMENTS, 2021).

Todos os nutrientes digeridos e a água são absorvidos através das paredes intestinais (enterócitos das vilosidades), enquanto os produtos residuais (material não absorvido) são impelidos para o cólon, intestino grosso (KONG; SINGH, 2010). O cólon é caracterizado como um ambiente anaeróbico que contém uma população diversa de microrganismos intestinais. As principais funções do cólon são a absorção de água e eletrólitos, fermentação de polissacarídeos e proteínas pela microbiota colônica, reabsorção de sais biliares, formação, armazenamento e eliminação de fezes (GUERRA *et al*., 2012).

2.9.1 Biodisponibilidade e bioacessibilidade de compostos bioativos lipofílicos

O termo bioacessibilidade pode ser descrito como a quantidade de um nutriente entregue pela matriz alimentar e apto para ser absorvido no TGI; enquanto a biodisponibilidade apresenta um sentido mais amplo, sendo definida como a porção de nutrientes absorvida pelas células do epitélio intestinal. Os fatores que regem a biodisponibilidade podem ser divididos em três categorias principais: bioacessibilidade (liberação e solubilização), transformação (química e bioquímica) e absorção (transporte e captação) (MCCLEMENTS *et al*., 2015).

A natureza da matriz alimentar influencia a bioacessibilidade, a transformação e a absorção dos compostos bioativos lipossolúveis por processos de modulação, como taxa de esvaziamento gástrico, secreções hormonais, atividades enzimáticas, remoção de produtos da digestão, solubilização e transporte de micelas mistas e absorção nas células epiteliais

(GOLDING; WOOSTER, 2010). O impacto das características da matriz lipídica na biodisponibilidade dos compostos bioativos incorporados a estas, é dependente de fatores como a concentração e a composição da fase lipídica, a estrutura do composto bioativo e o TP lipídica (TAN; MCCLEMENTS, 2021).

A composição química da fase lipídica utilizada para incorporação de compostos bioativos lipossolúveis impacta fortemente sua bioacessibilidade e consequentemente sua biodisponibilidade. A capacidade de solubilização das micelas mistas é fortemente influenciada pela composição da matriz lipídica. Quanto maior o comprimento da cadeia e menor grau de insaturação dos AG das matrizes lipídicas, maior será a capacidade de solubilização, ou seja, as micelas mistas apresentarão domínios hidrofóbicos grandes o suficiente para incorporar compostos bioativos (TAN; MCCLEMENTS, 2021).

A concentração da fase lipídica é um fator determinante para a biodisponibilidade pois está altamente relacionada à formação das micelas mistas durante o processo digestivo. Segundo Tan *et al*. (2020) se a concentração lipídica for muito baixa, não há a formação de micelas mistas em quantidade suficiente para solubilizar totalmente o composto incorporado à esta fase; porém se a concentração da fase lipídica for muito alta, poderá ocorrer precipitação do composto bioativo juntamente com os TAG que não foram digeridos durante a passagem pelo TGI.

O aumento de lipólise pela lipase pode gerar mais produtos de hidrólise (MAG e AGL, por exemplo), aumentando assim a produção de micelas mistas e consequentemente a solubilização do BC dentro das micelas (VERRIJSSEN *et al.*, 2015). No entanto, estudos vêm evidenciando que não apenas o grau de lipólise durante a digestão aumenta a capacidade de solubilização de BC, mas também o tipo de espécie lipídica micelarizado (ABREU-MARTINS *et al*., 2020).

O grau de saturação de AG pode determinar a capacidade de solubilização de compostos bioativos em micelas mistas. Estudos relataram que a liberação de AG monoinsaturados de cadeia longa durante o processo de digestão, como o ácido oleico, proporcionou maior capacidade de solubilização para micelas mistas e consequentemente maior bioacessibilidade de carotenoides, quando comparado a liberação de AG poliinsaturados (ABREU-MARTINS *et al.*, 2020; VERKEMPINCK *et al.*, 2018).

O TP seguido pela composição da matriz lipídica, são os fatores que mais afetam a bioacessibilidade de compostos incorporados aos sistemas de entrega à base de emulsões (ZHOU *et al.*, 2018). O TP afeta o destino gastrointestinal dos compostos bioativos incorporados às estruturas CLN (TAN; MCCLEMENTS, 2021) principalmente por estar diretamente relacionado à área superficial das partículas lipídicas. Quanto menor o TP lipídica, maior a área superficial disponível para ligação da lipase. A lipase apresenta uma forma globular de aproximadamente 5nm, sendo assim, quanto menor for o tamanho da partícula

lipídica/gota de óleo, maior será o espaço coberto pela lipase e consequentemente maior a taxa e a extensão da digestibilidade lipídica (conversão de TAG em AGL) (SALVIA-TRUJILLO *et al*., 2017a) aumentando assim a liberação e solubilização dos compostos bioativos incorporados à fase lipídica, e consequentemente a bioacessibilidade (LI; MCCLEMENTS, 2010; SALVIA-TRUJILLO *et al.*, 2017b).

Estudo realizado por Salvia-Trujillo *et al*. (2017a) demonstrou que a cinética de hidrólise lipídica foi fortemente influenciada pelo tamanho da gota de óleo presente nas emulsões testadas. Neste estudo a quantidade de TAG diminuiu em função do tempo durante a fase intestinal, enquanto a concentração de MAG, AGL e glicerol aumentou em todas as amostras estudadas. No entanto a formação dos produtos de hidrólise lipídica foi diferente de acordo com o tamanho inicial das gotículas presentes na emulsão. Emulsões com TP inferior (0,72μm) apresentaram maior área de superfície para ação da lipase na interface óleo-água levando a conversão de MAG em AGL e glicerol em maior intensidade quando comparado a emulsões com TP médio (1,93 μm). Ainda neste estudo, foi demonstrado que a produção de AGL no final da fase intestinal (120 min) foi 50% superior em emulsões com TP inferior (0,72 μm) do que emulsões com TP superior (15,1 μm), correspondendo a 60 mg/mL e 30mg/mL respectivamente.

No entanto é importante salientar, que, dificilmente o TP ao ser ingerida será o mesmo durante a passagem pelo TGI, devido a fenômenos de fragmentação, floculação e coalescência (TAN *et al*., 2020). Durante a digestão lipídica, as partículas de óleo podem flocular ou coalescer. A estabilidade das partículas durante a passagem pelo TGI depende do tipo de emulsificante utilizado em sua obtenção (GOLDING; WOOSTER, 2010; TAN; MCCLEMENTS, 2021). Alguns emulsificantes produzem partículas que são relativamente estáveis durante a passagem pelo TGI, enquanto outros produzem partículas que floculam e/ou coalescem em determinadas regiões do TGI. Essa agregação pode ocorrer por diversos fatores incluindo hidrólise enzimática, redução da repulsão elestrostática (PZ) ou efeitos de depleção ou floculação (TAN; MCCLEMENTS, 2021).

O tipo de emulsificante pode também influenciar a biodisponibilidade através de outras formas, como por exemplo afetar também a adsorção da lipase na superfície da partícula. Com o auxílio de sais biliares, a lipase se adsorve a superfície desencadeando a reação de lipólise. No entanto, há alguns emulsificantes que não podem ser totalmente deslocados pelos sais biliares, inibindo a adsorção da lipase e reduzindo assim a digestão de lipídios (SALVIA-TRUJILLO *et al*., 2019). Os emulsificantes podem ainda ter ação antioxidante, contribuindo para o aumento da biodisponibilidade através da manutenção da estabilidade dos compostos (TAN *et al*., 2020). Alguns emulsificantes podem inibir ou estimular a formação de micelas mistas que solubilizam os compostos bioativos após serem

liberados da matriz lipídica, influenciando assim a biodisponibilidade destes compostos (GASA-FALCON *et al.*, 2017).

As características estruturais e físico-químicas dos compostos bioativos também afetam sua biodisponibilidade (TAN; MCCLEMENTS, 2021). Para compostos bioativos que apresentam baixo grau de hidrofobicidade ou dimensões moleculares pequenas, o impacto do tipo da matriz lipídica utilizada em sua bioacessibilidade e biodisponibilidade é inferior (AHMED *et al.*, 2012). Isso ocorre devido ao fato de serem facilmente solubilizados tanto em micelas mistas grandes quanto pequenas (TAN; MCCLEMENTS, 2021).

De forma geral, a polaridade dos compostos bioativos determina sua transferência para as micelas na fase intestinal. Normalmente, carotenoides com maior hidrofobicidade, como o BC requerem a presença de maior quantidade de AGL do que MAG na fração micelar para serem transferidos. Devido a maior solubilidade em água do glicerol presente na estrutura de MAG, estes compostos podem apresentar BHL superior a AGL, portanto a solubilização de BC em micelas formadas por maiores quantidades de MAG é ineficiente (PALMERO *et al.*, 2014; SALVIA-TRUJILLO *et al.*, 2017b).

O grau de hidrofobicidade, porém, não afeta a absorção de compostos bioativos nas células epiteliais, conforme demonstrado em estudo de Sy *et al*. (2012), demonstrando assim que a bioacessibilidade é mais importante que a absorção para determinar a biodisponibilidade total de compostos bioativos lipossolúveis (TAN; MCCLEMENTS, 2021). Patel *et al*. (2010) demonstraram que nanopartículas apresentaram propriedades de mucoadesão no intestino delgado e dessa forma, proporcionaram o aumento na absorção do composto bioativo incorporado ao liberá-lo por um tempo prolongado nas proximidades da membrana celular.

2.9.2 Modelos para estudos de digestibilidade in vitro.

Estudos de digestibilidade envolvendo humanos e animais são os meios mais precisos para elucidar os principais fatores que afetam a biodisponibilidade de bioativos lipossolúveis, porém devido a fatores éticos, financeiros, de segurança e de tempo, a realização destes estudos é limitada (TAN; MCCLEMENTS, 2021). Por esta razão, um número considerável de abordagens *in vitro*, que variam em sua simplicidade, custo, tempo, reprodutibilidade e capacidade de simular de forma confiável as condições reais do TGI, vêm sendo desenvolvidas para estudar o destino gastrointestinal de nanopartículas (MCCLEMENTS; LI, 2010; MCCLEMENTS; MCCLEMENTS, 2016; MINEKUS *et al.*, 2014) devido principalmente às suas vantagens de redução de tempo e custo, ausência de restrições éticas e melhoria da precisão de reprodutibilidade em relação aos modelos *in vivo* (KONG; SINGH, 2010; MCCLEMENTS; LI, 2010).

O modelo de digestibilidade *in vitro* mais utilizado para estudar o destino dos alimentos no TGI humano é o método INFOGEST harmonizado, que se baseia nas condições fisiológicas que ocorrem no TGI durante o processo de digestão (MINEKUS *et al*., 2014). Este método descreve um conjunto de parâmetros, incluindo as fases oral, gástrica e intestinal, que foram padronizados e validados para que seja possível a comparação entre resultados obtidos por diferentes grupos de pesquisa (LIN *et al.*, 2018; TAN; MCCLEMENTS, 2021).

Os modelos de digestibilidade *in vitro* são divididos em estáticos e dinâmicos. Modelos de digestibilidade *in vitro* estática, geralmente incluindo um estágio (intestinal), dois estágios (gástrico e intestinal) ou três estágios (oral, gástrico e intestinal), mimetizam as condições fisiológicas e processos bioquímicos no TGI (LIN *et al*., 2018). Entretanto, a maior parte dos modelos estáticos não reproduz os processos físicos que ocorrem durante o processo de digestão humana, como mistura, cisalhamento, esvaziamento gástrico e peristaltismo, ou mudanças contínuas no pH e taxas de secreção, permitindo uma menor comparação dos resultados obtidos com estes modelos com os estudos *in vivo* (GUERRA *et al.*, 2012; LIN *et al.*, 2018). Além disso, durante os ensaios de digestibilidade *in vitro* utilizando modelos estáticos não há processo de absorção, ou seja, os produtos de digestão formados durante o processo não são removidos (WICKHAM; FAULKS; MILLS, 2009).

Os modelos dinâmicos de digestibilidade *in vitro* têm sido desenvolvidos com o intuito de superar as limitações dos modelos estáticos (GUERRA *et al*., 2012). Na tentativa de alcançar uma melhor correlação entre os comportamentos *in vivo* e *in vitro*, esses modelos dinâmicos simulam mais efetivamente os atributos bioquímicos, biomecânicos e temporais que ocorrem *in vivo* (LIN *et al*., 2018). Nos métodos de digestibilidade *in vitro* dinâmicos há renovação contínua dos fluidos digestivos intestinais, promovendo a formação contínua de micelas de sais biliares, o que não leva a saturação das mesmas com os compostos bioativos incorporados a fase lipídica em contraste com os métodos de digestibilidade estáticos, em que as micelas saturadas não são substituídas (MARZE, 2017).

Em comparação aos modelos estáticos, os modelos dinâmicos de digestibilidade *in vitro* são considerados mais adequados para fornecer uma melhor previsão do destino biológico de sistemas de entrega devido à sua maior semelhança com as condições *in vivo* (LIN *et al*., 2018). O modelo intestinal TIM-1 é um sistema dinâmico multicompartimental de digestibilidade *in vitro* que simula as condições *in vivo* e eventos cinéticos que ocorrem no estômago, duodeno, jejuno e íleo; fornecendo informações sobre o caminho percorrido por nutrientes e compostos no TGI; liberação, estabilidade e disponibilidade de nutrientes para absorção intestinal (RIBNICKY *et al.*, 2014).

Esse sistema é composto por quatro sucessivos compartimentos simulando o estômago, duodeno, jejuno e íleo. Cada compartimento é formado por duas unidades que consistem em um reator de vidro ou acrílico com uma parede flexível interna. A água é

bombeada para a área entre o reator e a parede flexível para manter a temperatura a 37°C e para alternar os movimentos de compressão/relaxamento, simulando assim os movimentos peristálticos. As mudanças na pressão da água que originam esses movimentos são alcançadas por bombas rotativas, e garantem assim, a mistura do quimo. Eletrodos de pH estão dispostos em cada compartimento para monitoramento das alterações que ocorrem durante as fases da digestão. A passagem do conteúdo pelo TIM-1 é regulada pela abertura e fechamento das válvulas peristálticas que conectam cada compartimento (PINHEIRO *et al.*, 2013). A fase de absorção é simulada através do uso de membranas de diálise que removem a água e pequenas moléculas (incluindo os produtos de digestão e o composto bioativo dissolvido). Os compartimentos do jejuno e do íleo são conectados a unidades de filtração (membranas ocas) que permitem que a bioacessibilidade seja quantificada. Frações não bioacessíveis são coletadas ao final do compartimento do íleo e representam o material não absorvido que entrará no intestino grosso (KONG; SINGH, 2010; RIBNICKY *et al.*, 2014).

Em ensaios de digestibilidade *in vitro* considerando sistemas de entrega nanoestruturados normalmente uma amostra contendo as nanopartículas em dispersão é preparada e em seguida, submetida a um ou mais tratamentos para simular o TGI (MCCLEMENTS; MCCLEMENTS, 2016). Esses métodos normalmente envolvem a passagem sequencial da amostra por uma série de fluidos gastrointestinais simulados mantidos a temperatura corporal (37°C) que apresentam composição específica (pH, minerais, ácidos, bases, sais biliares, enzimas etc.) sob condições de fluxo e tempo de incubação que imitam as regiões do TGI. Inicialmente, soluções estoque de fluido salivar (SSF), gástrico (SGF) e intestinal (SIF) são preparadas com composições e valores de pH específicos. Além disso, soluções de estoque de outros constituintes principais do TGI são preparadas, como enzimas, sais biliares e cloreto de cálcio. Essas soluções adicionais são misturadas com os fluidos simulados, para formar os fluidos finais (MCCLEMENTS; MCCLEMENTS, 2016; MINEKUS *et al.*, 2014).

O SSF final é uma solução neutra, contendo constituintes que simulam a saliva humana, como ácidos, tampões minerais, biopolímeros (mucina) e enzimas (amilase). O SGF final é uma solução aquosa altamente ácida (pH=3) com uma composição que simula condições gástricas, por exemplo ácidos, tampões, sais e enzimas digestivas (proteases e lipases). O SIF final é uma solução aquosa neutra (pH=7) que contém vários componentes que simulam a composição do intestino delgado, como sais biliares, fosfolipídios, bases, tampões, sais minerais e enzimas digestivas (MCCLEMENTS; MCCLEMENTS, 2016).

A amostra a ser testada passa então, sequencialmente, pelas fases oral, gástrica e intestinal (intestino delgado). Na fase oral, o SSF é adicionado à amostra sob agitação por aproximadamente 60 segundos e a amostra é então, submetida à fase gástrica. Na fase gástrica, há adição do SGF. O quimo é levado para o intestino delgado. O material coletado

após a passagem pelo intestino delgado é denominado de digerido. O digerido pode passar para um estágio de cólon simulado, utilizado para a análise da liberação e absorção de compostos bioativos e/ou utilizado para estudar mudanças na estrutura e composição de nanopartículas (MCCLEMENTS; MCCLEMENTS, 2016). O colón é uma das partes mais difíceis para simulação em laboratório, pois normalmente requer condições de anaerobiose para o cultivo de bactérias (YOO; CHEN, 2006).

Para a realização dos ensaios de digestibilidade *in vitro* são necessários alguns cuidados para obtenção de resultados precisos. A secreção das enzimas e fluidos gastrointestinais, a diluição da amostra durante a digestão e o preparo das amostras recolhidas durante o processo para posterior análise, podem influenciar os resultados obtidos a partir dos ensaios de digestibilidade *in vitro* (bioacessibilidade, por exemplo) (PINHEIRO *et al*., 2017).

2.10 Citotoxicidade

O conhecimento sobre a toxicidade de estruturas em macro e microescala pode não ser confiável para predizer a toxicidade em nanoescala, portanto estudos adicionais para avaliar a nanotoxicidade são obrigatórios (MARTINS *et al*., 2015). A diminuição no TP conduz a um aumento exponencial da área superficial, o que torna a superfície do nanomaterial mais reativo com o ambiente em que ele está circundado. O aumento da absorção, das nanopartículas, em certos tecidos pode levar a seu acúmulo, o que pode ser pode interferir nas funções biológicas críticas destas células (AILLON *et al.*, 2009).

Apesar da grande quantidade de trabalhos relacionados a regulamentação do uso de nanoestruturas em alimentos e aspectos relacionados à segurança de seu consumo, ainda não está totalmente esclarecido como as nanoestruturas se comportam após processos de ingestão e digestão e quais serão as mudanças experimentadas após sua absorção (MARTINS *et al*., 2015). Somente através da compreensão do destino digestivo das nanoestruturas/compostos bioativos é possível melhorar seu desempenho e ter informações conclusivas sobre a segurança das nanoestruturas (PINHEIRO *et al.*, 2017).

As nanopartículas ao serem introduzidas em formulações alimentícias, após serem ingeridas, serão primeiramente absorvidas no intestino, para depois serem transportadas até o fígado. Se tóxicas, podem prejudicar as células do epitélio intestinal, causando o seu rompimento e prejudicando assim sua função protetora (YU; HUANG, 2013). A citotoxicidade de nanopartículas é normalmente avaliada através do estudo da viabilidade celular, que consiste em uma abordagem *in vitro* de cultura de células (HUR *et al.*, 2011; LOH *et al.*, 2010). Modelos de culturas de células são amplamente utilizados para simular as células do epitélio que revestem a superfície interna do intestino delgado, onde a absorção dos

compostos bioativos e das nanopartículas normalmente ocorre (MCCLEMENTS; MCCLEMENTS, 2016).

O epitélio intestinal humano é composto por vários tipos de células: enterócitos, calciformes, endócrinas, de *Panet* e tronco. Para o estudo de mecanismos de transporte de nanoestruturas, dois tipos de células intestinais são considerados preferencialmente: os enterócitos e as células M, principais transportes para uma ampla gama de nanoestruturas (HE *et al.*, 2013). A linhagem celular de adenocarcinoma do cólon humano - Caco-2, vem sendo amplamente utilizada para estudar a absorção dos compostos bioativos e nanopartículas (REBOUL *et al.*, 2006) pois se assemelham aos enterócitos, que por sua vez representam 90% das células epiteliais do intestino (ARAÚJO *et al.*, 2014).

Para este estudo, uma camada de células Caco-2 cresce diretamente em uma placa de petri ou em uma membrana semi-permeável colocada dentro da placa de petri. Uma suspensão aquosa de amostra (que pode ter sido previamente exposta a condições do TGI) é colocada sobre as células epiteliais, e a quantidade de composto absorvido ou que atravessa as células é medida através de uma técnica analítica adequada (microscopia, cromatografia, espectrometria, entre outros) (MCCLEMENTS; MCCLEMENTS, 2016). O MTT é o método mais utilizado para ensaios de viabilidade celular de NL. Este é um método colorimétrico que mede a capacidade de células metabolicamente ativas reduzirem o MTT (brometo de 3-4,5-dimetil-tiazol-2-il-2,5-difeniltetrazólio) em formazan, que modifica a cor do meio, medido através de espectrometria (AHMAD *et al.*, 2012; DOKTOROVOVA; SOUTO; SILVA, 2014; HUR *et al.*, 2011).

Em contraste com micropartículas que são muito grandes para passar pelo epitélio intestinal e devem assim, liberar os compostos bioativos no TGI, nanoestruturas podem ser retiradas e atravessar a barreira intestinal (DES RIEUX *et al.*, 2006). A manipulação de materiais em nanoescala pode levar a formação de novas estruturas com características potencialmente tóxicas. Suas dimensões reduzidas permitem que penetre com facilidade nos tecidos biológicos, o que pode causar sua função normal ou morte celular. Exemplos de efeitos tóxicos incluem a inflamação do tecido e modificação do equilíbrio redox celular (ARORA; RAJWADE; PAKNIKAR, 2012).

Uma das maiores preocupações do uso de nanoestruturas na área de alimentos é a falta de conhecimento sobre como as propriedades físico-químicas em nanoescala podem alterar o destino biológico de nanoestruturas e a biodisponibilidade dos compostos bioativos incorporados a elas. Isto pode influenciar suas propriedades toxicológicas e causar efeitos adversos na saúde humana. Os efeitos tóxicos potenciais no TGI ou a nível sistêmico, manutenção de sua integridade após a passagem pelas barreiras do TGI, ou como as nanoestruturas são absorvidas, distribuídas e excretadas do corpo precisam ser avaliados (MARTINS *et al*., 2015).

2.11 Referências

ABREU-MARTINS, H.H. *et al*. The lipid type affects the in vitro digestibility and β-carotene bioaccessibility of liquid or solid lipid nanoparticles. **Food Chemistry**, v. 311, 126024, 2020.

ACOSTA, E. Bioavailability of nanoparticles in nutrient and nutraceutical delivery**. Current Opinion in Colloid & Interface Science**, v.14, p. 3-15, 2009.

ADITYA, N.P. *et al*. Curcumin and genistein coloaded nanostructured lipid carriers: *in vitro* digestion and antiprostate cancer activity. **Journal of Agricultural and Food Chemistry**, v. 61, n. 8, p. 1878–1883, 2013.

ADITYA, N.P.; KO, S. Solid lipid nanoparticles (SLNs): delivery vehicles for food bioactives. **RSC Advances**, v. 5, n. 39, p. 30902–30911, 2015.

AHMAD, J *et al*. Apoptosis induction by silica nanoparticles mediated through reactive oxygen species in human liver cell line HepG2. **Toxicology and Applied Pharmacology**, v. 259, n. 2, p. 160–168, 2012.

AHMED, K.; LI, Y.; MCCLEMENTS, D.J.; XIAO, H. Nanoemulsion- and emulsion-based delivery systems for curcumin: Encapsulation and release properties. **Food Chemistry**, v. 132, n. 2, p. 799–807, 2012.

AILLON, K.L. *et al*. Effects of nanomaterial physicochemical properties on in vivo toxicity. **Advanced Drug Delivery Reviews**, v. 61, p. 457-466, 2009.

AKHAVAN, S.; ASSADPOUR, E.; KATOUZIAN, I.; JAFARI, S.M. Lipid nano scale cargos for the protection and delivery of food bioactive ingredients and nutraceuticals. **Trends in Food Science & Technology**, v.74, p.132-146, 2018.

ANTON N.; BENOIT J.P.; SAULNIER P. Design and production of nanoparticles formulated from nano-emulsion templates: A review. **Journal of Controlled Release**, v. 128, n. 3, p. 185–199, 2008.

ARAÚJO, F *et al.* The impact of nanoparticles on the mucosal translocation and transport of GLP-1 across the intestinal epithelium. **Biomaterials**, v. 35, n. 33, p. 9199-9207, 2014.

ARORA, S., RAJWADE, J.M.; PAKNIKAR, K.M. Nanotoxicology and in vitro studies: The need of the hour. **Toxicology and Applied Pharmacology**, v. 258, p. 151-165, 2012.

ASHKAR, A.; SOSNIK, A.; DAVIDOVICH-PINHAS, M. Structured edible lipid-based particle systems for oral drug-delivery. **Biotechnology Advances**, 107789,2021.

ASSIS, L.M.; ZAVAREZE, E.R.; PRENTICE-HERNÁNDEZ, C.; SOUZA-SOARES, L.A. Characteristics of nanoparticles and their potential applications in foods. **Brazilian Journal of Food Technology,** v. 15, n. 2, p. 99-109, 2012.

ATTAMA, A.A.; MOMOH, M.A.; BUILDERS, P.F. Lipid Nanoparticulate Drug Delivery Systems: A Revolution in Dosage Form Design and Development. In: Sezer, Ali Demir (Ed). **Recent Advances in Novel Drug Carrier Systems**, 107-140, 2012. Intech.

BABAZADEH, A.; GHANBARZADEH, B.; HAMISHEHKAR, H. Formulation of food grade nanostructured lipid carrier (NLC) for potential applications in medicinal-functional foods. **Journal of Drug Delivery Science and Technology**, v. 39, p. 50–58, 2017.

BELOQUI, A.; DES RIEUX, A.; PRÉAT, V. *et al*. Mechanisms of transport of polymeric and lipidic nanoparticles across the intestinal barrier. **Advanced Drug Delivery Reviews**, v. 106, p. 242–255, 2016.

BOISTELLE, R. Fundamentals of nucleation and crystal growth. In: GARTI, N.; SATO, K. (Eds). **Crystallization and Polymorphism of Fats and Fatty Acids**. New York: Marcel Dekker, p. 189-226, 1988.

BONAIRE *et al*. Influence of Lipid Physical State on the in Vitro Digestibility of Emulsified Lipids. **Journal of Agricultural and Food Chemistry**, v. 56, n. 10, p. 3791–3797, 2008.

BUMMER, P.M. Physical chemical considerations of lipid-based oral drug delivery-- solid lipid nanoparticles **Critical Reviews in Therapeutic Drug Carrier Systems,** v. 21, n.1, p. 1-20, 2004.

BUNJES, H. Characterization of Solid Lipid Nano and Microparticles. In: **Lipospheres in Drug Targets and Delivery: Approaches, Methods, and Applications**. Ed. NASTRUZZI, C. CRC Press LLC, p.43-70, 2004.

BUNJES, H.; KOCH, M.H.J.; WESTESEN, K. Influence of emulsifiers on the crystallization of solid lipid nanoparticles. **Journal of Pharmaceutical Sciences**, v. 92, n. 7, 2003.

BUNJES, H.; UNRUH, T. Characterization of lipid nanoparticles by differential scanning calorimetry, X-ray and neutron scattering. **Advanced Drug Delivery Reviews**, v. 59, p. 379–402, 2007.

CARRIÈRE, F. Impact of gastrointestinal lipolysis on oral lipid-based formulations and bioavailability of lipophilic drugs. **Biochimie**, v.125, p.297-305, 2016.

CARVALHO, S.M. *et al*. Optimization of α-tocopherol loaded solid lipid nanoparticles bycentral composite design. **Industrial Crops and Products**, v. 49, p. 278– 285, 2013.

CERQUEIRA, M.A. *et al*. Design of bio-nanosystems for oral delivery of functional compounds. **Food Engineering Reviews**. v.5, p.1-19, 2014.

CHATTERTON, D.E.W.; SMITHERS, G.; ROUPAS, P.; BRODKORB, A. Bioactivity of β-lactoglobulin and α-lactalbumin-Technological implications for processing. **International Dairy Journal**, v.16, p.1299-1240, 2006.

CHAU, C.F., WU, S.H., YEN, G.C. The development of regulations for food nanotechnology. **Trends in Food Science & Technology**, v.18, p. 269-280, 2007.

CHE MAN, Y. B.; TAN, C. P. The carotenoids. In F. D. Gunstone (Ed.), **Lipids for functional foods and nutraceuticals**, Bridgewater: The Oily Press, p. 25–52, 2003.

CHEN, C.C.; TSAI, T.H.; HUANG, Z.R.; FANG, J. Y. Effects of lipophilic emulsifiers on the oral administration of lovastatin from nanostructured lipid carriers: Physicochemical characterization and pharmacokinetics.European **Journal of Pharmaceutics and Biopharmaceutics**, v.74, n.3, p. 474–482, 2010.

CHEN, L.; REMONDETTO, G. E.; SUBIRADE, M. Food protein-based materials as nutraceutical delivery systems**. Trends in Food Science and Technology**, v. 17, 272– 283, 2006.

CHOI, K.; ADITYA, N.P.; KO, S. Effect of aqueous pH and electrolyte concentration on structure, stability and flow behavior of non-ionic surfactant based solid lipid nanoparticles. **Food Chemistry**, v.147, p.239–244, 2014.

CHU, B.; ICHIKAWA, S.; KANAFUSA, S.; NAKAJIMA, M. Preparation of Protein-Stabilized b-Carotene Nanodispersions by Emulsification–Evaporation Method. **Journal of the American Oil Chemists' Society**, v. 84, n. 11, p. 1053–1062, 2007.

DAN, N. Compound release from nanostructured lipid carriers (NLCs). **Journal of Food Engineering**, v.171, v. 171, p. 37–43, 2016.

DAVIDOV-PARDO, G.; GUMUS, C.E., MCCLEMENTS, D.J., Lutein-enriched emulsion-based delivery systems: Influence of pH and temperature on physical and chemical stability. **Food Chemistry**, v. 196, p. 821–827, 2016.

DES RIEUX, A *et al*. Nanoparticles as potential oral delivery systems of proteins and vaccines: A mechanistic approach. **Journal of Controlled Release**, v. 116, p. 1-27, 2006.

DOKTOROVOVÁ, S *et al*. Formulating fluticasone propionate in novel PEG-containing nanostructured lipid carriers (PEG-NLC). **Colloids and Surfaces B: Biointerfaces**, v. 75, n. 2, p. 538–542, 2010.

DOKTOROVOVA, S.; SOUTO, E.B.; SILVA, A.M. Nanotoxicology applied to solid lipid nanoparticles and nanostructured lipid carriers – A systematic review of in vitro data. **European Journal of Pharmaceutics and Biopharmaceutics**, v. 87, p. 1-18, 2014.

DORA, C.D *et al*. Physicochemical and morphological characterizations of glyceryl tristearate/castor oil nanocarriers prepared by the solvent diffusion method. **Journal of the Brazilian Chemical Society**, v. 23, n. 11, p. 1972–1971, 2012.

DUNCAN, T.V. Applications of nanotechnology in food packaging and food safety: Barrier materials, antimicrobials and sensors. **Journal of Colloid and Interface Science**, v. 363, n. 1, p. 1–24, 2011.

ELTAYEB, M.; BAKHSHI, P.K.; STRIDE, E.; EDIRISINGHE, M. Preparation of solid lipid nanoparticles containing active compoundby electrohydrodynamic spraying. **Food Research International**, v. 53, n. 1, p. 88–95, 2013.

FOUBERT, I.; VAN DE WALLE, D.; DEWETTINCK, K. Physical properties: structural and physical characteristics. In: GUNSTONE, F. D.; HARWOOD, J. L.; DIJKSTRA, A. J. (Eds). **The Lipid Handbook**. 3 ed. Boca Raton: CRC Press, p. 471-534, 2007.

FREITAS, S.; MERKLE, H.P.; GANDER, B. Microencapsulation by solvent extraction/evaporation: Reviewing the state of the art of microsphere preparation process technology. **Journal of Controlled Release**, v.102, p. 313–332, 2005.

FREITAS, C.; MÜLLER, R.H. Correlation between long-term stability of solid lipid nanoparticles (SLN^{TM}) and crystallinity of the lipid phase. **European Journal of Pharmaceutics and Biopharmaceutics**, v. 47, n. 2, 1999.

FU, D. *et al*. Encapsulation of β-carotene in wheat gluten nanoparticle-xanthan gum stabilized Pickering emulsions: Enhancement of carotenoid stability and bioaccessibility. **Food Hydrocolloids**, v. 89, p. 80–89, 2019.

GASA-FALCON, A.; ODRIOZOLA-SERRANO, I.; OMS-OLIU, G.; MARTÍN-BELLOSO, O. Influence of mandarin fiber addition on physico-chemical properties of nanoemulsions containing β-carotene under simulated gastrointestinal digestion conditions**. LWT - Food Science and Technology**, v. 84, p. 331–337, 2017.

GOLDING, M.; WOOSTER, T.M. The influence of emulsion structure and stability on lipid digestion. **Current Opinion in Colloid & Interface Science**, v. 15, p. 90-101, 2010.

GROMPONE, M.A. Sunflower Oil. In: SHAHIDI, F. **Bailey's Industrial Oil and Fat Products**. Edible Oil and Fat Products: Chemistry, Chemical properties, and health effects. Sixth Edition v.2, Hoboken, New Jersey: John Wiley & Sons, 2005.

GUERRA, A *et al*. Relevance and challenges in modeling human gastric and small intestinal digestion. **Trends in Biotechnology November**, v. 30, n. 11, p. 591-600, 2012.

GUNSTONE, F.D. Vegetable Oils. In: SHAHIDI, F. **Bailey's Industrial Oil and Fat Products**. Edible Oil and Fat Products: Chemistry, Chemical properties, and health effects. Sixth Edition v.2, Hoboken, New Jersey: John Wiley & Sons, 2011.

GUZEY, D.; MCCLEMENTS, D.J. Formation, stability and properties of multilayer emulsions for application in the food industry. **Advances in Colloid and Interface Science**, v.128, p. 227-248, 2006.

HAN, F *et* al. Effect of surfactants on the formation and characterization of a new type of colloidal drug delivery system: Nanostructured lipid carriers. **Colloids and Surfaces A: Physicochemical and Engineering Aspects**, v. 315, n. 1–3, p. 210-216, 2008.

HANDFORD, C.E. *et al*. Awareness and attitudes towards the emerging use of nanotechnology in the agri-food sector. **Food Control**, 57, 24-34, 2015.

HARTEL, J.W. Advances in Food Crystallization. **Annual Review of Food Science and Technology**, v. 4, p. 277-292, 2013.

HE, B *et al*. The transport mechanisms of polymer nanoparticles in Caco-2 epithelial cells. **Biomaterials**, v. 34, n.25, p. 6082-6098, 2013.

HEJRI, A *et al.* Effect of edible antioxidants on chemical stability of ß-carotene loaded nanostructured lipid carriers. **LWT - Food Science and Technology**, v. 113, 108272, 2019.

HEJRI, A *et al.* Optimisation of the formulation of β-carotene loaded nanostructured lipid carriers prepared by solvent diffusion method. **Food Chemistry**, v. 141, n. 1, p. 117–123, 2013.

HELGASON, T *et al*. Impact of surfactant properties on oxidative stability of β-carotene encapsulated within solid lipid nanoparticles. **Journal of Agricultural and Food Chemistry,** v. 57, n. 17, p. 8033–8040, 2009.

HENTSCHEL, A.; GRAMDORF, S.; MÜLLER, R.H.; KURZ, T. β-Carotene-Loaded Nanostructured Lipid Carriers. **Journal of Food Science**, v. 73, n. 2, p. 1-6, 2008.

HIMAVAN, C.; STAROV, V.M.; STAPLEY, A.G.F. Thermodynamic and kinetic aspects of fat crystallization. **Advances in Colloid andInterface Science**, v.122, p. 3-33, 2006.

HORN, D.; RIEGER, J. Organic Nanoparticles in the Aqueous Phase—Theory, Experiment, and Use. **Angewandte Chemie International Edition**, v. 40, n. 23, p. 4330-4361, 2001.

HOW, C.W.; RASEDEE, A.; ABBASALIPOURKABIR, R. Characterization and Cytotoxicity of Nanostructured Lipid Carriers Formulated With Olive Oil, Hydrogenated Palm Oil, and Polysorbate 80. **IEEE TRANSACTIONS ON NANOBIOSCIENCE**, v. 12, n. 2, p. 72–78, 2013.

HU, M.; MCCLEMENTS, D. J.; DECKER, E.A. Lipid Oxidation in Corn Oil-in-Water Emulsions Stabilized by Casein, Whey Protein Isolate, and Soy Protein Isolate. **Journal of Agricultural and Food Chemistry**, v. 51, n. 6, p. 1696–1700, 2003.

HUANG, Z.; HUA, S.; YANG, Y.; FANG, J. Development and evaluation of lipid nanoparticles for camptothecin delivery: a comparison of solid lipid nanoparticles, nanostructured lipid carriers, and lipid emulsion. **Acta Pharmacologica Sinica**, v. 29, n. 9, p. 1094–1102, 2008.

HUANG, Q.; YU, H.; RU, Q. Bioavailability and delivery of nutraceuticals using nanotechnology. **Journal of Food Science**, v. 75, n. 1, p.50-57, 2010.

HUR, S.J.; LIM, B.O.; DECKER, E.A.; MCCLEMENTS, D.J. *In vitro* human digestion models for food applications. **Food Chemistry**, v. 125, p. 1-12, 2011.

JAFARI, S. M.; HE, Y.; BHANDARI, B. Effectiveness of encapsulating biopolymers to produce sub-micron emulsions by high energy emulsification techniques. **Food Research International**, v. 40, n. 7, p. 862-873, 2007.

JANNIN, V.; MUSAKHANIAN, J.; MARCHAUD, D. Approaches for the development of solid and semi-solid lipid-based formulations. **Advanced Drug Delivery Reviews**,v.60, p.734-746, 2008.

JENNING, V.; GOHLA, S. Comparison of wax and glyceride solid lipid nanoparticles (SLN). **International Journal of Pharmaceutic**, v.196, n.2, p. 219-222, 2000.

JOSEPH, S.; BUNJES, H. Preparation of nanoemulsions and solid lipid nanoparticles by premix membrane emulsification. **Journal of Pharmaceutical Sciences**, v. 101, n. 7, p. 2479–2489, 2012.

KAMAL-ELDIN, A. Minor Components of Fats and Oils. In: SHAHIDI, F. **Bailey's Industrial Oil and Fat Products**. Edible Oil and Fat Products: Chemistry, Chemical properties, and health effects. Sixth Edition v.2, Hoboken, New Jersey: John Wiley & Sons, 2005.

KATOUZIAN, I.; ESFANJANI, A.F.; JAFARI, S.M.; AKHAVAN, S. Formulation and application of a new generation of lipid nano-carriers for the food bioactive ingredients. **Trends in Food Science & Technology**, v.68, p. 14-25, 2017.

KHARAT, M.; MCCLEMENTS, D.J. Fabrication and characterization of nanostructured lipid carriers (NLC) using a plant-based emulsifier: Quillaja saponin. **Food Research International**, v.126, p. 1-11, 2019.

KHARE, A.R.; VASISHT, N. Nanoencapsulation in the Food Industry: Technology of the Future. **In: Process Technologies in Microencapsulation**, p. 151-155, 2014.

KHOSA, A.; REDDI, S.; SAHA, R.N. Nanostructured lipid carriers for site-specific drug delivery. **Biomedicine & Pharmacotherapy**, v. 103, p. 598-613, 2018.

KLANG, V.; MATSKO, N.B.; VALENTA, C.; HOFER, F. Electron microscopy of nanoemulsions: An essential tool for characterisation and stability assessment. **Micron**, v.43, n. 2-3, p. 85–103, 2012.

KONG, F.; SINGH, R.P.A. A human gastric simulator (hgs) to study food digestion in human stomach. **Journal of Food Science**, Chicago, v.75, n.9, p. 627-635, 2010.

KOPEC, R.E.; FAILLA, M.L. Recent advances in the bioaccessibility and bioavailability of carotenoids and effects of other dietary lipophiles. **Journal of Food Composition and Analysis**, v.68, p. 16-30, 2018.

LAKSHMI, P.; KUMAR, G.A. Nanosuspension technology: A review. **International Journal of Pharmacy and Pharmaceutical Sciences**, v.2, p. 35–40, 2010.

LAWLER, P.J.; DIMICK, P.S. Crystallization and polymorphism of fats. In: **Food Lipids: Chemistry, Nutrition, and Biotechnology**. Ed. AKOH, C.C. CRC Press, BocaRaton, p.275-300, 2002.

LEONG, T.; WOOSTER, T.; KENTISH, S.; ASHOKKUMAR, M. Minimising oil droplet size using ultrasonic emulsification. **Ultrasonics Sonochemistry**, v. 16, n. 6, p. 721–727, 2009.

LI, Y.; HU, M.; MCCLEMENTS, D.J. Factors affecting lipase digestibility of emulsified lipids using an in vitro digestion model: Proposal for a standardised pH-stat method. **Food Chemistry**, v. 126, n. 2, p. 498–505, 2011.

LI, Y.; MCCLEMENTS, D.J. New Mathematical Model for Interpreting pH-Stat Digestion Profiles: Impact of Lipid Droplet Characteristics on in Vitro Digestibility. **Journal of Agricultural and Food Chemistry**, v. 58, n. 13, p. 8085–8092, 2010.

LI, Q.; RUDOLPH, V.; WEIGL, B., EARL, A. Interparticle van der Waals force in powder flowability and compactibility. **International Journal of Pharmaceutics**, v.280, p. 77– 93, 2004.

LIN, Q.; LIANG, R.; WILLIAMS, P.A.; ZHONG, F. Factors affecting the bioaccessibility of β-carotene in lipid-based microcapsules: Digestive conditions, the composition, structure and physical state of microcapsules. **Food Hydrocolloids**, v.77, p. 187-203, 2018.

LIU, F.; TANG, C. Emulsifying Properties of Soy Protein Nanoparticles: Influence of theProtein Concentration and/or Emulsification Process. **Journal of Agricultural and Food Chemistry,** v. 62, n. 12, p. 2644–2654, 2014.

LIU, G.Y.; WANG, J.M.; XIA, Q. Application of nanostructured lipid carrier in food forthe improved bioavailability. **European Food Research and Technology**, v. 234, n. 3, p. 391–398, 2012.

LIU, C.H.; WU, C.T. Optimization of nanostructured lipid carriers for lutein delivery. **Colloids and Surfaces A: Physicochemical and Engineering Aspects**, v. 353, n.2- 3, p. 149–156, 2010.

LIVNEY, Y.D. Nanostructured delivery systems in food: latest developments and potential future directions. **Current Opinion in Food Science**, v. 3, p.25–135, 2015.

LOBATO, K.B.S *et al*. Characterization and stability evaluation of bixin nanocapsules. **Food Chemistry**, v. 141, n. 4, p. 3906–3912, 2013.

LOH, J.W.; YEOH, G.; SAUNDERS, M.; LIM, L. Uptake and cytotoxicity of chitosan nanoparticles in human liver cells. **Toxicology and Applied Pharmacology**, v. 249, n. 2, p. 148–157, 2010.

MACGIBBON, A. K. H.; TAYLOR, M. W. Composition and structure of bovine milk lipids. In: FOX, P. F. and McSWEENEY, P. L. H. **Advanced Dairy Chemistry. Lipids**. 3rd edition. New York: Springer. v. 2, cap. 1, p.1-35, 2006.

MARANGONI, A. G. Crystallization kinetics. In: MARANGONI, A. G. **Fat Crystal Networks.** New York: Marcel Dekker, p. 21-82, 2005.

MARANGONI, A.; ROUSSEAU, D. The Effects of Interesterification on the Physical Properties of Fats. *In*: **Physical properties of lipids**. CRC Press, 2002.

MARETTI, E *et al.* In vivo β-carotene skin permeation modulated by Nanostructured Lipid Carriers. **International Journal of Pharmaceutics**, v. 597, 120322, 2021.

MARTINI, S.; AWAD, T.; MARANGONI, A.G. Structure and properties of fat crystal networks. In: **Modifying Lipids for Use in Food**. Ed. GUNSTONE, F. Woodhead Publishing, Cambridge, p.142-169, 2006.

MARTINI, S.; HERRERA, M.L. Physical properties of shortenings with low-trans fatty acids as affected by emulsifiers and storage conditions**. European Journal of Lipid Science and Technology**, v. 110, n. 2, p. 172–182, 2008.

MARTINS, J.T. *et al*. Edible Bio-Based Nanostructures: Delivery, Absorption and Potential Toxicity. **Food Engineering Reviews**, v. 7, p. 419-513, 2015.

MARZE, S. Bioavailability of Nutrients and Micronutrients: Advances in Modeling and In Vitro Approaches. **Annual Review of Food Science and Technology**, v. 8, p. 35-55, 2017.

MCCLEMENTS, D.J. Critical Review of Techniques and Methodologies for Characterization of Emulsion Stability. **Critical Reviews in Food Science and Nutrition**,v. 47, n. 7, p. 611-649, 2007.

MCCLEMENTS, D.J. **Food Emulsions: Principles, Practices and Techniques**. (3rd ed.). CRC Press. Taylor & Francis Group, 2015, 690p.

MCCLEMENTS, D.J. Utilizing food effects to overcome challenges in delivery of lipophilic bioactives: Structural design of medical and functional foods. **Expert Opinion on Drug Delivery**, v. 10, n. 12, p. 1621-1632, 2013.

MCCLEMENTS, D.J.; JAFARI, S.M. Improving emulsion formation, stability and performance using mixed emulsifiers: A review. **Advances in Colloid and Interface Science**, p. 1-94, 2018.

MCCLEMENTS, D.J.; LI, Y. Structured emulsion-based delivery systems: Controlling the digestion and release of lipophilic food components. **Advances in Colloid and Interface Science**, v. 159, p. 213-288, 2010.

MCCLEMENTS, D.J.; LI, F.; XIAO, H. The Nutraceutical Bioavailability Classification Scheme: Classifying Nutraceuticals According to Factors Limiting their Oral Bioavailability. **Annual Review of Food Science and Technology**, v.6, p. 13.1-13.29, 2015.

MCCLEMENTS, D.J.; RAO, J. Food-Grade Nanoemulsions: Formulation, Fabrication, Properties, Performance, Biological Fate, and Potential Toxicity. **Critical Reviews in Food Science and Nutrition**, v, 51, p. 285-330, 2011.

MCCLEMENTS, D.J.; XIAO, H. Excipient foods: designing food matrices that improve the oral bioavailability of pharmaceuticals and nutraceuticals. **Food & Function**, v.5.; p. 1320-1333, 2014.

MCCLEMENTS, J.; MCCLEMENTS, D.J. Standardization of Nanoparticle Characterization: Methods for Testing Properties, Stability, and Functionality of Edible Nanoparticles. **Critical Reviews in Food Science and Nutrition**, v. 56, n. 8, p. 1334–1362, 2016.

MEHNERT, W.; MADER, K. Solid lipid nanoparticles: production, characterization and applications. **Advanced Drug Delivery Reviews**, v.64, p. 83-101, 2012.

MENSINK, R.P. Effects of stearic acid on plasma lipid and lipoproteins in humans. **Lipids**, v.40, n.12, p.1201-1205, 2005.

METIN, S.; HARTEL, R. W. Crystallization of fats and oils. In: SHAHIDI, F. (Ed.). **Bailey´s Industrial Oil and Fat Products**. New York: Wiley-Interscience, v.1, p. 45-76,2005.

MEYERS, D. **Surfactant Science and Technology**. Hoboken, NJ: John Wiley & Sons; 2006.

MINEKUS, M *et al*. A standardised static in vitro digestion method suitable for food – an international consensus. **Food & Function**, v. 5, n. 6, p. 1113–1124, 2014.

MITRI, K *et al*. Lipid nanocarriers for dermal delivery of lutein: preparation, characterization, stability and performance. **International Journal of Pharmaceutics**, v. 414, n. 1–2, p. 267–275, 2011.

MOHAMMADI, M.; ASSADPOUR, E.; JAFARI, S.M. Encapsulation of food ingredientes by nanostructured lipid carriers (NLCs). In: **Lipid-Based Nanostructures for Food Encapsulation Purposes**, v.2, p.217-270, 2019.

MORARU, C. I *et al*. Nanotechnology: a new frontier in food science. **Food Technology**, v. 57, n. 12, p. 24–29, 2003.

MORETTO, E.; FETT, R. **Tecnologia de óleos e gorduras vegetais na indústria de alimentos**. 1. ed. São Paulo: Livraria Varela, 1998. 150 p.

MOZAFARI, M.R. *et al*. Recent trends in the lipid-based nanoencapsulation of antioxidants and their role in foods. **Journal of the Science of Food and Agriculture**, v. 86, p. 2038-2045, 2006.

MÜLLER, R.H. *et al*. Lipid nanoparticles (SLN) - An alternative colloidal carrier systemfor controlled drug delivery. **European Journal of Pharmaceutics and Biopharmaceutics**, v.41, p. 62–69, 1995.

MÜLLER, R.H *et al*. Cytotoxicity of magnetite loaded polylactide polylactide/glycolide particle and solid lipid nanoparticles (SLN). **International Journal of Pharmaceutics,** v.138, p. 85–94, 1996.

MÜLLER, R.H.; KECK, C.M. Challenges and solutions for the delivery of biotech drugs-a review of drug nanocrystal technology and lipid nanoparticles. **Journal of Biotechnology**¸v. 113, n. 1-3, p. 151-170, 2004.

MÜLLER, R.H.; MÄDER, K.; GOHLA, S. Solid lipid nanoparticles (SLN) for controlled drug delivery - a review of the state of the art. **European Journal of Pharmaceutics and Biopharmaceutics**, v.50, p. 161–177, 2000.

MÜLLER, R.H.; RADTKE, M.; WISSING, S.A. Nanostructured lipid matrices for improved microencapsulation of drugs. **International Journal of Pharmaceutics**, v. 24, p.121–128, 2002.

MURPHY, Douglas B; DAVIDSON, Michael W. **Fundamentals of light microscopy and electronic imaging.** 2nd. ed. New York: John Wiley & Sons, 2012.

NATIONAL NANOTECHNOLOGY INITIATIVE. NNI. **Nanotechnology**. Disponível em: http://www.nano.gov/. Acesso em: 20 set 2016.

NEETHIRAJAN, S; JAYAS, D. S. Nanotechnology for the food and bioprocessing industries**. Food and Bioprocess Technology**, v.4, p. 39–47, 2011.

NGUYEN, H.M.; HWANG, I.C.; PARK, J.W.; PARK, H.J. Enhanced payload and photo-protection for pesticides using nanostructured lipid carriers with corn oil as liquid lipid. **Journal of Microencapsulation**, v. 29, n. 6, p. 596–604, 2012.

NIK, A.M.; LANGMAID, S.; WRIGHT, A.J. Nonionic surfactant and interfacial structure impact crystallinity and stability of β-carotene loaded lipid nanodispersions. **Journal of Agricultural and Food Chemistry**, v. 60, n. 16, p. 4126–4135, 2012.

O'BRIEN, R.D. Fats and Oils Analysis. In: **Fats and Oils – Formulating and Processing for Applications**. Ed. O'BRIEN, R.D. 3rd ed.CRC Press, New York, 2008.

OKONOGI, S.; RIANGJANAPATEE, P. Physicochemical characterization of lycopene-loaded nanostructured lipid carrier formulations for topical administration. **International Journal of Pharmaceutics**, v. 478, n. 2, p. 726–735, 2015.

OLIVEIRA, D.R.B *et al*. β-Carotene-loaded nanostructured lipid carriers produced by solvent displacement method. **Food Research International**, v. 90, p. 139-146, 2016.

OLIVEIRA, D.R.B.; FURTADO, G.F.; CUNHA, R.L. Solid lipid nanoparticles stabilized by sodium caseinate and lactoferrin. **Food Hydrocolloids**, v.90, p.321-329, 2019.

OLIVEIRA, G. M.; RIBEIRO, A. P. B.; KIECKBUSCH, T. G. Hardfats improve technological properties of palm oil for applications in fat-based products **LWT - Food Science and Technology**, v. 63, n. 2, p. 1155–1162, 2015.

PALMERO, P *et al*. Lycopene and β-carotene transfer to oil and micellar phases during in vitro digestion of tomato and red carrot based-fractions. **Food Research International**, v. 64, p. 831-838, 2014.

PAN, Y.; TIKEKAR, R.V.; NITIN, N. Distribution of a Model Bioactive within Solid Lipid Nanoparticles and Nanostructured Lipid Carriers Influences its Loading Efficiency and Oxidative Stability. **International Journal of Pharmaceutics**, v. 511, n.1, p. 322-330, 2016.

PARDEIKE, J.; HOMMOSS, A.; MÜLLER, R.H. Lipid nanoparticles (SLN, NLC) in cosmetic and pharmaceutical dermal products. **International Journal of Pharmaceutics**, v. 366, p. 170–184, 2009.

PATEL, A.; HU, Y.; TIWARI, J.K.; VELIKOV, K.P. Synthesis and characterisation of zein–curcumin colloidal particles. **Soft Matter**, v. 6, n. 24, p. 6192-6199, 2010.

PATEL, M.R.; MARTIN-GONZALEZ, F.S. Characterization of ergocalciferol loadedsolid lipid nanoparticles. **Journal of Food Science,** v.77, n.1, p.8-13, 2012.

PEZESHKI, A.; HAMISHEHKAR, H.; GHANBARZADEH, B.; FATHOLLAHYD, I.; NAHR, F.K.; HESHMATI, M.K.; MOHAMMADI, M. Nanostructured lipid carriers as a favorable delivery system for β-carotene. **Food Bioscience**, v.27, p.11-17, 2019.

PINHEIRO, A.C.; GONÇALVES, R.F.S.; MADALENA, D.A.; VICENTE, A. A. Towards the understanding of the behavior of bio-based nanostructures during in vitro digestion. **Current Opinion in Food Science**, v. 15, p. 79-86, 2017.

PINHEIRO, A.C *et al.* Unravelling the behaviour of curcumin nanoemulsions during in vitro digestion: Effect of the surface charge. **Soft Matter**, v. 9, n. 11, p. 3147–3154, 2013.

PINTO, F.; BARROS, D.P.C.; FONSECA, L.P. Design of multifunctional nanostructured lipid carriers enriched with α-tocopherol using vegetable oils. **Industrial Crops & Products**, v. 118, p. 149-159, 2018.

PORTER, C.J.H.; TREVASKIS, N.L.; CHARMAN, W.N. Lipids and lipid-based formulations: Optimizing the oral delivery of lipophilic drugs. **Nature Reviews. Drug Discovery**, v.6, n.3, p. 231–248, 2007.

POWELL, J.J.; FARIA, N.; THOMAS-MCKAY, E.; PELE, L.C. Origin and fate of dietary nanoparticles and microparticles in the gastrointestinal tract. **Journal of Autoimmunity**, v. 34, p. 226-233, 2010.

PURI, A. *et al*. Lipid based nanoparticles as pharmaceutical drug carriers: from conceptto clinic. **Critical Reviews in Therapeutic Drug Carrier Systems**, v.26, p.523-580, 2009.

PYO, S.M.; MÜLLER, R.H.; KECK, C.M. Encapsulation by nanostructured lipid carriers. In book: **Nanoencapsulation Technologies for the Food and Nutraceutical Industries**, p.114-137, 2017.

QIAN, C *et al*. Impact of lipid nanoparticle physical state on particle aggregation and β-carotene degradation: potential limitations of solid lipid nanoparticles. **Food Research International**, v. 52, n. 1, p. 342–349, 2013.

QIAN, C *et al*. Physical and chemical stability of β-carotene-enriched nanoemulsions: Influence of pH, ionic strength, temperature, and emulsifier type. **Food Chemistry**, v.132, p.1221-1229, 2012.

QUEIRÓS, M.S.; VIRIATO, R.L.S.; RIBEIRO, A.P.B.; GIGANTE, M.L. Development of solid lipid nanoparticle and nanostructured lipid carrier with dairy ingredients. **International Dairy Journal**, 105186, 2021.

RAWAL, S.U.; PATEL, M.M. Lipid nanoparticulate systems: Modern versatile drug carriers. In: **Lipid Nanocarriers for Drug Targeting**. Grumezescu, A, Eds.: William Andrew. Publishing. Elsevier, p. 49-138, 2018.

REBOUL, E. *et al*. Bioaccessibility of Carotenoids and Vitamin E from Their Main Dietary Sources. **Journal of Agricultural and Food Chemistry**, v. 54, n.8, p. 8749-8755, 2006.

RIBEIRO, A. P. B. *et al*. Influence of chemical interesterification on thermal behavior, microstructure, polymorphism and crystallization properties of canola oil and fully hydrogenated cottonseed oil blends. **Food Research International**, v. 42, n. 8, p. 1153–1162, 2009.

RIBEIRO, A. P. B.; BASSO, R.C.; KIECKBUSCH, T. G. Effect of the addition of hardfats on the physical properties of cocoa butter**. European Journal of Lipid Science and Technology**, v. 115, n. 13, p. 301-312, 2013.

RIBEIRO, H. S.; AX, K.; SCHUBERT, H. Stability of lycopene emulsions in food systems. **Journal of Food Science**, v. 68, n. 9, p.2730-2734, 2003.

RIBNICKY, D.M *et al*. Effects of a high fat meal matrix and protein complexation on the bioaccessibility of blueberry anthocyanins using the TNO gastrointestinal model (TIM-1). **Food Chemistry**, v. 142, p. 349-357, 2014.

ROBLES, L.V *et al*. Nanopartículas lipídicas sólidas. **Revista Mexicana de Ciências Farmacêuticas**, v.39, n.1, p.38-52, 2008.

RODRIGUEZ-RUIZ, V *et al.* Astaxanthin-loaded nanostructured lipid carriers for preservation of antioxidant activity. **Molecules**, v. 23, n. 10, 2018.

ROHMAH, M.; RAHARJO, S.; HIDAYAT, C.; MARTIEN, R. Application of Response Surface Methodology for the Optimization of β-Carotene-Loaded Nanostructured Lipid Carrier from Mixtures of Palm Stearin and Palm Olein. **Journal of the American Oil Chemists' Society**, v. 97, n. 2, p. 213–223, 2020.

SALVIA-TRUJILLO, L *et al*. Edible Nanoemulsions as Carriers of Active Ingredients: A Review. **Annual Review of Food Science and Technology**, p. 20.1-20.8, 2017b.

SALVIA-TRUJILLO, L *et al*. Lipid digestion, micelle formation and carotenoid bioaccessibility kinetics: Influence of emulsion droplet size. **Food Chemistry**, v. 229, p.653-662, 2017a.

SALVIA-TRUJILLO, L *et al*. Lipid nanoparticles with fats or oils containing β-carotene: Storage stability and in vitro digestibility kinetics. **Food Chemistry**, v.278, p.396-405, 2019.

SALVIA-TRUJILLO, L.; QIAN, C.; MARTÍN-BELLOSO, O.; MCCLEMENTS, D.J. Influence of particle size on lipid digestion and β-carotene bioaccessibility in emulsions and nanoemulsions. **Food Chemistry**, v. 141, n. 2, p. 1472–1480, 2013.

SANTOS, V *et al*. Nanostructured lipid carriers loaded with free phytosterols for food applications. **Food Chemistry**, v. 298, 125053, 2019.

SATO, K. Crystallization behavior of fats and lipids: a review. **Chemical Engineering Science.** Oxford, v. 56, n. 7, p. 2255-2265, 2001.

SAUVANT, P.; CANSELL, M.; SASSI, A.H.; ATGIÉ, C. Vitamin A enrichment: Caution with encapsulation strategies used for food applications. **Food Research International**, v. 46, p. 469-479, 2012.

SAWANT, K.K.; DODIYA, S.S. Recent advances and patents on solid lipid nanoparticles. **Recent Patents on Drug Delivery & Formulation**, v.2, n.2, p. 120– 135, 2008.

SCHUBERT, H.; ENGEL, R. Product and formulation engineering of emulsions. **Chemical Engineering Research & Design**, v. 82, n. 9, p. 1137–1143, 2004.

SCRIMGEOUR, C. Chemistry of Fatty Acids. In: SHAHIDI, F. **Bailey's Industrial Oil and Fat Products**. Edible Oil and Fat Products: Chemistry, Chemical properties, and health effects. Sixth Edition v.2, Hoboken, New Jersey: John Wiley & Sons, 2005.

SERRA, M.L.G. *et al*. Preparación de nanopartículas sólidas lipídicas (SLN), y eacarreadores lipídicos nanoestruturados (NLC). **Revista Mexicana de Ciências Farmacêuticas**, v.39, n.4, p.50-66, 2008.

SEVERINO, P.; PINHO, S.C.; SOUTO, E.B.; SANTANA, M.H.A. Polymorphism, crystallinity and hydrophilic-lipophilic balance of stearic acid and stearic acid-capric/caprylic triglyceride matrices for production of stablenanoparticles. **Colloids and Surfaces B: Biointerfaces**, v. 86, n. 1, p. 125–130, 2011.

SEVERINO, P.; SANTANA, M.H.A.; SOUTO, E.B. Optimizing SLN and NLC by 2^2 full factorial design: effect of homogeneization technique. **Materials Science and Engineering**, v. 32, n. 6, p. 1375–1379, 2012.

SHAH, R.; ELDRIDGE, D.; PALOMBO, E.; HARDING, I. **Lipid Nanoparticles: Production, Characterization and Stability**. SPRINGER BRIEFS IN PHARMACEUTICAL SCIENCE & DRUG DEVELOPMENT p.1-97, 2015.

SHANGGUAN, M *et al*. Binary lipids-based nanostructured lipid carriers for improved oral bioavailability of silymarin. **Journal of Biomaterials Applications**, v. 28, n. 6, p. 887–896, 2014.

SHARMA, V.K. *et al*. Solid lipid nanoparticles system: an overview. **International Journal of Research in Pharmaceutical Sciences,** v.2, p. 450-461, 2011.

SHUKAT, R.; BOURGAUX, C.; RELKIN, P. Crystallisation behaviour of palm oil nanoemulsions carrying vitamin E: DSC and synchrotron X-ray scattering studies. **Journal of Thermal Analysis and Calorimetry**, v. 108, n. 1, p. 153–161, 2012.

SOUTO, E.B *et al*. Nanopartículas de lipídios sólidos: métodos clássicos de produção laboratorial. **Química Nova**, v.34, p. 1762-1769, 2011.

SOUTO, E.B.; MEHNERT, W.; MÜLLER, R.H. Polymorphic behaviour of Compritol®888 ATO as bulk lipid and as SLN and NLC. **Journal of Microencapsulation,** v.23, p. 417-433, 2006.

SOUZA, A.L.R *et al.* Loading of praziquantel in the crystal lattice of solid lipid nanoparticles. **Journal of Thermal Analysis and Calorimetry**, v. 108, n.1, p. 353–360, 2012.

SY, C *et al*. Effects of physicochemical properties of carotenoids on their bioaccessibility, intestinal cell uptake, and blood and tissue concentrations. **Molecular Nutrition & Food Research**, v. 56, n. 9, p. 1385-397, 2012.

TAIZ, L.; ZEIGER, E. **Fisiologia e desenvolvimento vegetal**. 6.ed. Porto Alegre: Artmed, 2017, 888p.

TAMJIDI, F *et al.* Design and characterization of astaxanthin-loaded nanostructured lipid carriers. **Innovative Food Science and Emerging Technologies**, v. 26, p. 366–374, 2014.

TAMJIDI, F; SHADEDI, M.; VARSHOSAZ, J.; NASIRPOUR, J. Nanostructured lipid carriers (NLC): A potential delivery system for bioactive food molecules. **Innovative Food Science and Emerging Technologies**, v. 19, p. 29-43, 2013.

TAN, Y *et al*. Factors impacting lipid digestion and β-carotene bioaccessibility assessed by standardized gastrointestinal model (INFOGEST): oil droplet concentration. **Food Research International**, v. 11, n. 8, p. 7126–7137, 2020.

TAN, C.P.; CHE MAN, Y.B. Differential scanning calorimetric analysis of palm, palm oil based products and coconut oil: effects of scanning rate variation. **Food Chemistry**. v.76, p.89-102, 2002.

TAN, Y.; MCCLEMENTS, D.J. Improving the bioavailability of oil-soluble vitamins by optimizing food matrix effects: A review. **Food Chemistry**, v. 348, 129148, 2021.

TORO-VAZQUEZ, J. F.; RANGEL-VARGAS, E.; DIBILDOX-ALVARADO, E.; CHARÓ-ALONSO, M. A. Crystallization of cocoa butter with and without polar lipids evaluatedby rheometry, calorimetry and polarized light microscopy. **European Journal of Lipid Science and Technology**, v. 107, n. 9, p. 641–655, 2005.

VALENZUELA, A.; DELPALNQUE, B.; TAVELLA, M. Stearic acid: a possible substitute for *trans* fatty acids from industrial origin. **Grasas y Aceites**, v. 62, n. 2, p. 131–138, 2011.

VARSHOSAZ, J.; ESKANDARI, S.; TABAKHIAN, M. Production and optimization of valproic acid nanostructured lipid carriers by the Taguchi design. **Pharmaceutical Development and Technology**, v. 15, n. 1, p. 89–96, 2010.

VERKEMPINCK, S.H.E. Emulsion stability during gastrointestinal conditions effects lipid digestion kinetics. **Food Chemistry**, v. 246, p. 179-191, 2018.

VERRIJSSEN, T.A.J. *et al*. Relation between in vitro lipid digestion and β-carotene bioaccessibility in β-carotene-enriched emulsions with different concentrations of L-α-phosphatidylcholine. **Food Research International**, v. 67, p. 60-66, 2015.

WANG, X *et al*. Flocculation of oil-in-water emulsions stabilised by milk protein ingredients under gastric conditions: Impact on in vitro intestinal lipid digestion. **Food Hydrocolloids**, v.88, p. 272-282, 2019.

WANG, J *et al*. Preparation and characterization of novel lipid carriers containing microalgae oil for food applications. **Journal of Food Science**, v.79, n. 2, p.169-177, 2014.

WASSEL, P.; YOUNG, N.W.G. Food applications of trans fatty acid substitutes. **International Journal of Food Science and Technology**, v. 42, n. 5, p. 503-517, 2007.

WEISS, J *et al*. Solid lipid nanoparticles as delivery systems for bioactive food components. **Food Biophysics**, v. 3, n. 2, p. 146–154, 2008.

WEISS, J.; GAYSINSKY, S.; DAVIDSON, M.; MCCLEMENTS, D.J. Nanostructured Encapsulation Systems: Food Antimicrobials. **In: Global Issues in Food Science and Technology**, p. 425-479, 2009.

WEISS, J.; TAKHISTOV, P.; McCLEMENTS, J. Functional materials in foodnanotechnology. **Journal of Food Science**, v.71, n. 9, p.107-116, 2006.

WICKHAM, M.; FAULKS, R.; MILLS, C. In vitro digestion methods for assessing the effect of food structure on allergen breakdown. **Molecular Nutrition & Food Research**, v. 53, p. 952-958, 2009.

WILDE, P.J.; CHU, B.S. Interfacial & colloidal aspects of lipid digestion**. Advances in Colloid and Interface Science**, v. 165, n. 1, p. 14-22, 2011.

WINDBERGS, M.; STRACHAN, C.J; KLEINEBUDDE, P. Investigating the principles of recrystallization from glyceride melts. **AAPS PharmSciTech**, v. 10, n. 4, p. 1224–1233, 2009.

YANG *et al*. Preparation of 9Z-β-Carotene and 9Z-β-Carotene High-Loaded Nanostructured Lipid Carriers: Characterization and Storage Stability. **Journal of Agricultural and Food Chemistry**, v. 68, n. 47, p. 13844-13853, 2020.

YIN, L; CHU, B.; KOBAYASHI, I.; NAKAJIMA, M. Performance of selected emulsifiers and their combinations in the preparation of [beta]-carotene nanodispersions. **Food Hydrocolloids,** v. 23, n. 6, p. 1617–1622, 2009.

YOO, M.J.Y.; CHEN, X. D. GIT Physicochemical Modeling- A Critical Review. **International Journal of Food Engineering**, v. 2, n. 4, p. 1–10, 2006.

YOON, G.; PARK, J.W.; YONN, I. Solid lipid nanoparticles (SLNs) and nanostructured lipid carriers (NLCs): recent advances in drug delivery. **Journal of Pharmaceutical Investigation**, v. 43, p.353–362, 2013.

YOUNG, F.V.K. Interchangeability of fats and oils. **Journal of the American Oil Chemists' Society**, v. 62, n.2, p. 372-376, 1985.

YU, H.; HUANG, Q. Investigation of the cytotoxicity of food-grade nanoemulsions in Caco-2 cell monolayers and HepG2 cells. **Food Chemistry**, v. 141, n. 1, p. 29–33, 2013.

ZARDINI, A.A *et al.* Production and characterization of nanostructured lipid carriers and solid lipid nanoparticles containing lycopene for food fortification. **Journal of Food Science and Technology**, v. 55, n. 1, p. 287–298, 2018.

ZHANG, L. *et al*. Transparent dispersions of milk-fat-based nanostructured lipid carriersfor delivery of β-carotene. **Journal of Agricultural and Food Chemistry**, v. 61, n. 39, p. 9435–9443, 2013.

ZHENG, K. *et al*. The effect of polymer surfactant emulsifying agent on the formation and stability of aciaded nanostructured lipid carriers (NLC). **Food Hydrocolloids**, v. 32, p.72-78, 2013.

ZHOU, X. *et al*. Stability and in vitro digestibility of beta-carotene in nanoemulsions fabricated with different carrier oils. **Food Science & Nutrition**, v. 6, n. 8, p. 2537–2544, 2018.

CAPÍTULO III

Performance of natural and synthetic emulsifiers in the optimization of high pressure homogenization conditions to produce nanostructured lipid carriers

Submitted to Journal of Food Engineering

3. Performance of natural and synthetic emulsifiers in the optimization of high pressure homogenization conditions to produce nanostructured lipid carriers

Fernanda Luisa Lüdtke[a], Marcella Aparecida Stahl[a], Renato Grimaldi[a], Marcus Bruno Soares Forte[a], Mirna Lúcia Gigante[a], Ana Paula Badan Ribeiro[a]

[a]Department of Food Engineering and Technology, School of Food Engineering, State University of Campinas (UNICAMP), 13083-862, Campinas, SP, Brazil.

ABSTRACT

Lipid-based nanoparticles are one of the most promising encapsulation technologies in the field of nanotechnology, and solid lipid nanoparticles were the first generation of such structures. The second generation of lipid nanostructures is the nanostructured lipid carriers (NLC), which are composed of lipid materials with different melting points (MP). High pressure homogenization (HPH) is one of the main methods used on an industrial scale to produce NLC, and the process conditions affect the characteristics and physical stability of the produced NLC. The objective of this study was to optimize the HPH process conditions (number of cycles and homogenization pressure) to produce NLC formulated with different emulsifiers. The pre-emulsion for producing NLC was composed of an aqueous phase (90%) with a single emulsifier (ethoxylated sorbitan monooleate (Tween 80), sorbitan monostearate (Span 60), soy protein isolate (SPI), whey protein isolate (WPI), or enzymatically modified soy lecithin (SL) in a 2% (w/w) proportion, and a lipid phase composed of glyceryl tristearate (TS) and glyceryl trioleate (TO) in a 40:60 (w/w) proportion, corresponding to a model system containing similar contents of saturated and unsaturated fatty acids. The influence of the homogenization pressure (HP) and the number of cycles (NC) on the characteristics of the NLC was assessed separately for each emulsifier using a full 2^2 factorial design. The NLC were characterized by the particle size (PS), polydispersity index (PDI), and zeta potential (ZP) at 24 h and 15 days after production. The results indicated that SL, Tween 80, and WPI promoted the production of NLC in the nanometric range (PS ranging from 136.00 to 277.17 nm) that were stable (ZP > |20 mV|) during 15 days of storage at 25 °C. Of all the process conditions, 700 bar and 2 cycles were the optimal conditions for producing NLC with the different emulsifiers used in this study.

Keywords: Lipid nanoparticles, emulsifiers, high pressure homogenization, lipid matrices.

3.1 Introduction

Nanotechnology has emerged as an important area of public interest worldwide, with the potential to drastically affect the scientific community and world market (Chen et al., 2006; Weiss et al., 2008). Nanodelivery systems present great prospects for nanotechnology in the food industry and are one of the most promising technologies for revolutionizing conventional food science and the food industry (He and Hwang, 2016; Sawant and Dodiya, 2008).

Nanoparticles developed from lipids have gained prominence among nanodelivery systems, mainly for their ability to carry lipophilic bioactive compounds to the adsorption site in the human gastrointestinal tract. As lipids are part of human nutrition and an integral part of many physiological and biochemical processes, lipid-based nanoparticulate systems are

considered one of the safest, most biocompatible, most versatile, and affordable means of delivering compounds (Attama et al., 2012). In addition, they present advantages such as high physical and chemical stability, possibility of large-scale production, and controlled delivery of compounds (Helgason et al., 2009; Rawal and Patel, 2018).

Nanostructured lipid carriers (NLC) were developed to overcome some problems and limitations of other lipid-based delivery systems, such as solid lipid nanoparticles (SLN), which not only have a lower capacity for incorporating bioactives but also have high water content (70-99%), a disadvantage that often makes this type of nanostructure unsuitable for compound delivery and for application in some foods (Chen et al., 2020; Dumont et al., 2018). NLC are a type of oil-in-water emulsion composed of high- and low-melting-point lipids in their matrix, together with emulsifiers in the external phase to obtain a fine dispersion of these lipids in an aqueous medium (Akhavan et al., 2018).

NLC can be produced through several methods; high pressure homogenization (HPH) is the most used method for producing particles in the nanometric range in the food industry (Katouzian et al., 2017; Schubert and Engel, 2004), mainly due to the ease of scale transposition, absence of organic solvents, and short production time compared to other production methods (Pardeike et al., 2009). The homogenization step can be performed with different cycles and at different pressures, which directly affect the characteristics of the produced NLC (Jafari et al., 2007).

The essential components for producing NLC consist of the lipid phase, emulsifiers, and water (Tamjidi et al., 2013). Emulsifiers are amphiphilic molecules that have hydrophobic and hydrophilic groups in their structure, and include small-molecular-size surfactants, phospholipids (PL), proteins, and polysaccharides, among others (McClements and Gumus, 2016). They play two fundamental roles in the formation of emulsions: firstly, they facilitate emulsion formation, and secondly, they promote emulsion stability (Ozturk and McClements, 2016).

Emulsifiers are essential to stabilize lipid nanoparticles (LN) dispersions and prevent their agglomeration. The selection of the ideal emulsifier for producing LN is based on its properties, such as charge, molecular weight, chemical structure, and hydrophilic/lipophilic balance (HLB) (Attama et al., 2012). There are great differences in the ability of an emulsifier to rapidly adsorb onto lipid droplets during homogenization, and therefore, in its ability to reduce interfacial tension, resulting in the production of particles of different sizes, even using the same process conditions (McClements and Gumus, 2016). In general, the greater the ability of an emulsifier to reduce surface tension, the smaller the particle sizes produced by HPH (Håkansson et al., 2013).

The emulsifiers used to produce NLC can be synthetic or natural. Synthetic emulsifiers have been used in many studies to produce NLC, but studies using natural

emulsifiers are gaining ground owing to the growing appeal for clean-label products. Moreover, they can be used separately or combined (McClements and Jafari, 2018). Each emulsifier was used separately in this study to determine the individual effect of natural (SL, WPI, and SPI) and synthetic (Tween 80 and Span 60) emulsifiers on the production of NLC.

Sorbitan fatty acid esters correspond to a class of nonionic emulsifiers widely used in the food industry. They are derived from a reaction between sorbitol and a variety of commercially available fatty acids, such as lauric, palmitic, oleic, and stearic acid. The larger the chain length of the fatty acid ester, the lower the HLB, and therefore, the more hydrophobic the molecule. Sorbitan monostearate (Span 60) is an ester obtained by the reaction of sorbitan with stearic acid, a non-ionic emulsifier that presents a HLB of 4.7 (Cottrell and van Peiji, 2004).

Tween 80 is a nonionic, water-soluble emulsifier derived from polyethoxylated sorbitan and oleic acid. It is considered suitable to stabilize NLC owing to its HLB (~15) (Mohammadi et al., 2019). Nonionic emulsifiers form a compact film around nanoparticle surfaces and stabilize NLC formulations by creating steric hindrance (Souto et al., 2004). Such stabilization by steric hindrance typically results in the production of particles with smaller dimensions and that resist changes in pH and electrolyte concentration (McClements and Rao, 2011).

Lecithins are neutral surfactants that are found naturally in plant sources, such as soy and canola, and animal sources, such as eggs, and are generally recognized as safe (GRAS). Owing to their wide availability, they are considered low-cost emulsifiers with potential for producing NLC (Katouzian et al., 2017; McClements, 2015; Mohammadi et al., 2019). Standard (commercial) soy lecithin, obtained from the degumming step during oil refining, is composed of a mixture of PL and other substances. Physical, chemical, and enzymatic modifications are performed on standard lecithin to improve its emulsifying properties, heat resistance, and dispersion in aqueous or oily systems. Soy lecithin (SOLEC™ AE IP) (HLB 7-8) is an enzymatically hydrolyzed lecithin; enzymatic treatment produces lecithin with a high lysophospholipid/PL ratio, thereby increasing its emulsifying capacity for stabilization of O/A-type emulsified systems (Fernandes et al., 2012; Tanno, 2012). Although most emulsifiers used for producing NLC are small molecules, macromolecules such as proteins are natural and biocompatible ingredients that have been used in the stabilization of lipid nanoparticles (Mohammadi et al., 2019). WPI and SPI are among such emulsifiers. WPI is one of the ingredients most used in the food industry to obtain oil-in-water emulsions. It is composed of two main fractions, β-lactoglobulin and α-lactalbumin, which together account for about 70% of the protein content in whey (Chatterton et al., 2006). SPI is a byproduct of soybean oil extraction and is a natural and low-cost constituent of commercial products (Wang et al., 2019). SPI is composed of two main protein fractions, glycine and β-conglycinin, which in combination account for more than 70% of the protein content in soybeans (Nik et al., 2011).

Some challenges are to be overcome for the application of NL in food products. Some of these are related to formulation components, since the number of emulsifiers approved for food use is limited. Consequently, the search for new alternatives to replace known emulsifiers is an ongoing challenge (Katouzian et al., 2017; Oliveira et al., 2019). Therefore, the objective of this study was to optimize the HPH process conditions (number of cycles and homogenization pressure) to produce NLC from a model emulsion, as well as to assess the effect of different emulsifiers on the physical characteristics and stability of the produced NLC. In particular, this study investigated distinct macromolecules with a wide range of HLB values and emulsifying capacities for a better understanding of the performance of these agents in HPH processes for producing NLC with regular lipid composition.

3.2 Materials and methods

3.2.1 Materials

Glyceryl tristearate (TS; technical-grade tristearin) and glyceryl trioleate (TO; technical-grade triolein), both produced by Sigma-Aldrich (USA), were used as lipid matrices. Whey Protein Isolate (WPI) produced by Alibra (Brazil), Soy Protein Isolate (SPI) SUPRO® 500E IP produced by Solae (Brazil), Enzymatically Hydrolyzed Soy Lecithin (SL) SOLEC™ AE IP (HLB 7-8) produced by Solae (Brazil), Sorbitan Monostearate (Span 60) manufactured by Sigma-Aldrich (USA), and Ethoxylated Sorbitan Monooleate (Tween 80) produced by Sigma-Aldrich (USA) were used as emulsifying agents.

3.2.2 Methods

3.2.2.1 Characterization of raw materials

3.2.2.1.1 Fatty acid composition

Analysis of the composition of FA (FAC) was performed by gas chromatography using the Agilent 6850 GC USA chromatograph system (Santa Clara, CA, USA) after esterification using the Hartman and Lago (1973) method. FA methyl esters were separated according to the AOCS Ce 1f-96 method (AOCS, 2009) using an Agilent DB-23 column (50% cyanopropyl-methylpolysiloxane) 60 m in length, 0.25 mm inner diameter, and 0.25 µm film. The analysis conditions were as follows: oven temperature of 110 °C for 5 min, 110–215 °C (5 °C/min), 215 °C for 24 min; detector temperature of 280 °C; injector temperature of 250 °C; carrier gas: helium; split ratio of 1:50; injected volume of 1.0 µL. The qualitative composition was determined by comparing the peak retention times with those of FA standards.

3.2.2.1.2 Triacylglycerol composition

Analysis of TAG composition was performed by gas chromatography with capillary column (50% phenyl methylpolysiloxane) (DB-17HT Agilent, catalog no. 122-1811) 15 m in length, 0.25 mm inner diameter, and 0.15 μm film. The analysis conditions were as follows: split ratio of 1:100; column temperature of 250 ºC, programed to 350 ºC at a rate of 5ºC/min; carrier gas: helium, flow rate of 1.0 mL/min; injector temperature of 360 ºC; detector temperature 375 ºC; injected volume of 1.0 μL; and sample concentration of 100 mg/5 mL of tetrahydrofuran. The identification of TAG groups was performed by comparing retention times with those of TAG standards, according to the method reported by Antoniosi Filho et al. (1995).

3.2.2.1.3 Solid fat content (SFC)

SFC was determined by pulsed low-resolution nuclear magnetic resonance spectroscopy (NMR) Bruker pc120 Minispec (Silberstreifen, Rheinstetten, Germany), using high precision dry baths with temperature controlled (0–70°C) by the Peltier Tcon 2000 system (Duratech, Garden Grove, USA), according to the direct AOCS Cd 16b- 93 method. Samples were analyzed in series, with tempering of unstabilized fats (AOCS, 2009). MP were calculated using equations for the straight lines of the solid profiles obtained by NMR that corresponded to the temperature at which the lipid systems had a SFC of 4% (Ribeiro et al., 2009).

3.2.2.2 Production of NLC

The pre-emulsion for producing NLC was formulated according to conditions established and consolidated in the scientific literature (Helgason et al., 2009; Qian et al., 2013; Severino et al., 2012; Yang et al., 2014). For SPI and WPI, 2% aqueous solutions were prepared by dissolving the protein isolates in distilled water and were kept under magnetic stirring for 1 h at room temperature (approximately 25 °C). Sodium azide (0.02%) was added as an antimicrobial agent. The solutions were stored overnight under refrigeration (5-7 °C) for complete protein hydration.

The aqueous dispersion of NLC was prepared with 10% (w/w) of the total lipid phase, composed of TS and TO (40:60 TS:TO w/w). The aqueous phase comprised 2% (w/w) of emulsifier in distilled water, in accordance with the protocols of Helgason et al. (2009), Qian et al. (2013), and Yang et al. (2014). The lipid phase was heated to 85 °C. The aqueous solution containing the emulsifier was heated to the temperature of the lipid phase. To prepare the pre-emulsion, the melted lipid phase was added to the aqueous phase at 85 °C under continuous agitation using a model T18 ultra-turrax agitator (IKA, Germany) for 3 min at 10,000 rpm (Severino et al., 2012; Yang et al., 2014). Aqueous NLC dispersions were produced using the hot HPH technique in a high pressure homogenizer (Buffalo series, Homolab 2.20, FBF

Italia) according to the experimental design presented in section 2.2.2 (Rodrigues and Iemma, 2014; Severino et al., 2012).

The nanoemulsions formed were cooled at 5 °C for 24 h to recrystallize the lipid phase and obtain the NLC dispersions, which were subsequently stored at 25 °C for analysis (Kumbhar and Pokharkar, 2013; Qian et al., 2013; Yang et al., 2014). The analytical determinations were performed 48 h after producing the lipid nanostructures and after 15 days of storage at 25 °C (Das et al., 2020; Kumbhar and Pokharkar, 2013; Nik et al., 2012).

3.2.2.3 Experimental design and statistical analysis

The effects of the homogenization pressure (HP) and number of cycles (NC) on the characteristics of the NLC were assessed using a full 2^2 factorial design (Rodrigues and Iemma, 2014; Severino et al., 2012). Table 1 presents the full 2^2 factorial design along with the respective levels for the investigated variables. HP and NC were considered the independent variables of the experimental design, whereas the particle size (PS), polydispersity index (PI), and zeta potential (PZ) were the dependent variables. Individualized designs were prepared for the 40:60 TS:TO (w/w) lipid system, each containing one of the emulsifiers used in the study, with a total of 5 different designs with 7 experimental points each (Kumbhar and Pokharkar, 2013; Qian et al., 2013; Yang et al., 2014). The data were analyzed using Protimiza Experimental Design software. Polynomial equations were generated to establish the relationship between the independent variables (HP and NC) and the dependent or response variables (PS, PDI, and ZP). The proposed model was analyzed for each variable effect and for the interactions between them.

Table 1: 2^2 factorial design, providing the lower (−1), upper (+1) and (0) central point level values for each variable independent.

Variables	Coded levels		Real levels	
	HP (bar)	**NC**	**HP (bar)**	**NC**
1	-1	-1	500	1
2	+1	-1	900	1
3	-1	+1	500	3
4	+1	+1	900	3
5	0	0	700	2
6	0	0	700	2
7	0	0	700	2

HP: homogenization pressure; **NC**: number of cycles.

3.2.2.4 Characterization and stability study of NLC

The characterization and stability study of NLC were carried out by determining the PS, PDI, and ZP (Das et al., 2020; Severino et al., 2012). The analyses were performed in triplicate at room temperature (25 °C), 24 h and 15 days after producing the NLC.

3.2.2.4.1 Particle Size and Polydispersity Index

PS and PDI were determined using a Mastersizer 2000 laser diffractometer (Malvern Instruments). NLC aliquots were added to the equipment reading unit and filled with distilled water at 25 °C under agitation (1750 rpm) until a 2% obscuration rate was obtained. The analyses were performed in triplicate at room temperature (Averina et al., 2011). The mean PS values of the NLC were expressed in terms of the mean surface diameter (D32) obtained using equation 1, and the PDI was determined by calculating the Span (Equation 2).

$$D_{32} \quad \frac{\sum n_i d^3_i}{\sum n_i d^2_i} \qquad \text{(Equation 1)}$$

$$Span = \quad \frac{d_{90}-d_{10}}{d_{50}} \qquad \text{(Equation 2)}$$

where n_i is the number of particles with diameter d_i; and d10, d50, and d90 represent 10%, 50%, and 90% of the cumulative volume of the droplets, respectively.

3.2.2.4.2 Zeta potential

ZP was determined using a Zetasizer Nano-ZS (Malvern Instruments, Malvern, UK), and the samples were diluted (1:100) in distilled water for further analytical determination (Averina et al., 2011). The analyses were performed in triplicate at room temperature.

3.3 Results

3.3.1 Characterization of raw materials

Table 2 shows the fatty acid composition (FAC) of TS, TO, and the 40:60 TS:TO (w/w) lipid system. TS was mostly composed of saturated fatty acids (SFA), corresponding to 99.71% of the fatty acids found in this raw material. Approximately 64% of its composition corresponds to stearic acid (C18:0), followed by palmitic acid (28.71%). This high SFA content explains the high MP of this raw material and its solid state at room temperature.

Table 2. Fatty acid composition (%) of TS, TO and lipid system TS:TO (w/w) 40:60.

Fatty acid (%)	**TS**	**40:60**	**TO**
C10:0 Capric acid	0.08	0.10	0.12
C12:0 Lauric acid	0.09	0.14	0.18
C14:0 Myristic acid	3.51	3.43	3.37
C15:0 Pentadecanoic acid	0.52	0.38	0.29
C16:0 Palmitic acid	28.71	13.97	4.14
C16:1 Palmitoleic acid	0	2.75	4.59
C17:0 Margaric acid	1.88	0.93	0.3
C17:1 8-heptadecanoic acid	0	0.69	1.15
C18:0 Stearic acid	64.15	26.75	1.81
C18:1t Elaidic	0	6.44	10.74
C18:1 Oleic acid	0.14	38.88	64.71
C18:2t Linoleic *trans* acid	0	0.63	1.05
C18:2 Linoleic acid	0.14	4.05	6.66
C18:3 Linolenic acid	0	0.19	0.31
C20:0 Arachidic acid	0.77	0.43	0.21
C20:1 Eicosenoic acid	0	0.22	0.36
ΣSFA	**99.71**	**46.17**	**10.42**
ΣUFA	**0.28**	**53.85**	**89.57**

TO: triolein; **TS:** tristearin; **ΣSFA=** total amount of saturated fatty acids; **ΣAGI=** total amount of unsaturated fatty acids.

TO showed a high concentration of unsaturated fatty acids (UFA) (approximately 90%); oleic acid (C18:1) was the most abundant fatty acid, representing approximately 65% of the FAC of this raw material. The 40:60 TS:TO (w/w) lipid system had a balanced composition of SFA and UFA, justifying its use as a model system in this study, since this ratio between SFA and UFA is quite representative of the composition of NLC structures, given the balance of solid and liquid lipid fractions, as well as the MP characteristic of lipid matrices for this purpose.

Table 3 shows the TAG composition of TS, TO, and the 40:60 TS:TO (w/w) lipid system. There were 6 species of TAG with 46 to 56 carbon atoms in TS, and those with 52 carbon atoms were the most abundant (40.5%), with PSS species being predominant. TS was

composed of approximately 99.55% tri-saturated TAG (SSS). TO contained 15 species of TAG with 48 to 54 carbon atoms; OOO species, a TAG formed by the esterification of glycerol with 3 oleic fatty acids, were predominant. Tri-unsaturated TAG (UUU) were found in greater proportion in this raw material, followed by di-unsaturated groups (SUU), corresponding to 64.67% and 32.56% of the groups, respectively.

Table 3. Triacylglycerol composition (%) of TS, TO and lipid system TS:TO (w/w) 40:60.

Group	TAG (%)	TS	40:60	TO
C46	MPP	3.60	1.44	0
	MPO	0	0.70	1.16
C48	MPoO	0	0.91	1.51
	MPS	13.28	5.31	0
C50	PPS	27.70	11.08	0
	PPO	0	0.97	1.61
	MOO	0	7.92	13.20
	MOL	0	3.97	6.61
	PSS	40.50	16.20	0
C52	POO	0	5.79	9.65
	PoOO	0	9.58	15.96
	PoOL	0	2.63	4.38
	SSS	14.47	5.79	0
	SOO	0	0.95	1.59
C54	OOO	0	22.27	37.12
	OOL	0	4.33	7.21
C56	SSA	0.45	0.18	0
Σ S_3	-	99.55	39.82	0
Σ S_2U	-	0.45	1.84	2.77
Σ SU_2	-	0	19.54	32.56
Σ U_3	-	0	38.80	64.67

TO: triolein; **TS:** tristearin; **P**: Palmitic acid; **M**: Myristic acid; **O**: Oleic acid; **S**: Stearic acid; **L:** Linoleic acid; **Ln**: Linolenic acid; **Po**: Palmitoleic acid; **A**: Arachidonic acid; **S_3**: trisaturated; **S_2U**: monounsaturated; **SU_2:** diunsaturated; **U_3:** triunsaturated.

The 40:60 TS:TO (w/w) lipid system showed a wide range of triacylglycerol species with 46 to 56 carbon atoms, representing a balance between SSS (39.82%) and UUU (38.80%)

TAG, and a significant SUU content (19.54%). The most abundant TAG in this mixture were OOO (22.27%), followed by PSS (16.20%). Since tri-unsaturated TAG have a MP between 54 and 65 °C and tri-unsaturated TAG have a MP between -14 and 5.6 °C (O'Brien, 2008), it can be inferred that the considered lipid mixture has adequate melting characteristics for producing NLC.

Figure 1 shows the solid fat contents of TS, TO, and the 40:60 TS:TO (w/w) lipid system, for a wide temperature range, until complete melting. There was a directly proportional relationship between the percentage of saturated fatty acids in the mixture and the solid fat content, which can be explained by the physical and chemical characteristics of these fatty acids. From this result, it was possible to calculate the MP of lipid materials, considering the temperature of the 4% solids content in the obtained solids curve as a reference value (Ribeiro et al., 2009). TS had the highest MP (60 °C) among all the samples, followed by the 40:60 TS:TO (w/w) lipid system (55 °C). Conversely, TO, owing to its FAC, had a MP below 10 °C (data not shown). These observations confirmed the potential of this lipid system to produce NLC, since it had a MP higher than body temperature (37 ºC).

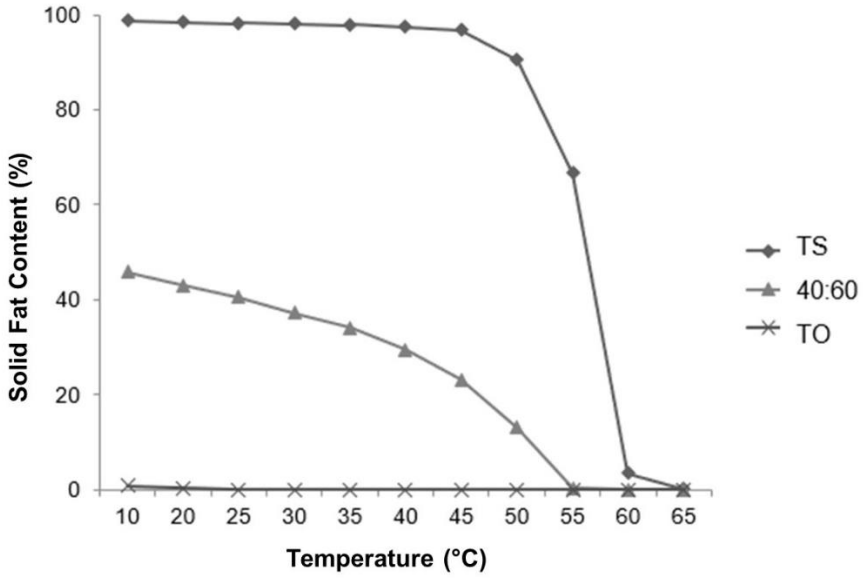

Figure 1. Solid fat content (SFC) (%) as a function of temperature of TS, TO and lipid system TS:TO (w/w) 40:60.

3.3.2 Characterization and stability study of NLC

The experimental conditions for producing NLC using HPH were assessed using a full 2^2 factorial design to analyze the factors that affect the characteristics of nanocarriers, such as PS, PDI, and ZP. For this purpose, it was decided to prepare a design for each emulsifier used in this study and assess its influence on the characteristics of the produced NLC.

For some NLC, the independent variables considered in this study did not show significant effects. Hence, it was not possible to obtain statistical models, and consequently, prepare response surfaces and contour curves. Therefore, Tables 4 to 8 show the effects of HP and NC on the PS, PDI, and ZP of NLC produced with SL, Span 60, SPI, Tween 80, and WPI as emulsifiers, respectively.

The effects of the independent variables on the PS, PDI, and ZP of NLC produced with SL are shown in Figures 2, 3, and 4. The linear model for each of the dependent variables is described below:

$$PS = 157,90 - 15,67_{HP} - 20,25_{NC}$$

$$PDI = 1,62 - 0,17_{HP} - 0,44_{NC}$$

$$ZP = - 48,70 + 1,68_{HP} + 4,26_{NC} + 1,36_{HP.NC}$$

where HP corresponds to the homogenization pressure and NC to the number of cycles.

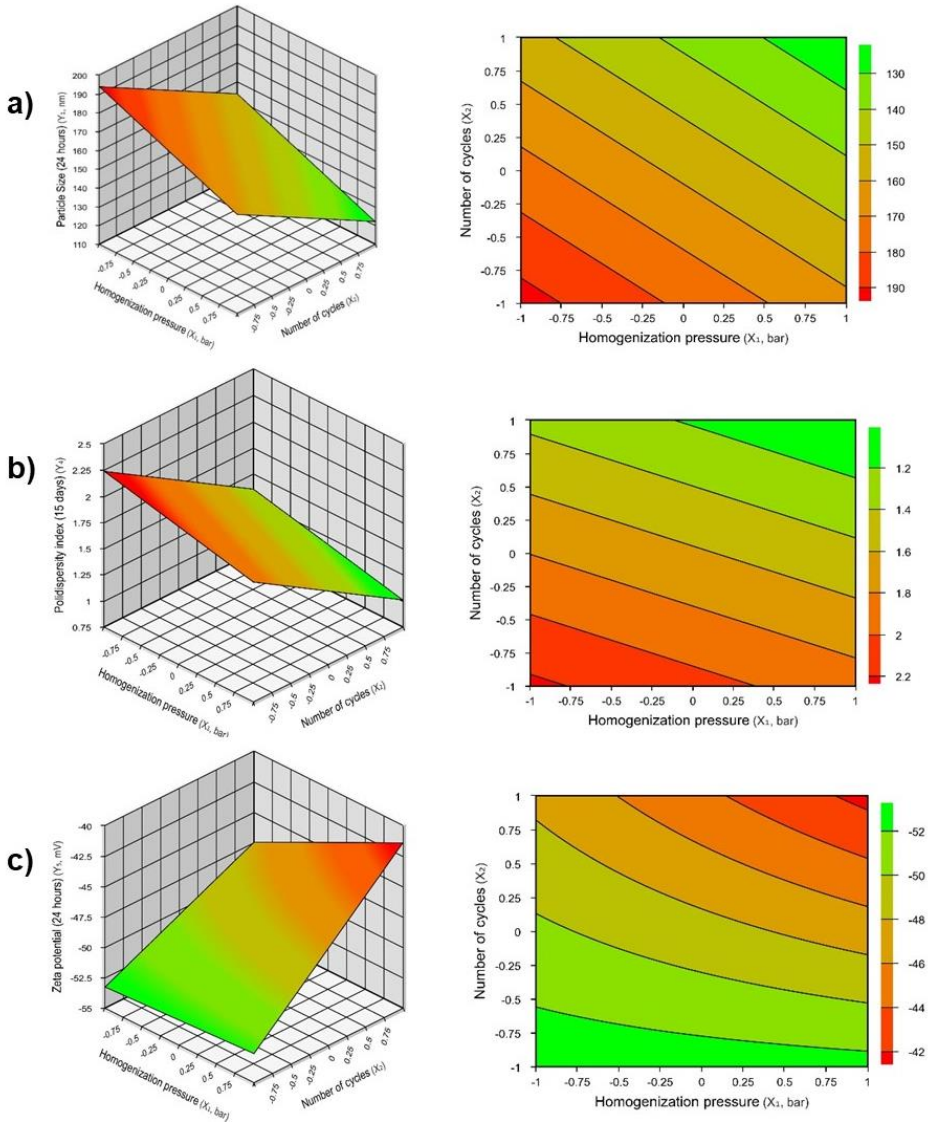

Figure 2. Contour plots and response surface charts of experimental design of NLC obtained with enzymatically modified soy lecithin. a) particle size; b) polydispersity index; c) zeta potential.

The linear models show that the dependent variables considered in the factorial design were affected by both independent variables (NC and HP) when SL was used to produce NLC. The results, presented in Table 4, indicate that the use of SL resulted in the production of NLC in the nanometric range with PS below 208 nm, PDI below 2.30, and ZP above │47 mV│ during 15 days of storage.

Table 4: Influence of pressure and number of homogenization cycles on the obtainment of NLC using enzymatically modified soy lecithin as emulsifier.

HP (bar)	NC	PS 24 h	PS 15 days	PDI 24 h	PDI 15 days	ZP 24 h	ZP 15 days
500	1	208.17±2.40	202.50±3.27	2.12±0.04	2.30±0.06	-53.87±1.59	-60.43±0.38
500	3	153.83±0.75	157.33±0.82	1.21±0.00	1.37±0.01	-48.07±1.36	-52.97±1.10
700	2	148.00±0.60	139.67±0.50	1.19±0.05	1.57±0.18	-47.90±0.68	-53.32±1.77
700	2	149.00±0.20	137.33±0.60	1.17±0.01	1.58±0.33	-47.80±0.56	-52.78±1.32
700	2	147.00±0.56	138.00±0.33	1.18±0.02	1.55±0.30	-48.10±0.07	-53.56±1.20
900	1	163.00±0.63	161.83±0.98	1.63±0.01	1.91±0.08	-53.23±0.40	-54.13±1.46
900	3	136.33±2.66	188.00±4.36	1.03±0.03	1.07±0.08	-52.00±1.15	-51.50±0.46

HP: homogenization pressure; **NC**: number of cycles; **PS**: Particle size; **PDI**: Polydispersity index; **ZP**: Zeta potential. Average of three replicates ± Standard Deviation.

For NLC produced with Span 60, only the independent variable, NC, influenced PS, whereas none of the independent variables considered in this study influenced the PDI and ZP. The linear model for the dependent variable, PS, is described below:

$$TP = 208{,}88 - 18{,}71_{NC}$$

where NC is the number of cycles.

Table 5: Influence of pressure and number of homogenization cycles on the obtainment of NLC using Span 60 as emulsifier.

HP (bar)	NC	PS 24 h	PS 15 days	PDI 24 h	PDI 15 days	ZP 24 h	ZP 15 days
500	1	247.67±6.28	277.17±17.3	10.04±1.21	15.99±0.55	-44.20±1.04	-41.97±0.85
500	3	193.33±9.87	236.83±14.8	8.42±5.28	51.48±23.1	-34.10±1.05	-42.63±0.55
700	2	195.00±9.02	195.33±8.38	3.57±6.53	4.38±1.55	-41.23±0.84	-34.87±0.26
700	2	203.33±7.01	251.00±6.12	12.83±9.04	30.36±7.05	-40.57±1.03	-38.77±0.24
700	2	213.67±5.61	215.27±5.08	16.18±3.82	16.19±12.1	-39.27±0.52	-38.80±0.64
900	1	215.33±3.44	215.83±19.2	14.84±4.21	11.17±7.86	-39.43±1.36	-39.17±0.60
900	3	194.83±5.04	231.67±5.01	14.84±1.69	25.28±9.43	-39.67±1.96	-35.53±1.00

HP: homogenization pressure; **NC**: number of cycles; **PS**: Particle size; **PDI**: Polydispersity index; **ZP**: Zeta potential. Average of three replicates ± Standard Deviation.

None of the independent variables considered in this study had a significant effect on the dependent variables (PS, PDI, and ZP) of NLC produced with SPI as an emulsifier. The use of SPI as an emulsifier promoted the production of NLC in the nanometric range, as shown in Table 6, but it was not possible to characterize the NLC dispersion after 15 days of storage, since the dispersion solidified, impairing sample dilution.

Table 6: Influence of pressure and number of homogenization cycles on the obtainment of NLC using soy protein isolate (SPI) as emulsifier.

HP (bar)	NC	PS 24 h	PS 15 days	PDI 24 h	PDI 15 days	ZP 24 h	ZP 15 days
500	1	197.17±2.40	-	2.08±0.04	-	-55.20±1.59	-
500	3	158.17±0.75	-	1.25±0.00	-	-55.93±1.36	-
700	2	160.33±0.60	-	1.40±0.05	-	-52.43±0.68	-
700	2	156.01±0.06	-	1.33±0.04	-	-55.23±0.40	-
700	2	158.00±0.33	-	1.34±0.00	-	-54.70±0.40	-
900	1	172.00±2.66	-	2.16±0.01	-	-56.30±0.40	-
900	3	147.83±0.63	-	1.20±0.03	-	-52.00±1.15	-

HP: homogenization pressure; **NC**: number of cycles; **PS**: Particle size; **PDI**: Polydispersity index; **ZP**: Zeta potential. Average of three replicates ± Standard Deviation.

For NLC produced with Tween 80, only the independent variable, NC, had a significant effect on the dependent variables, PS and PDI. ZP was not significantly affected by

any of the variables considered in this study. The linear model for each of the dependent variables is described below:

$$PS = 145{,}86 - 9{,}50_{NC}$$

$$PDI = 1{,}36 - 0{,}48_{NC}$$

where NC is the number of cycles. As indicated in Table 7, the NLC produced with Tween 80 had a PS below 168 nm, PDI below 2.01, and ZP above $\left|20\ mV\right|$.

Table 7: Influence of pressure and number of homogenization cycles on the obtainment of NLC using Tween 80 as emulsifier.

HP (bar)	NC	PS 24 h	PS 15 days	PDI 24 h	PDI 15 days	ZP 24 h	ZP 15 days
500	1	156.00±0.00	166.33±0.58	2.01±0.00	1.61±0.01	-26.87±0.38	-24.37±0.06
500	3	138.00±0.00	157.00±0.00	1.04±0.00	1.04±0.00	-23.80±0.75	-22.63±0.21
700	2	149.00±0.11	157.00±0.38	1.24±0.12	1.20±0.08	-24.9±0.38	-22.57±0.40
700	2	142.00±0.01	151.00±0.12	1.45±0.04	1.13±0.05	-24.2±1.53	-23.67±0.24
700	2	144.00±0.61	161.00±0.08	1.13±0.08	1.03±0.01	-25.13±0.57	-22.47±0.64
900	1	156.00±0.00	168.00±0.00	2.01±0.00	1.86±0.01	-27.37±0.65	-24.43±0.65
900	3	136.00±0.00	160.33±0.58	1.05±0.00	1.01±0.00	-27.63±0.15	-23.47±0.45

HP: homogenization pressure; **NC**: number of cycles; **PS**: Particle size; **PDI**: Polydispersity index; **ZP**: Zeta potential. Average of three replicates ± Standard Deviation.

The effects of the independent variables on the ZP of NLC produced with WPI are shown in Figure 5. The linear model for each of the dependent variables, PS and ZP, is described below:

$$PS = 222{,}48 - 43{,}17_{HP}$$

$$ZP = -33{,}01 - 4{,}63_{HP} + 5{,}60_{NC} - 5{,}09_{HP.NC}$$

where HP corresponds to the homogenization pressure and NC to the number of cycles.

a)

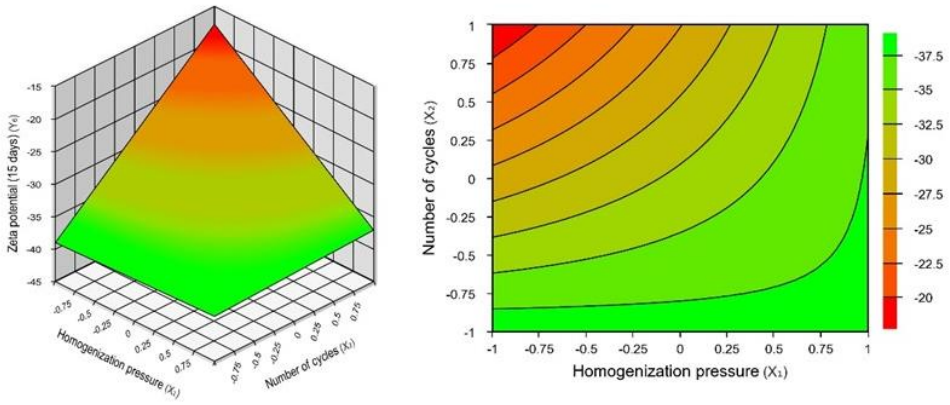

Figure 3. Contour plots and response surface charts of experimental design of NLC obtained with WPI. a) zeta potential.

The linear models show that only HP affected the PS of NLC produced with this emulsifier, whereas ZP was affected by both HP and NC. Table 8 shows the results obtained for each of the dependent variables (PS, PDI, and ZP) considered in this study. The NLC produced with WPI showed a PS below 274 nm, PI below 3.8, and ZP above $\left|32\ mV\right|$.

Table 8: Influence of pressure and number of homogenization cycles on the obtainment of NLC using whey protein isolate (WPI) as emulsifier.

HP (bar)	NC	PS 24 h	PS 15 days	PDI 24 h	PDI 15 days	ZP 24 h	ZP 15 days
500	1	274,00±4,05	203,33±1,03	3,57±0,03	2,60±0,03	-37,43±0,40	-37,70±0,60
500	3	259,50±2,88	240,67±1,47	3,81±0,03	3,37±0,16	-35,50±0,69	-36,33±0,59
700	2	219,00±2,04	267,17±2,07	3,89±1,02	3,80±0,71	-38,1±0,28	-32,9±0,29
700	2	264,33±0,51	207,00±3,15	2,94±0,04	3,30±0,05	-33,77±0,03	-36,87±0,46
700	2	180,67±1,61	191,27±1,08	2,91±0,82	2,89±0,10	-37,20±0,50	-34,67±0,64
900	1	201,00±2,10	195,17±1,57	3,77±0,05	3,15±0,29	-38,13±0,35	-36,80±0,36
900	3	159,83±0,75	177,00±0,89	3,06±0,03	3,27±0,02	-38,90±0,44	-35,77±0,76

HP: homogenization pressure; **NC**: number of cycles; **PS**: Particle size; **PDI**: Polydispersity index; **ZP**: Zeta potential. Average of three replicates ± Standard Deviation.

3.4. Discussion

The characteristics of nanoparticles (structure, size, composition, and charge) influence their physicochemical properties and functional performance, including optical properties, rheological properties, stability, biological fate, and delivery rate of bioactive

compounds (McClements, 2013). These physicochemical and stability-related characteristics depend on the composition of LN formulations (Shah et al., 2015).

Considered as derivatives of oil-in-water emulsions, in which liquid lipids of the oil droplets are replaced by lipids existing in solid form at body temperature, NLC can be stabilized using different emulsifiers (Rawal and Patel, 2018). Emulsifiers are amphiphilic molecules that have a lipophilic (nonpolar) and a hydrophilic (polar) fraction that form the typical head and tail of these molecules, respectively (Shah et al., 2015). The relative proportions of the hydrophilic and lipophilic fractions of an emulsifier are reflected in its HLB value (Attama et al., 2012).

In general, the efficacy of emulsifiers for producing NLC is related to two main factors: the speed at which the emulsifier covers the particle and the interaction between the emulsifier molecule and the dispersed lipid phase. HPH was the process used in this study to produce NLC; it generally promotes a rapid adsorption of emulsifiers after the disruption of oil droplets (Jafari et al., 2008). However, the emulsifier adsorption rate should be higher than the particle fragmentation rate for complete coating of all the produced particles (Lee et al., 2013). Therefore, the process should ideally provide a continuous increase in the number of droplets, which should then be rapidly coated by the emulsifiers used for particle stabilization.

As structural characteristics (molecular weight and number and location of hydrophobic and hydrophilic groups) strongly affect the ability of an emulsifier to reduce the surface tension between lipid and aqueous phases (McClements and Jafari, 2018), the performance of five different emulsifiers (natural and synthetic) with different HLB values were assessed in this study for optimizing the HPH conditions to produce NLC. Hot HPH is the most used method to produce NLC and it can be performed with different HP and NC (Ganesan and Narayanasamy, 2017). The process conditions of HPH (HP and NC) corresponded to the independent variables of the full 2^2 factorial design used for such optimization in this study. The NLC were characterized 24 h and 15 days after storage, with regard to PS and its distribution and the electric charge of the surface of the particles (ZP), which corresponded to the dependent variables of the design. Five factorial designs were prepared, one for each emulsifier considered in the study (SL, Span 60, SPI, Tween 80, and WPI), to determine the individual effect of the emulsifiers on the characteristics of the NLC.

As described in section 3.3.2, the independent variables (PH and NC) considered in this study did not have a significant effect on the dependent variables (PS, PDI, and ZP) for some NLC, as indicated by a very low standard error, thereby preventing the preparation of contour curves and response surfaces. Nevertheless, the main results of this study, as well as the effect of independent variables on the efficiency of emulsifiers used for NLC stabilization, are discussed below.

The use of SL as an emulsifier promoted the production of stable NLC ($ZP > |20$ mV$|$) in the nanometric range (PS < 200 nm) and with a narrow PS distribution, expressed as

PDI. In the case of this emulsifier, the independent variables considered in this study had a significant effect on the dependent variables, and it was therefore possible to obtain linear models, contour curves, and a response surface. The efficacy of SL for producing NLC can be explained by the similarity of the chemical structure of this emulsifier with that of the lipid phase, and its intermediate molecular weight in relation to the other emulsifiers used, which resulted in an effective interaction with the lipid components and an effective coating rate of the produced particles. The response surface shows that the optimal conditions were at levels +1 for HP (900 bar) and +1 for NC (3 cycles) for the dependent variables, PS and PDI, whereas they were at levels -1 for HP (500 bar) and -1 for NC (1 cycle) for the dependent variable, ZP.

As for Span 60, only the independent variable, NC, affected the dependent variable, PS, which was confirmed by the linear model obtained after ANOVA, indicating that a greater number of cycles is required for complete coating of the particles, owing to the high hydrophilicity of this emulsifier. Therefore, it was not possible to obtain contour curves or response surfaces. However, as shown in Table 5, the use of this emulsifier resulted in the production of NLC in the nanometric range, but these NLC were unstable, as confirmed by the increase in PS after 15 days of storage and the PDI of these nanostructures, which indicates a very heterogeneous PS distribution. Span 60 is obtained by the esterification of sorbitan with stearic acid, an 18-carbon saturated fatty acid. The increase in PS can be mainly attributed to differences between the chemical structure of this emulsifier and its compatibility and conformational arrangement and those of the lipid matrices used to produce NLC in this study (Saberi et al., 2011). Sorbitol, in addition to conferring greater hydrophilicity onto the molecule, is responsible for the dissimilarity between the structure of the emulsifier and that of the lipid phase of the NLC, thereby contributing to the instability of the produced nanostructures.

The use of SPI as an emulsifier supported the production of NLC in the nanometric range, as shown in Table 6, but physically unstable, as confirmed by the destabilization of the dispersion of the NLC after 15 days of storage, preventing the analytical determinations at this time point. As it is a protein, SPI can destabilize close to its isoelectric point, which considerably reduces its water solubility and emulsifying capacity (Xiang et al., 2015). Some of the characteristics of this emulsifier, such as its high molecular weight, weak electrostatic repulsions, and low water solubility, reduce its movement and the adsorption rate of SPI molecules to the oil-water interface, thereby decreasing its emulsifying capacity and the stability of the NLC dispersion (McClements and Jafari, 2018; Nishinari et al., 2014).

Compared with other proteins, SPI has a relatively low emulsifying capacity. This can be explained by the commercial production process of this emulsifier that involves alkaline extraction, acid precipitation, and spray-drying. The extraction and drying process leads to protein denaturation, causing commercially available SPI to be mostly present in a denatured

and/or aggregated form, which considerably reduces its emulsifying properties (Chen et al., 2011; Tang and Li, 2013).

Among all the emulsifiers used in this study, Tween 80 produced the smallest NLC, as shown in Table 7. When producing NLC by HPH, the greater the ability of an emulsifier to reduce surface tension, the smaller the particles (Håkansson et al., 2013). Therefore, compared to those of the other emulsifiers, the smaller PS of NLC produced with Tween 80 is related to the differential capacity of this emulsifier to adsorb rapidly at the interface, thereby reducing the tension between the aqueous and lipid phases. Only NC had a significant effect on PS and PDI, according to the linear model obtained after ANOVA. None of the considered independent variables had a significant effect on the dependent variable, ZP. In general, particles with high ZP values (in modulus) repel each other, thereby preventing agglomeration and ensuring particle stability. The use of Tween 80 resulted in the lowest ZP values after 15 days of storage (ZP > |22 mV|). NLC stabilized with ionic emulsifiers should present values above |30 mV| to be considered stable. However, the ZP values are lower when using nonionic emulsifiers instead of ionic emulsifiers. For NLC formulations produced with nonionic emulsifiers, such as Tween 80, stability is provided by the steric hindrance resulting from the complex structure of these emulsifiers (McClements and Rao, 2011). The other emulsifiers considered in this study presented ZP above |30 mV|.

The use of different emulsifiers in this study resulted in different ZP values probably due to their composition and the specific interaction with the lipid/aqueous phases. Protein-stabilized NLC had a negative charge, possibly because the isoelectric point of these proteins is below pH 7.0 (around 5). The negative charge of SL stabilized NLC was probably caused by the presence of anionic PL. In the case of Span 60, although it is a nonionic emulsifier, the presence of negative charges may have been due to anionic impurities present in the emulsifier or oil, or due to the adsorption of OH^- from water onto the surface of the droplets (Mun et al., 2007). Pinto et al. (2018) found that NLC produced with emulsifiers with low HLB values showed higher ZP values when compared with those produced with emulsifiers with higher HLB values, such as Tween 80.

When using WPI as an emulsifier to produce NLC, only the independent variable, HP, significantly affected the PS of the NLC, whereas PDI was not significantly affected by any of the independent variables considered in this study. ZP, on the other hand, was significantly affected by the independent variables, and it was hence possible to obtain linear models, contour curves, and a response surface. The response surface shows that the optimal conditions were found at all levels with respect to HP and at level -1 for NC (1 cycle), indicating that NC exerted greater influence on the dependent variable, ZP.

The homogenization step can be carried out with different cycles and pressures. In general, 1 to 5 cycles under 500-1500 bar are sufficient (Jafari et al., 2007). PS generally

decreases with an increase in pressure and the number of passages of the emulsion through HPH (NC) (McClements and Rao, 2011).

At the end point, this study showed that the independent variables considered in the factorial design affected the production of NLC in different ways: HP was responsible for disrupting the oil droplets present in the pre-emulsion, and NC, for the formation of new interfaces and the coating of the formed droplets. In general, the linear models obtained after ANOVA indicate that the PS values of NLC produced with nonionic emulsifiers, namely, Tween 80 and Span 60, were affected only by the NC of the HPH, suggesting that higher NC supports greater particle coating by these emulsifiers, thereby promoting a reduction in PS and PDI.

In the case of proteins, owing to the physical instability of the NLC dispersion stabilized with SPI, it was impossible to determine how each variable (HP and NC) affected the production of nanostructures. The PS of NLC produced with WPI were affected only by the applied HP, indicating that emulsifiers with higher molecular weight and size require higher pressures to reduce surface tension, and thus, to produce smaller NLC. The linear models obtained for this emulsifier also indicate that the ZP of the NLC was affected by both variables (HP and NC). However, as mentioned above, the optimal conditions for HP were found at all levels considered in the experimental design. In the case of NC, as ZP indicates the stability of the system during storage (Mohammadi et al., 2019), the stabilization of NLC using emulsifiers of higher molecular weight and size, such as WPI, responded positively to a higher NC. This indicates that, owing to the structural and molecular characteristics of WPI, the increase in NC caused greater coating of the droplets formed by this emulsifier, thus conferring greater stability onto the NLC.

The use of SL for NLC stabilization resulted in linear models indicating that the dependent variables (PS, PDI, and ZP) were affected by all the independent variables (HP and NC) considered in this study. Commercial lecithins are mainly composed of PL and TAG (Fernandes et al., 2012). The chemical structures of PL and TAG are similar. TAG are formed by the esterification of three FA molecules with a glycerol molecule, whereas esterification of two FA molecules and a phosphate group with glycerol results in SL. The SL in this study mostly comprised lysophospholipids, obtained by enzymatic hydrolysis of conventional soy lecithin using phospholipases (A_1 or A_2). In this case, the structure of PL changes, and the glycerol molecule is esterified to only one FA and one phosphate group, corresponding to lysophospholipids. This structural modification increases the polarity of the molecule, thereby increasing the emulsifying capacity of lysophospholipids when compared to conventional PL. For NLC produced with SL, the independent variables considered in this study (HP and NC) had a significant effect on the dependent variables (PS, PDI, and ZP), which can be mainly attributed to the structural and chemical similarity of this emulsifier with the lipid phase and its intermediate molecular weight in relation to the other emulsifiers. Although the linear models

obtained for the dependent variables provided the levels for the optimal conditions, the results were satisfactory at all levels, mainly due to the effective interaction with the lipid components and the good particle coating rate presented by this emulsifier.

Factorial design is a powerful tool for optimizing process conditions, and the strategy should reflect the number of factors (variables) to be studied and the initial knowledge of the process, always considering the interplay between common sense and statistical analysis (Rodrigues and Iemma, 2014). HPH was the process used in this study to produce NLC, in which very intense forces are applied to promote the disruption of particles in the nanometric range, typically causing a very high wear on the high pressure homogenizers. Therefore, the mildest possible process conditions should be used to prevent wear of the equipment parts, thereby increasing their durability. The process conditions considered in this study (HP and NC) significantly affected some of the dependent variables, thereby indicating the optimal conditions for each variable and emulsifier through response surfaces and contour curves. The efficacy of the emulsifiers used in this study was affected according to their physicochemical and structural characteristics. The production of NLC using Span 60 and SPI was not feasible, mainly owing to the structural characteristics of these emulsifiers, which were incompatible with the speed required for particle coating and the interaction between the emulsifier molecule and the dispersed lipid phase. The other emulsifiers (Tween 80, SL, and WPI) were effective for producing NLC. Although the optimal process conditions have been indicated for each variable and emulsifier, considering a standard lipid system, represented in this study by a model system with equivalent amounts of saturated and unsaturated fatty acids, the central point conditions (HP = 700 bar and NC = 2) are recommended to produce NLC, as they are satisfactory and represent, in practice, intermediate process conditions in terms of preventing equipment wear.

The results of this study demonstrate the importance of preparing experimental designs for optimizing the process conditions to produce NLC. Although many studies have been carried out to produce carriers, and their results suggest optimal HP and NC, preliminary studies considering the raw materials and equipment to be used should be carried out for each case. A rational selection of suitable raw materials and process conditions can enhance the physicochemical characteristics of the produced NLC.

3.5 Conclusions

In this study, the optimal experimental conditions for producing NLC were determined through a factorial design, considering the HPH process variables that influence the characteristics of the produced particles. Five different factorial designs were prepared, one for each analyzed emulsifier, considering HP and NC as independent variables, and PS,

PDI, and ZP as dependent variables. Although the independent variables considered in this study did not have a significant effect on the dependent variables for some emulsifiers, the factorial design allowed the determination of the optimal process conditions and the most suitable emulsifiers to produce stable NLC.

With regard to the effectiveness of the emulsifiers used, it was concluded that technologically obtaining NLC using Span 60 and SPI as emulsifiers was not feasible under the evaluated process conditions. On the other hand, the emulsifiers, Tween 80, LS, and WPI, enabled the production of NLC in the nanometric range, with adequate PDI and high physical stability (ZP) during 15 days of storage, thus demonstrating that the application of the HPH method was satisfactory for obtaining NLC.

The linear models obtained for the dependent variables indicated the levels for the optimal conditions; all the levels were satisfactory to produce NLC with the effective emulsifiers. Therefore, the central point conditions (NC of 2 cycles and HP of 700 bar) were satisfactory to produce NLC with adequate PS, obviating the need to validate the experiment.

3.6 Acknowledgments

The authors are grateful to the Coordination for the Improvement of Higher Education Personnel (*Coordenação de Aperfeiçoamento de Pessoal de Nível Superior* - CAPES) for the financial support. Fernanda Luisa Lüdtke thanks FAPESP (grants # 18/03172-0, # 19/05176-6, #16/11261-8 and 19/27354-3, São Paulo Research Foundation -FAPESP). Ana Paula Badan Ribeiro thanks CNPq (303429/2018-6) for the productivity grant.

3.7 References

Akhavan, S., Assadpour, E., Katouzian, I., Jafari, S.M., 2018. Lipid nano scale cargos for the protection and delivery of food bioactive ingredients and nutraceuticals. Trends in Food Science and Technology 74, 132–146. https://doi.org/10.1016/j.tifs.2018.02.001

Antoniosi Filho, N.R., Mendes, O.L., Lan, F.M., 1995. Computer Prediction of Triacylglycerol Composition of Vegetable Oils by HRGC. Chromatographia 40, 557–562.

AOCS. American Oil Chemists' Society, 2009. Official methods and recommended practices of the American Oil Chemists' Society.

Attama, A.A., Momoh, M.A., Builders, P.F., 2012. Lipid Nanoparticulate Drug Delivery Systems: A Revolution in Dosage Form Design and Development, in: Recent Advances in Novel Drug Carrier Systems. InTech, pp. 107–140. https://doi.org/10.5772/50486

Averina, E.S., Müller, R.H., Popov, D. v., Radnaeva, L.D., 2011. Physical and chemical stability of nanostructured lipid drug carriers (NLC) based on natural lipids from Baikal region (Siberia, Russia). Pharmazie 66, 348–356. https://doi.org/10.1691/ph.2011.0326

Chatterton, D.E.W., Smithers, G., Roupas, P., Brodkorb, A., 2006. Bioactivity of β–lactoglobulin and α–lactalbumin–Technological implications for processing. International Dairy Journal 16, 1229–1240. https://doi.org/10.1016/j.idairyj.2006.06.001

Chen, L., Chen, J., Ren, J., Zhao, M., 2011. Effects of ultrasound pretreatment on the enzymatic hydrolysis of soy protein isolates and on the emulsifying properties of hydrolysates. Journal of Agricultural and Food Chemistry 59, 2600–2609. https://doi.org/10.1021/jf103771x

Chen, L., Liang, R., Yokoyama, W., Alves, P., Pan, J., Zhong, F., 2020. Effect of the co–existing and excipient oil on the bioaccessibility of β–carotene loaded oil–free nanoparticles. Food Hydrocolloids 106. https://doi.org/10.1016/j.foodhyd.2020.105847

Chen, L., Remondetto, G.E., Subirade, M., 2006. Food protein–based materials as nutraceutical delivery systems. Trends in Food Science and Technology 17, 272–283. https://doi.org/10.1016/j.tifs.2005.12.011

Cottrell, T., van Peiji, J., 2004. Sorbitan esters and polysorbates, in: Whitehurst, R.J. (Ed.), Emulsifiers in Food Technology. Blackwell Publishing, Oxford, pp. 162–167.

Das, N.M.A., Kobayashi, I., Nakajima, M., 2020. Nanotechnology for bioactives delivery systems. Journal of Food and Drug Analysis 20, 184–188. https://doi.org/10.38212/2224–6614.2118

Dumont, C., Bourgeois, S., Fessi, H., Jannin, V., 2018. Lipid–based nanosuspensions for oral delivery of peptides, a critical review. International Journal of Pharmaceutics 541, 117–135. https://doi.org/10.1016/j.ijpharm.2018.02.038

Fernandes, G.D., Alberici, R.M., Pereira, G.G., Cabral, E.C., Eberlin, M.N., Barrera–Arellano, D., 2012. Direct characterization of commercial lecithins by easy ambient sonic–spray ionization mass spectrometry. Food Chemistry 135, 1855–1860. https://doi.org/10.1016/j.foodchem.2012.06.072

Ganesan, P., Narayanasamy, D., 2017. Lipid nanoparticles: Different preparation techniques, characterization, hurdles, and strategies for the production of solid lipid nanoparticles and nanostructured lipid carriers for oral drug delivery. Sustainable Chemistry and Pharmacy. https://doi.org/10.1016/j.scp.2017.07.002

Håkansson, A., Innings, F., Trägårdh, C., Bergenståhl, B., 2013. A high–pressure homogenization emulsification model—Improved emulsifier transport and hydrodynamic coupling. Chemical Engineering Science 91, 44–53. https://doi.org/10.1016/j.ces.2013.01.011

Hartman, L., Lago, R.C., 1973. Rapid preparation of fatty acid methyl esters from lipids. Laboratory practice 22, 475–476.

He, X., Hwang, H.M., 2016. Nanotechnology in food science: Functionality, applicability, and safety assessment. Journal of Food and Drug Analysis 24, 671–681. https://doi.org/10.1016/j.jfda.2016.06.001

Helgason, T., Awad, T.S., Kristbergsson, K., Decker, E.A., Mcclements, D.J., Weiss, J., 2009. Impact of surfactant properties on oxidative stability of β–carotene encapsulated within solid lipid nanoparticles. Journal of Agricultural and Food Chemistry 57, 8033–8040. https://doi.org/10.1021/jf901682m

Jafari, S.M., Assadpoor, E., He, Y., Bhandari, B., 2008. Encapsulation efficiency of food flavours and oils during spray drying. Drying Technology 26, 816–835. https://doi.org/10.1080/07373930802135972

Jafari, S.M., He, Y., Bhandari, B., 2007. Effectiveness of encapsulating biopolymers to produce sub–micron emulsions by high energy emulsification techniques. Food Research International 40, 862–873. https://doi.org/10.1016/j.foodres.2007.02.002

Katouzian, I., Faridi Esfanjani, A., Jafari, S.M., Akhavan, S., 2017. Formulation and application of a new generation of lipid nano–carriers for the food bioactive ingredients. Trends in Food Science and Technology 68, 14–25. https://doi.org/10.1016/j.tifs.2017.07.017

Kumbhar, D.D., Pokharkar, V.B., 2013. Engineering of a nanostructured lipid carrier for the poorly water–soluble drug, bicalutamide: Physicochemical investigations. Colloids and Surfaces A: Physicochemical and Engineering Aspects 416, 32–42. https://doi.org/10.1016/j.colsurfa.2012.10.031

Lee, L.L., Niknafs, N., Hancocks, R.D., Norton, I.T., 2013. Emulsification: Mechanistic understanding. Trends in Food Science and Technology 31, 72–78. https://doi.org/10.1016/j.tifs.2012.08.006

McClements, D.J., 2015. Food Emulsions: Principles, Practices and Techniques, 3rd ed.

McClements, D.J., 2013. Utilizing food effects to overcome challenges in delivery of lipophilic bioactives: Structural design of medical and functional foods. Expert Opinion on Drug Delivery 10, 1621–1632. https://doi.org/10.1517/17425247.2013.837448

McClements, D.J., Gumus, C.E., 2016. Natural emulsifiers — Biosurfactants, phospholipids, biopolymers, and colloidal particles: Molecular and physicochemical basis of functional performance. Advances in Colloid and Interface Science 234, 3–26. https://doi.org/10.1016/j.cis.2016.03.002

McClements, D.J., Jafari, S.M., 2018. Improving emulsion formation, stability and performance using mixed emulsifiers: A review. Advances in Colloid and Interface Science 251, 55–79. https://doi.org/10.1016/j.cis.2017.12.001

McClements, D.J., Rao, J., 2011. Food–Grade nanoemulsions: Formulation, fabrication, properties, performance, Biological fate, and Potential Toxicity. Critical Reviews in Food Science and Nutrition 51, 285–330. https://doi.org/10.1080/10408398.2011.559558

Mohammadi, M., Assadpour, E., Jafari, S.M., 2019. Encapsulation of food ingredients by nanostructured lipid carriers (NLCs), in: Lipid–Based Nanostructures for Food Encapsulation Purposes. Elsevier, pp. 217–270. https://doi.org/10.1016/b978–0–12–815673–5.00007–6

Mun, S., Decker, E.A., McClements, D.J., 2007. Influence of emulsifier type on in vitro digestibility of lipid droplets by pancreatic lipase. Food Research International 40, 770–781. https://doi.org/10.1016/j.foodres.2007.01.007

Nik, A.M., Langmaid, S., Wright, A.J., 2012. Nonionic surfactant and interfacial structure impact crystallinity and stability of β–carotene loaded lipid nanodispersions. Journal of Agricultural and Food Chemistry 60, 4126–4135. https://doi.org/10.1021/jf204810m

Nik, A.M., Wright, A.J., Corredig, M., 2011. Impact of interfacial composition on emulsion digestion and rate of lipid hydrolysis using different in vitro digestion models. Colloids and Surfaces B: Biointerfaces 83, 321–330. https://doi.org/10.1016/j.colsurfb.2010.12.001

Nishinari, K., Fang, Y., Guo, S., Phillips, G.O., 2014. Soy proteins: A review on composition, aggregation and emulsification. Food Hydrocolloids 39, 301–318. https://doi.org/10.1016/j.foodhyd.2014.01.013

O'Brien, R.D., 2008. Fats and Oils, 3rd ed. CRC Press, New York. https://doi.org/10.1201/9781420061673

Oliveira, D.R.B., Furtado, G. de F., Cunha, R.L., 2019. Solid lipid nanoparticles stabilized by sodium caseinate and lactoferrin. Food Hydrocolloids 90, 321–329. https://doi.org/10.1016/j.foodhyd.2018.12.025

Ozturk, B., McClements, D.J., 2016. Progress in natural emulsifiers for utilization in food emulsions. Current Opinion in Food Science 7, 1–6. https://doi.org/10.1016/j.cofs.2015.07.008

Pardeike, J., Hommoss, A., Müller, R.H., 2009. Lipid nanoparticles (SLN, NLC) in cosmetic and pharmaceutical dermal products. International Journal of Pharmaceutics 27, 11–17. https://doi.org/10.1016/j.ijpharm.2008.10.003

Pinto, F., de Barros, D.P.C., Fonseca, L.P., 2018. Design of multifunctional nanostructured lipid carriers enriched with α–tocopherol using vegetable oils. Industrial Crops and Products 118, 149–159. https://doi.org/10.1016/j.indcrop.2018.03.042

Qian, C., Decker, E.A., Xiao, H., McClements, D.J., 2013. Impact of lipid nanoparticle physical state on particle aggregation and β–carotene degradation: Potential limitations of solid lipid nanoparticles. Food Research International 52, 342–349. https://doi.org/10.1016/j.foodres.2013.03.035

Queirós, M. de S., Viriato, R.L.S., Ribeiro, A.P.B., Gigante, M.L., 2021. Development of solid lipid nanoparticle and nanostructured lipid carrier with dairy ingredients. International Dairy Journal 105186. https://doi.org/10.1016/j.idairyj.2021.105186

Rawal, S.U., Patel, M.M., 2018. Lipid nanoparticulate systems: Modern versatile drug carriers, in: Lipid Nanocarriers for Drug Targeting. Elsevier, pp. 49–138. https://doi.org/10.1016/B978–0–12–813687–4.00002–5

Ribeiro, A.P.B., Basso, R.C., Grimaldi, R., Gioielli, L.A., dos Santos, A.O., Cardoso, L.P., Guaraldo Gonçalves, L.A., 2009. Influence of chemical interesterification on thermal behavior, microstructure, polymorphism and crystallization properties of canola oil and fully hydrogenated cottonseed oil blends. Food Research International 42, 1153–1162. https://doi.org/10.1016/j.foodres.2009.05.016

Rodrigues, M.I., Iemma, A.F., 2014. Planejamento de Experimentos e Otimização de Processos: uma estratégia sequencial de planejamentos, 3rd ed. Casa do Espírito Amigo Fraternidade Fé e Amor, Campinas.

Saberi, A.H., Lai, O.M., Toro–Vázquez, J.F., 2011. Crystallization kinetics of palm oil in blends with palm–based diacylglycerol. Food Research International 44, 425–435. https://doi.org/10.1016/j.foodres.2010.09.029

Sawant, K.K., Dodiya, S.S., 2008. Recent Advances and Patents on Solid Lipid Nanoparticles, Recent Patents on Drug Delivery & Formulation.

Schubert, H., Engel, R., 2004. Product and formulation engineering of emulsions. Chemical Engineering Research and Design 82, 1137–1143. https://doi.org/10.1205/cerd.82.9.1137.44154

Severino, P., Santana, M.H.A., Souto, E.B., 2012. Optimizing SLN and NLC by 2 2 full factorial design: Effect of homogenization technique. Materials Science and Engineering C 32, 1375–1379. https://doi.org/10.1016/j.msec.2012.04.017

Shah, R., Eldridge, D., Palombo, E., Harding, I., 2015. Lipid Nanoparticles: Production, Characterization and Stability. Springer briefs in pharmaceutical science & drug development

Souto, E.B., Wissing, S.A., Barbosa, C.M., Müller, R.H., 2004. Evaluation of the physical stability of SLN and NLC before and after incorporation into hydrogel formulations. European Journal of Pharmaceutics and Biopharmaceutics 58, 83–90. https://doi.org/10.1016/j.ejpb.2004.02.015

Tamjidi, F., Shahedi, M., Varshosaz, J., Nasirpour, A., 2013. Nanostructured lipid carriers (NLC): A potential delivery system for bioactive food molecules. Innovative Food Science and Emerging Technologies 19, 29–43. https://doi.org/10.1016/j.ifset.2013.03.002

Tang, C.H., Li, X.R., 2013. Microencapsulation properties of soy protein isolate: Influence of preheating and/or blending with lactose. Journal of Food Engineering 117, 281–290. https://doi.org/10.1016/j.jfoodeng.2013.03.018

Tanno, H., 2012. Lecithin, in: Ullmann's Encyclopedia of Industrial Chemistry. Wiley–VCH Verlag GmbH & Co. KGaA, Weinheim, Germany. https://doi.org/10.1002/14356007.a15_293

Wang, X., Lin, Q., Ye, A., Han, J., Singh, H., 2019. Flocculation of oil–in–water emulsions stabilised by milk protein ingredients under gastric conditions: Impact on in vitro intestinal lipid digestion. Food Hydrocolloids 88, 272–282. https://doi.org/10.1016/j.foodhyd.2018.10.001

Weiss, J., Decker, E.A., McClements, D.J., Kristbergsson, K., Helgason, T., Awad, T., 2008. Solid lipid nanoparticles as delivery systems for bioactive food components. Food Biophysics 3, 146–154. https://doi.org/10.1007/s11483–008–9065–8

Xiang, J., Liu, F., Fan, R., Gao, Y., 2015. Physicochemical stability of citral emulsions stabilized by milk proteins (lactoferrin, α–lactalbumin, β–lactoglobulin) and beet pectin. Colloids and Surfaces A: Physicochemical and Engineering Aspects 487, 104–112. https://doi.org/10.1016/j.colsurfa.2015.09.033

Yang, Y., Corona, A., Schubert, B., Reeder, R., Henson, M.A., 2014. The effect of oil type on the aggregation stability of nanostructured lipid carriers. Journal of Colloid and Interface Science 418, 261–272. https://doi.org/10.1016/j.jcis.2013.12.024

CAPÍTULO IV

Lipid systems based on fully hydrogenated soybean oil and high oleic sunflower oil to obtain nanostructured lipid carriers: composition, physical properties, and crystallization parameters

Submitted to Food Structure

4. Lipid systems based on fully hydrogenated soybean oil and high oleic sunflower oil to obtain nanostructured lipid carriers: composition, physical properties, and crystallization parameters

Fernanda Luisa Lüdtke[a], Renato Grimaldi[a], Lisandro Pavie Cardoso[b], Ana Paula Badan Ribeiro[a]

[a]Department of Food Engineering and Technology, School of Food Engineering, State University of Campinas (UNICAMP), 13083-862, Campinas, SP, Brazil.
[b]Department of Applied Physics, Institute of Physics Gleb Wataghin, State University of Campinas (UNICAMP), 13083-859, Campinas, SP, Brazil.

ABSTRACT

The choice of lipid matrix for nanostructured lipid carriers (NLC) is essential because structural characteristics, physical and chemical properties, and retention and release of compounds incorporated into the structure are directly influenced. Resistance to chemical degradation, a melting point above body temperature, biodegradability, and generally regarded as safe status are some of the prerequisites for a lipid matrix to ensure that the formulation of NLC are biocompatible, stable, and highly efficient in the incorporation and delivery of bioactive compounds. Thus, the objective of the present study was to evaluate the composition and physical and crystallization properties of lipid systems composed of fully hydrogenated soybean oil (FHSO) and high oleic sunflower oil (HOSO). The lipid systems were composed of FHSO:HOSO (w/w) at the following ratios: 90:10, 80:20, 70:30, 60:40, 50:50, 40:60, 30:70, 20:80, and 10:90. They were characterized by their composition in fatty acids and triacylglycerol (TAG), thermal behavior during melting and crystallization, solid fat content (SFC), microscopical features, and polymorphism. Elevated HOSO in lipid systems promoted an increase in unsaturated fatty acids (UFA) and di- and tri-unsaturated TAG, as well as a reduction in SFC at tested temperatures (10–60 °C). In addition, variations in thermal behavior occurred due to increased HOSO levels, which allowed for establishing lipid systems with suitable thermal behavior to obtain NLC owing to less-ordered crystalline structures (amorphous, low crystallinity). With the exception of the lipid system with 10:90 FHSO:HOSO (w/w), all systems exhibited polymorphic stabilization in the most stable form (β form) after 60 days. Moreover, increasing HOSO in lipid systems led to a reduction in crystalized areas, which indicated that the crystalline structure was modified by the presence of the raw material. Findings of the present study demonstrated that the raw materials are compatible for the formulation of NLC.

Keywords: lipid matrices, fatty acid composition, triacylglycerol, crystallization, thermal resistance

4.1 Introduction

Increasing public awareness regarding the relationship between food and disease prevention has led to a growing interest in the production of foods that incorporate nutraceutical and functional compounds. However, the addition of these compounds to foods is infrequent due to their typically low solubility in water or oil and chemical instability, and consequently the low bioavailability of most of these compounds. In this context, lipid nanoparticles (LN) represent an alternative to overcome such limitations (Tamjidi et al., 2013).

Nanostructured lipid carriers (NLC) are second generation LN (Mohammadi et al., 2019; Yoon et al., 2013) and have been widely used to carry fat-soluble bioactive “cargo” compounds to sites of absorption in the gastrointestinal tract (GIT). These nanostructures have been recognized as ideal systems for loading functional or bioactive compounds that are toxicologically safe, technologically scalable, and show high performance, and have been the focus of a series of recent studies on the topic (Aditya & Ko, 2015).

Lipid matrices are the main ingredients of LN because they exert a direct influence on the load-carrying capacity and stability, and on the release of compounds incorporated into their structure (Katouzian et al., 2017; Shah et al., 2015). Physical and chemical properties of lipids used to obtain delivery systems based on emulsions directly impact their digestibility and, consequently, the bioavailability of lipophilic bioactive compounds solubilized within oil droplets (Salvia-Trujillo et al., 2017).

NLC are obtained by combining lipid matrices of high and low melting point (MP), whose structural incompatibility results in the formation of structures with characteristics that are imperfect for crystallization (Yoon et al., 2013). The incorporation of a lipid matrix with lower MP (liquid matrix) into a solid matrix results in the formation of a less-ordered crystalline structure and, therefore, expulsion of the compound during storage, and undesired changes to particle morphology, aggregation, and gelification are avoided (Gonçalves et al., 2018).

Major lipid components used to obtain NLC are synthetic materials, usually expensive, and whose chemical composition varies according to the manufacturer; these small differences in the content of acylglycerols can create difficulties in terms of standardization of the formulation and characterization of LN (Jannin et al., 2008; Mehnert & Mäder, 2012; Tamjidi et al., 2013).

The combination of characteristics of triacylglycerol (TAG) present in common lipid sources such as oils and fats of vegetable origin is very promising for the development of nanostructured lipid systems with specific release properties. Different mixtures of natural fats represent biocompatible sources for this purpose, exhibiting crystallographic characteristics that are adequate for the formulation of NLC (Cerqueira et al., 2014; Livney, 2015; Serra et al., 2008).

High MP lipids that can be used to obtain NLC include TAG, fatty acids (FA), waxes, fully hydrogenated vegetable oils, or an amalgamation of these raw materials. NLC have been investigated in several studies involving beeswax (Mojahedian et al., 2013; Soleimanian et al., 2019; Tan et al., 2010), propolis wax (Soleimanian et al., 2019), and fully hydrogenated vegetable oils (Kharat & McClements, 2019; Santos et al., 2019; Zheng et al., 2013).

Edible vegetable oils may be used as lipid matrices with lower MP for the production of NLC. The incorporation of these natural oils changes the crystallinity of the lipid

matrix and, in general, improves solubilization of encapsulated components. These raw materials are environmentally adequate, inexpensive, and commercially available on large scales. NLC production from soybean, corn, and sunflower oils have been reported and have a great potential for the application of NLC in foods (Liu & Wu, 2010; Nguyen et al., 2012).

The requirements for an ideal lipid matrix of high and low MP to generate NLC include solubility of the bioactive compound in the matrix, different FA and TAG compositions, stability against degradation (oxidation, lipolysis), biodegradability, and biocompatibility (Tamjidi et al., 2013). Moreover, proportions between lipid matrices with high and low MP used to obtain NLC should be assessed because the mixture formed by these lipid matrices should be homogeneous and solid at body temperature (Müller et al., 2000).

The production of NLC from vegetable raw materials that are widely available in the oil and fat industry has great potential, especially when incorporation of these nanostructures in foods is aimed for. Vegetables derived lipid raw materials allow for the synthesis of NLC at lower cost, provided that they are widely available regionally, and are healthier and more biocompatible; furthermore their chemical composition and physical properties of selected lipid matrices is considered. In this sense, fully hydrogenated soybean oil (FHSO) and high oleic sunflower oil (HOSO) have great potential for use as lipid matrices of high and low MP, respectively, in the production of NLC.

FHSO is obtained through the full hydrogenation of soybean oil, a process that consists of the catalytic addition of hydrogen to double-bonds of unsaturated fatty acids (UFA), thus promoting the conversion of UFA into saturated fatty acids (SFA) (Ribeiro et al., 2009, 2013).. This lipid matrix is a natural and low-cost source of stearic acid, a FA known for its neutral atherogenic effect and for not posing a risk for the development of heart diseases compared to other FA (Hunter et al., 2010).

HOSO is obtained from the genetic modification of conventional sunflowers and is considered a premium lipid raw material in terms of resistance to oxidation because of its significant oleic acid content, a monounsaturated FA (MUFA) that is less susceptible to oxidative processes than polyunsaturated FA (PUFA) due to its single double-bond in the carbon chain (Cardenia et al., 2011; Gunstone, 2011). Therefore, HOSO has a high potential for use as a lipid matrix with low MP in lipid systems in order to obtain NLC.

Properties of nanomaterials differ from those of conventional materials due to their greater surface area and varied physical forces that act on these particles (Siegrist et al., 2008). Knowledge of the physical and crystallization characteristics of the lipid matrices used to obtain NLC is important to optimize their formation, stability, and functionality (Kharat & McClements, 2019). Complete characterization of the lipid matrix and of lipid systems formed with varying ratios of these matrices is essential for the formulation of NLC with adequate crystallinity suitable for the incorporation of bioactive compounds. Therefore, the objective of

the present study was to determine the composition and physical and crystallization properties of lipid systems composed of FHSO and HOSO at different ratios to obtain NLC.

4.2 Materials and Methods

4.2.1 Materials

HOSO and FHSO were supplied by Cargill Foods (Campinas, Sao Paulo, Brazil).

4.2.2 Methods

4.2.2.1 Preparation of lipid systems

Lipid systems were prepared from mixtures of FHSO and HOSO in the following ratios of FHSO:HOSO (w/w)—90:10, 80:20, 70:30, 60:40, 50:50, 40:60, 30:70, 20:80, and 10:90. For this purpose, a simple mixture of the lipid matrices (FHSO and HOSO) was made and subsequently heated (85 °C) and completed melted and homogenized with a magnetic stirrer at 300 rpm for 30 min.

4.2.2.2 Fatty acid composition (FAC)

Analysis of the composition of FA (FAC) was performed by gas chromatography using the Agilent 6850 GC USA chromatograph system (Santa Clara, CA, USA) after esterification using the Hartman and Lago (1973) method. FA methyl esters were separated according to the AOCS Ce 1f-96 method (AOCS, 2009) using an Agilent DB-23 column (50% cyanopropyl-methylpolysiloxane) 60 m in length, 0.25 mm inner diameter, and 0.25 µm film. The analysis conditions were as follows: oven temperature of 110 °C for 5 min, 110–215 °C (5 °C/min), 215 °C for 24 min; detector temperature of 280 °C; injector temperature of 250 °C; carrier gas: helium; split ratio of 1:50; injected volume of 1.0 µL. The qualitative composition was determined by comparing the peak retention times with those of FA standards.

4.2.2.3 TAG composition

Analysis of TAG composition was performed by gas chromatography with capillary column (50% phenyl methylpolysiloxane) (DB-17HT Agilent, catalog no. 122-1811) 15 m in length, 0.25 mm inner diameter, and 0.15 µm film. The analysis conditions were as follows: split ratio of 1:100; column temperature of 250 ºC, programed to 350 ºC at a rate of 5ºC/min; carrier gas: helium, flow rate of 1.0 mL/min; injector temperature of 360 ºC; detector temperature 375 ºC; injected volume of 1.0 µL; and sample concentration of 100 mg/5 mL of tetrahydrofuran. The identification of TAG groups was performed by comparing retention times with those of TAG standards, according to the method reported by Antoniosi Filho et al. (1995).

4.2.2.4 Solid fat content (SFC)

SFC was determined by pulsed low-resolution nuclear magnetic resonance spectroscopy (NMR) Bruker pc120 Minispec (Silberstreifen, Rheinstetten, Germany), using high precision dry baths with temperature controlled (0–70°C) by the Peltier Tcon 2000 system (Duratech, Garden Grove, USA), according to the direct AOCS Cd 16b- 93 method. Samples were analyzed in series, with tempering of unstabilized fats (AOCS, 2009). SFC data were used to obtain a diagram of compatibility and MP of the lipid systems by correlations between FHSO and HOSO content and the SFC at 10, 20, 25, 30, 35, 40, 45, 50, 55, and 60 °C. MP were calculated using equations for the straight lines of the solid profiles obtained by NMR that corresponded to the temperature at which the lipid systems had a SFC of 4% (Karabulut et al., 2004).

4.2.2.5 Thermal behavior

Thermal behavior of samples during the melting and crystallization processes was evaluated using a TA Q2000 differential scanning calorimeter (DSC) coupled to a RCS90 refrigerated cooling system (TA Instruments, Waters LLC, New Castle, USA), according to the AOCS Cj 1-94 method. Samples were melted (85 °C/30 min) and stored in airtight aluminum capsules. The analysis conditions were as follows: weight of samples: ~ 10 mg; crystallization curves: 80 ºC for 10 min, 80 ºC to 40 ºC (10 ºC/ min), 40 ºC for 30 min. Melting events were evaluated between 25 °C and 100 °C, at a rate of 10 °C/min (Wang et al., 2014). The following parameters were used to assess results: onset temperature, peak temperature, offset temperature, and enthalpy of melting and crystallization events.

4.2.2.6 Polymorphic forms

Polymorphic forms of lipid systems were determined by X-ray diffraction, according to the AOCS Cj 2-95 method (AOCS, 2009). Samples were stabilized by two methods, where they were melted and stored in metal plates. However, in the first method (MI) samples were stabilized and maintained at 25 ºC during the entire analysis, whereas the second method (MII) involved using a protocol usually applied for recrystallization of NLC, in which samples are stabilized at 5 ºC for 24 h and subsequently stored at 25 ºC throughout the analysis period. Analysis was performed using a Philips PW 1710 diffractometer (PANalytical, Almelo, The Netherlands) using Bragg-Bretano geometry (θ: 2θ) with Cu-Kα radiation (λ = 1.54056 Å, tension of 40 KV, and current of 30 mA). The measurements were obtained with 0.02 degrees step-sizes in 2θ over an acquisition time of 2 s, with scans of 5° to 40° (2θ range). Identification of polymorphic forms was performed using short spacing intervals (distance between the acyl groups parallel to the TAG), which are characteristic of lipid crystals. Evaluation of polymorphic

forms was performed at 48 h and thereafter at 7, 15, 30, and 60 days after preparation of the lipid systems.

4.2.2.7 Microstructure

Determination of the microstructure (morphology and crystallinity) of the lipid systems was evaluated by polarized light microscopy at 25 °C using a BX 50 microscope (Olympus, San Jose, USA) coupled to a digital video camera (Media Cybernetics, Bethesda, USA). For this analysis, samples were also conditioned using two methods, where they were melted in an oven at 90 °C and the glass microscope slide and cover slips were pre-warmed at 90 °C for 15 min. Approximately 10 µL of samples was transferred using a capillary tube to the pre-warmed glass slide and subsequently covered with a cover slip. Then, samples were stabilized using distinct protocols. In MI they were stabilized and kept at 25 ºC, whereas in MII they were stabilized at 5 ºC for 24 h and subsequently kept at 25º C during the analysis period, according to the method of recrystallization commonly used for NLC. Three fields of view were imaged for each sample and only one was selected to be presented herein as being representative of each lipid system. Images were analyzed with Image-Pro Plus software, v.7.01 (Media Cybernetic, Bethesda, USA) using polarized light at 20 × magnification. The analysis were performed at 48 h and then at 7, 15, 30, and 60 days after preparation of the lipid systems.

4.3 Results and Discussion

4.3.1 Fatty acid composition (FAC)

The chemical composition of the lipid phase used to obtain NLC with incorporated bioactive compounds has a strong effect both on characteristics of the NLC and on the bioaccessibility of the bioactive compound incorporated into the structure. Characteristics of FA for NLC that comprised of lipid matrices with high and low MP promoted the formation of a more viscous lipid phase, which could lead to increased surface tension and, consequently, to the formation of larger particles (Pinto et al., 2018). Moreover, the composition of the lipid matrix affected the chain length and the degree of unsaturation of free fatty acids and monoacylglycerols produced during the digestion of lipids, thereby influencing the rate of lipid digestibility and the solubilization capacity of formed mixed micelles (Tan & McClements, 2021).

Table 1 shows the FAC of lipid systems composed of FHSO:HOSO (w/w) at distinct ratios. The FA predominantly found in HOSO were the UFA oleic acid (C18:1 = 78.51%) and linoleic acid (C18:2 = 12.49%), which accounted for approximately 91% of FA detected in this

lipid source. Oleic acid, a FA with only one *cis* unsaturation in its carbon chain, confers high oxidative stability to HOSO, which renders this raw material a low-MP lipid matrix ideal for the production of NLC for incorporation of bioactive compounds that are normally susceptible to oxidation. The SFA palmitic acid (C16:0 = 4.02%) and stearic acid (C18:0 = 2.69%) were also detected, albeit in lower proportions.

The process of full hydrogenation of vegetable oils promoted the full saturation of UFA present in the initial raw material (Ribeiro et al., 2013), as was observed in the FAC of the HOSO where SFA predominated. The FA that predominated in the FHSO were stearic acid (C18:0 = 87.31%) and palmitic acid (C16:0 =10.70%), accounting for 98% of the FA that comprise this lipid matrix. Stearic acid has a neutral effect on the body compared to cholesterol and, as a result, does not increase the risk of developing cardiovascular diseases (Sanders & Berry, 2005). The FAC in FHSO indicates that this lipid matrix has great potential for use as a high-MP lipid matrix for the production of NLC because its high content in SFA means that it is solid at room temperature.

Vegetable oils have great potential as lipid matrices with low MP for the production of NLC as they allow the formation of nanostructures from natural sources that are less expensive and that often have natural antioxidants in their composition. However, the choice of a raw material with lower MP is important because many vegetable oils exhibit a high degree of unsaturation and high viscosity, which may compromise the formation of NLC in terms of oxidative instability, problems related to droplets rupture during size reduction, and low efficiency of incorporation of bioactive compounds (Tamjidi et al., 2013). Furthermore, the solubilization capacity of the mixed micelles is strongly influenced by the composition of the lipid matrix—the greater the chain length and the lower the degree of unsaturation of the FA in lipid matrices, the greater the solubilization capacity, i.e., mixed micelles exhibit hydrophobic domains sufficiently large enough to incorporate bioactive compounds (Tan & McClements, 2021).

Several authors have reported that the release of long-chain MUFA, such as oleic acid, during digestion provides a greater solubilization capacity of mixed micelles and, consequently, greater bioaccessibility of carotenoids compared to those in the release of PUFA (Abreu-Martins et al., 2020; Verkempinck et al., 2018). As shown in Figure 1, the addition of HOSO to the lipid systems allowed obtaining systems with low SFA content and, consequently, with increased MUFA content, proportional to the amount of this raw material added to the lipid system.

Table 1. Fatty acid composition (%) of FHSO:HOSO (w/w) lipid systems.

	FHSO:HOSO (w/w)										
Fatty acid (%)	**100:0**	**90:10**	**80:20**	**70:30**	**60:40**	**50:50**	**40:60**	**30:70**	**20:80**	**10:90**	**0:100**
C14:0 Myristic acid	0.10	0.10	0.09	0.09	0.08	0.08	0.07	0.07	0.06	0.06	0.05
C15:0 Pentadecanoic acid	0.05	0.05	0.04	0.04	0.04	0.04	0.04	0.04	0.03	0.03	0.03
C16:0 Palmitic acid	10.70	10.03	9.37	8.70	8.03	7.36	6.69	6.02	5.35	4.69	4.02
C16:1 Palmitoleic acid	-	0.01	0.02	0.03	0.04	0.06	0.07	0.08	0.09	0.10	0.11
C17:0 Margaric acid	0.19	0.18	0.17	0.15	0.14	0.13	0.12	0.10	0.09	0.08	0.06
C17:1 8-heptadecanoic acid	-	0.01	0.01	0.02	0.02	0.03	0.03	0.04	0.04	0.05	0.05
C18:0 Stearic acid	87.31	78.85	70.38	61.92	53.46	45.00	36.54	28.08	19.62	11.15	2.69
C18:1 Oleic acid	0.12	7.96	15.80	23.64	31.48	39.32	47.16	55.00	62.84	70.68	78.51
C18:2*t* Linoleic *trans* acid	-	0.01	0.02	0.02	0.03	0.04	0.05	0.06	0.06	0.07	0.08
C18:2 Linoleic acid	0.05	1.29	2.52	3.76	4.99	6.23	7.46	8.70	9.93	11.17	12.40
C18:3 Linolenic acid	-	0.02	0.04	0.06	0.07	0.09	0.11	0.13	0.15	0.17	0.18
C20:0 Arachidic acid	0.74	0.70	0.65	0.61	0.56	0.52	0.47	0.43	0.38	0.34	0.29
C20:1 Eicosenoic acid	-	0.03	0.06	0.09	0.12	0.15	0.17	0.20	0.23	0.26	0.29
C22:0 Behenic acid	0.53	0.57	0.61	0.64	0.68	0.72	0.75	0.79	0.83	0.86	0.90
C24:0 Lignoceric acid	0.20	0.22	0.23	0.24	0.25	0.26	0.28	0.29	0.30	0.31	0.32

The FAC of this raw material (Table 1 and Figure 1) confirmed its potential as a lipid matrix for NLC with lower MP, mainly due to the high oleic acid (C18:1 = 78.51%) content which allowed for the following: a less viscous lipid phase and NLC of lower size; greater solubilization and protection of bioactive compounds merged into the structure because this FA exhibited high oxidative stability and increased bioaccessibility of the compound due to the greater solubilization capacity of mixed micelles. However, further characterization is necessary to identify optimal lipid systems for the formation of NLC, as discussed below.

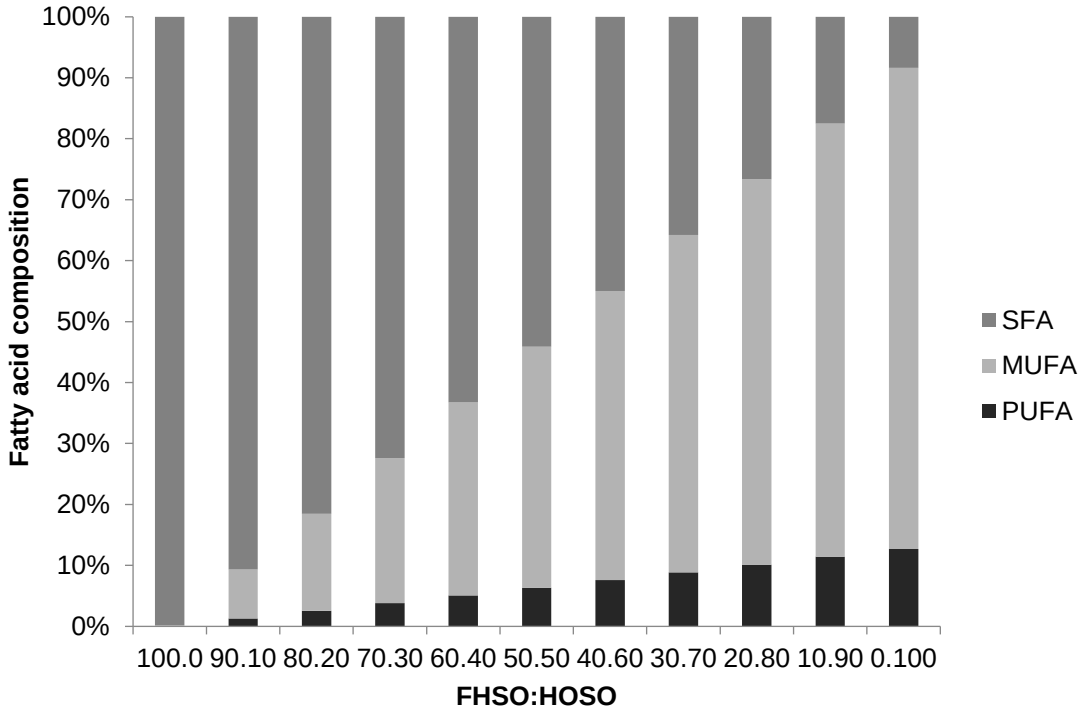

Figure 1. Saturated (SFA), monounsaturated (MUFA), and polyunsaturated fatty acids (PUFA) of the FHSO:HOSO (w/w) lipid systems.

4.3.2 Triacylglycerol (TAG) composition

The TAG content in FHSO, HOSO, and in respective lipid systems formed using mixtures of these raw materials (FHSO:HOSO w/w) is presented in Table 2. Eleven species of TAG with 50 to 58 carbon atoms in HOSO were identified, those majorly with 54 carbon (approximately 79%). Because TAG are formed by the esterification of a glycerol molecule with three FA, triolein (OOO) accounted for approximately 50.67% of the TAG in HOSO, mainly because of the high oleic acid content found in this lipid matrix. Other TAG were detected in significant amounts, such as OLO (20.09%), POO (10.24%), and OLL (6.16%).

Because of the homogeneity of the FAC in HOSO, only three TAG that were tri-saturated were identified. As shown in Table 2, the TAG in HOSO were PSP, PSS, and SSS, and the latter accounted for 62.66% of all TAG content in this lipid matrix. Increasing the proportion of HOSO in the lipid system resulted in elevated levels of tri-unsaturated TAG and resulted in a reduction in the concentration of tri-saturated TAG (Table 2). Nevertheless, the TAG composition in all lipid systems consisted predominantly of species with 54 carbons, formed by FA of 18 carbons, corresponding to the FA found in greater proportion in both lipid matrices (oleic and stearic acids).

Table 2: Triacylglycerol composition (%) of FHSO:HOSO (w/w) lipid systems.

		FHSO:HOSO (w/w)										
Group	**TAG**	**100:0**	**90:10**	**80:20**	**70:30**	**60:40**	**50:50**	**40:60**	**30:70**	**20:80**	**10:90**	**0:100**
C50	POP	-	0.04	0.09	0.13	0.18	0.22	0.26	0.31	0.35	0.40	0.44
	PSP	3.62	3.26	2.90	2.54	2.17	1.81	1.45	1.09	0.72	0.36	-
C52	POO	-	1.02	2.05	3.07	4.09	5.12	6.14	7.17	8.19	9.21	10.24
	POL	-	0.20	0.40	0.60	0.80	1.00	1.20	1.40	1.60	1.80	2.00
	PLL	-	0.15	0.30	0.45	0.61	0.76	0.91	1.06	1.21	1.36	1.51
	POS	-	0.04	0.09	0.13	0.17	0.21	0.26	0.30	0.34	0.39	0.43
	PSS	33.71	30.34	26.97	23.60	20.23	16.86	13.48	10.11	6.74	3.37	-
C54	OOO	-	5.07	10.13	15.20	20.27	25.34	30.40	35.47	40.54	45.60	50.67
	OLO	-	2.01	4.02	6.03	8.04	10.04	12.05	14.06	16.07	18.08	20.09
	OLL	-	0.62	1.23	1.85	2.46	3.08	3.69	4.31	4.92	5.54	6.16
	SOO	-	0.21	0.41	0.62	0.83	1.03	1.24	1.45	1.65	1.86	2.07
	SSS	62.66	56.40	50.13	43.87	37.60	31.33	25.07	18.80	12.53	6.27	-
C56	OOA	-	0.38	0.77	1.15	1.54	1.92	2.30	2.69	3.07	3.45	3.84
C58	OOBe	-	0.25	0.51	0.76	1.02	1.27	1.53	1.78	2.04	2.29	2.55
S_3		100.00	90.00	80.00	70.00	60.00	50.00	40.00	30.00	20.00	10.00	-
S_2U		-	0.29	0.59	0.88	1.17	1.47	1.76	2.06	2.35	2.64	2.94
SU_2		-	2.01	4.03	6.04	8.06	10.07	12.09	14.10	16.11	18.13	20.14
U_3		-	7.69	15.38	23.07	30.77	38.46	46.15	53.84	61.53	69.22	76.92

P: Palmitic acid; **O**: Oleic acid; **S**: Stearic acid; **L:** Linoleic acid; **Be:** Behenic acid; **A**: Arachidic acid; **S_3**: trisaturated; **S_2U**: monounsaturated; **SU_2**: diunsaturated; **U_3:** triunsaturated; **-**: not detectable.

4.3.3 Solid fat content (SFC)

Crystalline lattice growth begins when TAG molecules in the sample reorganize and crystallize from melted lipids as “primary crystals”. Once primary crystals are formed, they aggregate via the transference of mass and heat to form polycrystals and crystal aggregates at the microstructural scale, which continues until a three-dimensional lattice is created (Acevedo & Marangoni, 2010). The structural arrangement of TAG as crystals is commonly measured by X-ray diffraction, whereas crystal aggregates and the crystalline lattice are analyzed by NMR.

NMR is based on the measurement of the response of a sample to pulses of high frequency magnetic radiation. After a pulse is applied, the hydrogen nuclei present in the sample shift to an excited state and return to the ground state after some time, known as the decay rate. The latter depends on the physical state of the sample: the signal in solids decays much faster than that in liquids. Therefore, the SFC of lipid systems may be determined by the rate of decay of the NMR signal (McClements & McClements, 2016).

SFC values should be considered when lipid systems are applied to foods because they are directly related to the general behavior of lipid matrices when subjected to different temperatures. Values of SFC obtained at temperatures > 40 °C provide information regarding fat melting profiles; at temperatures < 25 °C they characterized hardness; temperatures between 20 °C and 25 °C they indicate thermal resistance to ambient temperature; and 37 °C they relate to the behavior of a specific lipid matrix at body temperature (O’Brien, 2008).

Because lipid matrices used to obtain LN should have a MP above body temperature (37 °C) and exhibit high thermal resistance (to avoid mobility of bioactive compounds incorporated into the nanostructure and to allow the technological application of such nanostructures in foods subjected to thermal treatments) (Salminen et al., 2014), we assessed the SFC of lipid systems with different FHSO:HOSO (w/w) ratios and at different temperatures. Figure 2 and Table 3 demonstrate SFC obtained for different lipid systems composed of FHSO:HOSO (w/w).

FHSO induces the formation of the initial crystals because of its chemical composition. Therefore, in this study, a reduction in FHSO content in lipid systems was accompanied by a proportional reduction in SFC because of the diminished levels of TAG with high MP (tri-saturated TAG) and an increase in di- and tri-unsaturated TAG from HOSO, which have lower MP. Moreover, the reduction in SFC with increasing temperature was less marked in lipid systems whose content in HOSO was higher, which might be explained by the increase in TAG concentrations with low MP in the system. The greatest reduction in SFC in lipid systems was observed between 60 °C and 65 °C (Table 3) and was associated with the temperature range within which most TAG in FHSO melt. Lipid systems in this study had an

SFC > 10% at 20 ºC and therefore, are classified as being resistant to oil exudation (Grimaldi et al., 2000).

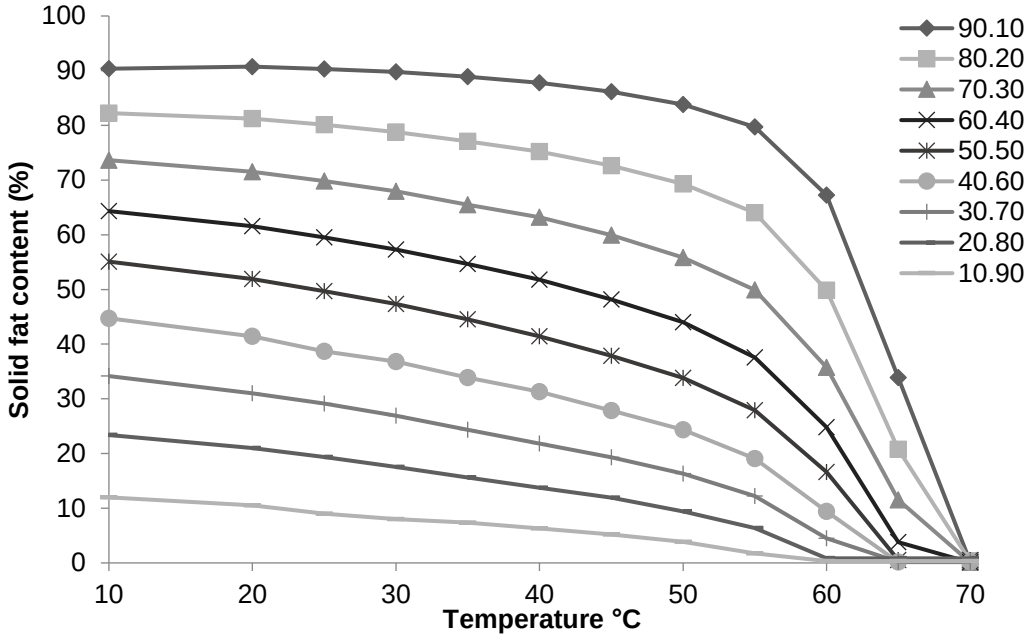

Figure 2: Solid fat content (SFC) (%) as a function of temperature of FHSO:HOSO (w/w) lipid systems.

The MP of lipid systems used to obtain NLC are extremely important because NLC need to remain stable during their passage through the GIT, whereas their melting temperature must be adequate for the TAG that compose the particle to be available to attach to the lipase so that digestion occurs and the compound incorporated in the structure is released. Similarly to SFC, MP of the FHSO:HOSO (w/w) lipid systems was lessen (data not shown) with an increased HOSO in the system. Because the MP of a lipid raw material is mainly affected by its chemical composition, the increase in HOSO in lipid systems promoted the inclusion of tri-unsaturated TAG that have lower MP; as a result, MP in lipid systems was reduced. Considering that the MP corresponded to the temperature at which the content in solids was 4% (Karabulut et al., 2004), analyzed lipid systems had MP between 49.1 °C and 69.5 °C (data not shown).

Table 3. Solid fat content (SFC) (%) as a function of temperature of FHSO:HOSO (w/w) lipid systems

FHSO:HOSO	10°C	20°C	25°C	30°C	35°C	40°C	45°C	50°C	55°C	60°C	65°C	70°C
100.00	98.87±0.02^{Aa}	98.67±0.01^{Aab}	98.50±0.01^{Abc}	98.33 ±0.02^{Abcd}	98.19±0.01^{Abcd}	98.02±0.02^{Ad}	97.4±0.02^{Ae}	96.89±0.02^{Af}	94.85±0.04^{Ag}	84.89±0.27^{Ah}	52.62±0.2 ^{Ai}	0.18±0.19 ^{ABj}
90.10	90.34±0.05^{Bb}	90.74±0.05 ^{Ba}	90.3±0.06 ^{Bb}	89.77±0.04 ^{Bc}	88.88±0.07^{Bd}	87.76±0.03^{Be}	86.14±0.12^{Bf}	83.83±0.06^{Bg}	79.7±0.08 ^{Bh}	67.26±0.18 ^{Bi}	33.86±0.16^{Bj}	0.19±0.19^{ABk}
80.20	82.25±0.03^{Ca}	81.22±0.02 ^{Cb}	80.15±0.04 ^{Cc}	78.79±0.06 ^{Cd}	77.09±0.06^{Ce}	75.2±0.06 ^{Cf}	72.65±0.05^{Cg}	69.31±0.02^{Ch}	64±0.13 ^{Ci}	49.85±0.31 ^{Cj}	20.79±0.31^{Ck}	0.32±.16 ^{Ai}
70.30	73.64±0.12^{Da}	71.52±0.09 ^{Db}	69.83±0.06 ^{Dc}	67.92±0.09 ^{Dd}	65.51±0.06 ^{De}	63.22±0.05 ^{Df}	59.93±0.14^{Dg}	55.81±0.08 ^{Dh}	49.93±0.12 ^{Di}	35.76±0.05 ^{Dj}	11.5±0.15 ^{Dk}	0.09±0.12 ^{ABi}
60.40	64.32±0.18^{Ea}	61.55±0.23 ^{Eb}	59.52±0.07 ^{Ec}	57.28±0.07 ^{Ed}	54.64±0.07 ^{Ee}	51.79±0.07 ^{Ef}	48.14±0.19^{Eg}	44.03±0.09^{Eh}	37.55±0.18 ^{Ei}	24.82±0.47 ^{Ej}	3.81±0.15 ^{Ek}	0.08±0.02 ^{ABi}
50.50	55.09±1.15^{Fa}	51.93±1.19 ^{Fab}	49.69±1.23^{Fbc}	47.35±1.39 ^{Fcd}	44.50±1.32 ^{Fde}	41.41±1.37 ^{Fe}	37.87±1.36 ^{Ff}	33.80±1.45 ^{Fg}	27.93±1.12^{Fh}	16.61±1.27 ^{Fi}	0.53±0.34 ^{Fj}	0±0.0 ^{Aj}
40.60	44.73±0.49^{Ga}	41.43±0.35 ^{Gb}	38.71±0.63 ^{Gc}	36.81±0.43 ^{Gd}	33.89±0.43 ^{Ge}	31.31±0.39 ^{Gf}	27.85±0.41^{Gg}	24.34±0.04 ^{Gh}	19.05±0.18 ^{Gi}	9.4±0.29 ^{Gj}	0.14±0.19 ^{Fk}	0±0.0 ^{Ak}
30.70	34.16±0.12^{Ha}	31.0±0.09 ^{Hb}	29.12±0.06 ^{Hc}	26.91±0.17 ^{Hd}	24.35±0.04 ^{He}	21.85±0.05 ^{Hf}	19.33±0.04^{Hg}	16.31±0.17 ^{Hh}	12.19±0.30 ^{Hi}	4.50±0.23 ^{Hj}	0.18±0.13 ^{Fk}	0±0.0 ^{Ak}
20.80	23.39±1.00 ^{Ia}	20.99±067 ^{Ib}	19.38±0.62 ^{Ic}	17.52±0.54 ^{Id}	15.64±0.36 ^{Ie}	13.76±0.21 ^{If}	11.91±0.27 ^{Ig}	9.39±0.28 ^{Ih}	6.36±0.35 ^{Ii}	0.84±0.24 ^{Ij}	0±0.0 ^{Fj}	0±0.0 ^{Aj}
10.90	11.99±0.09^{Ja}	10.55±0.18 ^{Jb}	8.98±1.22 ^{Jc}	7.99±0.78 ^{Jcd}	7.38±0.24 ^{Jde}	6.30±0.11 ^{Jef}	5.21±0.24 ^{Jf}	3.84±0.16 ^{Jg}	1.74±0.09 ^{Jh}	0.34±0.24 ^{Ji}	0±0.0 ^{Fi}	0±0.0 ^{Ai}

*Average of three replicates ± Standard Deviation. $^{A-J}$ Different capital letters indicate significant difference ($p< 0.05$) related to the evaluation of SFC between the lipid systems at the same temperature. $^{a-k}$ Different lower-case letters indicate significant difference ($p< 0.05$) related to the evaluation of the FSC of the same lipid system at the different temperatures.

Because lipid phases of high (solid) and low (liquid) MP considered for the formation of NLC must exhibit good miscibility and compatibility (Müller et al., 2002), we evaluated the compatibility of lipid systems composed of FHSO:HOSO (w/w) using compatibility diagrams. The results of a compatibility study involving the components of lipid systems where the SFC at different temperatures was plotted against the percentage of HOSO in the systems are shown in Figure 3.

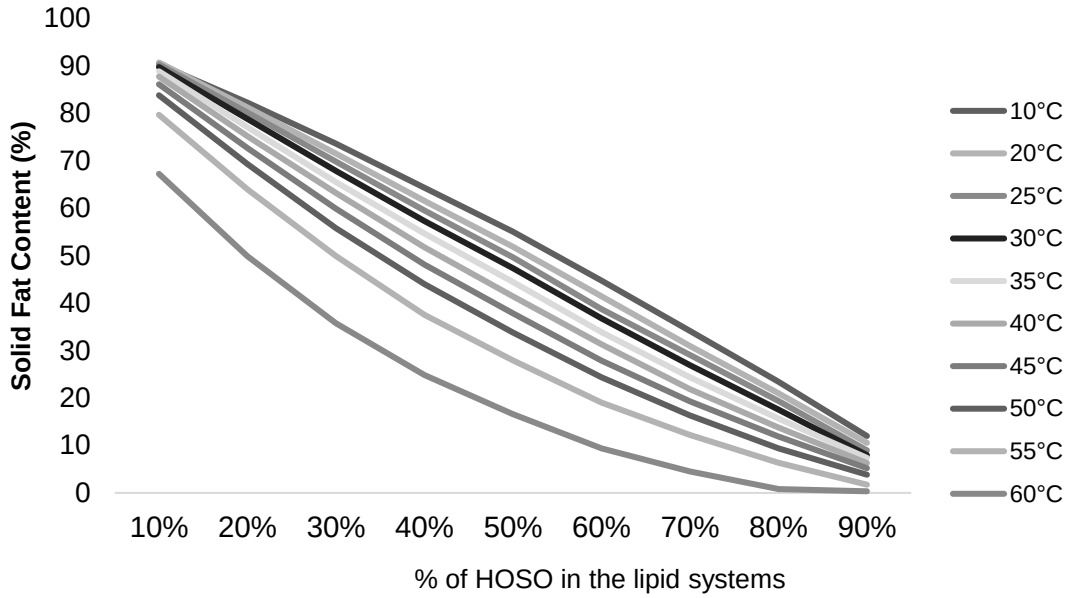

Figure 3: Compatibility diagram of FHSO:HOSO lipid systems (w/w).

Incompatible lipid systems are characterized by discontinuities in the lines of solids in compatibility diagrams (Timms, 1984). In this sense, the linear evolution of SFC according to composition (% of HOSO in the lipid system), presented in Figure 3, is an indicator of a complete compatibility between components through dilution effects in all FHSO:HOSO (w/w) lipid systems (Timms, 1984).

The profile of solids is a tool that helps guiding the use or replacement of fats in specific formulations because it provides indications about the general behavior of a lipid source. Data regarding the profile of solids, compatibility diagrams, and melting points allow for selection of the optimal lipid system for obtaining an NLC that meets the application requirements (incorporation of bioactive compounds, crystallization seeding, varying degrees of crystallinity, and thermal resistance). In lipid-based semi-solid formulations such as NLC, bioactive compounds are solubilized in the lipid phase at lower MP, which increases the load-carrying capacity of the particle, whereas the lipid phase at higher MP provides protection during the passage of the structure through the GIT. The combination of lipid components of high and low MP provides protection and promotes the micellization of compounds after

digestion (Ashkar et al., 2021). Therefore, NLC for the incorporation of bioactive compounds is aimed for, considering the crystallinity of the lipid system as a whole is necessary because this parameter is directly related to the structural stability of the particle during its passage through the GIT. In this sense, the results obtained for lipid system 10:90 indicated that this FHSO:HOSO (w/w) ratio was not adequate for the formation of a NCL because it could compromise the function of the structure in specific applications.

4.3.4 Thermal behavior

DSC is a sensitive technique that aids in the understanding of structural properties of a sample by measuring the loss or gain of heat, i.e., absorption or emission of thermal energy during melting or crystallization, respectively, that result from physical or chemical changes within a sample under controlled temperatures (Khosa et al., 2018). DSC analysis is useful to elucidate the behavior of mixtures of lipids with lower and higher MP and provides relevant information concerning the thermal behavior of lipid systems (Han et al., 2008).

Table 4 highlights parameters of thermal behavior during crystallization of different lipid systems (FHSO:HOSO w/w). The parameters considered for discussion of thermal behavior during crystallization were as follows: onset temperature of crystallization (Tco), which is the temperature at the beginning of the liquid-solid transition; offset temperature of crystallization (Toff c) denoting the temperature at the end of the thermal effects of crystallization; maximum temperature of the crystallization peak (Tcp), which indicates the point at which the maximum thermal effect occurred; and crystallization enthalpy (ΔHc), which reflects the energy required for change of phase to occur (Ribeiro et al., 2009).

The crystallization curves in Figure 4 show that FHSO and the lipid system 90:10 exhibited only one crystallization peak as a result of the homogeneity of TAG present in this lipid system, which was predominantly of high MP, and composed of long-chain FA, as described in 4.3.2. There was also only one crystallization peak in HOSO, the lipid source of lower MP, in this case due to the predominance of TAG with low MP (tri-unsaturated).

The remaining lipid systems exhibited two crystallization events—the first and second corresponded to the crystallization of the high MP TAG (trisaturated) and medium and low MP TAG, respectively. Moreover, the increase in the content of tri-unsaturated TAG from HOSO in the lipid systems led to a reduction in the energy required for crystallization (ΔHc), which indicated the formation of less-compact crystalline networks desired for obtaining NLC that are intended for bioactive compound incorporation. The incorporation of a lipid phase of lower MP leads to the formation of less-ordered amorphous crystalline structures, which results in a higher bioactive compound load-carrying capacity, reduced expulsion of the bioactive compound incorporated in the structure during storage and, consequently, decreased

tendency for undesirable changes involving the morphology of the particles, as well as greater colloidal stability (Gonçalves et al., 2018; Mohammadi et al., 2019).

The initial temperature of crystallization is a very important parameter in the evaluation of lipid systems used to obtain NLC with incorporated bioactive compounds. A high initial temperature of crystallization indicates faster recrystallization, higher crystallinity, and greater thermal resistance of the lipid system, which affects the capacity for incorporation and retention of bioactive compounds. Because Tco is the temperature at which tri-saturated TAG begin to crystalize, Tco values increased in proportion to the increased HOSO content of the lipid system.

Table 4. Thermal parameters of crystallization behavior of FHSO:HOSO (w/w) lipid systems.

FHSO:HOSO	**Tco**	**Tcp1**	**Tcp2**	**ΔHc 1**	**ΔHc 2**	**Toff c**
	(°C)			(J/g)		(°C)
100:0	50.42±0.34	47.67±0.08	-	111.80±0.12	-	41.17±0.50
90:10	48.58±0.06	45.52±0.57	-	90.75±2.17	-	35.03±1.66
80:20	47.51±0.10	44.65±0.16	-44.87±0.14	73.59±1.88	1.17±0.32	-50.81±0.56
70:30	46.39±0.06	43.87±0.36	-42.64±0.19	67.25±1.54	3.13±0.19	-50.22±0.58
60:40	45.38±0.08	43.82±0.15	-41.42±0.26	69.20±2.74	6.67±0.99	-51.34±1.31
50:50	43.65±0.25	42.34±0.40	-38.63±1.56	39.56±1.81	6.35±0.82	-47.67±1.70
40:60	41.21±0.13	40.15±0.15	-36.35±0.28	46.72±2.60	17.33±0.68	-46.54±0.48
30:70	39.57±0.78	38.43±0.27	-29.20±0.98	30.11±2.77	23.28±2.16	-40.20±1.67
20:80	35.85±0.35	35.52±0.39	-36.43±5.28	28.31±6.03	29.22±2.16	-48.78±5.82
10:90	31.20±0.22	30.53±0.21	-41.07±0.18	12.78±1.42	31.40±0.75	-53.26±0.48
0:100	-43.28±0.03	-46.94±0.03	-	31.63±0.81	-	-55.17±0.69

Tco: crystallization onset temperature; **Tcp:** crystallization peak temperature; **Toff c:** crystallization offset temperature; ∆**Hc**: crystallization enthalpy. Average of three replicates ± Standard Deviation

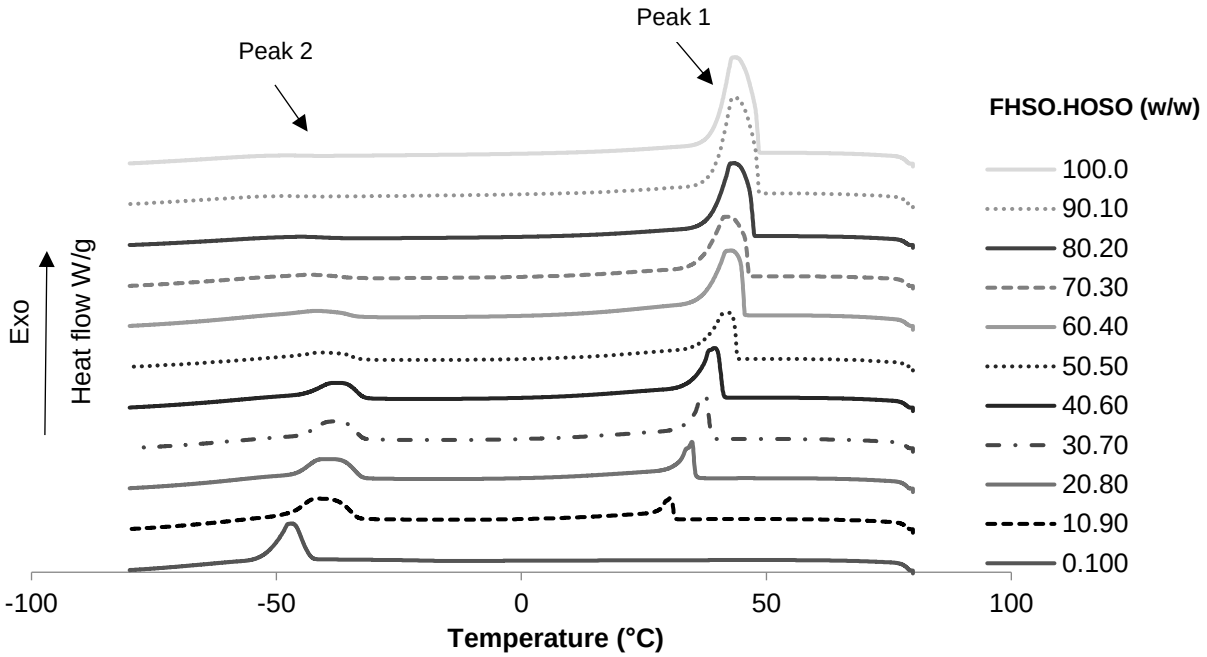

Figure 4. Crystallization behavior obtained from differential scanning calorimetry (DSC) of lipid systems composed by fully hydrogenated soybean oil (FHSO) and high oleic sunflower oil (HOSO).

The parameters that affected the thermal behavior of the melting process in the different systems lipids (FHSO:HOSO w/w) are shown in Table 5. The following parameters were considered for the discussion of the thermal behavior during melting: melting onset temperature (Tmo), which is the temperature at the beginning of the solid-liquid transition; final temperature of melting (Toff m), which is at the end of the thermal effect of melting; maximum temperature of the melting peak (Tmp), which indicates the point at which the maximum thermal effect occurred; and melting enthalpy (∆Hm), which reflects the energy required for the change of phase to occur.

As in the analysis of the thermal behavior during crystallization, FHSO, the lipid system 90:10 and HOSO exhibited only one melting event, which once again stipulated that TAG that composed it had similar thermal behaviors, reflected as a single melting peak. The increase in HOSO in the lipid systems led to the occurrence of a second melting peak, promoted the displacement of the initial and final peak temperatures, and a reduction in the energy required for the melting process, as shown in Table 5 and Figure 5. Changes involving these parameters may be explained by the TAG composition of this lipid matrix, which consists of TAG with a lower MP than that of the TAG present in FHSO.

Lipid nanoparticles are derivations of oil-water emulsions where liquid lipids of oil droplets are replaced by lipids that remain in solid form at body temperature (Rawal & Patel, 2018). Stability of the solid state at body temperature (37 °C) is therefore a requirement for selecting lipid systems for the formation of NLC with incorporated bioactive compounds,

because stability implies that the maintenance of structural integrity of particles during their passage through the GIT. This characteristic ensures that bioactive compounds incorporated into the structure are only released once in the intestine, which is the best site for its efficient absorption; hence, the compound is bioaccessible and can be used in vital biological functions (Ashkar et al., 2021).

Table 5. Thermal parameters of melting behavior of FHSO:HOSO (w/w) lipid systems.

FHSO:HOSO	Tmo	Tmp1	Tmp2	ΔHm 1	ΔHm 2	Toff m
		(°C)		(J/g)		(°C)
100:0	49.87±0.14	-	64.36±0.03	-	88.76±0.44	69.20±0.05
90:10	49.89±0.24	-	62.63±0.31	-	72.54±1.28	68.42±0.21
80:20	-13.53±0.49	-6.43±0.14	67.91±0.08	5.29±0.82	88.91±2.78	71.69±0.40
70:30	-13.16±0.44	-6.07±0.27	67.21±0.17	7.38±0.82	77.98±1.91	71.15±0.61
60:40	-13.01±0.05	-5.79±0.19	66.20±0.03	11.32±1.91	58.84±2.86	68.75±0.46
50:50	-12.20±0.26	-4.86±0.07	64.38±0.06	7.12±1.46	28.69±2.31	67.92±0.33
40:60	-12.27±0.65	-4.48±0.22	63.48±1.28	15.69±2.42	33.66±3.33	66.89±1.18
30:70	-12.38±0.64	-4.22±0.63	62.64±1.42	20.44±2.36	21.16±0.82	65.02±1.18
20:80	-12.26±1.53	-3.46±2.37	60.89±0.08	27.19±4.54	12.21±0.94	63.06±0.09
10:90	-13.38±0.10	-4.78±0.14	57.76±0.10	36.88±1.78	4.79±0.69	57.76±0.10
0:100	-13.45±0.17	-4.61±0.04	-	41.34±1.76	-	-1.10±0.18

Tmo: melting onset temperature; **Tmp:** melting peak temperature; **Toff m:** melting offset temperature; ∆**Hm**: melting enthalpy. Average of three replicates ± Standard Deviation.

Table 5 shows one melting event above 37 °C for all lipid systems analyzed in this study, which indicates thermal resistance at body temperature. However, Toff m needs to be considered in the production of NLC because it must be high enough to allow for stability of the particle structure during its passage through the GIT, but should also allow the particle to be digested by lipases during the digestion process. Like Tco, Toff m elevated proportionally to the content of FHSO in the lipid system as a result of increased trisaturated TAG levels in this lipid matrix.

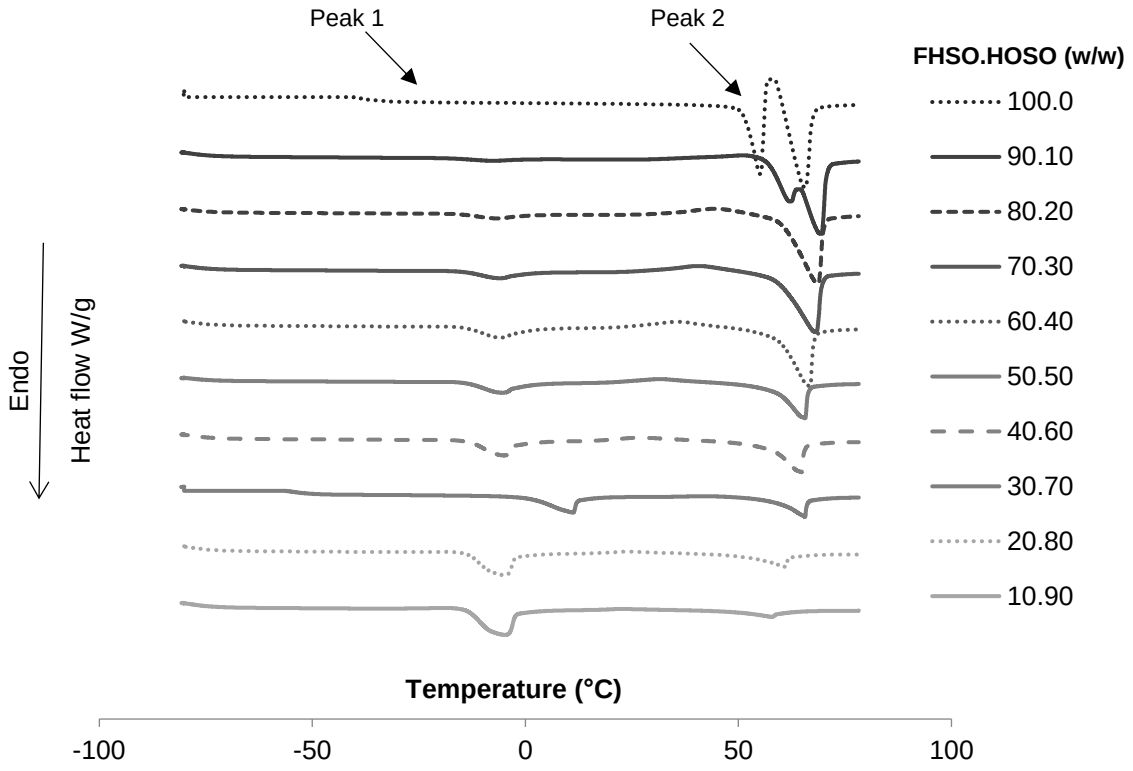

Figure 5. Melting behavior obtained from differential scanning calorimetry (DSC) of lipid systems composed by fully hydrogenated soybean oil (FHSO) and high oleic sunflower oil (HOSO).

The melting temperature observed by DSC was lower than the MP determined by SFC analysis using NMR, as described in section 4.3.3. In the determination of SFC by NMR, sample stabilization was performed to obtain a more stable polymorph. Thus, the MP obtained using this technique was determined when the sample exhibited high crystalline order and, in the case of NLC production, which indicated the temperature at which the particle SFC would be < 4% if they were stabilized in the polymorphic β form. Thermal behavior analysis by DSC did not take into account pre-treatment of samples and, therefore, the observed phenomenon encompassed the melting of different polymorphs. In this case, crystalline order was poorer but corresponded to the sample's polymorphic form, thereby resulting in a melting range lower than the MP detected by NMR.

Overall, rising HOSO in the lipid systems led to a modification of the thermal behavior of the fully saturated lipid base (FHSO), which allowed obtaining lipid systems with adequate behavior for the formation of NLC and incorporation of bioactive compounds. Lipid systems whose melting processes occurred at high temperatures could be used to produce NLC that will be submitted to thermal treatments, including pasteurization and sterilization.

4.3.6 Polymorphic form

The pattern of lipid crystallization is directly related to the phenomenon of polymorphism (behavior of the crystal). Crystallization of TAG results in the structural arrangement of these molecules when stacked in three polymorphic forms, including hexagonal (α), orthorhombic (β'), and triclinic (β) forms, which can be determined by X-ray diffraction, one of the most powerful tools to determine the spatial arrangement of molecules in a substance that provides valuable information concerning its physical state (liquid or crystalline) and polymorphic form (Hartel, 2013).

The polymorphic forms α, β', and β, in increasing order of stability and well-defined regarding their specific interplanar distances, or short spacing intervals —4.15 Å (α), 4.2 Å and 3.8 Å (β'), and 4.6 Å (β)— were determined by wide-angle X-ray diffraction. Short spacing intervals, peak intensity, and polymorphic forms are described in Table 6 for lipid systems stabilized by MI (crystallization and storage at 25 °C) and in Table 7 for lipid systems stabilized by MII (crystallization at 5°C/24 h followed by storage at 25 °C).

The results presented in Tables 6 and 7 show that stabilization using the method with a protocol commonly used for the recrystallization of NLC (MII) led to the formation of more stable polymorphs earlier than stabilization using MI in the majority of the lipid systems analyzed in this study. Crystal growth involves the diffusion of TAG into solution through a stagnated layer adjacent to the interface and their incorporation in the pre-existing crystalline network (crystallites). These mechanisms depend on the degree of supercooling, rate of diffusion of molecules to the surface of the crystal, and time required for the TAG molecules to be embedded in the growing crystalline lattice (Marangoni, 2005).

The synthesis of NLC is usually associated with variations of the following technological approaches: i) creation of an oil-in-water nanoemulsion as a precursor to subsequent steps; ii) subsequent solidification of the dispersed lipid phase (Sharma et al., 2011). The results obtained with MI revealed the importance of using lower temperatures for solidification of the dispersed lipid phase to obtain NLC. The earlier stabilization obtained with MII might be attributed to the lower temperature at which the sample was stored immediately after the melting process, which favored a more ordered association between TAG in the lipid systems.

However, regardless of the method used to stabilize samples, with the exception of the lipid system with a FHSO:HOSO (w/w) ratio of 10:90 and which exhibited the polymorphic forms β'+ β after 60 days, most lipid systems became stabilized in the polymorphic β form at the end of this period. This result might be explained by the similarity between FA chains that were predominant in the lipid matrices. HOSO was mostly composed of oleic acid (C18:1), whereas stearic acid predominated in FHSO (C18:0), with both FA having 18 carbon

atoms and therefore, high chemical homogeneity. Homogeneous TAG, i.e., TAG formed by FA with the same chain length, stacked easily and crystallized in the most stable polymorphic β form (Acevedo & Marangoni, 2010; Ribeiro et al., 2013).

Stabilization in polymorphic form β at the end of the 60-day period was therefore an indication that addition of nanoparticles obtained from these lipid systems to foods would occur in the most stable configuration, thus avoiding problems associated with subsequent polymorphic transitions. It should be emphasized that, although the macroscale results indicated the potential of using these lipid systems as the lipid phase of NLC, determining the polymorphic form of the nanoparticles obtained from these systems is crucial, because polymorphic transitions can be accelerated at the nanoscale.

Table 6: Polymorphic forms, short spacings and peak intensities of the diffractograms obtained for FHSO:HOSO lipid systems (w/w) stabilized through **Method I**.

		Short spacings (nm)					
Lipid system	**Time of storage**	**4.6**	**4.1**	**4.2**	**3.8**	**3.6**	**Polymorphic form**
	48 h	4.6 (vs)	4.1 (s)	4.2 (s)	3.9 (vs)	3.7 (w)	α + β’ + β
	7 days	4.6 (s)	4.1 (vs)	4.3 (vs)	3.8 (s)	3.6 (m)	α + β’ + β
10:90	15 days	4.6 (w)	4.1 (m)	4.2 (m)	3.8 (w)	3.6 (w)	α + β’ + β
	30 days	4.6 (w)	4.1 (m)	4.2 (m)	3.8 (w)	3.6 (vw)	α + β’ + β
	60 days	4.6 (w)	-	4.2 (w)	3.8 (w)	3.6 (vw)	β’ + β
	48 h	4.6 (vs)	-	-	3.8 (m)	3.7 (m)	β
	7 days	4.6 (vs)	-	-	3.9 (m)	3.7 (m)	β
20:80	15 days	4.6 (m)	-	-	3.8 (w)	3.6 (w)	β
	30 days	4.6 (w)	-	-	3.8 (w)	3.7 (w)	β
	60 days	4.6 (m)	-	-	3.8 (w)	3.7 (w)	β
	48 h	4.6 (vs)	-	4.2 (s)	3.8 (s)	3.6 (w)	β’ + β
	7 days	4.6 (vs)	-	4.3 (s)	3.8 (m)	3.7 (m)	β’ + β
30:70	15 days	4.6 (vs)	-	-	3.8 (m)	3.7 (m)	β
	30 days	4.6 (m)	-	-	3.8 (m)	3.7 (w)	β
	60 days	4.6 (w)	-	-	3.9 (w)	3.7 (w)	β
	48 h	4.6 (s)	-	4.2 (s)	3.8 (m)	3.7 (w)	β’ + β
	7 days	4.6 (vs)	-	4.2 (s)	3.9 (s)	3.7 (m)	β’ + β
40:60	15 days	4.6 (vs)	-	-	3.8 (s)	3.7 (s)	β
	30 days	4.6 (m)	-	-	3.9 (w)	3.7 (w)	β
	60 days	4.6 (w)	-	-	3.9 (w)	3.7 (w)	β

	48 h	4.6 (s)	-	4.3 (m)	3.9 (m)	3.7 (m)	β' + β
	7 days	4.6 (vs)	-	4.3 (s)	3.8 (s)	3.7 (m)	β' + β
50:50	15 days	4.6 (vs)	-	4.3 (s)	3.8 (s)	3.7 (m)	β' + β
	30 days	4.6 (m)	-	-	3.9 (w)	3.7 (m)	β
	60 days	4.6 (w)	-	-	3.9 (w)	3.7 (w)	β
	48 h	4.6 (vs)	-	4.2 (m)	3.9 (s)	3.7 (s)	β' + β
	7 days	4.6 (vs)	-	4.2 (s)	3.9 (s)	3.6 (s)	β' + β
60:40	15 days	4.6 (vs)	-	4.2 (s)	3.9 (s)	3.7 (s)	β' + β
	30 days	4.6 (s)	-	-	3.9 (m)	3.7 (m)	β
	60 days	4.6 (m)	-	-	3.9 (w)	3.7 (w)	β
	48 h	4.6 (vs)	-	4.2 (m)	3.8 (vs)	3.7 (s)	β' + β
	7 days	4.6 (s)	-	4.2 (m)	3.8 (s)	3.7 (s)	β' + β
70:30	15 days	4.6 (vs)	-	4.2 (s)	3.8 (s)	3.7 (s)	β' + β
	30 days	4.6 (m)	-	-	3.8 (m)	3.7 (m)	β
	60 days	4.6 (m)	-	-	3.8 (m)	3.7 (m)	β
	48 h	4.6 (s)	-	4.2 (vs)	3.8 (s)	3.7 (m)	β' + β
	7 days	4.6 (vs)	-	4.3 (s)	3.8 (vs)	3.7 (s)	β' + β
80:20	15 days	4.6 (m)	-	4.3(vs)	3.8 (s)	3.7 (m)	β' + β
	30 days	4.6 (m)	-	-	3.8 (m)	3.7 (m)	β
	60 days	4.6 (m)	-	-	3.8 (m)	3.7 (m)	β
	48 h	4.6 (m)	-	4.2 (vs)	3.8 (s)	-	β' + β
	7 days	4.6 (vs)	-	4.2 (s)	3.9 (vs)	3.7 (s)	β' + β
90:10	15 days	4.6 (vs)	-	4.2(s)	3.9 (vs)	3.7 (s)	β' + β
	30 days	4.6 (w)	-	4.2 (w)	3.8 (w)	3.7 (w)	β' + β
	60 days	4.6 (m)	-	-	3.9 (m)	3.7 (m)	B

Intensities: **v.** very; **w.** weak; **m.** medium; **s.** strong.

Table 7: Polymorphic forms, short spacings and peak intensities of the diffractograms obtained for FHSO:HOSO lipid systems (w/w) stabilized through **Method II**.

		Short spacings (nm)					
Lipid system	**Time of storage**	**4.6**	**4.1**	**4.2**	**3.8**	**3.6**	**Polymorphic form**
	48 h	4.6 (s)	4.1 (m)	4.4 (s)	3.9 (s)	3.6 (w)	α + β' + β
	7 days	4.5 (w)	4.1 (w)	4.3 (m)	3.9 (m)	3.6 (vw)	α + β' + β
10:90	15 days	4.5 (w)	-	4.3 (m)	3.9 (m)	3.6 (vw)	β' + β
	30 days	4.5 (w)	-	4.3 (m)	3.9 (m)	3.6 (vw)	β' + β
	60 days	4.5 (w)	-	4.3 (w)	3.9 (w)	3.6 (vw)	β' + β

	48 h	4.5 (m)	4.1 (m)	4.2 (m)	3.9 (s)	-	α + β’ + β
	7 days	4.6 (s)	-	4.2 (w)	3.9 (m)	3.7 (m)	β’ + β
20:80	15 days	4.6 (m)	-	-	3.8 (w)	3.7 (w)	β
	30 days	4.6 (w)	-	-	3.8 (w)	3.6 (vw)	β
	60 days	4.6 (w)	-	-	3.8 (vw)	3.7 (vw)	β
	48 h	4.6 (m)	-	4.3 (w)	3.9 (w)	3.7 (w)	β’ + β
	7 days	4.6 (m)	-	4.2 (m)	3.8 (w)	3.7 (w)	β’ + β
30:70	15 days	4.6 (m)	-	-	3.9 (w)	3.7 (w)	β
	30 days	4.6 (w)	-	-	3.8 (w)	3.7 (w)	β
	60 days	4.6 (w)	-	-	3.8 (vw)	3.7 (vw)	β
	48 h	4.6 (s)	-	4.3 (w)	3.8 (m)	3.7 (m)	β’ + β
	7 days	4.6 (s)	-	4.3 (m)	3.9 (m)	3.7 (m)	β’ + β
40:60	15 days	4.6 (s)	-	-	3.9 (m)	3.7 (m)	β
	30 days	4.6 (w)	-	-	3.9 (w)	3.7 (w)	β
	60 days	4.6 (w)	-	-	3.9 (w)	3.7 (w)	β
	48 h	4.6 (s)	-	4.3 (m)	3.9 (m)	3.7 (m)	β’ + β
	7 days	4.6 (s)	-	4.2 (m)	3.9 (m)	3.7 (m)	β’ + β
50:50	15 days	4.6 (s)	-	-	3.9 (m)	3.7 (m)	β
	30 days	4.6 (m)	-	-	3.9 (w)	3.7 (w)	β
	60 days	4.6 (w)	-	-	3.9 (w)	3.7 (w)	β
	48 h	4.6 (s)	-	-	3.9 (s)	3.7 (m)	β
	7 days	4.6 (vs)	-	-	3.9 (s)	3.7 (s)	β
60:40	15 days	4.6 (s)	-	-	3.9 (m)	3.7 (m)	β
	30 days	4.6 (m)	-	-	3.9 (w)	3.7 (w)	β
	60 days	4.6 (m)	-	-	3.9 (w)	3.7 (w)	β
	48 h	4.6 (s)	-	4.3 (m)	3.9 (m)	3.7 (m)	β’ + β
	7 days	4.6 (vs)	-	4.2 (w)	3.9 (s)	3.7 (s)	β’ + β
70:30	15 days	4.6 (m)	-	4.2 (w)	3.8 (m)	3.7 (w)	β’ + β
	30 days	4.6 (m)	-	4.2 (w)	3.8 (m)	3.7 (w)	β’ + β
	60 days	4.6 (m)	-	-	3.8 (vw)	3.7 (m)	B
	48 h	4.6 (vs)	-	4.3 (w)	3. (s)	3.7 (s)	β’ + β
	7 days	4.6 (s)	-	4.3 (w)	3.9 (s)	3.7 (s)	β’ + β
80:20	15 days	4.6 (s)	-	-	3.8 (m)	3.7 (m)	β
	30 days	4.6 (m)	-	-	3.8 (w)	3.7 (w)	β
	60 days	4.6 (w)	-	-	3.9 (w)	3.7 (w)	β

	48 h	4.6 (m)	-	4.3 (m)	3.8 (m)	3.7 (w)	β' + β
	7 days	4.7 (s)	-	4.3 (w)	3.9 (s)	3.7 (m)	β' + β
90:10	15 days	4.6 (s)	-	4.2(vw)	3.8 (s)	3.7 (m)	β' + β
	30 days	4.6 (m)	-	-	3.8 (w)	3.7 (w)	β
	60 days	4.6 (m)	-	-	3.9 (w)	3.7 (w)	β

Intensities: **v.** very; **w.** weak; **m.** medium; **s.** strong.

4.3.7 Microstructure

The structure of the crystalline lattice formed by the TAG that compose the lipid systems can be assessed by polarized light microscopy, which detects the presence and location of crystalline or liquid regions in a sample and allows microstructure evaluation in terms of dimensions, morphology, and density of the TAG crystals (Li et al., 2012; McClements & McClements, 2016). In the present study we assessed the microstructure of lipid systems composed of FHSO:HOSO (w/w) stabilized by two different methods. In the first method (MI), as recommended by the AOCS (2009), the samples were directly stabilized at 25 °C. In MII, lipid systems were stabilized according to a protocol commonly used to recrystallize NLC.

Table 8 presents quantitative parameters of the lipid systems visualized at 25 °C, corresponding to the mean diameter of the crystals and the percentage of crystalized area. Figure 6 presents the crystalline lattice of the lipid systems formed by FHSO and HOSO after stabilization by both methods (MI and MII). Images were acquired at 25 °C. Figure 6 illustrates the visualization of crystals with nuclei and elongated ramifications that are characteristic of TAG that initially crystallized as spherulite-type crystals and grow radially from the central nuclei as a result of aggregation of the crystalline lamellae (Marangoni & Rousseau, 2002).

Figure 6 and Table 8 show that lipid systems with a higher proportion of HOSO had a lower percentage of crystallized area (in white in the images) due to the presence of tri-unsaturated TAG and liquid oil. In addition, crystals were sparsely distributed along the formed network. Increasing the proportion of HOSO in the lipid systems also resulted in reduced mean diameter of crystals (Table 8). Thus, the addition of HOSO led to modification to the crystalline lattice structure and promoted a reduction in the crystallinity of the FHSO:HOSO (w/w) lipid systems. Crystallization of tri-unsaturated TAG from HOSO created greater spacing between formed crystals and reduced the crystallinity of lipid systems.

As mentioned previously, the formation of NLC is a complex process that involves heating the lipid matrix above its MP and its recrystallization by supercooling (Attama et al., 2012). The method used to stabilize lipid systems influenced the formation of the crystalline lattice. With the exception of the lipid systems FHSO:HOSO (w/w) at ratios of 90:10 and 30:70, the percentage of crystallized area was lower and the mean diameter of the crystals was

greater in MII than in MI. The results obtained herein emphasized the importance of recrystallization of the lipid phase used to obtain NLC at low temperatures after rupture of the particles at the nanometric scale.

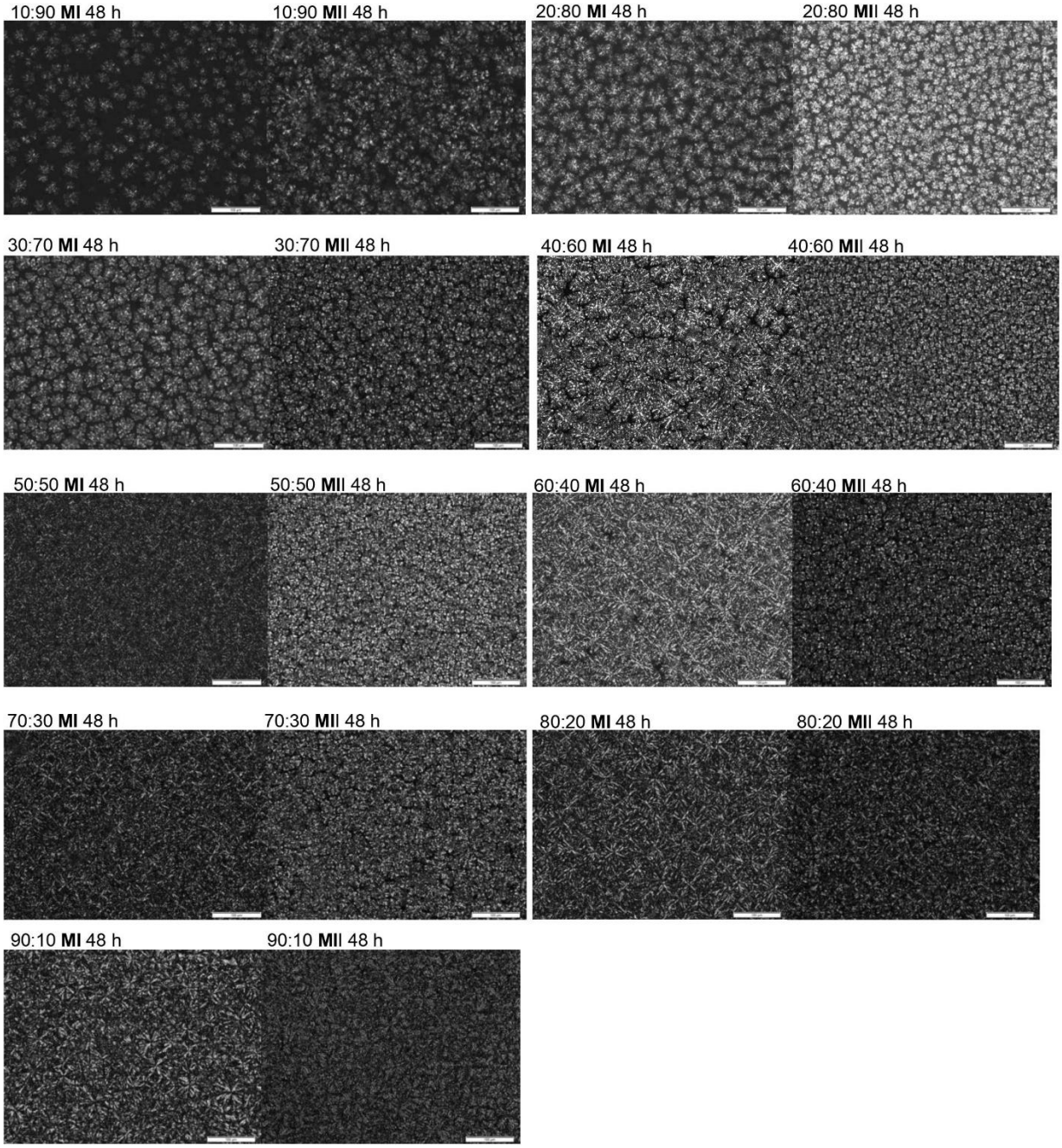

Figure 6: Polarized light microscopy images of crystals at 20× magnification obtained for FHSO:HOSO (w/w) lipid systems at 25°C after stabilization by MI and MII methods. MI: protocol recommended by AOCS; MII: protocol normally used for NLC recrystallization.

Table 8: Mean crystal diameters (Dmean) and percentage of crystalized area of FHSO:HOSO (w/w) lipid systems stabilized by two methods (MI and MII).

FSHO:HOSO (w/w)	Stabilization method	Dmean (μm)	Crystallized Area (%)
90:10	MI	60.84	41.86
	MII	67.37	57.21
80:20	MI	52.78	53.21
	MII	59.73	40.75
70:30	MI	43.44	42.54
	MII	43.01	33.16
60:40	MI	40.47	36.77
	MII	43.11	37.98
50:50	MI	38.98	39.04
	MII	40.04	29.47
40:60	MI	34.99	26.82
	MII	36.12	6.13
30:70	MI	27.99	15.75
	MII	21.20	16.09
20:80	MI	23.72	11.08
	MII	27.22	8.03
10:90	MI	14.52	7.32
	MII	17.41	5.58

MI: protocol recommended by AOCS; **MII:** protocol normally used for NLC recrystallization

The FAC obtained for the lipid systems demonstrated that FHSO and HOSO had great potential for the development of NLC. FHSO had a significant content of stearic acid, a FA that contributes to the protection and delivery of bioactive compounds incorporated into the structure as a result of its higher MP, in addition to allowing the formation of biocompatible NLC. HOSO had a significant content in terms of oleic acid, which allowed obtaining NLC with adequate physical and chemical properties for the incorporation of bioactive compounds, as well as the possibility of solubilization, protection, and delivery of these compounds to absorption sites in the human GIT.

Similarly to the analysis of SFC, the MP of the lipid systems FHSO:HOSO was diminished with increasing percentage of HOSO in the system. In general, increased HOSO abundance in the lipid systems modified the thermal behavior of the fully saturated lipid base (FHSO), thereby decreasing Toc and Toff m as a result of elevated tri-unsaturated TAG in the system. Because melting temperature increases with increased polymorphic stability due to differences in molecular stacking density, lipid systems with more unstable polymorphic forms had a lower melting temperature. All lipid systems examined in the present study exhibited at

least one melting event at or above 37 °C, which indicated thermal resistance at body temperature.

Both the method and the time of stabilization influenced polymorphic forms detected in the lipid systems by X-ray diffraction. The method with a protocol commonly used for recrystallization of the dispersed lipid phase of the NLC (MII) resulted in stabilization in the most stable polymorphic form (β form) earlier than the method suggested in the official protocols (MI). However, after 60 days of storage systems exhibited polymorphic stabilization in the β form, with the exception of the lipid system FHSO:HOSO (w/w) at a ratio of 10:90.

Increasing HOSO levels in lipid systems modified their thermal properties, crystallinity, and TAG and FA composition of the fully saturated lipid base (FHSO), which yielded lipid systems with adequate behavior for the production of NLC, with the exception of the lipid system FHSO:HOSO (w/w) at a ratio of 10:90. However, the selection of an adequate ratio between the lower and upper MP lipid raw material to compose the lipid systems for NLC should be considered with respect to nanostructures.

The results derived in this study allow defining specific purposes if lipid systems according to their physical and chemical properties and crystallization characteristics to obtain NLC. Thus, the lipid systems FHSO:HOSO (w/w) at ratios of 90:10, 80:20, and 70:30 exhibited high crystallinity; lipid systems at ratios of 60:40, 50:50, and 40:60 had medium crystallinity; and the systems at ratios of 30:70 and 20:80 exhibited low crystallinity. The crystallization characteristics of the lipid system FHSO:HOSO (w/w) at a 10:90 ratio were not suitable for the formation of NLC.

4.4 Conclusions

The mixture of different TAG present in lipid matrices used to compose the lipid systems led to differences in their melting and crystallization characteristics. HOSO contributed to reduce the crystallinity of the lipid system, which is in accordance with the use of this type of nanostructure to carry lipophilic bioactive compounds. Lipid matrices commonly used in the food industry and derived from vegetable sources produced on large scales to be used to obtain LN are an alternative in terms of economic viability and availability because the lipid materials commonly used for this purpose are expensive purified materials (e.g., tristearin and triolein). Findings of the lipid system characterization demonstrated that with the exception of the lipid system FHSO:HOSO at a ratio of 10:90 (w/w), systems were adequate for the formulation of NLC in terms of chemical composition, crystallinity, and overall physical properties.

4.5 Acknowledgments

The authors are grateful to the Coordination for the Improvement of Higher Education Personnel (*Coordenação de Aperfeiçoamento de Pessoal de Nível Superior* - CAPES) for the financial support. Fernanda Luisa Lüdtke thanks FAPESP (grants # 18/03172-0, # 19/05176-6, #16/11261-8 and 19/27354-3, São Paulo Research Foundation -FAPESP). Ana Paula Badan Ribeiro thanks CNPq (303429/2018-6) for the productivity grant.

4.6 References

Abreu–Martins, H., Artiga-Artigas, M., Hilsdorf Piccoli, R., Martín-Belloso, O., & Salvia-Trujillo, L. (2020). The lipid type affects the in vitro digestibility and β–carotene bioaccessibility of liquid or solid lipid nanoparticles. *Food Chemistry*, *311*. https://doi.org/10.1016/j.foodchem.2019.126024

Acevedo, N. C., & Marangoni, A. G. (2010). Characterization of the nanoscale in triacylglycerol crystal networks. *Crystal Growth and Design*, *10*(8), 3327–3333. https://doi.org/10.1021/cg100468e

Aditya, N. P., & Ko, S. (2015). Solid lipid nanoparticles (SLNs): Delivery vehicles for food bioactives. *RSC Advances*, *5*(39), 30902–30911. https://doi.org/10.1039/c4ra17127f

Attama, A.A., Momoh, M.A., & Builders, P.F. (2012). Lipid Nanoparticulate Drug Delivery Systems: A Revolution in Dosage Form Design and Development. Recent Advances in Novel Drug Carrier Systems (pp. 107–140). InTech. https://doi.org/10.5772/50486

Antoniosi Filho, N. R., Mendes, O. L., & Lan, F. M. (1995). Computer Prediction of Triacylglycerol Composition of Vegetable Oils by HRGC. *Chromatographia*, *40*, 557–562.

AOCS. American Oil Chemists' Society. (2009). *Official methods and recommended practices of the American Oil Chemists' Society* (Issue 6ed).

Ashkar, A., Sosnik, A., & Davidovich–Pinhas, M. (2021). Structured edible lipid–based particle systems for oral drug–delivery. In *Biotechnology Advances*. Elsevier Inc. https://doi.org/10.1016/j.biotechadv.2021.107789

Cardenia, V., Rodriguez–Estrada, M. T., Cumella, F., Sardi, L., della Casa, G., & Lercker, G. (2011). Oxidative stability of pork meat lipids as related to high–oleic sunflower oil and vitamin E diet supplementation and storage conditions. *Meat Science*, *88*(2), 271–279. https://doi.org/10.1016/j.meatsci.2010.12.034

Cerqueira, M. A., Pinheiro, A. C., Silva, H. D., Ramos, P. E., Azevedo, M. A., Flores–López, M. L., Rivera, M. C., Bourbon, A. I., Ramos, Ó. L., & Vicente, A. A. (2014). Design of Bio–nanosystems for Oral Delivery of Functional Compounds. *Food Engineering Reviews, 6*(1–2), 1–19. https://doi.org/10.1007/s12393–013–9074–3

Gonçalves, R. F. S., Martins, J. T., Duarte, C. M. M., Vicente, A. A., & Pinheiro, A. C. (2018). Advances in nutraceutical delivery systems: From formulation design for bioavailability enhancement to efficacy and safety evaluation. *Trends in Food Science and Technology, 78*, 270–291. https://doi.org/10.1016/j.tifs.2018.06.011

Grimaldi, R., Gonçalves, L. A. G., & Esteves, W. (2000). Características de Gorduras Comerciais Brasileiras. *Brazilian Journal of Food Technology*, *3*, 159–164.

Gunstone, F. D. (2011). Production and Trade of Vegetable Oils. In *Vegetable Oils in Food Technology* (6th ed., Vol. 2). Wiley–Blackwell. https://doi.org/10.1002/9781444339925.ch1

Han, F., Li, S., Yin, R., Liu, H., & Xu, L. (2008). Effect of surfactants on the formation and characterization of a new type of colloidal drug delivery system: Nanostructured lipid carriers. Colloids and Surfaces A: Physicochemical and Engineering Aspects, 315(1–3), 210–216. https://doi.org/10.1016/j.colsurfa.2007.08.005

Hartel, R. W. (2013). Advances in food crystallization. *Annual Review of Food Science and Technology, 4*(1), 277–292. https://doi.org/10.1146/annurev–food–030212–182530

Hunter, J. E., Zhang, J., Kris-Etherton, P. M., & Childs, L. (2010). Cardiovascular disease risk of dietary stearic acid compared with trans, other saturated, and unsaturated fatty acids: A systematic review. *American Journal of Clinical Nutrition*, *91*(1), 46–63. https://doi.org/10.3945/ajcn.2009.27661

Jannin, V., Musakhanian, J., & Marchaud, D. (2008). Approaches for the development of solid and semi–solid lipid–based formulations. *Advanced Drug Delivery Reviews, 60*(6), 734–746. https://doi.org/10.1016/j.addr.2007.09.006

Karabulut, I., Turan, S., & Ergin, G. (2004). Effects of chemical interesterification on solid fat content and slip melting point of fat/oil blends. *European Food Research and Technology*, *218*(3), 224–229. https://doi.org/10.1007/s00217–003–0847–4

Katouzian, I., Faridi Esfanjani, A., Jafari, S. M., & Akhavan, S. (2017). Formulation and application of a new generation of lipid nano–carriers for the food bioactive ingredients. Trends in Food Science and Technology, 68, 14–25. https://doi.org/10.1016/j.tifs.2017.07.017

Kharat, M., & McClements, D. J. (2019). Fabrication and characterization of nanostructured lipid carriers (NLC) using a plant–based emulsifier: Quillaja saponin. *Food Research International*, *126*, 1–11. https://doi.org/10.1016/j.foodres.2019.108601

Khosa, A., Reddi, S., & Saha, R. N. (2018). Nanostructured lipid carriers for site–specific drug delivery. *Biomedicine and Pharmacotherapy, 103*, 598–613. https://doi.org/10.1016/j.biopha.2018.04.055

Li, Y., Xiao, H., & McClements, D. J. (2012). Encapsulation and Delivery of Crystalline Hydrophobic Nutraceuticals using Nanoemulsions: Factors Affecting Polymethoxyflavone Solubility. *Food Biophysics*, *7*(4), 341–353. https://doi.org/10.1007/s11483–012–9272–1

Liu, C. H., & Wu, C. T. (2010). Optimization of nanostructured lipid carriers for lutein delivery. *Colloids and Surfaces A: Physicochemical and Engineering Aspects*, *353*(2–3), 149–156. https://doi.org/10.1016/j.colsurfa.2009.11.006

Livney, Y. D. (2015). Nanostructured delivery systems in food: Latest developments and potential future directions. *Current Opinion in Food Science, 3*, 125–135. https://doi.org/10.1016/j.cofs.2015.06.010

Marangoni, A. (2005). Crystallization Kinetics. In A. Marangoni (Ed.), *Fat Crystal Networks* (pp. 21–82).

Marangoni, A., & Rousseau, D. (2002). The Effects of Interesterification on the Physical Properties of Fats. In *Physical Properties of Lipids*. CRC Press. https://doi.org/10.1201/9780203909171.ch13

McClements, J., & McClements, D. J. (2016). Standardization of Nanoparticle Characterization: Methods for Testing Properties, Stability, and Functionality of Edible Nanoparticles. *Critical Reviews in Food Science and Nutrition*, *56*(8), 1334–1362. https://doi.org/10.1080/10408398.2014.970267

Mehnert, W., & Mäder, K. (2012). Solid lipid nanoparticles: Production, characterization and applications. *Advanced Drug Delivery Reviews, 64*, 83–101. https://doi.org/10.1016/j.addr.2012.09.021

Mohammadi, M., Assadpour, E., & Jafari, S. M. (2019). Encapsulation of food ingredients by nanostructured lipid carriers (NLCs). In *Lipid–Based Nanostructures for Food Encapsulation Purposes* (pp. 217–270). Elsevier. https://doi.org/10.1016/b978–0–12–815673–5.00007–6

Mojahedian, M. M., Daneshamouz, S., Samani, S. M., & Zargaran, A. (2013). A novel method to produce solid lipid nanoparticles using n–butanol as an additional co–surfactant according to the o/w microemulsion quenching technique. *Chemistry and Physics of Lipids*, *174*, 32–38. https://doi.org/10.1016/j.chemphyslip.2013.05.001

Müller, R. H., Mäder, K., & Gohla, S. (2000). Solid lipid nanoparticles (SLN) for controlled drug delivery ± a review of the state of the art. *European Journal of Pharmaceutics and biopharmaceutics, 50*(1),161–167. https://doi.org/10.1016/s0939–6411(00)00087–4

Müller, R. H., Radtke, M., & Wissing, S. A. (2002). Nanostructured lipid matrices for improved microencapsulation of drugs. *International Journal of Pharmaceutics, 242*(1–2), 121–128. https://doi.org/ 10.1016/s0378–5173(02)00180–1

Nguyen, H. M., Hwang, I. C., Park, J. W., & Park, H. J. (2012). Enhanced payload and photo–protection for pesticides using nanostructured lipid carriers with corn oil as liquid lipid. *Journal of Microencapsulation*, *29*(6), 596–604. https://doi.org/10.3109/02652048.2012.668960

O'Brien, R. D. (2008). *Fats and Oils* (CRC Press, Ed.; 3rd ed.). CRC Press. https://doi.org/10.1201/9781420061673

Pinto, F., de Barros, D. P. C., & Fonseca, L. P. (2018). Design of multifunctional nanostructured lipid carriers enriched with α–tocopherol using vegetable oils. *Industrial Crops and Products*, *118*, 149–159. https://doi.org/10.1016/j.indcrop.2018.03.042

Rawal, S. U., & Patel, M. M. (2018). Lipid nanoparticulate systems: Modern versatile drug carriers. In *Lipid Nanocarriers for Drug Targeting* (pp. 49–138). Elsevier. https://doi.org/10.1016/B978–0–12–813687–4.00002–5

Ribeiro, A. P. B., Basso, R. C., Grimaldi, R., Gioielli, L. A., dos Santos, A. O., Cardoso, L. P., & Guaraldo Gonçalves, L. A. (2009). Influence of chemical interesterification on thermal behavior, microstructure, polymorphism and crystallization properties of canola oil and fully hydrogenated cottonseed oil blends. *Food Research International*, *42*(8), 1153–1162. https://doi.org/10.1016/j.foodres.2009.05.016

Ribeiro, A. P. B., Basso, R. C., & Kieckbusch, T. G. (2013). Effect of the addition of hardfats on the physical properties of cocoa butter. *European Journal of Lipid Science and Technology*, *115*(3), 301–312. https://doi.org/10.1002/ejlt.201200170

Salminen, H., Helgason, T., Aulbach, S., Kristinsson, B., Kristbergsson, K., & Weiss, J. (2014). Influence of co–surfactants on crystallization and stability of solid lipid nanoparticles. *Journal of Colloid and Interface Science*, *426*, 256–263. https://doi.org/10.1016/j.jcis.2014.04.009

Salvia–Trujillo, L., Soliva-Fortuny, R., Rojas-Graü, M. A., McClements, D. J., & Martín–Belloso, O. (2017). Edible Nanoemulsions as Carriers of Active Ingredients: A Review. *Annual Review of Food Science and Technology, 8*, 439–466. Annual Reviews Inc. https://doi.org/10.1146/annurev–food–030216–025908

Sanders, T. A. B., & Berry, S. E. E. (2005). Influence of Stearic Acid on Postprandial Lipemia and Hemostatic Function. *Lipids*, *40*(12), 1221–1227. https://doi.org/10.1007/s11745-005-1489-7.

Santos, V. S., Braz, B. B., Silva, A. Á., Cardoso, L. P., Ribeiro, A. P. B., & Santana, M. H. A. (2019). Nanostructured lipid carriers loaded with free phytosterols for food applications. *Food Chemistry*, *298*. https://doi.org/10.1016/j.foodchem.2019.125053

Serra, M. de L. G., Hernández L, A., Vázquez R, M. L., Villafuerte R, L., & García F, B. (2008). Revista Mexicana de Ciencias Farmacéuticas. *Revista Mexicana de Ciencias Farmacéuticas*, *39*, 50–66. http://www.redalyc.org/articulo.oa?id=57911113008

Shah, R., Eldridge, D., Palombo, E., & Harding, I. (2015). Lipid Nanoparticles: Production, Characterization and Stability. In *Springer briefs in pharmaceutical science & drug development.* http://www.springer.com/series/10224

Sharma, V. K., Diwan, A., Sardana, S., & Dhall, V. (2011). Solid Lipid Nanoparticles System: An Overview.*International Journal of Research in Pharmaceutical Sciences, 2*(3), 450–461. www.ijrps.pharmascope.org

Siegrist, M., Stampfli, N., Kastenholz, H., & Keller, C. (2008). Perceived risks and perceived benefits of different nanotechnology foods and nanotechnology food packaging. *Appetite*, *51*(2), 283–290. https://doi.org/10.1016/j.appet.2008.02.020

Soleimanian, Y., Goli, S. A. H., Varshosaz, J., & Maestrelli, F. (2019). β–sitosterol Lipid Nano Carrier Based on Propolis Wax and Pomegranate Seed Oil: Effect of Thermal Processing, pH, and Ionic Strength on Stability and Structure. *European Journal of Lipid Science and Technology*, *121*(1), 1–31. https://doi.org/10.1002/ejlt.201800347

Tamjidi, F., Shahedi, M., Varshosaz, J., & Nasirpour, A. (2013). Nanostructured lipid carriers (NLC): A potential delivery system for bioactive food molecules. In *Innovative Food Science and Emerging Technologies, 19*, 29–43. https://doi.org/10.1016/j.ifset.2013.03.002

Tan, S. W., Billa, N., Roberts, C. R., & Burley, J. C. (2010). Surfactant effects on the physical characteristics of Amphotericin B–containing nanostructured lipid carriers. *Colloids and Surfaces A: Physicochemical and Engineering Aspects*, *372*(1–3), 73–79. https://doi.org/10.1016/j.colsurfa.2010.09.030

Tan, Y., & McClements, D. J. (2021). Improving the bioavailability of oil–soluble vitamins by optimizing food matrix effects: A review. *Food Chemistry*, *348*. https://doi.org/10.1016/j.foodchem.2021.129148

Timms, R. E. (1984). Phase behavior of fats and their mixtures. *Progress in Lipid Research*, *23*, 1–38. https://doi.org/10.1016/0163-7827(84)90004-3

Verkempinck, S. H. E., Salvia-Trujillo, L., Moens, L. G., Charleer, L., van Loey, A. M., Hendrickx, M. E., & Grauwet, T. (2018). Emulsion stability during gastrointestinal conditions effects lipid digestion kinetics. *Food Chemistry*, *246*, 179–191. https://doi.org/10.1016/j.foodchem.2017.11.001

Wang, J. L., Dong, X. Y., Wei, F., Zhong, J., Liu, B., Yao, M. H., Yang, M., Zheng, C., Quek, S. Y., & Chen, H. (2014). Preparation and characterization of novel lipid carriers containing microalgae oil for food applications. *Journal of Food Science*, *79*(2), 169–177. https://doi.org/10.1111/1750–3841.12334

Yoon, G., Park, J. W., & Yoon, I. S. (2013). Solid lipid nanoparticles (SLNs) and nanostructured lipid carriers (NLCs): Recent advances in drug delivery. *Journal of Pharmaceutical Investigation, 43*(5), 353–362. https://doi.org/10.1007/s40005–013–0087–y

Zheng, M., Falkeborg, M., Zheng, Y., Yang, T., & Xu, X. (2013). Formulation and characterization of nanostructured lipid carriers containing a mixed lipids core. *Colloids and Surfaces A: Physicochemical and Engineering Aspects*, *430*, 76–84. https://doi.org/10.1016/j.colsurfa.2013.03.070

CAPÍTULO V

High oleic sunflower oil and fully hydrogenated soybean oil nanostructured lipid carriers: development and characterization

Submitted to Food Structure

5. High oleic sunflower oil and fully hydrogenated soybean oil nanostructured lipid carriers: development and characterization

Fernanda Luisa Lüdtke[a], Marcella Aparecida Stahl[a], Renato Grimaldi[a], Lisandro Pavie Cardoso[b], Mirna Lúcia Gigante[a], Ana Paula Badan Ribeiro[a]

[a]Department of Engineering and Food Technology, School of Food Engineering, State University of Campinas (UNICAMP), 13083-862, Campinas, SP, Brazil.

[b]Department of Applied Physics, Institute of Physics Gleb Wataghin, State University of Campinas (UNICAMP), 13083-859, Campinas, SP, Brazil.

ABSTRACT

Nanotechnology has proven to be an important focus of public attention worldwide due to its wide range of applications and the superior functionality of nanoscale delivery systems. Lipid-based nanoparticles are among the most promising encapsulation technologies in the field of nanotechnology. As one of the main trends in the development of these structures, the use of edible and/or commercially available oils and fats in the food industry stands out, replacing synthetic lipid matrices, which are not as viable for food applications in terms of cost, availability, or regulatory aspects. The objective of this work was to obtain and characterize nanostructured lipid carriers (NLC) using fully hydrogenated soybean oil (FHSO) and high oleic sunflower oil (HOSO) as lipid matrices. NLC were formulated from different lipid systems, 80:20, 60:40, 40:60, and 20:80 FHSO:HOSO (w/w), using soy lecithin (SL), Tween 80, or whey protein isolate as an emulsifier. In general, the increase in the unsaturation degree of the FHSO:HOSO lipid system resulted in larger NLC when obtained with Tween 80 or SL, greater physical instability, and lower peak temperature and melting enthalpy, although for the 20:80 system, it was not possible to observe melting peaks by differential scanning calorimetry. The increase in the unsaturation degree, however, did not change the polymorphic shape of NLC, which stabilized in the β form 48 h after their obtainment. Among the considered lipid systems, 80:20, 60:40, and 40:60 FHSO:HOSO (w/w) systems form stable particles, with crystallinity properties suitable for food incorporation.

Keywords: lipid nanoparticles, emulsifiers, physical stability, crystallization, degree of unsaturation

5.1 Introduction

Research advances in nanotechnology have shown that nanoscale delivery systems exhibit superior functionality in relation to conventional microencapsulation systems, justifying the great interest in nanocarriers (Chen et al., 2006; Weiss et al., 2008). Investigations related to nanoparticle development in the agricultural and food industries are still scarce compared with those in the biomedical and pharmaceutical fields (Barroso et al., 2021). However, nanotechnology has become one of the most promising technologies to revolutionize conventional food science and food industry (He & Hwang, 2016).

In the food field, nanoparticles can be obtained using polymers or lipids. Lipid

nanoparticles (LN) are considered complex extended release systems, with spherical shapes and sizes on the nanometer scale (between 50 and 1000 nm), although quite variable according to the materials and methods of obtainment (Villafuerte et al., 2008). Compared with biopolymer-based nanocarriers, they present low toxicity because they are obtained through biocompatible ingredients, high bioavailability because they are entirely formed of physiological lipids, and greater efficiency in bioactive compound incorporation (Rostamabadi et al., 2019; Villafuerte et al., 2008). However, nanostructures for food applications must be entirely produced with ingredients considered to be food grade and through processing operations that have already been approved (McClements, 2012). For this reason, there is a growing demand for natural ingredients to obtain nanostructures with suitable properties to be incorporated into food (Pinheiro et al., 2017).

Nanostructured lipid carriers (NLC) are composed of a mixture of high and low melting point (MP) lipids (oils) dispersed in an aqueous medium and stabilized by a drop of emulsifier (Niculae et al., 2014; Puri et al., 2009). Typically, solid lipids are mixed with liquid lipids in ratios of 70:30 up to 99.9:0.1, while the emulsifier content varies between 1.5% to 5% (v/v) (Pardeike et al., 2009). The choice of the lipid matrix is a fundamental element to obtaining NL, as bioactive ingredients are incorporated into this matrix. Some factors should be considered regarding the lipids used in NLC structure formulation: good solubility of lipophilic ingredients within the lipid matrix; high stability against decomposition factors such as oxidation; biodegradability and safety; and an adequate ratio between solid and liquid lipids in the matrix (Katouzian et al., 2017).

The type and concentration of solid and liquid lipids and the type of emulsifier used to obtain NLC are among the factors that most affect their physicochemical properties (Badea et al., 2015; How et al., 2013). The characteristics of nanoparticles (structure, dimension, and composition, among others) in turn influence their physicochemical properties and functional performance, such as optical and rheological properties, stability, biological fate, and delivery rate (McClements, 2013). Thus, the particle size (PS) and distribution, like its charge, are strongly influenced by the composition of the lipid matrix and the emulsifier used to obtain NLC (Pinto et al., 2018).

The lipid components used to obtain NLC can comprise a great diversity of molecules (Kamboj et al., 2010). To obtain NLC, the use of low-cost ingredients, such as components naturally found in foods that can be used for “clean” (green) formulation in the food industry, is recommended (Katouzian et al., 2017). Fatty acids (FA) extracted from natural edible oils and fats (for example, palmitic, oleic, and stearic oils) are Generally Recognized as Safe (GRAS) and approved food additives with great potential for this purpose (Babazadeh et al., 2017).

Fully hydrogenated vegetable oils (hardfats) have been used as a high MP lipid matrix to obtain NLC (Santos et al., 2019). The total hydrogenation process of vegetable oils promotes the addition of hydrogen to the double bonds of unsaturated fatty acids (UFA) through a catalytic reaction, cleaving them and thus promoting their conversion into saturated fatty acids (SFA). This process, considered of relatively low cost, represents an alternative for industrial plants previously used for the partial hydrogenation process and allows the obtainment of lipid bases with a MP, composed of tri-saturated triacylglycerols (TAG), from conventional vegetable oils (Ribeiro et al., 2009, 2013; Wassell & Young, 2007).

Fully hydrogenated soybean oil (FHSO) contains significant levels of stearic acid, normally higher than 85%, which highlights the use of this component, due to its neutral atherogenic effect, to obtain NLC. Indeed, FHSO does not present adverse effects on the risk of cardiovascular disease (Hunter et al., 2010; Valenzuela et al., 2011).

Oils from vegetable sources, such as soybean, corn, and sunflower, are great candidates for use as a lipid matrix with a lower MP to obtain NLC to be employed as food additives (Mohammadi et al., 2019). The limitation to using edible vegetable oils for NLC production is associated with the low oxidative stability presented by these raw materials (Liu & Wu, 2010; Nguyen et al., 2012). Low oxidation resistance can affect the oxidative stability of bioactive compounds incorporated into NLC during food processing and storage, as well as during its passage through the gastrointestinal tract (Tan & McClements, 2021). Therefore, raw materials resistant to chemical degradation should be selected (Tamjidi et al., 2013).

High oleic sunflower oil (HOSO) is considered a premium lipid raw material in terms of oxidation resistance. The genetic modification of sunflower to a high oleic variety promotes an increase in its oxidative stability, as it significantly raises the content of oleic acid, a monounsaturated FA (MUFA) that, compared with a polyunsaturated FA, is less susceptible to oxidative processes since it presents only one double bond in the carbon chain (Cardenia et al., 2011; Gunstone, 2011). This raw material has high potential to be used as a low MP lipid matrix to obtain NLC with incorporated bioactive compounds, since it is commercially available at a feasible cost, GRAS, and, as mentioned above, resistant to oxidative processes.

As HOSO and FHSO are composed of several FA with different MP, we hypothesize that they are excellent candidates for obtaining stable NLC. We chose FHSO for this study, seeking a lipid fraction in NLC that is solid when stored at room temperature, with a high MP lipid base and a high content of stearic acid (Hunter et al., 2010).

The percentage of liquid lipid in the lipid matrix can influence the physical properties of NLC, such as PS and melting temperature, and the beginning of the crystallization process, as well as produce particles with lower crystallinity, which promotes greater space for the incorporation of bioactive compounds (Zheng et al., 2013). Since bioactive compounds have greater solubility in liquid lipids than in solid lipids (Helgason et al., 2009; Tamjidi et al.,

2013), knowing the physicochemical and stability properties of NLC obtained with lipid systems of different solid/liquid ratios is essential when aiming to incorporate bioactive compounds in these nanostructures. Thus, the objective of this work was to obtain and characterize NLC obtained from lipid systems composed of different FHSO:HOSO (w/w) ratios. NLC were characterized by the general properties of PS distribution, structure, thermal behavior, crystallinity, and polymorphism, with consideration of the effects of lipid phase composition relative to the degree of unsaturation of the lipid systems used.

5.2 Materials and Methods

5.2.1 Materials

The lipid materials used to produce NLC were HOSO (C18:1 = 78.51 %, C18:2 = 12.40 %, and C16:0 = 4.02 %) and FHSO (C18:0 = 87.31 % and C16:0 = 10.70 %), both supplied by Cargill Foods (Brazil). The emulsifying agents were whey protein isolate (WPI) produced by Alibra (Brazil), the enzymatically hydrolysed soybean lecithin (SL) SOLEC^{TM} AE IP produced by Solae (Brazil), and the ethoxylated sorbitan monooleate (Tween 80) produced by Sigma-Aldrich (USA).

5.2.2 Methods

5.2.2.1 NLC obtainment

NLC were obtained from a pre-emulsion composed of an aqueous phase (88%), a lipid phase (10%), and an emulsifier (2%). Table 1 shows the FHSO:HOSO (w/w) lipid and emulsifier systems used to obtain NLC. The lipid phase was composed of different lipid systems using FHSO and HOSO in proportions of 80:20; 60:40; 40:60, and 20:80 (w/w). SL, Tween 80, or WPI was used to obtain NLC. In the case of WPI, a 2% aqueous solution was previously prepared to complete protein hydration. WPI was dissolved in distilled water and kept under magnetic stirring for 1 h at approximately 25°C. After obtaining the formulations, sodium azide (0.02%) was added as an antimicrobial agent, and the solution was stored overnight under refrigeration (5–7°C) (Queirós et al., 2021).

For the preparation of the pre-emulsion, the lipid phase was heated to 85°C and added slowly to the aqueous phase, which was previously heated to 85°C. The mixtures were then stirred at 10,000 rpm/3 min in an Ultra turrax model T18 (IKA, Germany) stirrer to form the pre-emulsion. The pre-emulsion was subjected to heat and high pressure using a two-stage homogenizer Homolab 2.20 (Buffalo series, FBF Italy). The process conditions used to obtain NLC were 700 bar and two homogenization cycles (Lüdtke et al., 2017), with the

pressure applied by the second stage valve corresponding to 10% of the total pressure applied, i.e. approximately 70 bar. The obtained nano-emulsions were cooled at 5°C for 24 h to recrystallize the lipid phase and obtain the dispersion containing NLC and subsequently stored in a biological oxygen demand-type incubator at 25°C for 60 days (Kumbhar & Pokharkar, 2013; Qian et al., 2013; Yang et al., 2014).

Table 1: Emulsifiers, and total amount of saturated (SFA) and unsaturated fatty acids (UFA) presented in lipid systems used to obtain NLC.

			∑ **FA (%)**		
NLC	**Emulsifier**	**FHSO:HOSO (w/w)**	**SFA (%)**	**UFA (%)**	**SFA/UFA ratio**
$\mathbf{L_{80:20}}$	SL	80:20	81.54	18.46	4.42
$\mathbf{L_{60:40}}$	SL	60:40	63.25	36.76	1.72
$\mathbf{L_{40:60}}$	SL	40:60	44.95	55.05	0.82
$\mathbf{L_{20:80}}$	SL	20:80	26.66	73.34	0.36
$\mathbf{T_{80:20}}$	Tween 80	80:20	81.54	18.46	4.42
$\mathbf{T_{60:40}}$	Tween 80	60:40	63.25	36.76	1.72
$\mathbf{T_{40:60}}$	Tween 80	40:60	44.95	55.05	0.82
$\mathbf{T_{20:80}}$	Tween 80	20:80	26.66	73.34	0.36
$\mathbf{W_{80:20}}$	WPI	80:20	81.54	18.46	4.42
$\mathbf{W_{60:40}}$	WPI	60:40	63.25	36.76	1.72
$\mathbf{W_{40:60}}$	WPI	40:60	44.95	55.05	0.82
$\mathbf{W_{20:80}}$	WPI	20:80	26.66	73.34	0.36

NLC: nanostructured lipid carries; **SL:** enzymatic modified soybean lecithin; **WPI**: whey protein isolate; **FHSO**: fully hydrogenated soybean oil; **HOSO:** high oleic sunflower oil; **FA**: fatty acids; **SFA**: saturated fatty acids; **UFA**: saturated fatty acids.

5.2.2.2 NLC characterization

5.2.2.2.1 Particle size and polydispersity index

PS and polydispersity index (PDI) were determined by a laser diffractometer using Mastersizer 2000 equipment (Malvern Instruments, Malvern, UK). NLC aliquots were added to the equipment reading unit filled with distilled water at 25°C and stirred at 1750 rpm until a 2% obscuration rate was obtained (Averina et al., 2011). The analyses were carried out in triplicate at 25° C. Results referring to the mean size of NLC were expressed as mean surface diameter (D_{32}), as calculated using Equation 1, while the PDI was obtained by calculating the span using Equation 2.

$$D_{32} \quad \frac{\sum n_i d^3_i}{\sum n_i d^2_i} \qquad \text{(Equation 1)}$$

$$Span \quad \frac{d_{90}-d_{10}}{d_{50}} \qquad \text{(Equation 2)}$$

where n_i is the number of particles with diameter d_i and d10, d50, and d90 represent 10%, 50%, and 90% of the cumulative droplet volume, respectively.

5.2.2.2.3 Zeta potential

The zeta potential (ZP) was determined using the Zetasizer Nano-ZS (Malvern Instruments, Malvern, UK), and the samples were diluted (1:100) in distilled water for further analytical determination (Averina et al., 2011). The analyses were carried out in triplicate at room temperature.

5.2.2.2.4 Physical stability

The physical stability of the dispersions containing NLC was determined by the light backscattering technique using Turbiscan® Lab equipment (Formulaction, l'Union, France). After the dispersions were obtained, they were immediately added to cylindrical tubes with a flat bottom where they were stored at 25°C. The operating principle of the equipment is based on the incidence of a light ray with a fixed wavelength (880 nm) on the cylindrical tube containing the sample. The tube is scanned vertically every 40 μm, with the height H = 0 mm associated with the bottom of the measuring cell. The light beam can then be transmitted or backscattered depending on the interaction of light with the medium. The equipment quantifies how much of a light beam incident on a sample is deflected by the dispersed particles (Buron et al., 2004). The physical stability of the dispersions was analyzed using light backscatter profiles (ΔBS) obtained through scans conducted at different periods of analysis (48 h and 7, 15, 30, and 60 days after the obtainment of NLC).

5.2.2.5 Solid fat content

The solid fat content (SFC) was determined by pulsed low-resolution nuclear magnetic resonance spectroscopy (NMR) Bruker pc120 Minispec (Silberstreifen, Rheinstetten, Germany), using high precision dry baths with temperature controlled (0–70°C) by the Peltier Tcon 2000 system (Duratech, Garden Grove, USA). The analysis was carried out using AOCS

Cd 16b-93 direct method, involving reading of samples in series (AOCS, 2009). The samples were transferred to NMR tubes and kept in an isothermal condition at 25°C (Nik et al., 2012).

5.2.2.2.6 Polymorphism

The polymorphic form of NLC was determined by X-ray diffraction according to the AOCS Cj 2-95 method (AOCS, 2009). Analyses were performed at 25°C in a Philips PW 1710 diffractometer (PANalytical, Almelo, Holanda) using Bragg-Bretano geometry (θ:2θ) with Cu-Kα radiation (λ = 1.54056 Å; voltage, 40 KV; current, 30 mA). The measurements were obtained with 0.02° steps from 5° to 40° 2θ and acquisition time of 2 s. The polymorphic form was identified from interplanar distances of the crystals (Schenk & Peschar, 2004).

5.2.2.2.7 Thermal melting behavior

The thermal behaviour during the melting of β-carotene-loaded NLC was assessed in a TA Q2000 differential scanning calorimeter (DSC) coupled to a RCS90 Refrigerated Cooling System (TA Instruments, Waters LLC, New Castle). Universal V4.7A (TA Instruments, Waters LLC, New Castle) was used for data processing. The analysis conditions were as follows: sample mass: ~ 10 mg; maintenance of isothermal condition: 25 °C for 10 min; melting events assessed between 25 and 100 °C at a rate of 10 °C/min (Wang et al., 2014).

5.2.2.2.8 Microstructure

The morphological and structural characteristics of NLC were evaluated by microscopy under polarized light at 25°C using an Olympus BX 50 polarized light microscope (San Jose, USA) coupled to a digital video camera (Media Cybernetics, Bethesda, USA) and by scanning electron microscopy (only for NLC obtained using Tween 80 as emulsifier) using a TM 3000 high vacuum scanning electron microscope (SEM; Hitachi, Japan) with a Swift ED3000 energy dispersive system with x-ray detection (Hitachi).

5.2.2.2.8 Statistical analysis

All analytical determinations were performed in triplicate. The results obtained were evaluated by analysis of variance (ANOVA) and Tukey's test for comparison of the means at a significance level of 5% using STATISTICA 7.0 software (StatSoft Inc, Tulsa, OK, USA).

5.2 Results and Discussion

NLC are carrier systems that can combine the advantages of different colloidal compound release systems and avoid some of their disadvantages (Mohammadi et al., 2019), such as low bioactive loading, low encapsulation efficiency, and system instability (Katouzian et al., 2017). They present great potential for industrial production (Rostamabadi et al., 2019) since the use of nanostructures proves to be a promising and differentiated alternative for the transport and protection of bioactive compounds in food systems (Mozafari et al., 2006; Weiss et al., 2006).

The efficiency of NLC as a compound delivery system is directly related to their physicochemical characteristics and properties, which in turn are linked to a series of factors, such as the type of lipid matrix and emulsifier used in their production. A study carried out by Pinto et al. (2018) showed that the PS, PI, and ZP of NLC are significantly influenced by the composition of the lipid matrix and the type of emulsifier used to obtain these structures. In this study we evaluated the physical and crystallization properties of NLC obtained from different FHSO:HOSO (w/w) lipid systems to verify the influence of the unsaturation degree present in the lipid systems, the interaction between the lipid phases with the highest and lowest MP, and the influence of emulsifiers on the characteristics of the obtained NLC.

5.3.1 Particle Size and Polydispersity Index

Table 2 shows the PS, expressed as the mean diameter (D_{32}) of NLC, obtained with different emulsifiers. The results demonstrate that the emulsifiers SL, WPI, and Tween 80 provided the obtainment of NLC on a nanometric scale for all lipid systems. However, significant differences were observed among the emulsifiers and lipid systems used, as described below.

The NLC obtained with SL showed a significant increase ($p < 0.05$) in PS as the unsaturation degree of the lipid system increased. The higher the SFA content, the greater the proportion of stearic acid in the lipid phase that forms the carrier. Stearic acid has a linear chain, which facilitates the packaging and, consequently, the ordering of TAG in the crystal. The SL used in this study is mainly formed of lysophospholipids, a class of phospholipids in which the glycerol molecule is esterified with an FA and a phosphate group. Due to the structural and chemical similarity of this emulsifier to TAG, which are composed of a glycerol molecule esterified to three FA, TAG/emulsifier association is easier. Thus, due to the ease of both TAG/TAG and TAG/emulsifier association, there was a decrease in the dimensions of NLC with an increase in the SFA content in the lipid system, with the smallest dimensions observed for the NLC obtained with the 80:20 FHSO:HOSO (PS < 226.33 nm) lipid system. In

general, less organized and less compact crystal structures tend to occupy more space, resulting in larger nanoparticles (O'Brien, 2008; Ribeiro et al., 2013), which may explain the increase in the system's unsaturation results in larger NLC. The PS of the NLC obtained with this emulsifier were below 260 nm during the 60 days of storage.

Table 2: Particle size (PS) of nanostructured lipid carriers (NLC) evaluated after 48 h, 7 days, 15 days, 30 days, and 60 days of storage.

NLC	48 h	7 days	15 days	30 days	60 days
$L_{80:20}$	216.67±1.53^{bA}	226.33±4.73^{cA}	203.00±1.73^{aA}	199.33±2.89^{aA}	202.00±5.29^{aA}
$L_{60:40}$	225.33±2.89^{bB}	231.00±0.00^{bcA}	208.00±6.24^{aA}	248.33±8.02^{dC}	241.67±5.51^{cdC}
$L_{40:60}$	233.00±1.73^{bC}	248.33±2.08^{cB}	244.33±3.06^{cB}	227.00±2.00^{bB}	216.00±5.20^{aB}
$L_{20:80}$	255.67±2.08^{bC}	251.67±2.08^{abB}	250.67±2.89^{abB}	251.00±1.73^{abC}	249.00±2.65^{aC}
$T_{80:20}$	160.67±0.58^{aA}	169.33±0.58^{bA}	170.00±1.00^{bcA}	169.67±3.21^{bcA}	174.00±1.00^{cA}
$T_{60:40}$	184.00±1.73^{aB}	195.00±1.00^{bB}	194.67±0.58^{bB}	202.33±4.04^{cA}	197.00±1.00^{bcB}
$T_{40:60}$	223.00±2.00^{aD}	222.33±2.31^{aD}	219.67±4.04^{aD}	220.67±2.31^{aC}	216.67±2.52^{aD}
$T_{20:80}$	216.33±1.15^{bC}	211.33±2.52^{abC}	207.33±3.51^{aC}	207.33±1.15^{aB}	206.67±2.31^{aC}
$W_{80:20}$	320.33±0.58^{aC}	320.33±1.53^{aD}	320.67±1.53^{aD}	321.00±2.00^{aD}	319.00±3.61^{aD}
$W_{60:40}$	260.67±2.08^{aA}	257.33±1.53^{aA}	257.33±0.58^{aA}	260.67±0.58^{aA}	256.33±4.04^{Aa}
$W_{40:60}$	276.67±3.06^{aB}	278.00±1.73^{aB}	277.33±1.53^{aB}	277.00±1.73^{aB}	274.33±2.31^{aB}
$W_{20:80}$	287.67±2.52^{aB}	282.67±0.58^{aC}	283.00±1.73^{aC}	285.00±1.73^{aC}	284.67±1.53^{Ac}

NLC L: nanostructured lipid carries obtained with enzymatic modified soybean lecithin as emulsifier; **NLC T**: nanostructured lipid carries obtained with Tween 80 as emulsifier; **NLC W**: nanostructured lipid carries obtained with whey protein isolate as emulsifier. Average of three replicates ± Standard Deviation. $^{a-d}$ Different lower-case letters indicate significant difference ($p< 0.05$) related to the evaluation of each parameter (PS, PDI and ZP) in comparison to the time of storage of NLC (48 h, 7, 15, 30, 45, and 60 days after processing) for the same NLC. $^{A-D}$ Different capital letters indicate significant difference ($p< 0.05$) related to the evaluation of the same parameter (PS, PDI or ZP) at the same time of storage of NLC (48 h, 7, 15, 30, 45, and 60 days after processing) between the NLC obtained with the same emulsifier.

Similar behaviors have been observed in studies that evaluated NLC obtained with different proportions of lipids with higher and lower MP. Babazadeh et al. (2017) obtained NLC using lipid sources of higher (lauric acid, stearic acid, and cocoa butter) and lower MP (glycerol, Miglyol 812, corn oil, and oleic acid) combined in different proportions and using different emulsifiers (Poloxamer 407, Tween 80, and Tween 20). The authors reported that, when the emulsifier concentration was 2%, the same concentration used in our study, PS significantly increased with an increase in the unsaturation of the lipid system. Pezeshki et al. (2019) evaluated NLC with β-carotene incorporation obtained using octyl octanoate and Precirol as

lipid matrices with higher and lower MP, respectively, in different proportions and Poloxamer 407 as the emulsifier at different concentrations (1%, 2%, 3%, or 4% w/v). At all emulsifier concentrations, the increase in unsaturation in the lipid system was found to be accompanied by an increase in the PS of the NLC obtained. A study carried out by Queirós et al. (2021) evaluated the influence of the degree of unsaturation of different lipid systems composed of fully hydrogenated milk fat, anhydrous milk fat, and HOSO on the characteristics of NLC obtained through polyaromatic hydrocarbons. In this study, WPI and sodium caseinate were used as emulsifiers. The authors reported that an increase in the unsaturation degree of the lipid system used to obtain NLC promoted a significant increase in PS, which agrees with the NLC results obtained with SL in our study.

NLC formation is similar to emulsions formation. Emulsifying agents are amphiphilic molecules that consist of a hydrophilic head and a hydrophobic tail. They perform two primary functions in NLC formation: facilitation of the dispersion of the molten lipid in an aqueous phase during the emulsification step and stabilization of the nanoparticles after the emulsion cooling phase (Rawal & Patel, 2018). In general, the greater the ability of an emulsifier to reduce surface tension, the smaller the PS obtained (Håkansson et al., 2013). Therefore, in this study, the use of Tween 80 promoted the obtainment of NLC with smaller dimensions (PS 160.07–223.00 nm) during the 60 days of storage. Tween 80, a nonionic emulsifier soluble in water, is derived from polyethoxylated sorbitan and oleic acid (Mohammadi et al., 2019) and, due to its structural characteristics and low molecular weight, quickly adsorbs at the oil–water interface, promoting the formation of NLC with smaller dimensions (Lee et al., 2013). In the case of Tween 80, in a manner similar to that used with SL, an increase in PS was verified to be accompanied by an increase in the unsaturation degree of the lipid system, but only up to a ratio of 40:60 FHSO:HOSO, with the smallest dimensions observed for the NLC $T_{80:20,}$ obtained via the lipid system with a higher proportion of SFA (81.54%) because of the ease of associating TAG/TAG and TAG/emulsifier. However, it was found that NLC $T_{20:80}$, obtained with the lipid system with the highest degree of unsaturation (73.34%), was smaller than NLC $T_{40:60}$. In this case, as Tween 80 has a MUFA in its structure, the high content of oleic acid present in the 20:80 FHSO:HOSO lipid system may have promoted a greater interaction of this emulsifier with the lipid phase, thus obtaining smaller particles (Pinto et al., 2018).

Compared with that of the other emulsifiers considered in this study, the use of WPI resulted in the obtainment of NLC with higher PS (256.33 to 360.67 nm) without significant changes ($p < 0.05$) during the 60 days of storage. There are large differences in the ability of different emulsifiers to adsorb rapidly onto lipid droplets during homogenization and therefore in their ability to reduce interfacial tension, resulting in different sized particles even under the same process conditions (McClements & Gumus, 2016). Some biopolymer-based emulsifiers

are not as efficient as emulsifiers with smaller molecular sizes, resulting in the obtainment of larger particles during homogenization (Chang et al., 2015). WPI has a globular and heterogeneous structure, which hinders its incorporation into the lipid phase due to the more ordered packaging of the TAG that compose the particle. This leaves less room to accommodate the emulsifying molecule, thus explaining the larger dimensions observed for lipid systems with higher percentages of FHSO. Furthermore, due to its high molecular weight, WPI diffuses more slowly towards the interface, thus resulting in larger particles, as verified in this study. In the case of this emulsifier, it was not possible to establish a linear relationship between the increase/decrease in the unsaturation degree of the lipid system with the decrease/increase in PS. NLC $W_{60:40}$ had the smallest dimensions, which were less than 260 nm during the 60 days of storage.

In general, studies that consider obtaining NLC from different systems, as our study did, present divergent results. For example, How et al. (2013) characterized NLC formulated with olive oil and hydrogenated palm oil in different proportions, obtained using Tween 80 as an emulsifier added in different ratios. The authors reported that the physicochemical characteristics of NLC seemed to exhibit a pattern independent of the proportion of the lipid matrix with the lowest MP in the lipid system. However, the NLC obtained with higher olive oil content had larger PS among the NLC evaluated. Oliveira et al. (2016) characterized NLC incorporated with β-carotene, obtained from tristearin and HOSO in different proportions, and found that the lipid composition did not change the PS. In a study conducted by Pan et al. (2016), there was no influence by the increase in unsaturation degree of the lipid system on the PS of the obtained NLC. In that study, the authors evaluated NLC prepared using lipid systems with different proportions of glyceryl trioctanoate (a lipid with a lower MP) and eicosanoid (a lipid with a higher MP) and SL with a high MP (Phospholipon® 80 H) as an emulsifier. The authors reported that the percentage of lipid with the lowest MP did not significantly influence the PS of the obtained NLC ($p < 0.05$). Pinto et al. (2018) developed NLC from vegetable oils (sunflower, sweet almond, coconut, and olive oils) as lipid matrices with lower MP and myristic acid (C14:0) as a lipid matrix with a higher MP in different proportions using four different emulsifiers (Tween 80, Span 60, Span 80, and Poloxamer 188). In that study, although the PS of NLC generally decreased with the increase in the percentage of vegetable oils, some exceptions were observed, indicating that, in addition to the proportion of the lipid matrix with a lower MP, the FA composition influences PS. The characteristics of FA form the lipid matrices with the highest and lowest MP used to obtain NLC and can promote the formation of a more viscous lipid phase, which leads to an increase in surface tension and, consequently, the formation of larger particles.

In general, the lipid systems that provided the smallest dimensions for the NLC obtained with SL and Tween 80 were those with the highest degree of saturation, $L_{80:20}$ (PS <

226 nm) and $T_{80:20}$ (PS < 174 nm), respectively, while these same systems produced NLC with larger dimensions when WPI ($W_{80:20}$) was used as the emulsifier (PS > 319 nm). The results found in this study demonstrate the importance of individually evaluating each emulsifier, since the influence of the degree of saturation/unsaturation of the lipid system on the dimensions of the obtained NLC varied according to the emulsifier used in their production.

Table 3: Polidispersity index (PDI) of nanostructured lipid carriers (NLC) evaluated after 48 h, 7 days, 15 days, 30 days, and 60 days of storage.

NLC	48 h	7 days	15 days	30 days	60 days
$L_{80:20}$	1.77±0.01^{aA}	1.82±0.01^{aA}	1.99±0.03^{bB}	2.04±0.02^{bAB}	2.02±0.09^{bB}
$L_{60:40}$	1.77±0.03^{aA}	1.90±0.04^{aBC}	2.02±0.05^{abB}	2.29±0.23^{bB}	2.29±0.05^{bC}
$L_{40:60}$	1.76±0.02^{aA}	1.91±0.01^{bC}	1.81±0.06^{abA}	1.85±0.02^{abA}	1.89±0.06^{bAB}
$L_{20:80}$	1.77±0.01^{aA}	1.84±0.01^{bAB}	1.84±0.04^{bA}	1.84±0.01^{bA}	1.83±0.03^{abA}
$T_{80:20}$	2.56±0.04^{bC}	2.44±0.01^{aC}	2.38±0.05^{aC}	2.41±0.06^{aD}	2.36±0.02^{aC}
$T_{60:40}$	2.31±0.06^{bB}	2.06±0.03^{aB}	2.05±0.12^{aB}	2.05±0.03^{aC}	1.93±0.06^{aB}
$T_{40:60}$	1.81±0.03^{aA}	1.94±0.05^{bA}	1.94±0.03^{bA}	1.92±0.04^{bB}	1.84±0.04^{abB}
$T_{20:80}$	1.80±0.01^{aA}	1.83±0.07^{aA}	1.75±0.07^{aA}	1.72±0.05^{aA}	1.72±0.03^{aA}
$W_{80:20}$	1.81±0.00^{aC}	1.80±0.01^{aC}	1.80±0.01^{aC}	1.80±0.02^{aC}	1.81±0.02^{aC}
$W_{60:40}$	1.63±0.02^{aB}	1.65±0.02^{aB}	1.65±0.00^{aB}	1.63±0.03^{aB}	1.64±0.03^{aB}
$W_{40:60}$	1.66±0.02^{aB}	1.65±0.02^{aB}	1.65±0.01^{aB}	1.66±0.01^{Ab}	1.67±0.02^{Ab}
$W_{20:80}$	1.58±0.02^{aA}	1.57±0.00^{aA}	1.57±0.00^{aA}	1.55±0.02^{aA}	1.56±0.01^{aA}

NLC L: nanostructured lipid carries obtained with enzymatic modified soybean lecithin as emulsifier; **NLC T**: nanostructured lipid carries obtained with Tween 80 as emulsifier; **NLC W**: nanostructured lipid carries obtained with whey protein isolate as emulsifier. Average of three replicates ± Standard Deviation. $^{a-d}$ Different lower-case letters indicate significant difference ($p< 0.05$) related to the evaluation of each parameter (PS, PDI and ZP) in comparison to the time of storage of NLC (48 h, 7, 15, 30, 45, and 60 days after processing) for the same NLC. $^{A-D}$ Different capital letters indicate significant difference ($p< 0.05$) related to the evaluation of the same parameter (PS, PDI or ZP) at the same time of storage of NLC (48 h, 7, 15, 30, 45, and 60 days after processing) between the NLC obtained with the same emulsifier.

The PDI is an indicator of the stability of the system (McClements, 2015), where a lower index indicates greater stability. In this study, the Span value, shown in Table 3, was considered an indicator of the PDI. All NLC obtained presented PDI less than 2.5, indicating homogeneous particles and narrow PS distribution of the system (Schaffazick et al., 2003).

Among the emulsifiers used in the study, WPI facilitated the obtainment of NLC with lower PDI (1.56–1.81) and better stability during 60 days of storage ($p < 0.05$). When SL was used to obtain NLC, it was not possible to verify a linear relationship between the increase/decrease in the unsaturation degree of the lipid system with the decrease/increase in

PDI. In the case of Tween 80, there was a decrease in the PDI with an increase in the UFA content in the system. This can be explained by the structural characteristics of Tween, which has a lipophilic tail composed of a MUFA (C17:1). The increased unsaturation of the lipid system allows for greater accommodation of the emulsifier within the NLC structure, resulting in more homogeneous particles.

5.3.2 Zeta Potential

Large ZP values, whether positive or negative, contribute to the stability of a suspension and minimize aggregation due to electrostatic repulsion between particles, especially those with pronounced ZP (Pinto et al., 2014). Regardless of the lipid system and emulsifiers used, all NLC presented ZP > |20 mV| (Table 4), indicating physical stability over the 60 days of evaluation.

The electrical characteristics of nanoparticles depend on the type, concentration, and location of any ionized groups on their surfaces as well as on the ionic composition and physical properties of the surrounding liquid (McClements & McClements, 2016). Differences were observed between NLC obtained with different emulsifiers and are related to the composition and structure of these emulsifiers. The lowest magnitude ZP values were found for NLC stabilized with Tween 80 (Table 4). Tween 80 is a water-soluble, nonionic emulsifier that stabilizes NLC dispersions through steric hindrance (Tamjidi et al., 2013). Even though particles stabilized by nonionic emulsifiers are not expected to be electrically charged, many studies have demonstrated that emulsion-based delivery systems stabilized by Tween 80 are negatively charged. This can be attributed to the presence of anionic impurities and other minor lipids in the oil (as free FA) or in the emulsifier (as free oleic acid). In addition, the adsorption of hydroxyl ions (OH-) from the aqueous phase can also impart a negative charge to the oil–water interface (McClements, 2015).

Previous studies have reported similar ZP values for NLC obtained with Tween 80 from different lipid matrices. Han et al. (2008) reported ZP values close to –20 mV when NLC were obtained from monostearin and Miglyol® 812; Pinto et al. (2018) found values between −23.0 and −32.0 mV in NLC obtained from sunflower, sweet almond, coconut, or olive oils and higher MP lipids rich in lauric (C12:0), myristic (C14:0), palmitic (C16:0), or stearic acid (C18:0); Salvia-Trujillo et al. (2019) reported ZP values between −25 and −28 mV for nano-lipids (NL) formulated with corn oil or olive oil; Santos et al. (2019) found ZP values between −22.27 and −29.70 mV in their characterization of NLC incorporated with phytosterols, obtained using HOSO and fully hydrogenated crambe and canola oils; and Tetyczka et al. (2019) reported ZP values close to −30 mV in their evaluation of NLC obtained using palmitic and oleic acids as lipid matrices.

Table 4: Zeta potential (ZP) of nanostructured lipid carriers (NLC) evaluated after 48 h, 7 days, 15 days, 30 days, and 60 days of storage.

NLC	48 h	7 days	15 days	30 days	60 days
$L_{80:20}$	-65.37±1.62^{aA}	-60.23±5.33^{abB}	-52.93±3.32^{Bbc}	-48.83±0.67^{Bcd}	-41.20±1.23^{Bd}
$L_{60:40}$	-65.73±0.81^{aA}	-59.57±1.72^{bB}	-51.07±1.57^{Bc}	-45.03±1.77^{Cd}	-40.13±0.47^{Be}
$L_{40:60}$	-65.90±1.14^{aA}	-60.20±0.10^{bB}	-53.10±0.62^{Bc}	-45.77±0.25^{Cd}	-42.53±1.12^{Be}
$L_{20:80}$	-68.03±2.18^{aA}	-69.37±1.00^{aA}	-64.00±0.20^{Ab}	-57.83±0.59^{Ac}	-49.60±0.98^{Ad}
$T_{80:20}$	-25.00±1.82^{Aa}	-22.20±0.69^{Aab}	-24.33±0.15^{abB}	-21.70±0.50^{bC}	-22.50±1.78^{abC}
$T_{60:40}$	-25.50±0.87^{Ac}	-23.67±0.81^{Ac}	-28.33±0.12^{bA}	-29.43±1.06^{bA}	-32.20±0.92^{aA}
$T_{40:60}$	-25.57±0.32^{Ab}	-23.20±0.66^{Ac}	-24.23±0.06^{cB}	-26.23±0.65^{bB}	-29.17±0.15^{aB}
$T_{20:80}$	-26.10±0.92^{Ab}	-21.27±1.79^{Ac}	-24.37±0.65^{bB}	-30.20±2.35^{aA}	-32.37±0.68^{aA}
$W_{80:20}$	-62.17±2.12^{aA}	-65.43±1.12^{aA}	-63.80±1.35^{aA}	-62.27±1.06^{aA}	-61.63±3.65^{aA}
$W_{60:40}$	-63.67±1.80^{aA}	-65.07±0.49^{aA}	-64.43±0.92^{aA}	-66.03±1.13^{aA}	-66.10±1.20^{aA}
$W_{40:60}$	-64.67±1.10^{aA}	-57.87±11.95^{aA}	-63.67±2.26^{aA}	-67.03±1.72^{aA}	-64.20±1.50^{aA}
$W_{20:80}$	-63.53±2.72^{aA}	-63.43±1.83^{aA}	-64.93±0.17^{aA}	-68.00±6.70^{aA}	-61.53±0.50^{aA}

NLC L: nanostructured lipid carries obtained with enzymatic modified soybean lecithin as emulsifier; **NLC T**: nanostructured lipid carries obtained with Tween 80 as emulsifier; **NLC W**: nanostructured lipid carries obtained with whey protein isolate as emulsifier. Average of three replicates ± Standard Deviation. $^{a-d}$ Different lower-case letters indicate significant difference ($p< 0.05$) related to the evaluation of each parameter (PS, PDI and ZP) in comparison to the time of storage of NLC (48 h, 7, 15, 30, 45, and 60 days after processing) for the same NLC. $^{A-D}$ Different capital letters indicate significant difference ($p< 0.05$) related to the evaluation of the same parameter (PS, PDI or ZP) at the same time of storage of NLC (48 h, 7, 15, 30, 45, and 60 days after processing) between the NLC obtained with the same emulsifier.

The highest magnitude ZP values were observed for NLC obtained with SL or WPI (Table 4). The nature of the emulsifying molecules surrounding the lipid droplets strongly influences the surface charge density, which in turn is dependent on the pH of the medium (McClements & Gumus, 2016). The negative charge observed for NLC stabilized with SL can be attributed to the presence of anionic phospholipids (Mun et al., 2007) and a pH close to neutral. In the case of SL, the magnitude of the ZP values observed for the NLC showed a significant reduction during the stabilization period; however, at the end of 60 days, all NLC obtained with SL presented ZP > |−40 mV|. Similar values were reported by Heo et al. (2016), who evaluated nano-emulsions obtained from conjugated linolenic acid (in the form of free FA and TAG) using SL (composed of 69.9% phosphatidylcholine and 8.4% phosphatidylethanolamine) as an emulsifier. The authors also found ZP values greater than |−40 mV| for all obtained nano-emulsions.

Among the emulsifiers considered, WPI facilitated the obtainment of NLC with higher magnitude ZP values (greater than |−60 mV|) regardless of the lipid system used as the lipid phase. Most emulsifiers used to obtain NLC are emulsifiers with smaller molecular size; however, macromolecules such as proteins are natural and biocompatible ingredients that have been used in the stabilization of LN (Mohammadi et al., 2019). Proteins have an amphiphilic region in their structure, which explains their potential as an emulsifier. When present at the lipid interface, proteins tend to organize themselves to expose their charged fractions to the outside of the particle, while their hydrophobic fractions interact with the lipid phase (Oliveira et al., 2018).

Similar results were reported by Lee et al. (2011), who evaluated the physicochemical properties of nano-emulsions stabilized with WPI and obtained using corn oil as a lipid matrix. The authors found ZP values of approximately −62 mV for nano-emulsions evaluated at pH 7.0. Yi et al. (2014) reported lower magnitude ZP values than those found in this study when they evaluated solid LN with incorporation of β-carotene prepared with WPI in different proportions (0.10−1.50% w/w). The authors found ZP values close to −30 mV with an emulsifier concentration of 1%, which may explain this difference, as the concentration of emulsifier we used in this study was 2%.

5.3.3 Physical stability

LN are heterogeneous and thermodynamically unstable systems and, therefore, have a significant tendency to lose physical stability during storage (Huang et al., 2008). ZP is a measure of particle surface load and can be considered an indicator of system stability during storage, since it determines the interaction of nanoparticles with other charged species, such as molecules, surfaces, or particles, in their environment (McClements, 2007; Mohammadi et al., 2019). However, as the NLC were kept in dispersions in our study, we chose to further evaluate the physical stability of the dispersions using the light backscattering technique.

The stability of the dispersions containing NLC was evaluated using Turbiscan® Lab equipment. This equipment can detect destabilization phenomena with a high degree of sensitivity, especially in cases of opaque systems (Araújo et al., 2011). Compared with other optical analytical methods, such as microscopy, PS, and ZP, the analysis of physical stability by Turbiscan has the advantage of being a non-destructive method that does not require sample dilution. In addition, it provides information on the type of destabilization process, discriminating between particle migration (creaming or sedimentation), which is normally reversible with agitation, and PS variation (flocculation or coalescence) (Buron et al., 2004).

The evaluation of the physical stability of the dispersions was conducted for a period of 60 days, as described in section 5.2.2.4. The curves obtained were superimposed

on an illustrative graph of the ΔBS, obtained through scans carried out 48 h and 7, 15, 30, and 60 days after NLC obtainment, and are shown in Figures 1, 2, and 3. In these graphs, the first reading of the dispersions (48 h) was recorded as time 00d:00h:00m (baseline) and is represented in the graph in royal blue, and the last reading at 60 days is represented in red. The ordinate axis corresponds to the percentage of backscattered light, while the abscissa axis represents the height of the cylindrical tube in which the samples were conditioned, where a height of 0 corresponds to the bottom of the tube. Through these graphs, it is possible to verify the instability or stability of the dispersions.

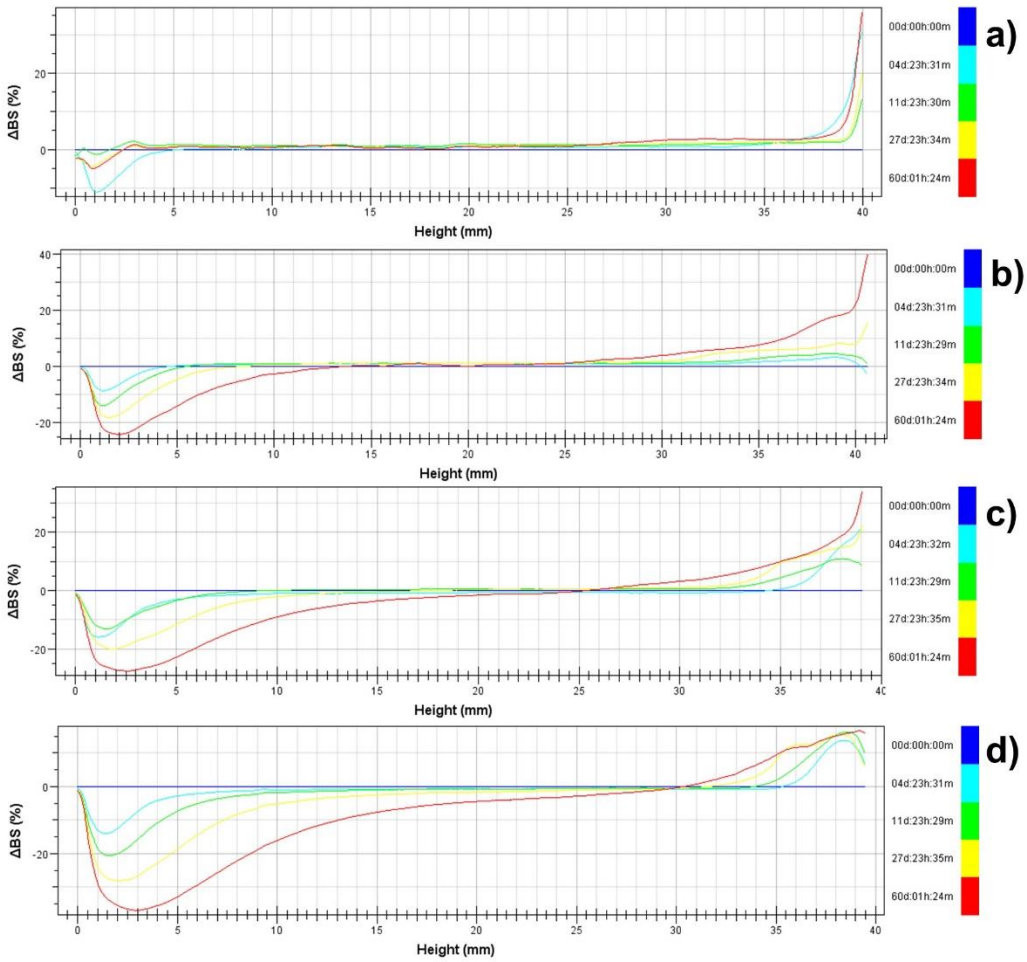

Figure 1: ΔBS variations of dispersions containing NLC obtained with enzymatic modified soybean lecithin. a) NLC obtained from the 80:20 (FHSO:HOSO w/w) lipid system; b) NLC obtained from the 60:40 (FHSO:HOSO w/w) lipid system; c) NLC obtained from the 40:60 (FHSO:HOSO w/w) lipid system; d) NLC obtained from the 20:80 (FHSO:HOSO w/w) lipid system.

The occurrence of destabilization and phase separation modifies the interaction mode of the light beam with the medium, causing an increase or decrease in ΔBS due to the variation and differences in PS and particle migration. In fact, for particles smaller than the

wavelength of incident light, an increase in PS leads to a decrease in the ΔBS. If ΔBS show a variation lower than or equal to ±10%, the samples are considered physically stable, while variations greater than ±10% indicate an unstable dispersion (Celia et al., 2009).

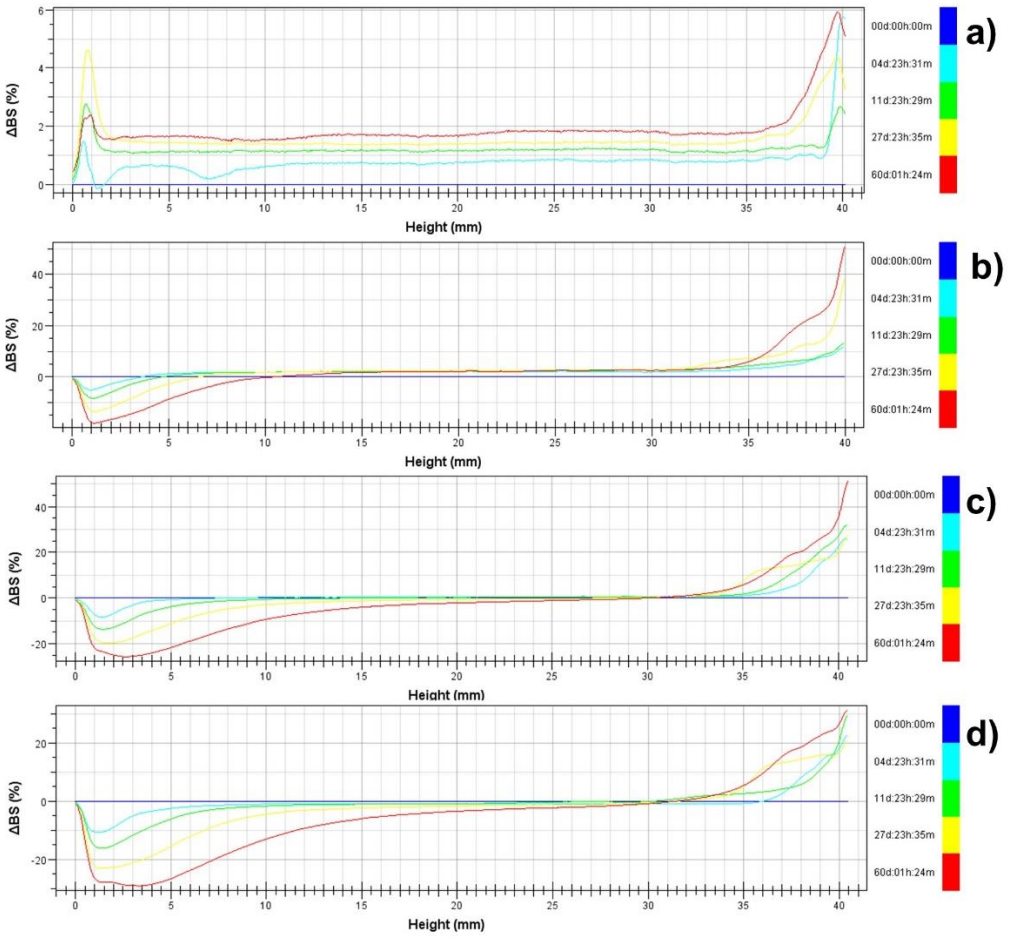

Figure 2: ΔBS variations of dispersions containing NLC obtained with Tween 80. a) NLC obtained from the 80:20 (FHSO:HOSO w/w) lipid system; b) NLC obtained from the 60:40 (FHSO:HOSO w/w) lipid system; c) NLC obtained from the 40:60 (FHSO:HOSO w/w) lipid system; d) NLC obtained from the 20:80 (FHSO:HOSO w/w) lipid system.

The graphs of ΔBS indicate the destabilization observed in the samples. The positive ΔBS variation at the bottom of the tube and negative ΔBS variation at the top (height = 40 mm) relative to the baseline are indicative of sample sedimentation; ΔBS variation in the middle of the tube (height = 20 mm) indicates the occurrence of flocculation or coalescence. ΔBS variations that are negative at the bottom of the tube and positive at the top relative to the baseline are indicative of sample creaming (Mengual et al., 1999).

In this study, obtaining NLC from different lipid systems was found to result in dispersions containing NLC with different ΔBS. The greater the unsaturation degree of the lipid system, the greater the physical instability verified for NLC, which was associated with changes in ΔBS at the end of the storage period. The lipid system that produced more stable dispersions

during the 60 days of storage was the 80:20 FHSO:HOSO (w/w) system. When NLC was obtained with Tween 80, the variation in ΔBS was lower than ±5% (Fig. 2), and with SL, the variation in ΔBS was lower than ±10% (Fig. 1) during the 60 days of storage. In the case of WPI, the NLC presented variations in ΔBS greater than ±10% (Fig. 3) at 60 days of storage. The greater stability can be explained by the higher content of stearic acid present in this system, which, due to its linear chain, makes intramolecular packaging easier and thus promotes the obtainment of more stable particles. However, the increase in the degree of unsaturation in the lipid system represents an increase in the content of oleic acid, the unsaturation of which hinders the intramolecular association and therefore reduces the stability of NLC in dispersion. Similar to our study, Queirós et al. (2021) reported that nanoparticulate systems containing lipid matrices with higher contents of UFA produce NLC with a greater mean diameter and, consequently, lower physical stability during storage.

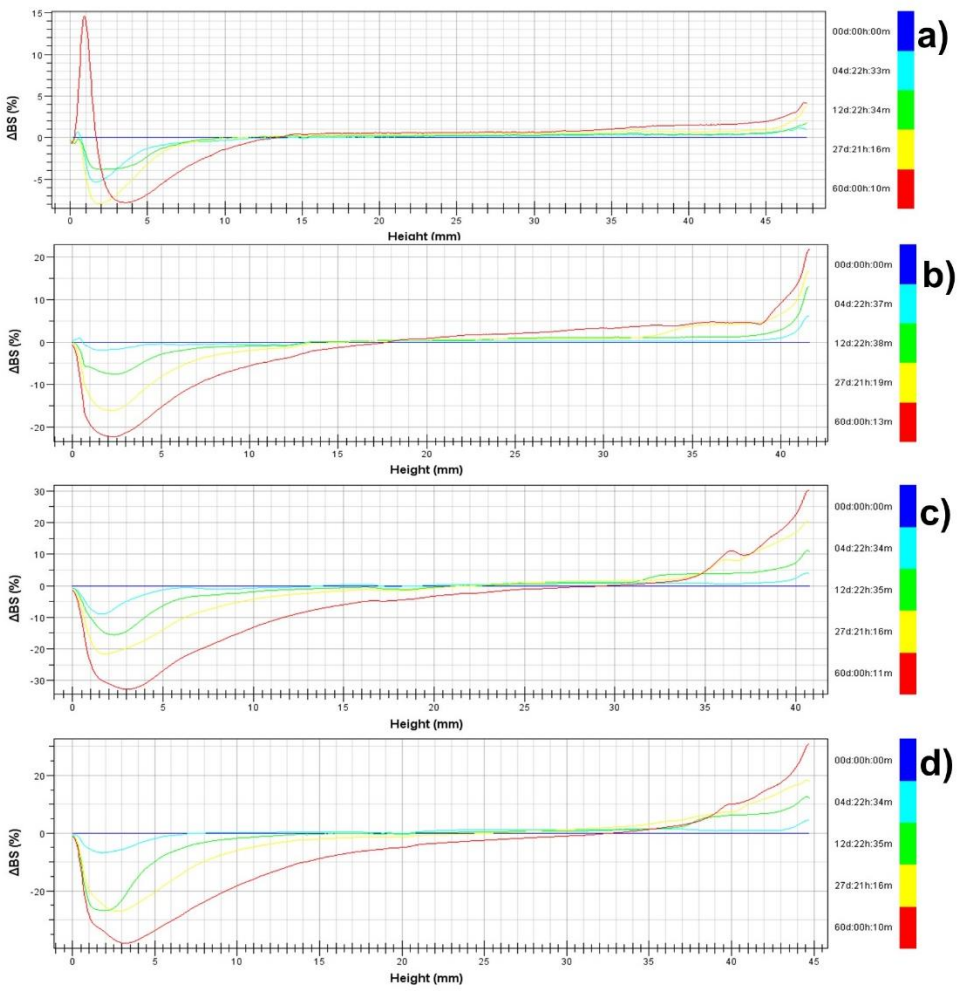

Figure 3: ΔBS variations of dispersions containing NLC obtained with WPI. a) NLC obtained from the 80:20 (FHSO:HOSO w/w) lipid system; b) NLC obtained from the 60:40 (FHSO:HOSO w/w) lipid system; c) NLC obtained from the 40:60 (FHSO:HOSO w/w) lipid system; d) NLC obtained from the 20:80 (FHSO:HOSO w/w) lipid system.

If we consider 10% as indicative of the stability of the system (Celia et al., 2009), we find that, in this study, except for NLC $W_{80:20}$ (W1), all NLC presented characteristic graphs of the creaming phenomenon, corresponding to a negative ΔBS variation at the bottom of the tube and positive ΔBS variation at the top. Up to 30 days, NLC $W_{80:20}$ (W1) presented the characteristic graph of the creaming phenomenon; however, after 60 days of storage, there was a variation in positive ΔBS up to approximately 2.5 mm in height, with subsequent variation in negative ΔBS still in the lower part of the tube, followed by positive variation at the top. Variation in positive ΔBS at the bottom of the tube may be indicative of sample sedimentation. As mentioned above, creaming is a phenomenon associated with particle migration, while sedimentation is associated with PS variation (Buron et al., 2004). However, the Turbiscan results must be supported by dynamic light scattering analysis, which assesses the characteristics of NLC as particles. Therefore, it was possible to verify that the observed sedimentation cannot be attributed to PS variation, since NLC $W_{80:20}$ maintained its dimensions during storage (Table 2).

The results obtained in this study also demonstrate that different emulsifiers result in different ΔBS variations for the same lipid system, indicating that the emulsifiers used to obtain NLC directly affect its physical stability in dispersions. In general, for NLC obtained with Tween 80 and WPI, ΔBS presents a variation greater than ±10% at 30 days of storage for the lipid system 60:40 FHSO:HOSO (w/w), at 15 days of storage for the lipid system 40:60 FHSO:HOSO (w/w), and at 7 days of storage for the lipid system 20:80 FHSO:HOSO (w/w). In the case of NLC obtained with SL, a variation in ΔBS greater than ±10% was observed for the lipid system 60:40 FHSO:HOSO (w/w) at 15 days of storage, while variation in ΔBS was observed at 7 days of storage for the other lipid systems.

Therefore, among the emulsifiers considered in this study, Tween 80 facilitated the obtainment of more stable systems during the 60-day storage period. As verified in section 5.3.1, the NLC obtained using Tween 80 had smaller dimensions compared with those of the NLC obtained with SL or WPI. The greater physical stability in dispersion observed for NLC obtained with Tween 80 can then be attributed to the smaller PS observed, since larger particles usually show greater destabilization. Thus, in addition to the effectiveness of this emulsifier in obtaining smaller NLC, the structural characteristics and the low molecular weight of Tween 80 were responsible for the greater physical stability of NLC in dispersion, observed through ΔBS variation graphs.

5.3.4 Solid fat content

NMR is based on measurements of a sample's responses to high-frequency magnetic radiation pulses. After applying the pulse, the hydrogen nuclei present in the sample

move to an excited state, returning to their ground state after a certain time, known as the decay rate. The decay rate depends on the physical state of the sample: the signal for solids decays much faster than that for liquids. Thus, the SFC of NLC can be determined by measuring the decay rate of the NMR signal (McClements & McClements, 2016).

Table 5 shows the SFC, at 25°C, of NLC obtained from different FHSO:HOSO (w/w) lipid systems. The NLC obtained with 80:20 FHSO:HOSO (w/w) showed the highest SFC during the 60 days of storage, mainly due to the high content of SFA present in this system. A reduction in SFC was observed with an increase in the unsaturation degree of the lipid system, as the NLC obtained with the lipid system 20:80 FHSO:HOSO (w/w) showed the lowest values during the entire storage period. The lower SFC presented by these NLC is explained by the liquid oil content in the system at 25°C, which is in line with the thermal behavior that will be discussed in section 5.3.6, by which these samples did not show melting peaks.

Table 5: Solid fat content (%) at 25°C of NLC evaluated after 48 h, 7 days, 15 days, 30 days, and 60 days of storage.

NLC	48 h	7 days	15 days	30 days	60 days
$L_{80:20}$	82.00±0.10^{aA}	91.90±0.37^{bA}	90.40±0.33^{bA}	90.70±0.32^{bA}	87.30±0.17^{abA}
$L_{60:40}$	62.70±0.09^{aB}	63.70±0.25^{abC}	68.90±0.29^{bA}	70.10±0.15^{bBC}	69.00±0.29^{bB}
$L_{40:60}$	44.40±0.13^{aB}	46.30±0.45^{aA}	47.60±0.18^{aA}	45.40±0.15^{aA}	43.70±0.03^{aA}
$L_{20:80}$	31.90±0.45^{aA}	25.90±0.33^{abA}	24.90±0.28^{abA}	26.00±0.09^{abB}	19.80±0.36^{bB}
$T_{80:20}$	71.60±0.15^{aB}	72.70±0.25^{abC}	71.00±0.40^{aB}	74.30±0.07^{bB}	72.40±0.49^{abB}
$T_{60:40}$	68.80±0.08^{aA}	76.80±0.15^{bA}	70.90±0.16^{abA}	76.50±0.45^{bAB}	74.70±0.32^{abA}
$T_{40:60}$	46.30±0.04^{abB}	51.00±0.10^{aA}	49.20±0.32^{aA}	48.90±0.17^{abA}	44.10±0.20^{bA}
$T_{20:80}$	26.80±0.08^{aA}	28.00±0.37^{aA}	30.80±0.14^{aA}	33.10±0.18^{aA}	31.50±0.32^{aA}
$W_{80:20}$	83.30±0.09^{aA}	82.90±0.17^{aB}	83.80±0.17^{aA}	78.80±0.44^{aB}	80.80±0.39^{baA}
$W_{60:40}$	71.50±0.27^{aA}	73.10±0.29^{aBC}	70.20±0.22^{aA}	69.50±0.19^{aC}	68.70±0.19^{aA}
$W_{40:60}$	52.20±0.12^{aA}	52.60±0.24^{aA}	51.20±0.07^{aA}	49.40±0.03^{aA}	48.50±0.27^{aA}
$W_{20:80}$	31.10±0.23^{aA}	31.20±0.11^{aA}	29.70±0.29^{aA}	29.10±0.14^{aAB}	28.20±0.03^{baA}

NLC L: nanostructured lipid carries obtained with enzymatic modified soybean lecithin as emulsifier; **NLC T**: nanostructured lipid carries obtained with Tween 80 as emulsifier; **NLC W**: nanostructured lipid carries obtained with whey protein isolate as emulsifier. Average of three replicates ± Standard Deviation. $^{a-d}$ Different lower-case letters indicate significant difference ($p< 0.05$) related to the evaluation of each parameter (PS, PDI and ZP) in comparison to the time of storage of NLC (48 h, 7, 15, 30, 45, and 60 days after processing) for the same NLC. $^{A-D}$ Different capital letters indicate significant difference ($p< 0.05$) related to the evaluation of the same parameter (PS, PDI or ZP) at the same time of storage of NLC (48 h, 7, 15, 30, 45, and 60 days after processing) between the NLC obtained with the same emulsifier.

The results obtained also indicate that the emulsifiers considered in this study facilitated the obtainment of NLC with different SFC according to each lipid system. For example, for the 80:20 FHSO:HOSO (w/w) system, the use of Tween 80 produced NLC ($T_{80:20}$) with lower SFC, presenting values lower than the SFA ratio present in this system. For the 60:40 FHSO:HOSO (w/w) system, superior and similar SFC ($p < 0.05$) were found for NLC obtained using Tween 80 ($T_{60:40}$) and WPI ($W_{60:40}$), respectively, as well as for the 20:80 FHSO:HOSO (w/w) system in which NLC were $T_{20:80}$ and $W_{20:80}$. In the case of the 40:60 FHSO:HOSO (w/w) lipid system, the highest SFC values were observed for NLC obtained with WPI ($W_{40:60}$).

The SFC observed for NLC obtained with WPI did not show significant changes during the storage period ($p < 0.05$), indicating that this NLC maintained its crystallinity. The storage time also did not promote significant changes at the end of 60 days for NLC obtained with Tween 80. Although some changes were observed in some NLC during this period, all NLC had similar SFC at 48 h after 60 days of storage. For NLC obtained with SL, NLC $L_{80:20}$ and $L_{20:80}$ maintained their crystallinity during the 60 days, although other NLC ($L_{60:40}$ and $L_{20:80}$) showed significant changes ($p < 0.05$) during the storage period.

SFC is directly related to the formation of crystals, the presence of crystalline agglomerates, and, consequently, the crystal lattice, indicating the degree of crystallinity presented by NLC. SFC values found in this study were mostly higher than the values found when we evaluated the SFC of the lipid systems on a macroscale (Lüdtke, et al., 2021). Hence, an increase in SFC can be attributed to both scale reduction and the addition of emulsifiers during the obtainment of NLC. Although the emulsifiers considered in this study did not influence the polymorphic habit of NLC, as discussed in section 5.3.5, the different SFC observed for NLC indicate that these emulsifiers participated in the formation of the crystal lattice.

5.3.5 Polymorphism

Since the incorporation efficiency and loading capacity of NL are strongly influenced by the crystalline characteristics of lipid matrices, it is essential to study the crystallinity of NL obtained from lipid matrices or unconventional techniques in order to assess the potential of these structures to incorporate bioactive compounds (Shah et al., 2015).

The lipid crystallization pattern is highly related to polymorphism (crystal behavior), which in turn is influenced by internal factors, such as molecular configuration and impurities, and some external factors, including temperature, pressure, and cooling rate. Polymorphism increases surface and hydrophobic interactions and, subsequently, increases colloidal instabilities (Mohammadi et al., 2019).

Short spacings, peak intensity, and identification of polymorphic forms found for NLC obtained from different lipid systems are described in Tables 6, 7, and 8. All NLC obtained in this study presented a polymorphic β form from 48 h of stabilization, which is characterized by short spacings at 4.6, 3.8, and 3.7 Å regardless of the lipid system or the type of emulsifier used. This can be attributed to the great homogeneity in the composition of FA and TAG of the FHSO and HOSO used to obtain NLC. HOSO mainly contains oleic acid (C18:1), and FHSO mainly contains stearic acid (C18:0), both FA with 18 carbon atoms. Homogeneous TAG, which are formed by FA of the same chain size, have their packaging facilitated, thus showing a tendency to crystallize in the more stable β polymorphic form (Acevedo & Marangoni, 2010; Ribeiro et al., 2013). Similar results were reported by Queirós et al. (2021), who evaluated the polymorphic habit of NLC obtained using fully hydrogenated milk fat, anhydrous milk fat, and HOSO in different proportions. The authors found that the NLC obtained with HOSO in the composition presented short spacings characteristic of the β polymorphic form.

Stabilization in the β polymorphic form is desirable, as the polymorphic alteration results in morphological modifications of the particles and, thus, expulsion of the bioactive compound incorporated into the structure. Additionally, it appears that none of the emulsifiers considered in this study interfered with the polymorphic form of the obtained NLC. Furthermore, the evaluation over 60 days showed that there was no fusion or recrystallization of NLC to less stable polymorphic forms, which is very positive when considering the application of these nanostructures in foods. This result can be associated with the maintenance of SFC values throughout the storage period, as discussed previously in section 5.3.4.

Additionally, we verified in this study that the scale reduction from macro to nano had an impact on the crystalline habit and speed of polymorphic transitions. Except for the 60:40 lipid system, which showed stabilization in the β form at 48 h, the lipid systems considered showed polymorphic stabilization in the β form only after 15 days when evaluated on a macroscale in a previous study (Lüdtke, et al., 2021). However, the NLC obtained in this study showed stabilization in the β polymorphic form at 48 h regardless of the lipid system. This was probably because, in smaller dimensions, the van der Waals forces between the TAG molecules are stronger, resulting in more compact crystal structures, whereas at the macroscale, the TAG have more space to organize, thus forming less compact structures.

Table 6: Polymorphic forms, short spacings and peak intensities of the diffractograms obtained for NLC produced with SL as emulsifier.

NLC	Time of storage	Short spacings (nm)					
		4.6	**4.1**	**4.2**	**3.8**	**3.6**	**Polymorphic form**
$L_{80.20}$	48 h	4.6 (vs)	-	-	3.8 (m)	3.6 (m)	β
	7 days	4.6 (vs)	-	-	3.8 (m)	3.7 (m)	β
	15 days	4.6 (vs)	-	-	3.8 (m)	3.7 (m)	β
	30 days	4.6 (vs)	-	-	3.8 (m)	3.6 (m)	β
	60 days	4.6 (vs)	-	-	3.8 (m)	3.6 (m)	β
$L_{60.40}$	48 h	4.6 (s)	-	-	3.8 (m)	3.6 (m)	β
	7 days	4.6 (vs)	-	-	3.8 (m)	3.6 (m)	β
	15 days	4.6 (vs)	-	-	3.8 (m)	3.6 (m)	β
	30 days	4.6 (vs)	-	-	3.8 (m)	3.6 (m)	β
	60 days	4.6 (m)	-	-	3.8 (w)	3.7 (w)	β
$L_{40.60}$	48 h	4.6 (vs)	-	-	3.8 (m)	3.6 (m)	β
	7 days	4.6 (s)	-	-	3.8 (m)	3.6 (w)	β
	15 days	4.6 (s)	-	-	3.8 (m)	3.6 (w)	β
	30 days	4.6 (vs)	-	-	3.8 (m)	3.6 (w)	β
	60 days	4.6 (m)	-	-	3.8 (w)	3.6 (w)	β
$L_{20.80}$	48 h	4.6 (m)	-	-	3.8 (m)	-	β
	7 days	4.6 (m)	-	-	3.8 (m)	3.6 (s)	β
	15 days	4.6 (m)	-	-	3.8 (m)	3.6 (w)	β
	30 days	4.6 (m)	-	-	3.8 (w)	3.6 (m)	β
	60 days	4.6 (m)	-	-	3.8 (m)	3.6 (m)	β

Intensities: **v.** very; **w.** weak; **m.** medium; **s.** strong.

Table 7: Polymorphic forms, short spacings and peak intensities of the diffractograms obtained for NLC produced with Tween 80 as emulsifier.

NLC	Time of storage	Short spacing (nm)					
		0.46	**0.41**	**0.42**	**0.38**	**0.36**	**Polymorphic form**
$T_{80.20}$	48 h	4.6 (s)	-	-	3.8 (w)	3.7 (m)	β
	7 days	4.6 (s)	-	-	3.9 (w)	3.6 (m)	β
	15 days	4.6 (s)	-	-	3.8 (m)	3.7 (m)	β
	30 days	4.6 (s)	-	-	3.8 (m)	3.6 (m)	β
	60 days	4.6 (s)	-	-	3.8 (w)	3.6 (w)	β
$T_{60.40}$	48 h	4.6 (vs)	-	-	3.9 (m)	3.6 (m)	β
	7 days	4.6 (vs)	-	-	3.9 (m)	3.6 (m)	β
	15 days	4.6 (vs)	-	-	3.8 (m)	3.6 (m)	β
	30 days	4.6 (vs)	-	-	3.8 (m)	3.6 (m)	β
	60 days	4.6 (s)	-	-	3.9 (w)	3.6 (w)	β
$T_{40.60}$	48 h	4.6 (s)	-	-	3.9 (w)	3.7 (w)	β
	7 days	4.6 (vs)	-	-	3.9 (m)	3.7 (w)	β
	15 days	4.6 (s)	-	-	3.9 (w)	3.7 (w)	β
	30 days	4.6 (s)	-	-	3.8 (m)	3.7 (w)	β
	60 days	4.6 (m)	-	-	3.9 (w)	3.7 (w)	β
$T_{20.80}$	48 h	4.6 (s)	-	-	3.9 (m)	3.7 (w)	β
	7 days	4.6 (vs)	-	-	3.9 (m)	3.7 (w)	β
	15 days	4.6 (s)	-	-	3.9 (m)	3.7 (w)	β
	30 days	4.6 (s)	-	-	3.9 (w)	3.6 (w)	β
	60 days	4.6 (m)	-	-	3.8 (w)	3.6 (w)	β

Intensities: **v.** very; **w.** weak; **m.** medium; **s.** strong.

Table 8: Polymorphic forms, short spacings and peak intensities of the diffractograms obtained for NLC produced with WPI as emulsifier.

NLC	Time of storage	Short spacing (nm)					
		0.46	**0.41**	**0.42**	**0.38**	**0.36**	**Polymorphic form**
$W_{80.20}$	48 h	4.6 (vs)	-	-	3.9 (m)	3.6 (m)	β
	7 days	4.6 (vs)	-	-	3.9 (m)	3.6 (s)	β
	15 days	4.6 (vs)	-	-	3.8 (s)	3.6 (s)	β
	30 days	4.6 (s)	-	-	3.8 (m)	3.7 (m)	β
	60 days	4.6 (m)	-	-	3.9 (vs)	3.7 (vs)	β
$W_{60.40}$	48 h	4.6 (vs)	-	-	3.8 (s)	3.6 (s)	β
	7 days	4.6 (vs)	-	-	3.8 (s)	3.6 (s)	β
	15 days	4.6 (vs)	-	-	3.8 (s)	3.6 (m)	β
	30 days	4.6 (vs)	-	-	3.8 (s)	3.6 (s)	β
	60 days	4.6 (m)	-	-	3.8 (vs)	3.6 (s)	β
$W_{40.60}$	48 h	4.6 (vs)	-	-	3.9 (s)	3.6 (m)	β
	7 days	4.6 (vs)	-	-	3.8 (s)	3.6 (m)	β
	15 days	4.6 (s)	-	-	3.8 (m)	3.6 (m)	β
	30 days	4.6 (vs)	-	-	3.8 (w)	3.6 (w)	β
	60 days	4.6 (s)	-	-	3.9 (m)	3.7 (m)	β
$W_{20.80}$	48 h	4.6 (vs)	-	-	3.9 (s)	3.6 (m)	β
	7 days	4.6 (vs)	-	-	3.8 (m)	3.6 (m)	β
	15 days	4.6 (s)	-	-	3.8 (m)	3.6 (m)	β
	30 days	4.6 (s)	-	-	3.9 (m)	3.7 (m)	β
	60 days	4.6 (vs)	-	-	3.8 (m)	3.7 (m)	β

Intensities: **v.** very; **w.** weak; **m.** medium; **s.** strong.

5.3.6 Thermal melting behavior

Differential scanning calorimetry (DSC) is commonly used to investigate the thermal properties of nanostructured lipid systems (Qian et al., 2012). Characterization by DSC improves understanding of the thermal behavior of lipid systems composed of high and low MP lipid matrices used to obtain NLC, providing information related to polymorphic transitions (Khosa et al., 2018). DSC is an important tool that can indicate whether the interaction of high and low MP lipid matrices is compatible with the obtainment of NLC with thermal properties suitable for the incorporation of bioactive compounds.

To this end, we evaluated the thermal behavior of NLC obtained from different FHSO:HOSO (w/w) lipid systems and SL, Tween 80, or WPI as the emulsifier. The parameters used to discuss the thermal melting behavior for the NLC obtained from SL, Tween 80, or WPI are found in Tables 9, 10, and 11, respectively, and correspond to the melting onset temperature (Tmo), which refers to the beginning of the solid–liquid transition; melting offset temperature (Toff m), which corresponds to the temperature at which the thermal melting effect was completed; melting peak temperature (Tmp), which indicates the point at which the maximum thermal effect occurred; and, melting enthalpy (ΔHm), which reflects the energy required for the phase change to occur.

The NLC obtained with the 20:80 FHSO:HOSO (w/w) lipid system did not present endothermic events under the conditions evaluated, indicating that this system did not shows crystallinity and, therefore, was not suitable for obtaining NLC. The melting curves of the NLC obtained for the other lipid systems showed a single endothermic event at around 60°C, which corresponded to the melting of the solid lipid matrix of the nanoparticles (FHSO). Because of the presence of TAG with a lower MP, the T_{fm} and enthalpy–ΔH decreased with an increase in the degree of unsaturation of the lipid systems used to obtain NLC.

The Tmo observed for NLC obtained from the 80:20 FHSO:HOSO (w/w) lipid system was found in the range of 57.19°C to 63.13°C; from the 60:40 FHSO:HOSO (w/w) lipid system, 56.93°C to 63.10°C; and from the 40:60 FHSO:HOSO (w/w) lipid system, 54.18°C to 62.16°C. The Toff m observed for the NLC obtained from the 80:20 FHSO:HOSO (w/w) lipid system was found in the range of 67.58°C to 75.04°C; from the 60:40 FHSO:HOSO (w/w) lipid system, 66.96°C to 71.87°C; and from the 40:60 FHSO:HOSO (w/w) lipid system, 65.59°C to 68.55°C.

The Tmp observed for NLC obtained from the 80:20 FHSO:HOSO (w/w) lipid system was found in the range of 65.53°C to 67.15°C; from the 60:40 FHSO:HOSO (w/w) lipid system, 65.17°C to 66,90°C; and from the 40:60 FHSO:HOSO (w/w) lipid system, 62.54°C to 64.25°C, indicating the possibility of applying these structures in foods submitted to thermal processing.

Table 9: Thermal melting parameters of NLC produced with SL as emulsifier.

NLC	Time of storage	Tmo (°C)	Tmp (°C)	Toff m (°C)	ΔH (J/g)
$L_{80.20}$	48 h	62.10±0.91	66.34±0.29	69.36±1.00	3.39±0.70
$L_{60.40}$	48 h	61.26±0.46	65.17±0.10	68.98±1.35	0.69±0.20
$L_{40.60}$	48 h	59.10±0.93	63.65±0.72	68.03±1.9	0.43±0.23
$L_{80.20}$	7 days	61.59±0.3	65.89±0.82	68.66±0.25	2.82±1.33
$L_{60.40}$	7 days	61.52±0.46	65.21±0.10	66.96±1.35	0.36±0.20
$L_{40.60}$	7 days	60.49±0.45	63.12±0.42	65.64±0.2	0.13±0.02
$L_{80.20}$	15 days	61.59±0.3	65.94±0.82	68.76±0.15	2.78±1.02
$L_{60.40}$	15 days	61.50±0.42	65.18±0.50	66.96±1.35	0.48±0.2
$L_{40.60}$	15 days	60.39±0.52	63.02±0.42	65.68±0.28	0.14±0.02
$L_{80.20}$	30 days	60.36±2.5	66.44±0.22	69.26±0.44	2.70±0.15
$L_{60.40}$	30 days	61.33±0.42	65.19±0.32	67.98±0.15	0.52±0.06
$L_{40.60}$	30 days	59.98±0.46	63.06±0.50	66.49±0.86	0.22±0.07
$L_{80.20}$	60 days	61.78±1.14	66.37±0.36	68.67±0.76	2.66±1.05
$L_{60.40}$	60 days	61.40±0.35	65.17±0.25	68.20±0.22	0.56±0.04
$L_{40.60}$	60 days	60.17±0.43	63.00±0.47	65.95±0.55	0.17±0.01

Tmo: melting onset temperature; **Tmp:** melting peak temperature; **Toff m:** melting offset temperature; **ΔH**: melting enthalpy. Average of three replicates ± Standard Deviation.

The addition of other components, such as emulsifiers or bioactive compounds, to the lipid or aqueous phase of NLC can promote changes in the thermal behavior of the particles obtained (Bunjes & Unruh, 2007). In this sense, differences in thermal parameters were not observed in NLC obtained from the same FHSO:HOSO (w/w) lipid system but different emulsifiers, demonstrating that the emulsifiers considered in this study did not interfere with the thermal parameters of lipid systems at the nanoscale. These results indicate that the thermal behavior in the fusion of the NLC obtained in this study was governed by the lipid matrices used in their production. NLC obtained from the 80:20, 60:40, and 40:60 FHSO:HOSO (w/w) lipid systems remained in a semi-solid state at body temperature (37°C),

which is an indispensable attribute when stable NLC are intended for food application and especially when bioactive compounds are incorporated.

Table 10: Thermal melting parameters of NLC produced with Tween 80 as emulsifier.

NLC	Time of storage	Tmo (°C)	Tmp (°C)	Toff m (°C)	ΔH (J/g)
$T_{80.20}$	48 h	63.13±0.46	66.66±0.04	70.56±1.20	0.98±0.06
$T_{60.40}$	48 h	61.02±0.75	65.34±0.15	69.19±0.62	0.89±0.03
$T_{40.60}$	48 h	59.65±0.39	63.13±0.22	68.55±2.25	0.42±0.22
$T_{80.20}$	7 days	62.92±0.43	66.52±0.13	68.36±0.29	0.65±0.15
$T_{60.40}$	7 days	61.61±0.23	65.48±0.05	67.13±0.12	0.46±0.02
$T_{40.60}$	7 days	59.77±0.05	62.92±0.30	66.07±0.6	0.21±0.04
$T_{80.20}$	15 days	62.23±0.92	66.01±0.12	67.58±1.51	0.82±0.18
$T_{60.40}$	15 days	62.53±1.28	66.90±0.06	71.87±1.05	0.57±0.0.27
$T_{40.60}$	15 days	62.16±0.57	63.84±0.24	66.46±0.49	0.04±0.03
$T_{80.20}$	30 days	61.14±01.67	66.14±0.93	68.84±0.5	0.87±1.06
$T_{60.40}$	30 days	62.77±1.44	66.08±0.19	71.68±6.65	0.43±33.99
$T_{40.60}$	30 days	61.94±1.00	64.06±4.12	66.49±3.87	0.18±0.74
$T_{80.20}$	60 days	62.25±2.54	65.53±0.91	75.04±6.20	0.73±4.03
$T_{60.40}$	60 days	63.10±1.71	66.02±1.72	69.97±3.65	0.31±10.66
$T_{40.60}$	60 days	58.21±1.46	62.74±5.28	67.82±5.83	0.12±6.55

Tmo: melting onset temperature; **Tmp**: melting peak temperature; **Toff m:** melting offset temperature; **ΔH**: melting enthalpy. Average of three replicates ± Standard Deviation.

When we evaluated the 80:20, 60:40, and 40:60 FHSO:HOSO (w/w) lipid systems on a macroscale, we observed different thermal behavior from that observed for the NLC obtained from them (Lüdtke, et al., 2021). In this study, all lipid systems on a macroscale showed two fusion events, one corresponding to the temperature of trisaturated TAG from FHSO and another from tri-unsaturated TAG from HOSO, while NLC showed only one endothermic event. In this case, the thermal behavior in the fusion of NLC was dictated by the lipid matrix with the highest MP used to obtain the NLC (FHSO). The macro-to-nano scale reduction did not change the general thermal behavior parameters of the lipid phase (Tom,

Tmp and Toff m). However, the melting profiles were sensitive to the mass concentration of lipids in the dispersion, which resulted in proportionally reduced values of ΔH.

Table 11: Thermal melting parameters of NLC produced with WPI as emulsifier.

NLC	Time of storage	Tmo (°C)	Tmp (°C)	Toff m(°C)	∆H (J/g)
$W_{80.20}$	48 h	63.03±0.16	67.15±0.23	70.92±1.47	0.96±0.3
$W_{60.40}$	48 h	61.90±0.46	65.37±0.10	68.34±1.35	0.44±0.2
$W_{40.60}$	48 h	59.62±0.15	63.11±0.14	65.86±0.68	0.23±0.03
$W_{80.20}$	7 days	60.88±3.01	66.96±0.05	72.18±4.94	1.62±1.47
$W_{60.40}$	7 days	61.99±0.14	65.78±0.11	68.86±0.39	0.66±0.07
$W_{40.60}$	7 days	60.19±0.49	63.53±0.28	66.68±0.59	0.25±0.09
$W_{80.20}$	15 days	60.81±2.84	66.98±0.4	71.51±4.57	1.45±1.15
$W_{60.40}$	15 days	59.98±0.19	65.52±0.22	69.38±0.25	0.83±0.06
$W_{40.60}$	15 days	60.71±0.34	63.46±0.38	66.04±0.43	0.16±0.00
$W_{80.20}$	30 days	61.26±1.99	67.01±0.25	70.92±3.3	1.29±0.87
$W_{60.40}$	30 days	60.81±0.42	65.84±0.32	69.26±0.15	0.76±0.06
$W_{40.60}$	30 days	61.35±0.94	64.25±1.01	66.68±0.89	0.21±0.08
$W_{80.20}$	60 days	57.19±0.19	66.50±0.81	69.31±1.05	6.47±0.33
$W_{60.40}$	60 days	56.93±0.35	65.22±0.25	68.53±0.22	5.48±0.04
$W_{40.60}$	60 days	54.18±2.65	62.54±1.7	65.59±1.9	3.88±2.34

Tmo: melting onset temperature; **Tmp**: melting peak temperature; **Toff m:** melting offset temperature; ∆**H**: melting enthalpy. Average of three replicates ± Standard Deviation.

Although DSC instruments are able to measure the endothermic events that occur in a lipid matrix very accurately, they are not able to report the cause of these thermal events. For the latter purpose, it is necessary to consider complementary instrumental techniques such as x-ray diffraction, which provides accurate information about polymorphic habit and polymorphic transitions (Khosa et al., 2018). As explained in section 5.3.5, all NLC obtained in this study presented polymorphic stabilization in the β form from 48 h, indicating that, compared with lipid systems on the macroscale, TAG organized themselves into a more compact crystal structure (Lüdtke, et al., 2021). This more compact crystal structure observed in NLC requires

greater energy to promote the solid–liquid phase transition, thus conferring a greater thermal resistance to nanocarriers. As observed for the polymorphism (section 5.3.5), the thermal behavior of NLC remained constant during the 60 days of storage.

5.3.7 Microstructure

In addition to PS, dispersity, and composition, the microstructure is an important feature of nanostructured lipid systems, as it provides important information about the physical state and properties such as incorporation efficiency of bioactive compounds (Shah et al., 2015). Several microscopy techniques can be used to provide information on the physical state of the NL. Optical polarized light microscopy (PLM) can be used to determine the presence and location of crystalline or liquid regions in a sample (Li et al., 2012). In this study, the morphology of NLC was evaluated using PLM (Figure 4) and scanning electron microscopy (SEM; Figure 5).

The images acquired by PLM were of the dispersion containing NLC. In the PLM evaluation of the microstructure of NLC, it is not possible to highlight morphology patterns, since this technique does not have adequate resolution. In practice, it is difficult to obtain reliable measurements below 1000 nm due to the mechanical limitations of the microscope components and the Brownian motion of nanoparticles (McClements & McClements, 2016).

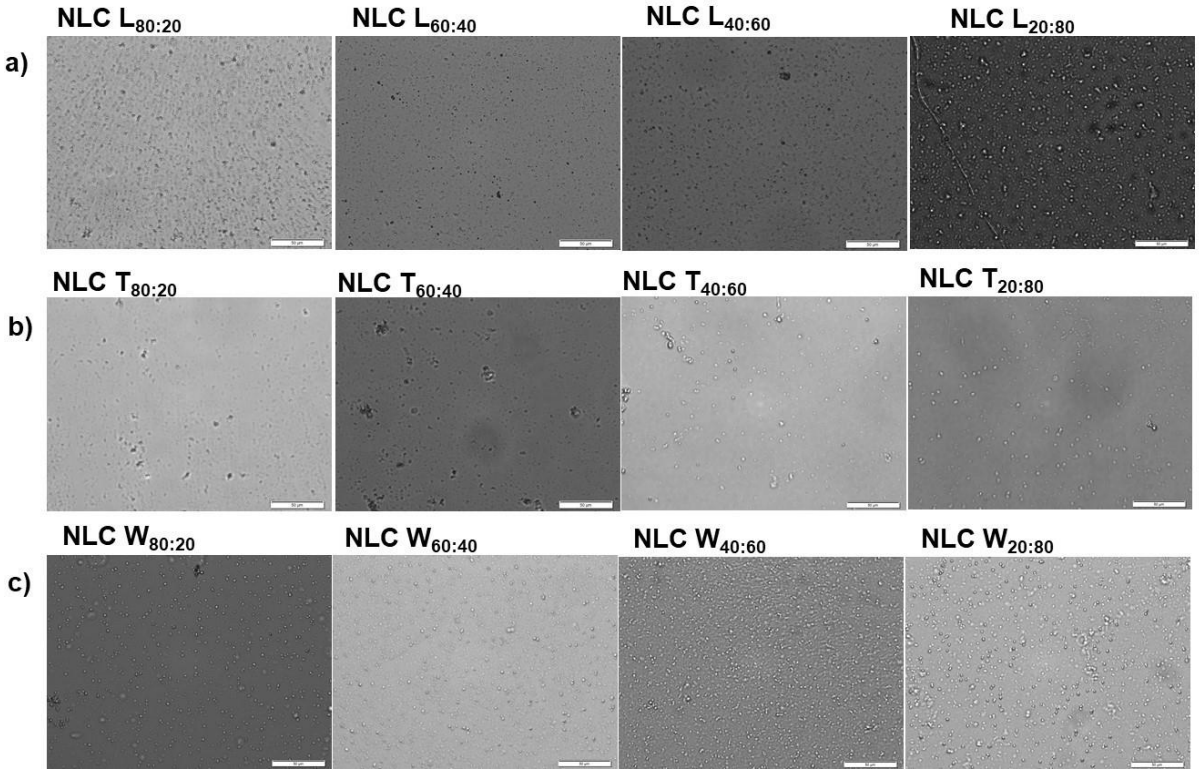

Figure 4: Polarized light microscopy images at 40x magnification obtained of NLC dispersions at 25°C. a) NLC obtained with SL as emulsifier; b) NLC obtained with Tween 80 as emulsifier; c) NLC obtained with WPI as emulsifier.

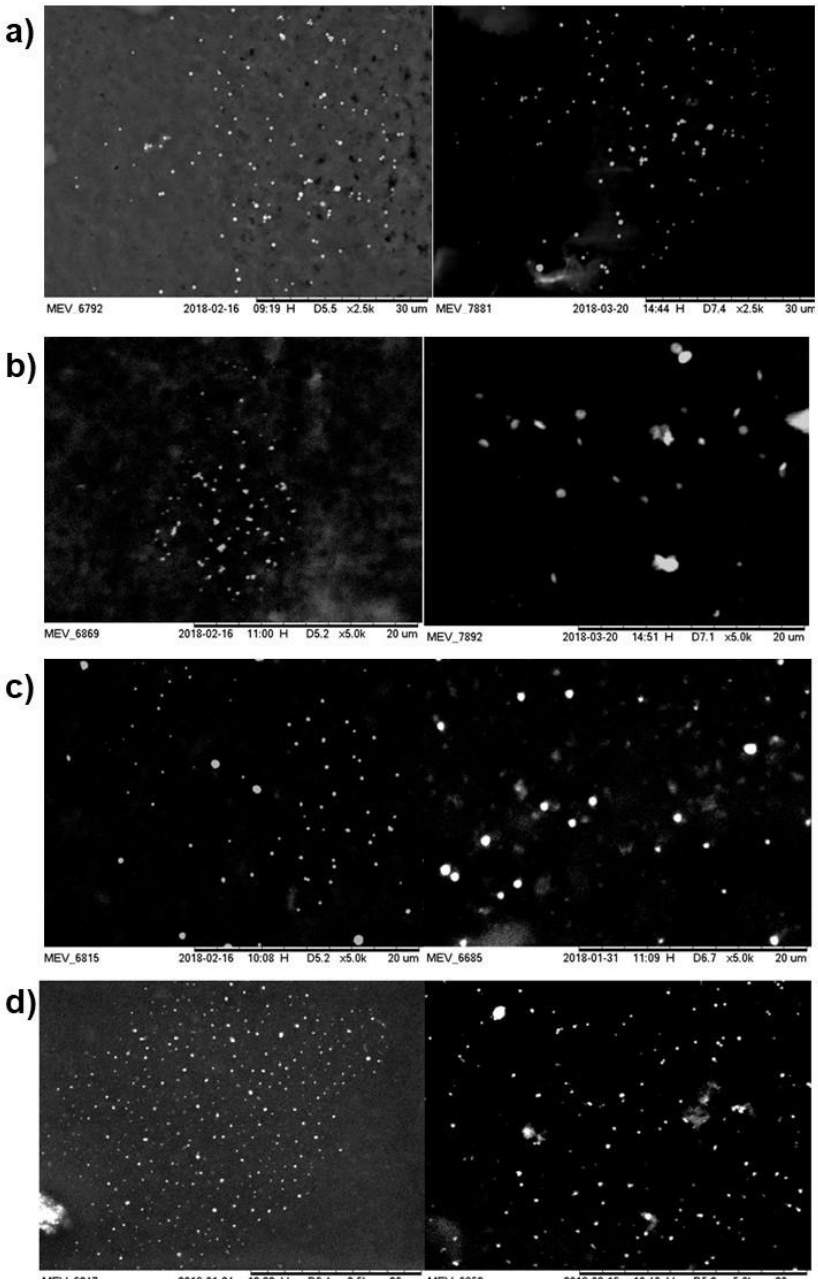

Figure 5: Scanning eletron microscopy images of NLC obtained with Tween 80 as emulsifier. a) NLC obtained with the 80:20 FHSO:HOSO lipid system at 2500x magnification; b) NLC obtained with the 60:40 FHSO:HOSO lipid system at 5000x magnification; c) NLC obtained with the 40:60 FHSO:HOSO lipid system at 5000x magnification; d) NLC obtained with the 20:80 FHSO:HOSO lipid system at 2500 and 5000x magnification.

Among microscopic techniques, electron microscopy is the most suitable for characterizing the microstructure and organization of nanoparticles, mainly due to its ability to detect through electron beams (approximately 1 nm resolution) structural elements that are too small to be visualized with light waves in optical microscopes (McClements & McClements, 2016). To this end, we evaluated the microstructure of NLC using SEM. The images obtained corresponded to the particles as structural elements, since the preparation of the samples for visualization involved prior drying, under ambient conditions, of the dispersions containing NLC

conditioned on the carbon strip. With this technique, however, it was only possible to obtain images of NLC formulated with Tween 80 as the emulsifier.

As shown in Figure 5, the NLC obtained with Tween 80, regardless of the lipid system, generally presented a spherical shape. The shape of the particle can influence the carrying capacity and release properties of bioactive compounds incorporated into NLC. Spherical particles have a smaller surface area and are therefore stabilized with smaller amounts of emulsifiers. Furthermore, they are characterized by a longer diffusion pathway, thus providing a controlled and slow release of incorporated compounds. The spherical shape also provides minimal contact with the surrounding liquid, conferring a greater stability to the compounds incorporated into the structure (Shah et al., 2015). Thus, we found that the use of Tween 80 provided NLC with an adequate format for the protection and incorporation of bioactive compounds.

It was not possible to identify through SEM any NLC obtained using SL or WPI as the emulsifier. For this type of lipid nanosystem, structural characterization can be adequately performed by transmission electron microscopy (TEM) techniques, which allow for the evaluation of the integrity and morphology of the nanoparticles.

The results obtained in this study demonstrate that the emulsifiers used to obtain NLC had greater influence on the physicochemical characteristics of the nanocarriers than on the thermal and crystallization properties. We verified that thermal behavior, polymorphism, and SFC were governed by the composition of the lipid systems. Evaluation of these parameters showed that the 20:80 FHSO:HOSO (w/w) lipid system could compromise both the structure and stability of the incorporated compounds. However, other lipid systems produced NLC with adequate physical characteristics and crystal stability, since thermal properties, SFC, and crystallization features were maintained during the 60 days of storage. Neither the polymorphic transitions nor the thermal properties were influenced by the evaluation time, mainly because the raw materials with high and low MP used to obtain NLC form very compatible systems, which can be considered robust crystallization systems.

The scale reduction from macro to nano promoted significant changes in thermal properties, degree of crystallinity, and polymorphic habit of the lipid matrices used in this study. NLC showed higher thermal resistance, higher SFC, and polymorphic stabilization in the β form in the last 48 h, indicating the absence of the late polymorphic transitions that occurred in the macroscale lipid systems (Lüdtke et al., 2021). These results suggest that, although the macroscale characterization provides important information about the behavior of lipid systems, it is always important to characterize them at the nanoscale in terms of thermal and crystallization properties.

At the end of this study, it was found that the 80:20, 60:40, and 40:60 FHSO:HOSO (w/w) lipid systems had adequate crystallinity properties for the development of NLC. However,

it is necessary to consider that the incorporation of a lipid phase with a lower MP in lipid systems used to obtain NLC provides greater space for the accommodation of bioactive compounds, thus resulting in a greater carrying capacity (Mohammadi et al., 2019). Therefore, we recommend that, when aiming to incorporate bioactive compounds in NLC, the choice should be lipid systems with an intermediate ratio between the lipid matrices of higher and lower MP, such as the 60:40 or 40:60 FHSO:HOSO (w/w) lipid systems. However, it is important to point out that, prior to the incorporation of these compounds, more studies are needed to verify the compatibility of the bioactive target with the lipid system and emulsifier.

5.3 Conclusion

The unsaturation degree of lipid systems composed of FHSO:HOSO (w/w) do not affect parameters such as zeta potential or polydispersity index when obtained from the same emulsifier. However, differences are observed when nanostructured lipid carriers are obtained using different emulsifiers, indicating that the type of emulsifier used has a direct influence on the zeta potential and polydispersity index of these nanostructures. Despite these differences, the nanostructured lipid carriers have homogeneous particles, narrow PS distribution of the system, and absolute zeta potential values greater than -20 mV, indicating good physical stability over 60 days.

The data obtained in this study confirm our initial hypothesis that lipid phase modulation affects thermal properties, SFC, and crystallization properties of NLC. When Tween 80 or soy lecithin are used as the emulsifier, the increase in the unsaturation degree of the system favors the obtainment of NLC with larger dimensions, greater physical instability, and lower peak temperature and melting enthalpy. The increase in the unsaturation degree, however, does not change the polymorphic form of the NLC obtained.

Among the lipid systems considered, the 80:20, 60:40, and 40:60 FHSO:HOSO (w/w) systems produce stable particles with adequate crystallinity characteristics to obtain NLC.

5.4 Acknowledgments

The authors are grateful to the Coordination for the Improvement of Higher Education Personnel (*Coordenação de Aperfeiçoamento de Pessoal de Nível Superior* - CAPES) for the financial support. Fernanda Luisa Lüdtke thanks FAPESP (grants # 18/03172-0, # 19/05176-6, #16/11261-8 and 19/27354-3, São Paulo Research Foundation -FAPESP). Ana Paula Badan Ribeiro thanks CNPq (303429/2018-6) for the productivity grant.

5.5 References

Acevedo, N. C., & Marangoni, A. G. (2010). Characterization of the nanoscale in triacylglycerol crystal networks. *Crystal Growth and Design*, *10*(8), 3327–3333. https://doi.org/10.1021/cg100468e

Araújo, J., Nikolic, S., Egea, M. A., Souto, E. B., & Garcia, M. L. (2011). Nanostructured lipid carriers for triamcinolone acetonide delivery to the posterior segment of the eye. *Colloids and Surfaces B: Biointerfaces*, *88*(1), 150–157. https://doi.org/10.1016/j.colsurfb.2011.06.025

Averina, E. S., Müller, R. H., Popov, D. v., & Radnaeva, L. D. (2011). Physical and chemical stability of nanostructured lipid drug carriers (NLC) based on natural lipids from Baikal region (Siberia, Russia). *Pharmazie*, *66*(5), 348–356. https://doi.org/10.1691/ph.2011.0326

Babazadeh, A., Ghanbarzadeh, B., & Hamishehkar, H. (2017). Formulation of food grade nanostructured lipid carrier (NLC) for potential applications in medicinal–functional foods. *Journal of Drug Delivery Science and Technology*, *39*, 50–58. https://doi.org/10.1016/j.jddst.2017.03.001

Badea, G., Lăcătuşu, I., Badea, N., Ott, C., & Meghea, A. (2015). Use of various vegetable oils in designing photoprotective nanostructured formulations for UV protection and antioxidant activity. *Industrial Crops and Products*, *67*, 18–24. https://doi.org/10.1016/j.indcrop.2014.12.049

Barroso, L., Viegas, C., Vieira, J., Ferreira–Pêgo, C., Costa, J., & Fonte, P. (2021). Lipid–based carriers for food ingredients delivery. *Journal of Food Engineering, 295*. https://doi.org/10.1016/j.jfoodeng.2020.110451

Bunjes, H., & Unruh, T. (2007). Characterization of lipid nanoparticles by differential scanning calorimetry, X–ray and neutron scattering. *Advanced Drug Delivery Reviews, 59*(6), 379–402. https://doi.org/10.1016/j.addr.2007.04.013

Buron, H., Mengual, O., Meunier, G., Cayré, I., & Snabre, P. (2004). Optical characterization of concentrated dispersions: applications to laboratory analyses and on–line process monitoring and control. *Polymer International*, *53*(9), 1205–1209. https://doi.org/10.1002/pi.1231

Cardenia, V., Rodriguez–Estrada, M. T., Cumella, F., Sardi, L., della Casa, G., & Lercker, G. (2011). Oxidative stability of pork meat lipids as related to high–oleic sunflower oil and vitamin E diet supplementation and storage conditions. *Meat Science*, *88*(2), 271–279. https://doi.org/10.1016/j.meatsci.2010.12.034

Celia, C., Trapasso, E., Cosco, D., Paolino, D., & Fresta, M. (2009). Turbiscan Lab® Expert analysis of the stability of ethosomes® and ultradeformable liposomes containing a bilayer fluidizing agent. *Colloids and Surfaces B: Biointerfaces*, *72*(1), 155–160. https://doi.org/10.1016/j.colsurfb.2009.03.007

Chang, C., Tu, S., Ghosh, S., & Nickerson, M. T. (2015). Effect of pH on the inter–relationships between the physicochemical, interfacial and emulsifying properties for pea, soy, lentil and canola protein isolates. *Food Research International*, *77*, 360–367. https://doi.org/10.1016/j.foodres.2015.08.012

Chen, L., Remondetto, G. E., & Subirade, M. (2006). Food protein–based materials as nutraceutical delivery systems. *Trends in Food Science and Technology*, *17*(5), 272–283. https://doi.org/10.1016/j.tifs.2005.12.011

Gunstone, F. D. (2011). Production and Trade of Vegetable Oils. In *Vegetable Oils in Food Technology* (6th ed., Vol. 2). Wiley–Blackwell. https://doi.org/10.1002/9781444339925.ch1

Håkansson, A., Innings, F., Trägårdh, C., & Bergenståhl, B. (2013). A high–pressure homogenization emulsification model—Improved emulsifier transport and hydrodynamic coupling. *Chemical Engineering Science*, *91,* 44–53. https://doi.org/10.1016/j.ces.2013.01.011

Han, F., Li, S., Yin, R., Liu, H., & Xu, L. (2008). Effect of surfactants on the formation and characterization of a new type of colloidal drug delivery system: Nanostructured lipid carriers. *Colloids and Surfaces A: Physicochemical and Engineering Aspects*, *315*(1–3), 210–216. https://doi.org/10.1016/j.colsurfa.2007.08.005

He, X., & Hwang, H. M. (2016). Nanotechnology in food science: Functionality, applicability, and safety assessment. *Journal of Food and Drug Analysis, 24*(4), 671–681. Elsevier Taiwan LLC. https://doi.org/10.1016/j.jfda.2016.06.001

Helgason, T., Awad, T. S., Kristberg, K., Decker, E. A., Mcclements, D. J., & Weiss, J. (2009). Impact of surfactant properties on oxidative stability of β–carotene encapsulated within solid lipid nanoparticles. *Journal of Agricultural and Food Chemistry*, *57*(17), 8033–8040. https://doi.org/10.1021/jf901682m

Heo, W., Kim, J. H., Pan, J. H., & Kim, Y. J. (2016). Lecithin–Based Nano–emulsification Improves the Bioavailability of Conjugated Linoleic Acid. *Journal of Agricultural and Food Chemistry*, *64*(6), 1355–1360. https://doi.org/10.1021/acs.jafc.5b05397

How, C. W., Rasedee, A., & Abbasalipourkabir, R. (2013). Characterization and cytotoxicity of nanostructured lipid carriers formulated with olive oil, hydrogenated palm oil, and polysorbate 80. *IEEE Transactions on Nanobioscience*, *12*(2), 72–78. https://doi.org/10.1109/TNB.2012.2232937

Huang, Z. R., Hua, S. C., Yang, Y. L., & Fang, J. Y. (2008). Development and evaluation of lipid nanoparticles for camptothecin delivery: A comparison of solid lipid nanoparticles, nanostructured lipid carriers, and lipid emulsion. *Acta Pharmacologica Sinica*, *29*(9), 1094–1102. https://doi.org/10.1111/j.1745–7254.2008.00829.x

Hunter, J. E., Zhang, J., Kris–Etherton, P. M., & Childs, L. (2010). Cardiovascular disease risk of dietary stearic acid compared with trans, other saturated, and unsaturated fatty acids: A systematic review. *American Journal of Clinical Nutrition*, *91*(1), 46–63. https://doi.org/10.3945/ajcn.2009.27661

Kamboj, S., Bala, S., & Nair, A. B. (2010). Solid lipid nanoparticles: an effective lipid based technology for poorly water soluble drugs. *International Journal of Pharmaceutical Sciences Review and Research*, *5*(2), 78–90. ISSN 0976 – 044X

Katouzian, I., Faridi Esfanjani, A., Jafari, S. M., & Akhavan, S. (2017). Formulation and application of a new generation of lipid nano–carriers for the food bioactive ingredients. *Trends in Food Science and Technology, 68*, 14–25. https://doi.org/10.1016/j.tifs.2017.07.017

Khosa, A., Reddi, S., & Saha, R. N. (2018). Nanostructured lipid carriers for site–specific drug delivery. *Biomedicine and Pharmacotherapy, 103*, 598–613. https://doi.org/10.1016/j.biopha.2018.04.055

Kumbhar, D. D., & Pokharkar, V. B. (2013). Engineering of a nanostructured lipid carrier for the poorly water–soluble drug, bicalutamide: Physicochemical investigations. *Colloids and Surfaces A: Physicochemical and Engineering Aspects*, *416*(1), 32–42. https://doi.org/10.1016/j.colsurfa.2012.10.031

Lee, L. L., Niknafs, N., Hancocks, R. D., & Norton, I. T. (2013). Emulsification: Mechanistic understanding. *Trends in Food Science and Technology, 31*(1), 72–78. https://doi.org/10.1016/j.tifs.2012.08.006

Li, Y., Xiao, H., & McClements, D. J. (2012). Encapsulation and Delivery of Crystalline Hydrophobic Nutraceuticals using Nanoemulsions: Factors Affecting Polymethoxyflavone Solubility. *Food Biophysics*, *7*(4), 341–353. https://doi.org/10.1007/s11483–012–9272–1

Liu, C. H., & Wu, C. T. (2010). Optimization of nanostructured lipid carriers for lutein delivery. *Colloids and Surfaces A: Physicochemical and Engineering Aspects*, *353*(2–3), 149–156. https://doi.org/10.1016/j.colsurfa.2009.11.006

Lüdtke, F.L., Grimaldi, R., Cardoso, L.P., Ribeiro, A.P.B. (2021b). Lipid systems based on fully hydrogenated soybean oil and high oleic sunflower oil to obtain nanostructured lipid carriers: composition, physical properties, and crystallization parameters. *To be submitted.*

Lüdtke, F. L., Stahl, M. A., Zaia, B. G., Santos, V.S., Hashimoto, J. C., & Ribeiro, A. P. B. (2017). Evaluation of process parameters for obtaining nanostructured lipid carriers by high pressure homogenization. *17th AOCS LatinAmerican Congress and Exhibition on Fats, Oils, and Lipids*.

McClements, D. J. (2007). Critical review of techniques and methodologies for characterization of emulsion stability. *Critical Reviews in Food Science and Nutrition, 47*(7), 611–649. https://doi.org/10.1080/10408390701289292

McClements, D. J. (2012). Requirements for food ingredient and nutraceutical delivery systems. In *Encapsulation Technologies and Delivery Systems for Food Ingredients and Nutraceuticals* (pp. 3–18). Elsevier. https://doi.org/10.1533/9780857095909.1.3

McClements, D. J. (2013). Utilizing food effects to overcome challenges in delivery of lipophilic bioactives: Structural design of medical and functional foods. *Expert Opinion on Drug Delivery, 10*(12), 1621–1632. https://doi.org/10.1517/17425247.2013.837448

McClements, D. J. (2015). *Food Emulsions: Principles, Practices and Techniques* (Taylor & Francis Group, Ed.; 3rd ed.).

McClements, D. J., & Gumus, C. E. (2016). Natural emulsifiers — Biosurfactants, phospholipids, biopolymers, and colloidal particles: Molecular and physicochemical basis of functional performance. *Advances in Colloid and Interface Science, 234*, 3–26. https://doi.org/10.1016/j.cis.2016.03.002

McClements, J., & McClements, D. J. (2016). Standardization of Nanoparticle Characterization: Methods for Testing Properties, Stability, and Functionality of Edible Nanoparticles. *Critical Reviews in Food Science and Nutrition*, *56*(8), 1334–1362. https://doi.org/10.1080/10408398.2014.970267

Mengual, O., Meunier, G., Cayre, I., Puech, K., & Snabre, P. (1999). Characterisation of instability of concentrated dispersions by a new optical analyser: the TURBISCAN MA 1000. *Colloids and Surfaces A: Physicochemical and Engineering Aspects*, *152*(1–2), 111–123. https://doi.org/10.1016/S0927–7757(98)00680–3

Mohammadi, M., Assadpour, E., & Jafari, S. M. (2019). Encapsulation of food ingredients by nanostructured lipid carriers (NLCs). In *Lipid–Based Nanostructures for Food Encapsulation Purposes* (pp. 217–270). Elsevier. https://doi.org/10.1016/b978–0–12–815673–5.00007–6

Mozafari, M. R., Flanagan, J., Matia–Merino, L., Awati, A., Omri, A., Suntres, Z. E., & Singh, H. (2006). Recent trends in the lipid–based nanoencapsulation of antioxidants and their role in foods. *Journal of the Science of Food and Agriculture, 86*(13), 2038–2045. https://doi.org/10.1002/jsfa.2576

Mun, S., Decker, E. A., & McClements, D. J. (2007). Influence of emulsifier type on in vitro digestibility of lipid droplets by pancreatic lipase. *Food Research International*, *40*(6), 770–781. https://doi.org/10.1016/j.foodres.2007.01.007

Nguyen, H. M., Hwang, I. C., Park, J. W., & Park, H. J. (2012). Enhanced payload and photo–protection for pesticides using nanostructured lipid carriers with corn oil as liquid lipid. *Journal of Microencapsulation*, *29*(6), 596–604. https://doi.org/10.3109/02652048.2012.668960

Niculae, G., Lacatusu, I., Badea, N., Meghea, A., & Stan, R. (2014). Influence of vegetable oil on the synthesis of bioactive nanocarriers with broad spectrum photoprotection. *Central European Journal of Chemistry*, *12*(8), 837–850. https://doi.org/10.2478/s11532–014–0503–9

Nik, A. M., Langmaid, S., & Wright, A. J. (2012). Nonionic surfactant and interfacial structure impact crystallinity and stability of β–carotene loaded lipid nanodispersions. *Journal of Agricultural and Food Chemistry*, *60*(16), 4126–4135. https://doi.org/10.1021/jf204810m

O'Brien, R. D. (2008). *Fats and Oils* (CRC Press, Ed.; 3rd ed.). CRC Press. https://doi.org/10.1201/9781420061673

Oliveira, D.R.B. (2018). Production of lipid nanostructures through low energy processes. [PhD thesis published]. Universidade Estadual de Campinas.

Oliveira, D. R. B., Michelon, M., de Figueiredo Furtado, G., Sinigaglia–Coimbra, R., & Cunha, R. L. (2016). β–Carotene–loaded nanostructured lipid carriers produced by solvent displacement method. *Food Research International*, *90*, 139–146. https://doi.org/10.1016/j.foodres.2016.10.038

Pan, Y., Tikekar, R. v, & Nitin, N. (2016). Distribution of a Model Bioactive within Solid Lipid Nanoparticles and Nanostructured Lipid Carriers Influences its Loading Efficiency and Oxidative Stability. *International Journal of Pharmaceutics, 511*(1), 322–330. https://doi.org/10.1016/j.ijpharm.2016.07.019

Pardeike, J., Hommoss, A., & Müller, R. H. (2009). Lipid nanoparticles (SLN, NLC) in cosmetic and pharmaceutical dermal products. *International Journal of Pharmaceutics, 366*(1–2), 170–184. https://doi.org/10.1016/j.ijpharm.2008.10.003

Pezeshki, A., Hamishehkar, H., Ghanbarzadeh, B., Fathollahy, I., Keivani Nahr, F., Khakbaz Heshmati, M., & Mohammadi, M. (2019). Nanostructured lipid carriers as a favorable delivery system for β–carotene. *Food Bioscience*, *27*, 11–17. https://doi.org/10.1016/j.fbio.2018.11.004

Pinheiro, A. C., Gonçalves, R. F., Madalena, D. A., & Vicente, A. A. (2017). Towards the understanding of the behavior of bio–based nanostructures during in vitro digestion. *Current Opinion in Food Science, 15*, 79–86. https://doi.org/10.1016/j.cofs.2017.06.005

Pinto, F., de Barros, D. P. C., & Fonseca, L. P. (2018). Design of multifunctional nanostructured lipid carriers enriched with α–tocopherol using vegetable oils. *Industrial Crops and Products*, *118*, 149–159. https://doi.org/10.1016/j.indcrop.2018.03.042

Pinto, M. F., Moura, C. C., Nunes, C., Segundo, M. A., Costa Lima, S. A., & Reis, S. (2014). A new topical formulation for psoriasis: Development of methotrexate–loaded nanostructured lipid carriers. *International Journal of Pharmaceutics*, *477*(1–2), 519–526. https://doi.org/10.1016/j.ijpharm.2014.10.067

Puri, A., Loomis, K., Smith, B., Lee, J.–H., Yavlovich, A., Heldman, E., & Blumenthal, R. (2009). Lipid–Based Nanoparticles as Pharmaceutical Drug Carriers: From Concepts to Clinic. *Critical Reviews in Therapeutic Drug Carrier Systems*, *26*, 523–580 https://doi.org/10.1615/critrevtherdrugcarriersyst.v26.i6.10.

Qian, C., Decker, E. A., Xiao, H., & McClements, D. J. (2012). Nanoemulsion delivery systems: Influence of carrier oil on β–carotene bioaccessibility. *Food Chemistry*, *135*(3), 1440–1447. https://doi.org/10.1016/j.foodchem.2012.06.047

Qian, C., Decker, E. A., Xiao, H., & McClements, D. J. (2013). Impact of lipid nanoparticle physical state on particle aggregation and β–carotene degradation: Potential limitations of solid lipid nanoparticles. *Food Research International*, *52*(1), 342–349. https://doi.org/10.1016/j.foodres.2013.03.035

Queirós, M. de S., Viriato, R. L. S., Ribeiro, A. P. B., & Gigante, M. L. (2021). Development of solid lipid nanoparticle and nanostructured lipid carrier with dairy ingredients. *International Dairy Journal*, 105186. https://doi.org/10.1016/j.idairyj.2021.105186

Rawal, S. U., & Patel, M. M. (2018). Lipid nanoparticulate systems: Modern versatile drug carriers. In *Lipid Nanocarriers for Drug Targeting* (pp. 49–138). Elsevier. https://doi.org/10.1016/B978–0–12–813687–4.00002–5

Ribeiro, A. P. B., Basso, R. C., Grimaldi, R., Gioielli, L. A., dos Santos, A. O., Cardoso, L. P., & Guaraldo Gonçalves, L. A. (2009). Influence of chemical interesterification on thermal behavior, microstructure, polymorphism and crystallization properties of canola oil and fully hydrogenated cottonseed oil blends. *Food Research International*, *42*(8), 1153–1162. https://doi.org/10.1016/j.foodres.2009.05.016

Ribeiro, A. P. B., Basso, R. C., & Kieckbusch, T. G. (2013). Effect of the addition of hardfats on the physical properties of cocoa butter. *European Journal of Lipid Science and Technology*, *115*(3), 301–312. https://doi.org/10.1002/ejlt.201200170

Rostamabadi, H., Falsafi, S. R., & Jafari, S. M. (2019). Nanoencapsulation of carotenoids within lipid–based nanocarriers. In *Journal of Controlled Release, 298*, 38–67. https://doi.org/10.1016/j.jconrel.2019.02.005

Salvia–Trujillo, L., Verkempinck, S. H. E., Zhang, X., van Loey, A. M., Grauwet, T., & Hendrickx, M. E. (2019). Comparative study on lipid digestion and carotenoid bioaccessibility of emulsions, nanoemulsions and vegetable–based in situ emulsions. *Food Hydrocolloids*, *87*, 119–128. https://doi.org/10.1016/j.foodhyd.2018.05.053

Santos, V. S., Braz, B. B., Silva, A. Á., Cardoso, L. P., Ribeiro, A. P. B., & Santana, M. H. A. (2019). Nanostructured lipid carriers loaded with free phytosterols for food applications. *Food Chemistry*, *298*. https://doi.org/10.1016/j.foodchem.2019.125053

Schaffazick, S. R., Guterres, S. S., Freitas, L. de L., & Pohlmann, A. R. (2003). Caracterização e estabilidade físico–química de sistemas poliméricos nanoparticulados para administração de fármacos. *Química Nova*, *26*(5), 726–737. https://doi.org/10.1590/S0100–40422003000500017

Schenk, H., & Peschar, R. (2004). Understanding the structure of chocolate. *Radiation Physics and Chemistry*, *71*(3–4). https://doi.org/10.1016/j.radphyschem.2004.04.105

Shah, R., Eldridge, D., Palombo, E., & Harding, I. (2015). Lipid Nanoparticles: Production, Characterization and Stability. In *Springer briefs in pharmaceutical science & drug development.* http://www.springer.com/series/10224

Tamjidi, F., Shahedi, M., Varshosaz, J., & Nasirpour, A. (2013). Nanostructured lipid carriers (NLC): A potential delivery system for bioactive food molecules. *Innovative Food Science and Emerging Technologies, 19,* 29–43. https://doi.org/10.1016/j.ifset.2013.03.002

Tan, Y., & McClements, D. J. (2021). Improving the bioavailability of oil–soluble vitamins by optimizing food matrix effects: A review. *Food Chemistry*, *348*. https://doi.org/10.1016/j.foodchem.2021.129148

Tetyczka, C., Hodzic, A., Kriechbaum, M., Juraić, K., Spirk, C., Hartl, S., Pritz, E., Leitinger, G., & Roblegg, E. (2019). Comprehensive characterization of nanostructured lipid carriers using laboratory and synchrotron X–ray scattering and diffraction. *European Journal of Pharmaceutics and Biopharmaceutics*, *139*, 153–160. https://doi.org/10.1016/j.ejpb.2019.03.017

Valenzuela, A., Delplanque, B., & Tavella, M. (2011). Stearic acid: A possible substitute for trans fatty acids from industrial origin. *Grasas y Aceites*, *62*(2), 131–138. https://doi.org/10.3989/gya.033910

Villafuerte, R., Leopoldo, García, F., Beatriz, Garzón, S., M. L., Hernández, L., Vázquez, R., & Luisa, M. (2008). Nanopartículas lipídicas sólidas. *Revista Mexicana de Ciencias Farmacéuticas*. *39*(1), 38–52. http://www.redalyc.org/articulo.oa?id=57939107

Wang, J. L., Dong, X. Y., Wei, F., Zhong, J., Liu, B., Yao, M. H., Yang, M., Zheng, C., Quek, S. Y., & Chen, H. (2014). Preparation and characterization of novel lipid carriers containing microalgae oil for food applications. *Journal of Food Science*, *79*(2), 169–177. https://doi.org/10.1111/1750–3841.12334

Wassell, P., & Young, N. W. G. (2007). Food applications of trans fatty acid substitutes. *International Journal of Food Science & Technology*, *42*(5), 503–517. https://doi.org/10.1111/j.1365–2621.2007.01571.x

Weiss, J., Decker, E. A., McClements, D. J., Kristbergsson, K., Helgason, T., & Awad, T. (2008). Solid lipid nanoparticles as delivery systems for bioactive food components. *Food Biophysics*, *3*(2), 146–154. https://doi.org/10.1007/s11483–008–9065–8

Weiss, J., Takhistov, P., & McClements, D. J. (2006). Functional Materials in Food Nanotechnology. *Journal of Food Science*, *71*(9), 107–116. https://doi.org/10.1111/j.1750–3841.2006.00195.x

Yang, Y., Corona, A., Schubert, B., Reeder, R., & Henson, M. A. (2014). The effect of oil type on the aggregation stability of nanostructured lipid carriers. *Journal of Colloid and Interface Science*, *418*, 261–272. https://doi.org/10.1016/j.jcis.2013.12.024

Yi, J., Lam, T. I., Yokoyama, W., Cheng, L. W., & Zhong, F. (2014). Controlled release of β–carotene in β–lactoglobulin–dextran– conjugated nanoparticles" in vitro digestion and transport with caco–2 monolayers. *Journal of Agricultural and Food Chemistry*, *62*(35), 8900–8907. https://doi.org/10.1021/jf502639k

Zheng, M., Falkeborg, M., Zheng, Y., Yang, T., & Xu, X. (2013). Formulation and characterization of nanostructured lipid carriers containing a mixed lipids core. *Colloids and Surfaces A: Physicochemical and Engineering Aspects*, *430*, 76–84. https://doi.org/10.1016/j.colsurfa.2013.03.070

CAPÍTULO VI

Development and characterization of fully hydrogenated soybean oil and high oleic sunflower oil β-carotene loaded nanostructured lipid carriers

Submitted to Food Research International

6. Development and characterization of fully hydrogenated soybean oil and high oleic sunflower oil β-carotene loaded nanostructured lipid carriers

Fernanda Luisa Lüdtke[a], Renato Grimaldi[a], Lisandro Pavie Cardoso[b], Mirna Lúcia Gigante[a], António Augusto Vicente[c], Ana Paula Badan Ribeiro[a]

[a]Department of Food Engineering and Technology, School of Food Engineering, State University of Campinas (UNICAMP), 13083-862, Campinas, SP, Brazil.

[b]Department of Applied Physics, Gleb Wataghin Institute of Physics, State University of Campinas (UNICAMP), 13083-859, Campinas, SP, Brazil.

[c] CEB - Centre of Biological Engineering, University of Minho, 4710-057 Braga, Portugal.

ABSTRACT

Nanostructured lipid carriers (NLC) have shown great potential as a delivery system for lipophilic bioactive compounds as they provide protection, high water dispersibility, chemical stability, and oral bioavailability. The less compact crystal structure created by high- and low-melting-point lipids has more space for the entrapment of bioactive compounds, such as β-carotene, the carotenoid with the highest provitamin A activity. The objective of this study was to produce and characterise β-carotene-loaded NLC. The study assessed the physical and crystallization properties, entrapment efficiency (EE), and loading capacity (LC) of NLC produced with fully hydrogenated soybean oil and high oleic sunflower oil as high- and low-melting-point lipid matrices, respectively, and soy lecithin, Tween 80, and whey protein isolate (WPI) as emulsifiers. WPI promoted the production of NLC with larger particle size, lower physical stability, and lower IE and LC, compared with other emulsifiers. The melting range of the resulting NLC was within a suitable range for incorporation in foods, with a peak melting temperature above body temperature.

Keywords: lipid nanoparticles, emulsifiers, physical stability, entrapment efficiency, polymorphic habit, bioactive compounds

6.1 Introduction

The growing incidence of diet-related diseases, such as obesity, cardiovascular diseases, hypertension, and cancer, has necessitated the continuous development of products with health-promoting effects, especially by using bioactive compounds (Livney, 2015). However, the application of bioactive compounds in food products is often limited by chemical instability and high hydrophobicity presented by these compounds (Pezeshki et al., 2019).

In recent decades, interest in the development of delivery systems has been considerably growing with the increasing awareness of the health benefits of consuming bioactive compounds. These delivery systems improve the uniform distribution of bioactive compounds in food matrices, protect their bioactivity during processing and storage, and increase their bioavailability in the body (McClements et al., 2007).

The need for food-grade nanotechnology systems that can encapsulate, protect, and release bioactive compounds has attracted the great interest of researchers and industries (Santos et al., 2018; Silva et al., 2012). The use of nanotechnology approaches has shown great potential for improving the delivery of bioactive compounds in functional foods to produce healthier products, resulting in increased solubility, bioavailability, and stability, and protection of the bioactive compound during processing, storage, and distribution (Chen et al., 2006).

Carotenoids are among the bioactive compounds used to produce functional foods; they are natural antioxidants associated with a decreased risk of developing degenerative diseases, such as cancer, cardiovascular diseases, age-related macular degeneration, and cataracts. In addition to their antioxidant capacity, some carotenoids, such as β-carotene, are precursors of other essential molecules, such as vitamin A (Grune et al., 2010).

The different types of carotenoids found in photosynthetic organisms consist of linear molecules with multiple conjugated double bonds (Taiz et al., 2017). This structure confers both antioxidant and provitamin functions to carotenoids but poses challenges to the incorporation of these compounds into foods. The use of β-carotene is limited by its highly hydrophobic nature, and thus, it is not easily incorporated into water-based foods, has low bioavailability in crystalline form and high reactivity, and is unstable upon exposure to heat, light, and oxygen (Brito-Oliveira et al., 2017).

Lipid-based delivery systems are considered suitable for the loading and protection of carotenoids (Katouzian et al., 2017). This is because the compounds remain isolated from the external aqueous phase as they are solubilised in oil droplets, thereby resulting in increased water dispersibility, chemical stability, and oral bioavailability (Park et al., 2018). Nanostructured lipid carriers (NLC) can be used as carriers of this lipophilic compound in water-based food products, protecting it from physical and chemical degradation, and thereby increasing its bioavailability (Hentschel et al., 2008; Liu & Wu, 2010).

NLC were developed to overcome the disadvantages and problems associated with solid lipid nanoparticles (SLN), such as low entrapment efficiency (EE) due to the highly crystalline structure that often leads to expulsion of the compound during storage (Assadpour & Jafari, 2019). The hydrophobic core of the particles within NLC consists of a crystallised lipid phase with a partially disorganised structure, which inhibits morphological changes and expulsion of the bioactive compound (Kharat & McClements, 2019). The most relevant factors that should be considered in the formulation of NLC for the loading of bioactive compounds are the use of ingredients generally recognised as safe that are compatible with food matrices, can protect the incorporated bioactive compound, have a high loading capacity (LC), and support a controlled and targeted delivery of the compounds for improved bioavailability (Jafari et al., 2017; McClements & Li, 2010; Mohammadi et al., 2019).

The conventional method for producing NLC involves the mixing of lipid molecules that are highly different spatially, that is, mixing solid lipids with liquid lipids (oils). The matrix of the lipid particles has a lower melting point compared with the solid lipids used to produce NLC, but it has a higher melting point compared with the body temperature (Attama et al., 2012). The selection of appropriate lipidic raw materials is crucial for the formulation of NLC and for the chemical stability of bioactive compounds incorporated into the structures (Tamjidi et al., 2013). Lipid sources presenting large amounts of unsaturated fatty acids (FA) are susceptible to auto-oxidation when dispersed in nanoemulsions due to the increased surface area provided by the reduction in particle size (PS) (Yi et al., 2015). Therefore, the selection of the lipid matrix for NLC is also crucial for increased bioavailability of carotenoids. This auto-oxidation can lead to the degradation of the lipophilic bioactive component incorporated into these lipid matrices (Liu et al., 2016). Therefore, the selection of oxidation-resistant lipid sources is important.

Because delivery systems need to be industrially viable for incorporation into foods, the used ingredients should meet the regulatory requirements, have verified beneficial effects and properties, be feasible for production on an industrial scale, and sufficiently cost-effective for the respective market segment (Pyo et al., 2017). The use of conventional vegetable oils is a promising alternative to produce NLC as they are commercially available, present a viable cost, and are approved for use in food (Pezeshki et al., 2019).

High oleic sunflower oil (HOSO) is a promising material for the production of NLC into which bioactive compounds can be incorporated, mainly due to the higher oxidative stability of this lipid matrix when compared with other vegetable oils rich in polyunsaturated FA (Oliveira et al., 2016). In addition to its high oxidative stability, HOSO has neutral taste and aroma, and therefore, it has been used to produce products with maximum toxicological safety and biodegradability (Gunstone, 2011). HOSO is a lipid source of high quality and low melting point for NLC production (Cerqueira et al., 2014; Tamjidi et al., 2013). A study by Zhou et al. (2018) has demonstrated that vegetable oils rich in C16 and C18 FA are good lipid sources for carrying lipophilic compounds, such as β-carotene. In addition, a study by Oliveira et al. (2016) demonstrated that the presence of HOSO in NLC provided a less organised crystal structure that improved entrapment and protected against the degradation of β-carotene, thereby further supporting the growing interest in this raw material.

Fully hydrogenated vegetable oils are a low-cost option with high potential as raw materials of high melting point for NLC production (Santos et al., 2019). Obtained after the process of total hydrogenation of soybean oil, fully hydrogenated soybean oil (FHSO) has significant levels of stearic acid (> 87 %) (Oliveira et al., 2015; Ribeiro et al., 2013), thereby favouring the use of these components in lipid nanoparticles (LN) for the neutral atherogenic

effect and the reduced risk of cardiovascular disease associated with this FA (Valenzuela et al., 2011).

Therefore, the objective of this study was to produce and characterize β-carotene loaded NLC using FHSO as a high melting point lipid matrix and HOSO as a low melting point lipid matrix, to determine the potential of low-cost, highly available, and food-grade lipid raw materials in the production of NLC.

6.2 Materials and Methods

6.2.1 Materials

The lipid materials used to produce NLC were HOSO (C18:1 = 78.51 %, C18:2 = 12.40 %, and C16:0 = 4.02 %) and FHSO (C18:0 = 87.31 % and C16:0 = 10.70 %), both supplied by Cargill Foods (Brazil). The emulsifying agents were whey protein isolate (WPI) produced by Alibra (Brazil), the enzymatically hydrolysed soybean lecithin (SL) SOLEC^{TM} AE IP produced by Solae (Brazil), and the ethoxylated sorbitan monooleate (Tween 80) produced by Sigma-Aldrich (USA).

6.2.2 Methods

6.2.2.1 Production of NLC

Table 1 presents the FHSO:HOSO (w/w) lipid systems and emulsifiers used in the formulation of NLC. NLC were produced from a pre-emulsion composed of aqueous phase (88 %), lipid phase (10 %), and emulsifier (2 %). The lipid phase was composed of 60:40 FHSO:HOSO (w/w) lipid system. SL, Tween 80, and WPI were used separately to produce NLC loaded with β-carotene. An aqueous solution of WPI (2 %) was previously prepared for complete hydration of proteins. WPI was dissolved in distilled water and kept under magnetic stirring for 1 h at room temperature (approximately 25 °C). Sodium azide (0.02 %) was then added as an antimicrobial agent and the solution was stored overnight under refrigeration (5–7 °C) (Queirós et al., 2021). The lipid phase was heated to 85 °C, and β-carotene (5 mg/g of lipid phase) was added after complete melting of the solid lipid matrix (FHSO). The mixture was then homogenised under magnetic stirring with heating until the complete solubilisation of the bioactive compound. The β-carotene solubilised in the melted lipid phase was added to the aqueous phase at 85 °C with continuous stirring (10,000 rpm for 3 min) in a model T18 Ultra Turrax shaker (IKA, Germany) to form the pre-emulsion. The pre-emulsion was then subjected to high pressure hot homogenisation using a two-stage Homolab 2.20 homogeniser (Buffalo series, FBF Italy). The process conditions used to produce the NLC were 700 bar and

two homogenisation cycles (Lüdtke et al., 2017), with the pressure applied by the second-stage valve corresponding to 10 % of the total applied pressure, that is, approximately 70 bar. The nanoemulsions were then refrigerated at 5 °C for 24 h to recrystallise the lipid phase to obtain the dispersion containing the NLC, which was subsequently stored in a BOD incubator at 25 °C for 60 days (Kumbhar & Pokharkar, 2013; Qian et al., 2013; Yang et al., 2014).

Table 1: Composition of β-carotene loaded NLC.

NLC	Emulsifier	FHSO: HOSO	β-carotene (%)	Ultrapure water (%)
$\mathbf{L_\beta}$	SL	60:40	0.05	90
$\mathbf{T_\beta}$	*Tween* 80	60:40	0.05	90
$\mathbf{W_\beta}$	WPI	60:40	0.05	90

NLC: nanostructured lipid carries; **SL:** enzymatic modified soybean lecithin; **WPI**: whey protein isolate; **FHSO**: fully hydrogenated soybean oil; **HOSO:** high oleic sunflower oil.

6.2.2.2 Characterization of NLC

6.2.2.2.1 Particle size and Polydispersity index

PS and the polydispersity index (PDI) were determined by photon correlation spectroscopy (PCS) using the dynamic light scattering (DLS) technique with a Mastersizer 2000 Laser Diffractometer (Malvern Instruments, Malvern, UK). The NLC were added to the equipment reading unit, filled with distilled water at 25 °C, and kept under constant stirring at 1750 rpm. The considered obscuration index was 2 %. The analyses were performed in triplicate at room temperature (25 °C) (Averina et al., 2011). The mean PS of the NLC were expressed as a function of the mean surface diameter (D_{32}) obtained with Equation 1 and the PDI was determined by calculating the Span (Equation 2).

$$D_{32=} \frac{\sum n_i d^3_i}{\sum n_i d^2_i} \quad \text{(Equation 1)}$$

$$Span= \frac{d_{90}-d_{10}}{d_{50}} \quad \text{(Equation 2)}$$

where n_i is the number of particles with diameter d_i; and d10, d50, and d90 represent 10%, 50%, and 90% of the cumulative volume of the droplets, respectively.

6.2.2.2.2 Zeta potential

The zeta potential (ZP) was determined by PCS using the DLS technique with a Zetasizer Nano-ZS (Malvern Instruments, Malvern, UK). For measuring the ZP, the samples were diluted (1:100) in ultrapure water and the conductivity (50 µS/cm) was adjusted with a solution of potassium chloride (0.1 % w/v). The ZP was determined using the electrophoretic mobility with the Helmholtz-Smoluchowski equation (Das et al., 2020; Severino et al., 2012). The analyses were performed in triplicate at room temperature.

6.2.2.2.2 Physical stability

The physical stability of the dispersions containing NLC was determined using the backscattering technique with a Turbiscan® Lab (Formulation, l'Union, France). After producing NLC, the dispersions were added to flat-bottomed cylindrical tubes and then stored at 25 °C. The stability was analysed using scattering profiles (ΔBS) with scans at 880 nm in length at different heights (mm), with the height, H = 0 mm, referring to the bottom of the measuring cell. The scanning was performed on the days of the analyses (after 48 h, and 7, 15, 30, and 60 days).

6.2.2.2.4 Solid fat content

The solid fat content (SFC) was determined by pulsed low-resolution nuclear magnetic resonance spectroscopy (NMR) Bruker pc120 Minispec (Silberstreifen, Rheinstetten, Germany), using high precision dry baths with temperature controlled (0–70°C) by the Peltier Tcon 2000 system (Duratech, Garden Grove, USA). The analysis was carried out using AOCS Cd 16b-93 direct method, involving reading of samples in series (AOCS, 2009).

6.2.2.2.5 Thermal behavior during melting

The thermal behavior during the melting of β-carotene-loaded NLC was assessed in a TA Q2000 differential scanning calorimeter (DSC) coupled to a RCS90 Refrigerated Cooling System (TA Instruments, Waters LLC, New Castle). Universal V4.7A (TA Instruments, Waters LLC, New Castle) was used for data processing. The analysis conditions were as follows: sample mass: ~ 10 mg; maintenance of isothermal condition: 25 °C for 10 min; melting events assessed between 25 and 100 °C at a rate of 10 °C/min (Wang et al., 2014). The following parameters were used to assess the results: melting onset temperature (Tmo), melting offset temperature (Toff m), melting peak temperature (Tmp), and melting enthalpy (∆Hm) (Campos, 2005).

6.2.2.2.6 Polymorphism

The polymorphic form of the NLC was determined by X-ray diffraction according to the AOCS Cj 2-95 method (AOCS, 2009). The analyses were performed at 25 °C in a Philips PW 1710 diffractometer (PANalytical, Almelo, Netherlands) using the Bragg-Brentan geometry (θ: 2θ) with Cu-Kα radiation (λ=1.54056 Å, voltage of 40 KV, and current of 30 mA). The measurements were obtained with 0.02° steps in 2θ and an acquisition time of 2 s, with scans from 5 to 40° (2θ scale). The polymorphic form was identified based on the interplanar distances of the crystals (Schenk & Peschar, 2004).

6.2.2.2.7 Entrapment efficiency and loading capacity

The extraction and quantification of β-carotene incorporated into NLC were performed using two methods for comparative purposes. The first method was based on Oliveira et al. (2016) and involved a liquid-liquid extraction of the β-carotene incorporated into NLC. For this, 1 mL of aqueous dispersion containing the NLC was transferred to a glass tube protected from light, and 4 mL of ethanol were added, and the mixture was stirred in a vortex. The tubes were placed in a heating block and incubated at 80 °C for 30 min to promote the destabilisation of the particles. Next, 3 mL of hexane was added, and the tubes were vortexed and centrifuged for 5 min at 3,000 rpm for phase separation. The upper hexane phase was transferred to a volumetric flask and diluted with hexane to a known volume to ensure that the absorbance was within the reading range (200–800 nm). The absorbance was then read at 450 nm in a model SP-2000UV UV/VIS spectrophotometer (TECNAL, Brazil).

The second method involved direct quantification by separating the NLC from the aqueous dispersion through ultracentrifugation. The aqueous dispersion containing the NLC was placed in tubes and centrifuged at 20,000 rpm for 15 min in a high-speed refrigerated Avanti J-26 XPI centrifuge (Beckman Coulter), followed by drying in a Tecnal vacuum oven (Model TE-395) at 40 °C overnight. The methodology was based on that of Babazadeh et al. (2017) and Li et al. (2016), with modifications. The process was performed 48 h after producing NLC, with subsequent storage of the ultracentrifuged material at 25 °C. The ultracentrifuged material was weighed (known mass) in a volumetric flask, diluted in a known volume of hexane for subsequent reading of the absorbance at 450 nm in a model SP-2000UV UV/VIS spectrophotometer (TECNAL, Brazil).

For both methods, the EE of β-carotene in the NLC structures and the LC of the NLC were calculated according to equations 3 and 4, respectively (Nguyen et al., 2012).

$$EE \quad \frac{Incorporated\ Mlc}{Total\ Mlc} \qquad \text{(Equation 3)}$$

$$LC\ (\%) = \frac{Incorporated\ Mlc}{Total\ Mlp} \qquad \text{(Equation 4)}$$

Where: LC = loading capacity, in %; EE = entrapment efficiency, in %; *Total Mlc* = total mass of lipophilic component added to the lipid phase of the NLC; *Incorporated Mlc* = total mass of lipophilic component incorporated into the NLC; *Total Mlp* = total mass of lipid phase used for preparing the NLC.

6.2.2.3 Statistical analysis

All analytical determinations were performed in triplicate. The results were assessed with analysis of variance (ANOVA) and Tukey's test was used for comparing means at a level of significance of 5 % using STATISTICA 7.0 (StatSoft Inc, Tulsa, OK, USA).

6.3 Results

6.3.1 Particle size, polydispersity index and zeta potential

Table 2 shows the PS, PDI and ZP of NLC produced with different emulsifiers. Tween 80 promoted the production of NLC with a lower PS (< 201.33 nm) during the 60 days of storage. In contrast, NLC produced with WPI (W_β) had a PS > 340 nm, but without a significant increase ($p < 0.05$) during the considered period. NLC produced with SL (L_β) showed an intermediate PS (PS < 266.67nm) during the storage period. There was a significant increase ($p < 0.05$) in PS from 48 h to 7 days of storage for the NLC produced with Tween 80 (T_β NLC), but this nanostructure had a PS close to 200 nm at the end of the storage period. As for L_β NLC, there was also a significant increase ($p < 0.05$) in the PS from 48 h to 7 days of storage, followed by a reduction ($p < 0.05$) at 15 and 30 days, an increase ($p < 0.05$) at 45 days, and a reduction ($p < 0.05$) at 60 days, with a PS close to 210 nm at the end of the storage period.

The PDI was expressed in terms of the Span value (Table 2). Of the emulsifiers analysed in this study, WPI produced NLC with the lowest PDI, differing statistically from those of the other emulsifiers used in this study. T_β NLC showed the highest PDI, compared with the other carriers at 48 h, but there was a significant reduction ($p < 0.05$) in this parameter at the end of the storage period. L_β NLC showed intermediate PDI during the storage period, but

there was a significant increase in this parameter at the end of the storage period when this carrier presented a PDI value statistically similar ($p < 0.05$) to that of T_β NLC.

Table 2: Particle size (PS), polydispersity index (PDI) and zeta potential (ZP) of the β-carotene loaded nanostructured lipid carriers (NLC) evaluated after 48 h, 7 days, 15 days, 30 days, 45 days, and 60 days of production.

NLC/time	PS (nm)	PDI	ZP (mV)
48 h			
L_β	238.33±1.53^{aB}	1.96±0.03^{aB}	-58.83±1.14^{aB}
T_β	176.00±1.00^{aA}	2.62±0.02^{aC}	-24.17±0.49^{aC}
W_β	347.67±3.51^{Ac}	1.58±0.01^{aA}	-61.27±0.65^{Aa}
7 days			
L_β	266.67±3.06^{bB}	2.29±0.02^{bB}	-55.17±0.80^{abA}
T_β	194.67±4.93^{Ba}	2.31±0.02^{bB}	-24.37±1.89^{aB}
W_β	351.00±1.73^{Ac}	1.56±0.01^{Aa}	-60.43±3.40^{Aa}
15 days			
L_β	237.33±2.89^{aB}	2.26±0.03^{bcB}	-55.37±0.38^{aA}
T_β	201.00±3.00^{bA}	2.27±0.03^{bcB}	-26.53±1.06^{abB}
W_β	343.33±0.58^{aC}	1.50±0.00^{aA}	-57.33±1.69^{Aa}
30 days			
L_β	218.33±4.73^{Bc}	2.25±0.02^{bcB}	-56.80±1.31^{aB}
T_β	195.67±1.53^{Ab}	2.15±0.02^{dB}	-26.70±0.95^{abC}
W_β	346.33±4.51^{Ca}	1.55±0.08^{aA}	-62.17±1.29^{aA}
45 days			
L_β	232.00±7.00^{Ba}	2.16±0.08^{Bc}	-56.47±0.74^{Aa}
T_β	199.67±4.16^{Ab}	2.21±0.06^{Bcd}	-28.73±0.91^{Bb}
W_β	344.33±4.93^{Ca}	1.53±0.08^{Aa}	-57.53±1.17^{Aa}
60 days			
L_β	208.67±2.52^{Bc}	2.25±0.05^{Bbc}	-51.30±2.82^{Bb}
T_β	201.33±1.53^{Ab}	2.24±0.01^{Bbc}	-27.10±0.44^{Cab}
W_β	347.67±3.06^{Ca}	1.47±0.02^{Aa}	-57.10±1.31^{Aa}

*Average of three replicates ± Standard Deviation. $^{a-d}$ Different lower-case letters indicate significant difference ($p < 0.05$) related to the evaluation of each parameter (PS, PDI and ZP) in comparison to the time of storage of NLC (48 h, 7, 15, 30, 45, and 60 days after processing) for the same NLC. $^{A-C}$ Different capital letters indicate significant difference ($p < 0.05$) related to the evaluation of the same parameter (PS, PDI or ZP) at the same time of storage of NLC (48 h, 7, 15, 30, 45, and 60 days after processing) between the NLC.

This study found that all NLC had a ZP > -20 mV, and the use of different emulsifiers produced particles with different charges (Table 2). Of the emulsifiers used in the study, the use of WPI led to the production of NLC with the highest ZP values in the considered period (ZP > -57 mV), and these values were maintained ($p < 0.05$) during the 60 days. Although there was a significant reduction ($p < 0.05$) in the ZP of NLC produced with SL at the end of the storage period, this NLC showed intermediate values compared with other carriers, corresponding to ZP > -51 mV during the that period. The NLC produced using Tween 80 had the lowest ZP values ($p < 0.05$) among the NLC assessed in this study, but these values were > -24 mV during the considered period and showed no significant changes ($p < 0.05$) at the end of the 60 days.

6.3.2 *Physical stability*

The physical stability of the dispersion containing NLC was assessed during a period of 60 days, as described in item 6.2.2.2, using a Turbiscan® Lab. The operating principle of this equipment is based on the incidence of a light with a fixed wavelength (880 nm) on the cylindrical tube containing the sample. This was followed by vertical scanning every 40 µm, upwards and downwards, from the bottom to the top of the cylindrical tube, with the height H = 0 mm referring to the bottom of the measuring cell. The light beam can then be transmitted or backscattered, depending on the interaction of the light with the medium. The equipment quantifies the extent to which that light beam is deflected by the dispersed particles (Buron et al., 2004). The scans were performed at 48 h and at 7, 15, 30, 45, and 60 days after producing the NLC and the curves were superimposed on a graph illustrating the light backscattering profiles (ΔBS) to analyse the variations in ΔBS in predetermined periods for the same sample. The first reading of dispersions containing NLC (48 h) was carried out at time 00 d:00 h:00 m (baseline), represented in the graph by the royal blue colour, and the last reading at 60 days, represented by the red colour. The vertical axis corresponds to the percentage of backscattered light, while the horizontal axis represents the height of the cylindrical tube in which the samples were stored, with the height of 0 mm corresponding to the bottom of the tube.

The graphs corresponding to ΔBS variations of dispersions containing L_β NLC, T_β NLC, and W_β NLC are shown in Figure 1. These graphs show the instability or stability of dispersions containing NLC based on the scanning profiles obtained in the indicated periods. The occurrence of destabilisation and phase separation phenomena changes the interaction of the light beam with the medium, causing increase or decrease in ΔBS due to variations and differences in PS and particle migration. Compared with the baseline, positive ΔBS variations at the bottom of the tube (H = 0 mm) and negative at the top (H = 40 mm) indicate sample

sedimentation, while ΔBS variations in the middle of the tube (H = 20 mm) indicate flocculation or coalescence phenomena. Negative ΔBS variations at the bottom of the tube (H = 0 mm) and positive at the top (H = 40 mm), compared with the baseline, indicate creaming of the sample (Mengual et al., 1999).

This study found that NLC produced with different emulsifiers resulted in dispersions containing NLC with different ΔBS profiles over the storage period. For NLC dispersions to be considered physically stable, their ΔBS profiles should present a variation ≤ ± 10 % (Celia et al., 2009). Of all the emulsifiers, the NLC produced with Tween 80 showed ΔBS variations of < ± 10 % at the end of 60 days. The NLC produced with SL showed variations > ± 10 % after 15 days and those produced with WPI showed the same variation after 7 days of storage.

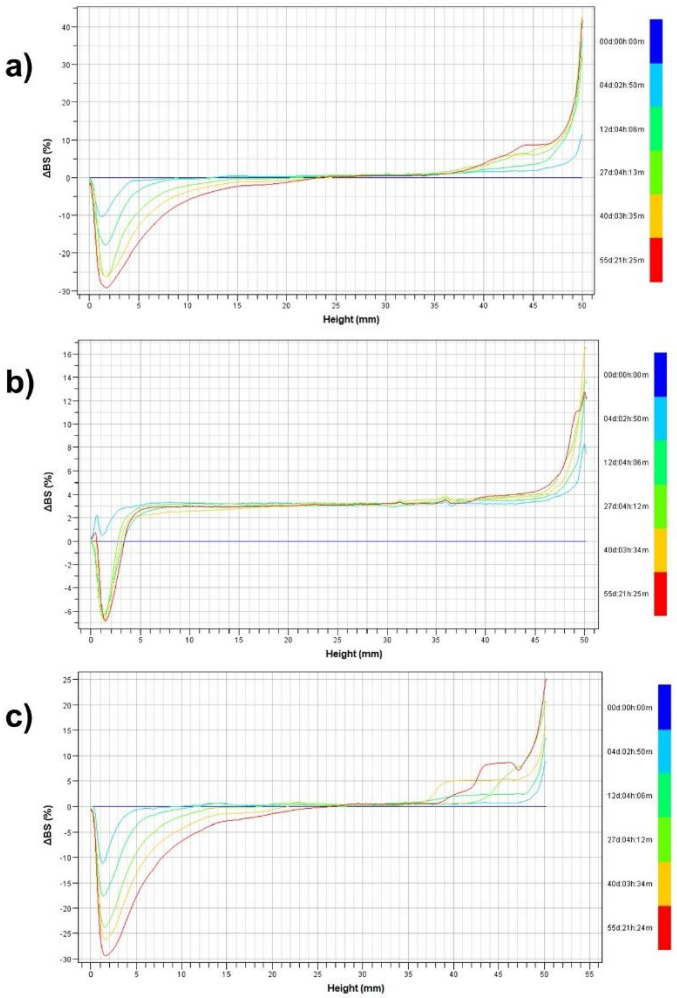

Figure 1: ΔBS variations of dispersions containing β-carotene loaded NLC. a) NLC L_β; obtained using enzymatically modified soy lecithin as emulsifier; b) NLC T_β, obtained using Tween 80 as emulsifier; c) NLC W_β, obtained using WPI as emulsifier.

6.3.3 *Solid Fat Content*

SFC values of the different β-carotene-loaded NLC samples are shown in Figure 2. At 25 °C, the SFC of NLC produced with different emulsifiers was generally > 65 % during the storage period. However, the SFC values varied with the different emulsifiers. The highest SFC was observed for T_β (> 85 %) during the storage period, which did not decrease significantly ($p < 0.05$) during the 60 days. The NLC produced with WPI showed SFC value similar to that of T_β NLC at 48 h, but there was a gradual and significant reduction ($p < 0.05$), which was 15 % lower at the end of 60 days, compared with the 48 h time-point. The SFC of the L_β NLC was significantly ($p < 0.05$) lower than those of all other NLC, approximately ranging from 65 to 75 %. The SFC of W_β NLC showed a gradual and significant reduction over the storage period.

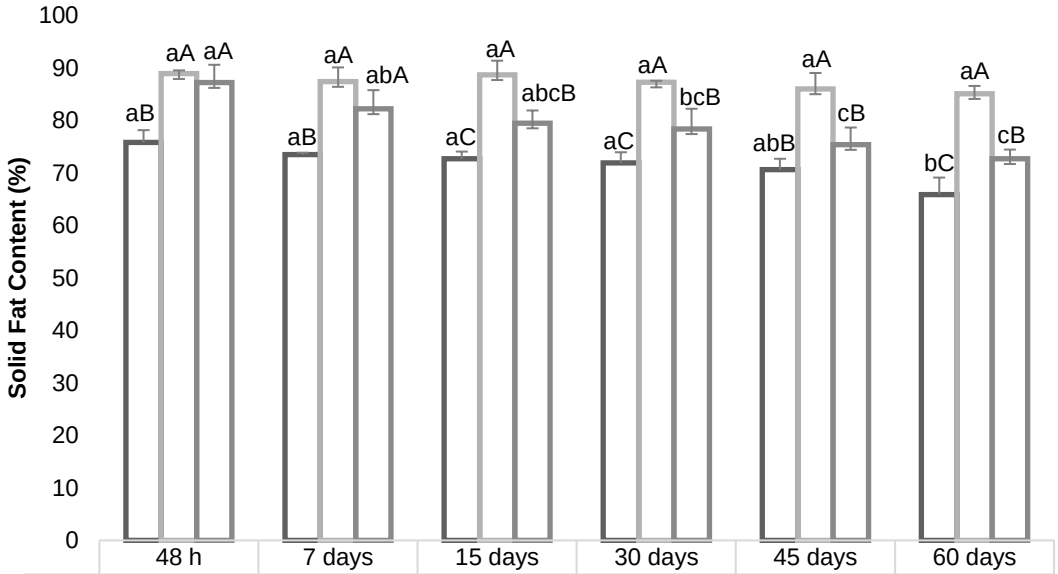

	48 h	7 days	15 days	30 days	45 days	60 days
Lβ	75.8	73.5	72.7	71.9	70.6	65.9
Tβ	88.9	87.4	88.7	87.3	86	85.1
Wβ	87.2	82.2	79.5	78.4	75.4	72.7

Figure 2: Solid fat content (%) at 25°C of β-carotene loaded NLC. Errors bars represent the standard deviation of n= 3 replicates. $^{A-C}$ Different capital letters indicate significant difference between NLC at the same time of storage ($p< 0.05$). $^{a-b}$ Different lower-case letters indicate significant difference in comparison to the time of storage of NLC ($p< 0.05$) for the same NLC.

6.3.4 *Thermal behavior during melting*

Table 3 presents the parameters related to the thermal behavior of β-carotene-loaded NLC during melting, namely melting onset temperature (Tmo), melting peak temperature (Tmp), melting offset temperature (Toff m), and melting enthalpy (ΔH).

Table 3. Thermal parameters of melting behavior of β-carotene loaded NLC.

NLC	Time of storage	Tmo (°C)	Tmp(°C)	Toff m (°C)	∆H (J/g)
	48 h	56.61±1.12	63.30±1.57	67.56±1.24	7.14±1.29
	7 days	56.98±2.53	63.20±1.34	67.63±1.36	7.30±1.20
L_β	15 days	57.12±0.89	63.30±0.96	67.37±2.02	6.88±0.75
	30 days	57.28±1.56	63.48±1.22	68.34±1.63	7.32±1.15
	45 days	57.38±1.45	63.46±1.78	69.12±1.38	7.58±1.35
	60 days	56.89±1.89	63.62±1.90	69.23±1.14	7.55±1.12
	48 h	56.80±1.75	63.32±0.78	67.20±0.85	6.79±0.45
	7 days	57.27±1.25	63.28±0.77	68.42±1.81	7.59±0.78
T_β	15 days	57.10±0.88	62.16±0.74	67.66±0.72	5.79±0.85
	30 days	57.52±0.79	63.64±1.62	69.20±1.15	6.96±0.45
	45 days	56.80±0.75	63.45±1.25	68.44±0.75	9.38±0.75
	60 days	57.92±1.32	64.29±1.42	68.98±0.98	9.44±0.95
	48 h	60.53±1.20	64.01±2.02	67.60±1.02	6.64±1.45
	7 days	57.04±1.35	63.66±1.52	67.68±0.85	7.58±1.60
W_β	15 days	56.94±1.32	63.59±1.64	67.32±1.28	7.52±1.15
	30 days	56.69±1.10	63.70±0.65	68.18±2.05	7.99±0.98
	45 days	56.30±0.98	63.76±1.40	68.13±1.32	8.52±1.25
	60 days	56.87±1.25	64.06±1.75	68.65±1.65	8.20±1.28

Tmo: melting onset temperature; **Tmp:** melting peak temperature; **Toff m:** melting offset temperature; ∆**H**: melting enthalpy. Average of three replicates ± Standard Deviation

All NLC samples analysed in this study had only one melting peak. The Tmo of L_β NLC, T_β NLC, and W_β NLC was within the range of 56.61–57.38 °C, 56.80–57.92 °C, and 56.30–60.53 °C, respectively. The Toff m for this same NLC sequence was within the range of 67.56–69.23 °C, 67.20–69.20 °C, and 67.32–68.65 °C, respectively. Moreover, the Tmp of this NLC sequence were in the range of 63.20–63.62 °C, 62.16–64.29 °C, and 63.59–64.06 °C, respectively.

6.3.5 Polymorphism

Table 4 shows the short spacings, peak intensities, and polymorphic forms of β-carotene-loaded NLC samples (L_β, T_β, and W_β). The polymorphic forms exhibited characteristic peaks. The α form showed a single peak at 4.15 Å, while the β' form was characterised by two short spacings (3.8 Å and 4.2 Å) and the β form by a relatively high intensity interplanar

distance at 4.6 Å and low intensity short spacings at 3.6 and 3.8 Å (Marangoni & Rousseau, 2002). The use of different emulsifiers to produce NLC did not affect the polymorphic habit of the obtained particles. The L_β, T_β, and W_β NLC showed the same proportion of β' and β polymorphic forms, which are characterised by short spacings at 4.6, 3.8, and 3.7 Å (polymorph β) and 4.2 and 3.8 Å (polymorph β'). This study also found that the polymorphic forms observed from 48 h (β' and β) were maintained during the storage period, indicating that no NLC presented late polymorphic transitions.

Table 4: Polymorphic forms, short spacings and peak intensities of the diffractograms obtained for β-carotene loaded NLC during 60 days of storage.

NLC	Time of storage	*Short spacings (nm)*					
		4.6	**4.1**	**4.2**	**3.8**	**3.6**	**Polymorphic form**
L_β	48 h	4.7 (vs)	-	4.2 (m)	3.8 (m)	3.6 (w)	β' + β
	7 days	4.7 (s)	-	4.2 (s)	3.8 (m)	3.6 (w)	β' + β
	15 days	4.7 (vs)	-	4.2 (vs)	3.8 (m)	3.6 (m)	β' + β
	30 days	4.7 (vs)	-	4.2 (m)	3.9 (m)	3.6 (m)	β' + β
	45 days	4.6 (m)	-	4.2 (m)	3.8 (m)	3.6 (m)	β' + β
	60 days	4.7 (vs)	-	4.2 (m)	3.9 (m)	3.6 (m)	β' + β
T_β	48 h	4.7 (s)	-	4.2 (s)	3.8 (m)	3.6 (m)	β' + β
	7 days	4.7 (s)	-	4.2 (s)	3.8 (m)	3.6 (w)	β' + β
	15 days	4.6 (vs)	-	4.2 (s)	3.9 (m)	3.7 (m)	β' + β
	30 days	4.7 (vs)	-	4.2 (m)	3.9 (s)	3.6 (m)	β' + β
	45 days	4.6 (m)	-	4.2 (m)	3.8 (s)	3.7 (m)	β' + β
	60 days	4.7 (vs)	-	4.2 (m)	3.9 (m)	3.7 (m)	β' + β
W_β	48 h	4.6 (w)	-	4.2 (w)	3.8 (vw)	3.6 (w)	β' + β
	7 days	4.6 (s)	-	4.2 (s)	3.8 (m)	3.6 (m)	β' + β
	15 days	4.7 (s)	-	4.2 (m)	3.8 (m)	3.7 (m)	β' + β
	30 days	4.6(s)	-	4.2 (m)	3.8 (m)	3.6 (m)	β' + β
	45 days	4.6 (m)	-	4.2 (vw)	3.8 (s)	3.7 (w)	β' + β
	60 days	4.7 (s)	-	4.2 (m)	3.9 (m)	3.7 (m)	β' + β

Intensities: **v.** very; **w.** weak; **m.** medium; **s.** strong.

6.3.6 *Entrapment efficiency and loading capacity of β-carotene*

Table 5 presents the LC and EE of β-carotene for all NLC determined by liquid-liquid extraction (Method 1). For this extraction method, the NLC produced with SL as emulsifier showed higher values for both parameters, compared with NLC produced using Tween 80 and WPI. The LC of the NLC ranged from 0.03 to 0.50 % and the EE from 6.09 to 100.25 % during the 60 days of storage. Table 5 also shows that the LC and EE of NLC separated by ultracentrifugation (Method 2) ranged from 1.77 to 5.23 % and from 35.32 to 104.53 %, respectively. For this extraction method, the NLC produced with Tween 80 as emulsifier showed higher values for both parameters. Moreover, these parameters decreased during the storage period for all the NLC samples, which can be attributed to the degradation of the lipophilic component incorporated into the structure.

Table 5: Entrapment efficiency (EE) and loading capacity (LC) of the β-carotene loaded nanostructured lipid carriers (NLC) considering the extraction through two distinct methods (MI and MII).

NLC/time	EE (%)	LC (%)	EE (%)	LC (%)
48 h	**MI**		**MII**	
L_β	14.28±2.82^{aA}	0.07±0.01^{aA}	91.26±2.14^{aA}	4.62±0.11^{aA}
T_β	12.30±2.19^{Aa}	0.06±0.01^{aAB}	104.53±2.48^{aA}	5.23±0.34^{aA}
W_β	5.86±1.72^{aB}	0.03±0.01^{aB}	68.75±0.55^{aB}	3.44±0.68^{acB}
7 days	**MI**		**MII**	
L_β	30.44±2.74^{aA}	0.15±0.01^{aA}	98.01±1.31^{aA}	4.87±0.07^{aA}
T_β	24.10±3.24^{aB}	0.12±0.02^{aB}	93.88±6.13^{aA}	4.69±0.71^{aA}
W_β	6.68±0.51^{aC}	0.03±0.00^{bC}	92.33±3.26^{bA}	4.62±0.16^{Ba}
15 days	**MI**		**MII**	
L_β	28.35±4.95^{aA}	0.14±0.02^{aA}	76.54±3.63^{bA}	3.83±0.18^{bA}
T_β	16.49±1.41^{aB}	0.08±0.01^{aB}	86.81±0.99^{aB}	4.34±0.05^{aB}
W_β	6.54±1.01^{aC}	0.03±0.01^{aC}	81.85±4.32^{bcAB}	4.09±0.22^{abAB}
30 days	**MI**		**MII**	
L_β	100.25±4.58^{bA}	0.50±0.02^{bA}	56.23±2.93^{cA}	2.89±0.75^{cA}
T_β	56.57±2.88^{bB}	0.28±0.10^{bB}	61.15±1.57^{bA}	3.06±0.08^{bA}
W_β	8.21±0.64^{aC}	0.04±0.00^{aC}	69.43±2.36^{acB}	3.47±0.12^{acB}
45 days	**MI**		**MII**	
L_β	22.99±4.32^{aA}	0.11±0.02^{aA}	49.23±3.36^{dA}	2.45±0.17^{dA}
T_β	14.08±3.02^{aB}	0.07±0.02^{aB}	53.48±6.09^{bcA}	2.67±0.30^{bA}
W_β	5.76±0.90^{aC}	0.03±0.00^{aC}	49.50±6.71^{adA}	2.47±0.55^{cdA}
60 days	**MI**		**MII**	
L_β	23.27±6.93^{AaA}	0.12±0.09^{aA}	38.65±0.78^{eA}	1.95±0.04^{eA}
T_β	11.51±1.49^{aA}	0.06±0.01^{aA}	38.82±0.32^{cA}	1.94±0.16^{cA}
W_β	6.09±0.74^{aA}	0.03±0.00^{aA}	35.32±0.46^{dA}	1.77±0.02^{dA}

MI: liquid-liquid extraction of β-carotene incorporated into NLC; **MII:** separation of NLC from aqueous dispersion by ultracentrifugation. Average of three replicates ± Standard Deviation. $^{a-e}$ Different lower-case letters indicate significant difference ($p< 0.05$) related to the evaluation of each parameter (IE and LC) in comparison to the time of storage of NLC (48 h, 7, 15, 30, 45, and 60 days after processing) for the same NLC and the same extraction method. $^{A-C}$ Different capital letters indicate significant difference ($p< 0.05$) related to the evaluation of the same parameter (EE or LC) at the same time of storage of NLC (48 h, 7, 15, 30, 45, and 60 days after processing) between the NLC.

6.4 Discussion

The composition, structure, and surface properties of lipid nanoparticles have a major impact on the functional performance of foods and beverages, as well as on their biological potential after ingestion. The surface of nanoparticles typically consists of a mixture of molecules and ions with different structures, orientations, properties, and interaction (McClements, 2013). The most important parameters for characterising lipid nanoparticles are the PS and size distribution, ZP, polymorphism, degree of crystallinity, LC, and IE of the bioactive compound (Ghasemiyeh & Mohammadi-Samani, 2018).

Among other factors, the PS is strongly affected by the production method. The high-pressure homogenisation (HPH) method is the most used method for NLC production, and PS is influenced by several factors, including the type of lipid matrix and the complete miscibility between them, the solubility of bioactive compounds in the lipid phase, and the type of emulsifier (Tamjidi et al., 2013). This study assessed the influence of three different emulsifiers (SL, Tween 80, and WPI) in the production of β-carotene-loaded NLC.

Due to the nature of the emulsion in NLC, the emulsifier should rapidly adsorb to the droplet surface to reduce interfacial tension, consequently reducing particle aggregation and destabilisation. Furthermore, the rapid adsorption of the emulsifier to the oil/water interface reduces the undesirable crystalline forms of nanoparticles (Mohammadi et al., 2019). In this study, NLC was produced by the HPH method, a process known to induce a rapid adsorption of emulsifiers after the disruption of oil droplets (Jafari et al., 2008). In this case, the emulsifier adsorption rate should be higher than the particle fragmentation rate to achieve full coating of all particles (Lee et al., 2013).

In this study, the use of different emulsifiers resulted in the production of NLC with varied dimensions (Table 2). This variation in PS can be largely attributed to the molecular and structural characteristics of each emulsifier and their interaction with the lipid phase and the bioactive compound incorporated into it. Emulsifiers with small molecular size, such as Tween 80, are more effective for producing smaller particles because they can quickly adsorb to the droplet surfaces during homogenisation, rapidly lower surface tension, and completely coat the particles, thereby preventing coalescence (Donsì et al., 2012; Lee et al., 2013). This explains that the smallest dimensions in this study were observed for T_{β} NLC (Table 2). Moreover, emulsifiers based on biopolymers, such as WPI, have a larger molecular size, and, therefore, adsorb to droplet surfaces slowly, and hence, they are less efficient in producing particles with small dimensions during homogenisation (Chang et al., 2015; Charoen et al., 2011). In addition, the beneficial properties of emulsifiers with larger molecular size, such as proteins, can change during the production of NLC, such as during hot HPH (Katouzian et al., 2017). Of the analysed emulsifiers, the SL produced NLC with intermediate dimensions, with

PS < 266.67 nm during the 60 days of storage (Table 2). These results can be mainly attributed to the similarity of the chemical structure of this emulsifier to that of the lipid phase and its intermediate molecular weight, which caused an effective interaction with the lipid components and sufficient particle coating rate during HPH.

The entrapment of β-carotene into NLC structures promoted a significant increase in PS for L_β and W_β NLC, while T_β NLC had similar dimensions to those of the nanostructure containing no bioactive compound (Lüdtke et al., 2021a). Although PS increased in L_β NLC, the PS values during the period considered in this study ranged from 208.67 to 266.67 nm (Table 2). In the case of W_β NLC, the entrapment of β-carotene into the structure promoted an increase of approximately 90 nm in PS, with unloaded NLC presenting a PS of approximately 260 nm in our earlier study (Lüdtke et al., 2021a) and of approximately 350 nm in the present study (Table 2). The increase in PS with the entrapment of β-carotene into the structure may have occurred due to an increase in interfacial tension and viscosity of the dispersed lipid phase with the solubilisation of the bioactive compound, which impaired size reduction during homogenisation (Tamjidi et al., 2014).

Similar results have been reported by studies that assessed the effect of incorporating carotenoids into NLC structures on PS. Tamjidi et al. (2014) characterised NLC with and without incorporating astaxanthin and found that the entrapment of the bioactive compound increased the PS of NLC, compared with that of empty NLC. Okonogi & Riangjanapatee (2015) performed the physicochemical characterization of NLC produced by HPH with different amounts of lycopene (5, 25, or 50 mg), Eumulgin SG (1 %), orange wax, and rice bran oil. The entrapment of the bioactive compound into the NLC structure promoted a small increase in PS, and this was proportional to the amount of lycopene incorporated into NLC. Zardini et al. (2018) characterised lycopene-loaded NLC, which was produced with a combination of high-shear and ultrasonic homogenisation methods, using MCT, glyceryl monostearate, and distearate as lipid matrices, and Tween 80 and SL together as emulsifiers. The authors found that the PS of lycopene loaded NLC was significantly higher than that of unloaded NLC.

The PDI is a direct measure of PS distribution, and it allows the determination of the degree of homogeneity of the assessed particles. Low PDI values indicate the production of homogeneous and poorly polydispersed NLC, while higher values suggest the heterogeneity of the particles. Particles with low PDI values are stable during storage (Lakshmi & Kumar, 2010). WPI, one of the emulsifiers analysed in this study, resulted in the production of NLC with the lowest PDI values, which differed statistically ($p < 0.05$) from the other emulsifiers used in this study (Table 2). Despite this difference between NLC produced with different emulsifiers, all NLC had a PDI < 2.5, indicating homogeneous particles and a narrow PS distribution of the system (Schaffazick et al., 2003).

ZP is directly related to particle aggregation or repulsion, and hence, it measures the particle surface charge and indicates the stability of the system during storage (Mohammadi et al., 2019). It reflects the repulsion force between charged particles; a minimum ZP of │30 mV│ is normally required to achieve good stability for an electrostatically stabilised nanosuspension. However, a ZP of │20 mV│ is sufficient to achieve the stability of nanosuspensions with a combination of electrostatic and steric forces as coating the particles with a hydrophilic emulsifier can further improve the stability of NLC by hydration in the surface layer (Tamjidi et al., 2014).

The use of different emulsifiers produced particles with different charges ($p < 0.05$) (Table 2). These charges are determined by the composition and structural conformation of the molecules of the emulsifier. The charges of nanoparticles can be attributed to the presence of ionised constituents on their surfaces, such as ionic emulsifiers, proteins, and phospholipids (McClements, 2007). In the case of L_β NLC, the presence of charges is mainly due to the presence of SL, an amphoteric lipophilic emulsifier of high molecular weight and negative charge at neutral pH conditions (Soleimanian et al., 2019). In the case of Tween 80, the negative ZP can be attributed to the hydroxyl groups present in the structure of the emulsifier (Tamjidi et al., 2013). Unlike polysorbates, proteins are charged molecules, and hence, they tend to organise by exposing their charged fractions to the outside when at the lipid interface, while their hydrophobic fractions interact with the lipid phase (Oliveira et al., 2016). In general, all the emulsifiers analysed in this study produced NLC with ZP > |20mV| (Table 2), which indicated adequate physical stability during the 60 days of storage due to electrostatic repulsion between particles, thus minimising any possible aggregation.

Lipid nanoparticles are thermodynamically unstable and heterogeneous systems, which usually tend to lose physical stability during storage (Huang et al., 2008). The NLC in this study remained suspended in dispersions; hence, the physical stability of the dispersions was also monitored because changes in the structural characteristics of the particles can change the physical stability of the entire system. Therefore, the stability of the dispersions containing the NLC was assessed using the light backscattering technique with a Turbiscan® Lab. This equipment can predict stability and monitor the destabilisation of dispersions, discriminating between particle migration (creaming or sedimentation), which is normally reversible with agitation, and PS variations (flocculation or coalescence) (Buron et al., 2004).

The ΔBS profiles, indicating destabilisation for dispersions with β-carotene, are shown in Figure 1. If 10 % is considered as an indication of the stability of the system (Celia et al., 2009), all dispersions containing NLC had creaming properties, corresponding to negative ΔBS variations at the bottom of the tube and positive variations at the top (Buron et al., 2004). However, the type of emulsifier used for stabilising NLC with β-carotene affected the physical stability of these nanostructures in dispersion. Of the emulsifiers analysed in this study, Tween

80 provided the most stable NLC dispersions during the 60 days of storage, with ΔBS variations of less than ± 10 % at the end of this period. The other emulsifiers used in this study provided less stable NLC dispersions. In general, NLC produced with SL and WPI showed ΔBS variations greater than ± 10 % after 15 days and after 7 days of storage, respectively, which indicated a more drastic destabilisation.

However, the physical stability results obtained with Turbiscan should be further supported with DLS analysis to assess the characteristics of NLC as particles. The different physical instability of NLC can be explained by their different structural characteristics. As earlier discussed, W_β NLC had the highest PS. Because smaller particles move faster due to Brownian motion leading to dispersion stability against gravity (Fathi et al., 2013), an increase in PS elevates the degree of turbidity of the system (Katouzian et al., 2017), and hence, the larger dimensions of this carrier can be associated with the ΔBS variations of the corresponding dispersion. In this case, the greater stability observed for T_β NLC, compared with that of L_β and W_β NLC, can be attributed to the smaller dimensions of the nanostructure during the 60 days of storage. Therefore, these results reinforce the effectiveness of Tween 80 to produce NLC on a smaller scale and with greater physical stability when contained in dispersions.

Although the ΔBS variations are indicative of creaming, normally associated with the movement of particles, and therefore, reversible with mechanical agitation (Buron et al., 2004), it is important to consider the destabilisation of the dispersions containing NLC as this can lead to degradation of the bioactive compound incorporated into NLC. In this regard, the destabilisation process performed during the storage period should be carefully selected and the most appropriate type of packaging (in dispersions, lyophilised) should be adopted.

SFC is directly related to the lipid crystallization process, and therefore, it is an indication of the degree of crystallinity of NLC. This study found that both scale reduction and the entrapment of bioactive compound did not decrease the crystallinity of the system. This is not consistent with the results of a previous study where the entrapment of β-carotene into the structure increased the crystallinity of the system as shown by the SFC (Figure 2), which was significantly higher compared with that of NLC produced without the compound (Lüdtke et al., 2021a). The 60:40 FHSO:HOSO (w/w) lipid system used to produce NLC contained 63.25 % of unsaturated FA. Figure 2 shows that the SFC values of all NLC samples was > 65 %, with significant differences ($p < 0.05$) between SFC at 25 °C for the NLC produced with different emulsifiers. Of the emulsifiers analysed in this study, Tween 80 provided the highest SFC values at 25 °C, which were > 85 %. The reduction in SFC ($p < 0.05$) for the L_β and W_β NLC was accompanied by a reduction in physical stability as determined by Turbiscan over the storage period.

Depending on its phospholipid composition, SL can act as a promoter or inhibitor of the fat crystallization process (Miskandar et al., 2006). Lecithins are surfactants obtained by extracting and purifying phospholipids from naturally occurring products, such as soy, canola, and eggs. The commercial soy lecithin is usually composed of a mixture of phospholipids and other substances, such as triacylglycerols (McClements, 2015). However, the SL used in this study was obtained by the hydroxylation of commercial lecithin through an enzymatic treatment that hydrolyses one of the glycerol-bound FA, thereby converting phosphatidylcholine (PC) into lysophosphatidylcholine (LPC) (Fernandes et al., 2012). Lecithins with nonpolar tail groups or lecithins with high concentrations of PC are usually more active in the nucleation of fat crystals. Conversely, lecithins mostly composed of polar tail groups, such as LPC, are poorly active in the nucleation and growth of crystals (Miskandar et al., 2006). Therefore, the lower SFC of L_β NLC can be explained by the anti-crystallising effect of SL, thereby yielding a lower number of crystals, and, consequently, reducing the crystallinity of the system.

The different polymorphic forms of NLC obtained with and without β-carotene (Lüdtke et al., 2021a) indicated that the entrapment of the bioactive compound interfered with the lipid crystallization process, explaining the higher SFC values of L_β, T_β, and W_β NLC. The high SFC of NLC with β-carotene can also be attributed to the crystallinity of this bioactive compound. The higher degree of crystallinity of T_β NLC (SFC > 85 %) did not lead to a lower LC and EE (Table 5), compared with those of other emulsifiers; hence, the high value can be attributed to the entrapment and maintenance of the bioactive compound in the structure.

As NLC must maintain their solid state during storage and under gastrointestinal tract (GIT) conditions (Mohammadi et al., 2019), it is crucial to assess their thermal behavior. Differential scanning calorimetry (DSC) is one of the most used analytical tools for providing information about the physical state of nanoparticles. The assessment is based on the measurement of enthalpy changes (heat released or absorbed) when a sample is subjected to a controlled temperature program (Qian et al., 2012; Shukat et al., 2012).

The DSC thermograms are widely used to assess the interaction between lipids and compounds incorporated into LN. The thermal behavior during melting and crystallization, melting and crystallization temperatures, enthalpy, and polymorphic transitions can be characterised through these graphs. The results obtained in this study demonstrated that the thermal behavior of NLC during melting was governed by the lipid matrix used to produce NLC that had the highest melting point. The thermal behavior of the carriers indicated the complete entrapment and solubilisation of β-carotene in the lipid matrices as there was only one melting peak. The melting curves of the NLC showed a single endothermic event around 60 °C, with the temperature corresponding to the melting of FHSO. There were no significant differences in the melting ranges of NLC produced with different emulsifiers, thereby indicating that the emulsifiers used in this study did not interfere in the thermal behavior of the carriers. The initial

melting temperature, the final melting temperature, and the peak maximum temperature of all NLC were in the range of 56.30–60.53 °C, 67.23–69.23°C, and 62.16–64.19 °C, respectively (Table 3).

The delivery of bioactive compounds in the GIT is a major challenge, mainly due to the unique physicochemical properties and physiological barriers, such as metabolism and gastrointestinal instability. Of all the GIT segments, the small intestine is the most efficient for the absorption of compounds, and this is mainly due to the presence of microvilli, which increases the surface area. Therefore, the release of the compound in the intestine is a prerequisite for its absorption (Ashkar et al., 2021). Therefore, an ideal nanostructured system for delivery should maintain its integrity up to the adsorption site, thereby allowing the compound to fulfil its biochemical and physiological function in the human body. The DSC confirmed that all carriers developed in this study (L_β, T_β and W_β NLC) remained solid at body temperature (37 °C), thus indicating that these NLC maintain their structural integrity during transit through the GIT and further reinforcing the potential of these nanostructures to increase the bioaccessibility of lipophilic bioactive compounds.

The thermal behavior of L_β, T_β and W_β NLC was different from that of the 60:40 HOSO : FHSO (w/w) lipid system when assessed on a macroscale (Lüdtke et al., 2021b). The 60:40 HOSO:FHSO (w/w) lipid system showed two melting events, corresponding to the melting temperature of the trisaturated triacylglycerols (TAG) of FHSO and the triunsaturated TAG of HOSO (Lüdtke et al., 2021b). Conversely, the NLC analysed in this study showed only one endothermic event, as earlier described. However, although the macro-to-nano scale reduction did not change the overall thermal behavior parameters of the lipid phase on a macroscale (Tmo, Toff m, and Tmp), the melting profiles were sensitive to the lipid mass concentration in the dispersion, which resulted in proportionally reduced enthalpy (ΔH) values.

In general, the entrapment of β-carotene into the NLC structure did not affect the initial, final, and peak maximum temperatures as determined by DSC (Lüdtke et al., 2021a). However, there was an increase in the energy required for melting (∆H J/g) in NLC with β-carotene, which can be attributed to the intrinsic crystallinity of this compound.

The degree of crystallinity of lipids and the polymorphic transitions of NLC are very important characteristics that directly affect the entrapment and release of bioactive compounds. Both characteristics are strongly dependent on the lipids used to produce the NLC (Mohammadi et al., 2019). The polymorphism is directly related to the crystallization temperature, which in turn depends on the composition of the nanosystem, the amount of bioactive compound that was incorporated, and the interactions among the ingredients of the LN (Rawal & Patel, 2018).

The lipid matrices used to produce the NLC in this study were FHSO and HOSO, which tend to stabilise crystals in the β polymorphic form for the strong homogeneity in FA and

triacylglycerols of the lipid raw materials. In addition to lipid materials, this study used emulsifiers and the bioactive compound, β-carotene, to produce NLC. The crystallization process refers to the spontaneous ordering of a lipid system, characterised by total or partial restriction of movement caused by chemical or physical interactions between triacylglycerol molecules. Different crystal structures result from different molecular packings. A crystal consists of molecules arranged in a fixed pattern known as a lattice (Sato, 2001). When molecules other than TAG are added to the lipid system, the arrangement of the molecules can change, which occur due to differences between the structural and chemical characteristics of these molecules and those of TAG. Table 4 shows that all NLC produced in this study had the β and β' polymorphic forms during the storage period. There were no differences between the polymorphic properties of NLC produced with different emulsifiers (SL, Tween 80, and WPI); hence, it was expected that the polymorphic characteristics of the different NLC samples would be similar.

However, the change in the polymorphic form of the particle can be attributed to the entrapment of β-carotene into the structure, as there was stabilisation in the β form from 48 h after production in NLC containing no β-carotene (Lüdtke et al., 2021a). Therefore, the change in the polymorphic form of the NLC caused by the entrapment of β-carotene can be explained by the structural dissimilarity of this bioactive compound with the other materials used in the production of the nanostructures. β-carotene was solubilised in the lipid phase of the NLC, which may have promoted an association with the TAG, as well as with the emulsifiers, thereby modifying the arrangement and recrystallization of the TAG during cooling.

In general, the different emulsifiers used in this study did not affect thermal resistance, nor the polymorphic property of the NLC, as there were no significant differences between the L_β, T_β, and W_β NLC. The polymorphic property of the NLC in this study was different from that shown by the lipid system used to produce NLC when assessed on a macroscale (Lüdtke et al., 2021b). On a macroscale, the 60:40 FHSO:HOSO (w/w) lipid system had the β'+ β polymorphic forms up to 15 days of storage, and there was a polymorphic transition to the more stable form after that period, thereby showing stabilisation in the β polymorphic form (Lüdtke et al., 2021b). As earlier discussed, all NLC in this study showed stabilisation in the β'+ β polymorphic forms during the 60 days of stabilisation. In this case, the stabilisation time had no effect on polymorphism, indicating that the NLC did not show late polymorphic transition, which is desirable for the entrapment of bioactive compounds. This is because polymorphic changes can be followed by changes in particle shape, consequently leading to the expulsion of the compound incorporated into the structure.

A delivery system based on nanoparticles should present several characteristics to be considered suitable for the entrapment of bioactive compounds, and high LC and IE are among those characteristics. LC is defined as the capacity of the delivery system to

accommodate bioactive compounds into its structure, and it is typically calculated considering the amount of entrapped bioactive compound in relation to the amount of lipid material (Mohammadi et al., 2019). This parameter can range from 0 (low) to 100 % (high) depending on the nature of the active ingredient and carrier nanoparticles, as well as the conditions used to obtain the nanoparticles (McClements & McClements, 2016).

The chemical stability of bioactive compounds entrapped into NLC is assessed by determining the EE during storage (Mohammadi et al., 2019). EE is defined as the percentage of active ingredient that is effectively entrapped into carrier nanoparticles rather than the surrounding fluid (McClements & McClements, 2016), and it is one of the key factors to assess the ability of delivery systems to retain bioactive compounds in their structure (Babazadeh et al., 2017).

The amount of active compound inside and outside nanoparticles in a delivery system can only be determined after isolating nanoparticles from the surrounding environment. There are several approaches to isolate nanoparticles from the surrounding matrix, such as dialysis, filtration, gravitational separation, and centrifugation. The concentration of the bioactive compound in nanoparticles can be measured using appropriate analytical tools, such as chromatography, electrophoresis, and spectroscopy (McClements & McClements, 2016).

This study assessed two distinct methods for isolating the bioactive compound. The first method consisted of a methodology described by Oliveira et al. (2016), which is based on the liquid-liquid extraction of β-carotene incorporated into NLC. Oliveira et al. (2016) reported difficulties in determining free β-carotene from NLC into which β-carotene has been incorporated because the nanoparticles precipitated together with the free form of the bioactive compound. This study had similar challenges when using this method for the separation of the bioactive compound incorporated into the structure, resulting in very low values of LC and EE, as shown in Table 5. Moreover, the quantification of β-carotene was low as early as from 48 h after production, which indicates that the values were probably low due to separation problems and not due to degradation of the compound.

The second method was based on the direct quantification of the incorporated β-carotene through the separation of the NLC from the aqueous dispersion by ultracentrifugation. This approach involves the use of a centrifugal force that is used to accelerate the movement of particles, precipitating and separating them from the aqueous fraction (McClements & McClements, 2016). It was possible to quantify the β-carotene in the ultracentrifuged fraction using this method, which was considered in this study as the loaded NLC.

A crucial factor to assess the suitability of a lipid carrier for a given compound is the LC of the nanocarrier. Factors that affect this LC include the solubility of the compound in the melted lipid and the degree of crystallinity of this lipid (Maiti et al., 2016). Considering the values obtained in this study after separating the NLC from the aqueous dispersion by

ultracentrifugation (Method II), Tween 80 produced NLC with the highest LC and EE values during the 60 days of storage, followed by the NLC produced with SL and WPI, as shown in Table 5. Moreover, there was degradation of the lipophilic component incorporated into the NLC during the storage period, corresponding to a significant reduction ($p < 0.05$) in LC and EE, which should be considered for the use of these nanostructures in food.

The LC and EE values obtained after quantification with Method II are in line with the results already reported in the literature, which explored the extraction and quantification of β-carotene using different methods. Pan et al. (2016) analysed the EE of NLC with β-carotene prepared by mixing different proportions of low- and high-melting-point lipids (10 : 90, 30 : 70, 50 : 50, and 70 : 30 of liquid : solid). The authors found that the amount of loaded β-carotene increased as the liquid lipid content increased, and the EE reached values close to 100 % in NLC with higher liquid-lipid content. Zardini et al. (2018) studied the EE and LC of NLC with lycopene, a carotenoid naturally found in plant sources. The authors reported that the EE of lycopene ranged from 64.79 to 78.89 %, whereas the LC ranged from 4.54 to 5.52 %. Pezeshki et al. (2019) developed NLC with β-carotene with different proportions of solid and liquid lipid matrices (2 : 1, 4 : 1, and 10 : 1 of solid lipid : liquid lipid) and emulsifier (1 %, 2 %, 3 %, and 4 %). The EE of β-carotene in the optimised NLC formulation with a concentration of 2 % emulsifier was approximately 97 %. Rohmah et al. (2020) assessed the EE of β-carotene in NLC by separating the NLC from the dispersion through ultracentrifugation. The optimised NLC formulation was obtained using stearin and palm olein as lipid matrices and Tween 80 as emulsifier, with an EE of approximately 91.2 %.

In this study, the LC and EE values of the same NLC sample varied according to the method used for β-carotene extraction. The values obtained after extraction using Method I indicated that this method was not suitable for separating β-carotene incorporated in NLC from free β-carotene. The LC and EE values for L_β, T_β and W_β NLC using this method were very low and varied during the storage period, indicating that this method did not reflect the changes in the dispersions and NLC that occurred over time. The LC and EE values found with Method II showed that the separation of NLC from dispersions by ultracentrifugation was more appropriate in this study for isolating β-carotene incorporated into NLC from free β-carotene. Therefore, this method reflected the characteristics observed for NLC more accurately through the analytical determinations previously mentioned. The LC and EE values were not only higher than the values obtained with Method I but there was a significant and expected decrease in these parameters over the storage time, which was related to the degradation of β-carotene incorporated into NLC. Therefore, based on the results of this study, separating NLC from dispersions by ultracentrifugation is an appropriate method for the extraction and quantification of β-carotene incorporated into NLC.

6.4 Conclusion

The melting range of the NLC produced with different proportions of FHSO and HOSO is in the appropriate range for incorporation into foods, with a peak maximum temperature above body temperature and no significant differences for the different emulsifiers used in this study (SL, Tween 80, and WPI). There were also no differences among the polymorphic properties of NLC produced with the different emulsifiers. However, the entrapment of β-carotene influenced the polymorphic property of NLC, as the lipid components used to produce the NLC preferentially stabilised in the β form, while the NLC produced in this study stabilised in the β and β' forms.

Although the use of different emulsifiers produced particles with different charges, all NLC showed a ZP > |20 mV|. Regarding PS, of all the emulsifiers used in this study, WPI produced the β-carotene-loaded NLC with the largest dimension. This emulsifier also produced NLC with lower physical stability, as determined by Turbiscan and lower EE and LC of the lipophilic bioactive compound. Moreover, the use of Tween 80 and SL produced NLC with lower PS, lower polydispersity, and higher EE and LC values. According to Turbiscan, the physical stability of NLC produced with Tween 80 was considerably higher than the stability of NLC produced with the other emulsifiers used in this study.

As for the two methods analysed in this study for extraction and quantification of β-carotene incorporated into NLC, separating the NLC from the aqueous phase by ultracentrifugation was more effective. However, the development of new methodologies for an adequate separation of NLC has become increasingly necessary.

This study showed, above all, the potential of NLC produced with lipid matrices, widely available in the oil and fat industry, for the loading of lipophilic bioactive compounds. In this regard, FHSO and HOSO proved to be suitable as high-and low- melting-point lipid matrices, respectively, for the development of lipid nanoparticles loaded with β-carotene.

6.5 Acknowledgments

Fernanda Luisa Lüdtke thanks FAPESP (grants # 18/03172-0, # 19/05176-6, #16/11261-8 and 19/27354-3, São Paulo Research Foundation -FAPESP). Ana Paula Badan Ribeiro thanks CNPq (303429/2018-6) for the productivity grant.

6.6 References

AOCS. American Oil Chemists' Society. (2009). *Official methods and recommended practices of the American Oil Chemists' Society* (Issue 6ed).

Ashkar, A., Sosnik, A., & Davidovich–Pinhas, M. (2021). Structured edible lipid–based particle systems for oral drug–delivery. In *Biotechnology Advances*. Elsevier Inc. https://doi.org/10.1016/j.biotechadv.2021.107789

Assadpour, E., & Jafari, S.M. (2019). A systematic review on nanoencapsulation of food bioactive ingredients and nutraceuticals by various nanocarriers. *Critical Reviews in Food Science and Nutrition*, *59*(19), 3129–3151. https://doi.org/10.1080/10408398.2018.1484687

Attama, A.A., Momoh, M.A., & Builders, P.F. (2012). Lipid Nanoparticulate Drug Delivery Systems: A Revolution in Dosage Form Design and Development. *Recent Advances in Novel Drug Carrier Systems* (pp. 107–140). InTech. https://doi.org/10.5772/50486

Averina, E. S., Müller, R. H., Popov, D. v., & Radnaeva, L. D. (2011). Physical and chemical stability of nanostructured lipid drug carriers (NLC) based on natural lipids from Baikal region (Siberia, Russia). *Pharmazie*, *66*(5), 348–356. https://doi.org/10.1691/ph.2011.0326

Babazadeh, A., Ghanbarzadeh, B., & Hamishehkar, H. (2017). Formulation of food grade nanostructured lipid carrier (NLC) for potential applications in medicinal–functional foods. *Journal of Drug Delivery Science and Technology*, *39*, 50–58. https://doi.org/10.1016/j.jddst.2017.03.001

Brito–Oliveira, T. C., Molina, C. V., Netto, F. M., & Pinho, S. C. (2017). Encapsulation of Beta–carotene in Lipid Microparticles Stabilized with Hydrolyzed Soy Protein Isolate: Production Parameters, Alpha–tocopherol Coencapsulation and Stability Under Stress Conditions. *Journal of Food Science*, *82*(3), 659–669. https://doi.org/10.1111/1750–3841.13642

Buron, H., Mengual, O., Meunier, G., Cayré, I., & Snabre, P. (2004). Optical characterization of concentrated dispersions: applications to laboratory analyses and on–line process monitoring and control. *Polymer International*, *53*(9), 1205–1209. https://doi.org/10.1002/pi.1231

Celia, C., Trapasso, E., Cosco, D., Paolino, D., & Fresta, M. (2009). Turbiscan Lab® Expert analysis of the stability of ethosomes® and ultradeformable liposomes containing a bilayer fluidizing agent. *Colloids and Surfaces B: Biointerfaces*, *72*(1), 155–160. https://doi.org/10.1016/j.colsurfb.2009.03.007

Cerqueira, M. A., Pinheiro, A. C., Silva, H. D., Ramos, P. E., Azevedo, M. A., Flores–López, M. L., Rivera, M. C., Bourbon, A. I., Ramos, Ó. L., & Vicente, A. A. (2014). Design of Bio–nanosystems for Oral Delivery of Functional Compounds. *Food Engineering Reviews*, *6*(1–2),1–19. https://doi.org/10.1007/s12393–013–9074–3

Chang, C., Tu, S., Ghosh, S., & Nickerson, M. T. (2015). Effect of pH on the inter–relationships between the physicochemical, interfacial and emulsifying properties for pea, soy, lentil and canola protein isolates. *Food Research International*, *77*, 360–367. https://doi.org/10.1016/j.foodres.2015.08.012

Charoen, R., Jangchud, A., Jangchud, K., Harnsilawat, T., Naivikul, O., & McClements, D. J. (2011). Influence of Biopolymer Emulsifier Type on Formation and Stability of Rice Bran Oil–in–Water Emulsions: Whey Protein, Gum Arabic, and Modified Starch. *Journal of Food Science*, *76*(1). https://doi.org/10.1111/j.1750–3841.2010.01959.x

Chen, L., Remondetto, G. E., & Subirade, M. (2006). Food protein–based materials as nutraceutical delivery systems. *Trends in Food Science and Technology*, *17*(5), 272–283. https://doi.org/10.1016/j.tifs.2005.12.011

Das, N. M. A., Kobayashi, I., & Nakajima, M. (2020). Nanotechnology for bioactives delivery systems. *Journal of Food and Drug Analysis*, *20*(1), 184–188. https://doi.org/10.38212/2224–6614.2118

Donsì, F., Annunziata, M., Vincensi, M., & Ferrari, G. (2012). Design of nanoemulsion–based delivery systems of natural antimicrobials: Effect of the emulsifier. *Journal of Biotechnology*, *159*(4), 342–350. https://doi.org/10.1016/j.jbiotec.2011.07.001

Fathi, M., Varshosaz, J., Mohebbi, M., & Shahidi, F. (2013). Hesperetin–Loaded Solid Lipid Nanoparticles and Nanostructure Lipid Carriers for Food Fortification: Preparation, Characterization, and Modeling. *Food and Bioprocess Technology*, *6*(6). https://doi.org/10.1007/s11947–012–0845–2

Fernandes, G. D., Alberici, R. M., Pereira, G. G., Cabral, E. C., Eberlin, M. N., & Barrera–Arellano, D. (2012). Direct characterization of commercial lecithins by easy ambient sonic–spray ionization mass spectrometry. *Food Chemistry*, *135*(3), 1855–1860. https://doi.org/10.1016/j.foodchem.2012.06.072

Ghasemiyeh, P., & Mohammadi–Samani, S. (2018). Solid lipid nanoparticles and nanostructured lipid carriers as novel drug delivery systems: applications, advantages and disadvantages. *Research in Pharmaceutical Sciences*, *3*(4):288–303. https://doi.org/10.4103/1735–5362.235156.

Grune, T., Lietz, G., Palou, A., Ross, A. C., Stahl, W., Tang, G., Thurnham, D., Yin, S. A., & Biesalski, H. K. (2010). β–carotene is an important vitamin A source for humans. *Journal of Nutrition*, *40*(12), 2268S–2285S. https://doi.org/10.3945/jn.109.119024

Gunstone, F. D. (2011). Production and Trade of Vegetable Oils. In *Vegetable Oils in Food Technology* (6th ed., Vol. 2). Wiley-Blackwell. https://doi.org/10.1002/9781444339925.ch1

Hentschel, A., Gramdorf, S., Müller, R. H., & Kurz, T. (2008). β–Carotene–loaded nanostructured lipid carriers. *Journal of Food Science*, *73*(2). https://doi.org/10.1111/j.1750–3841.2007.00641.x

Huang, Z. R., Hua, S. C., Yang, Y. L., & Fang, J. Y. (2008). Development and evaluation of lipid nanoparticles for camptothecin delivery: A comparison of solid lipid nanoparticles, nanostructured lipid carriers, and lipid emulsion. *Acta Pharmacologica Sinica*, *29*(9), 1094–1102. https://doi.org/10.1111/j.1745–7254.2008.00829.x

Jafari, S. M., Assadpoor, E., He, Y., & Bhandari, B. (2008). Encapsulation efficiency of food flavours and oils during spray drying.*Drying Technology, 26*(7), 816–835. https://doi.org/10.1080/07373930802135972

Jafari, S. M., Paximada, P., Mandala, I., Assadpour, E., & Mehrnia, M. A. (2017). Nanoencapsulation Technologies for the Food and Nutraceutical Industries Encapsulation by nanoemulsions. In *Nanoencapsulation Technologies for the Food and Nutraceutical Industries*. https://doi.org/10.1016/B978–0–12–809436–5/00002–1

Katouzian, I., Faridi Esfanjani, A., Jafari, S. M., & Akhavan, S. (2017). Formulation and application of a new generation of lipid nano–carriers for the food bioactive ingredients. *Trends in Food Science and Technology, 68*, 14–25. https://doi.org/10.1016/j.tifs.2017.07.017

Kharat, M., & McClements, D. J. (2019). Fabrication and characterization of nanostructured lipid carriers (NLC) using a plant–based emulsifier: Quillaja saponin. *Food Research International*, *126*. https://doi.org/10.1016/j.foodres.2019.108601

Kumbhar, D. D., & Pokharkar, V. B. (2013). Engineering of a nanostructured lipid carrier for the poorly water–soluble drug, bicalutamide: Physicochemical investigations. *Colloids and Surfaces A: Physicochemical and Engineering Aspects*, *416*(1), 32–42. https://doi.org/10.1016/j.colsurfa.2012.10.031

Lakshmi, P., & Kumar, G. A. (2010). Nanosuspension technology: a review. *International Journal of Pharmacy and Pharmaceutical Sciences*, *4*, 35–40.

Lee, L. L., Niknafs, N., Hancocks, R. D., & Norton, I. T. (2013). Emulsification: Mechanistic understanding. *Trends in Food Science and Technology*, *31*(1), 72–78. https://doi.org/10.1016/j.tifs.2012.08.006

Li et al. (2016). Development and Validation of a Method for Determination of Encapsulation Efficiency of CPT-11/DSPE-mPEG2000 Nanoparticles. *Medicinal chemistry, 6*, 345–348.

Liu, C. H., & Wu, C. T. (2010). Optimization of nanostructured lipid carriers for lutein delivery. *Colloids and Surfaces A: Physicochemical and Engineering Aspects*, *353*(2–3), 149–156. https://doi.org/10.1016/j.colsurfa.2009.11.006

Liu, F., Wang, D., Sun, C., McClements, D. J., & Gao, Y. (2016). Utilization of interfacial engineering to improve physicochemical stability of β–carotene emulsions: Multilayer coatings formed using protein and protein–polyphenol conjugates. *Food Chemistry*, *205*, 129–139. https://doi.org/10.1016/j.foodchem.2016.02.155

Livney, Y. D. (2015). Nanostructured delivery systems in food: Latest developments and potential future directions. *Current Opinion in Food Science, 3*, 125–135. https://doi.org/10.1016/j.cofs.2015.06.010

Lüdtke, F.L., Grimaldi, R., Cardoso, L.P., Ribeiro, A.P.B. (2021b). Lipid systems based on fully hydrogenated soybean oil and high oleic sunflower oil to obtain nanostructured lipid carriers: composition, physical properties, and crystallization parameters. *To be submitted.*

Lüdtke, F.L., Stahl, M.A., Grimaldi, R., Cardoso, L.P., Gigante, M.L., Ribeiro, A.P.B. (2021a). High oleic sunflower oil and fully hydrogenated soybean oil nanostructured lipid carriers: development and characterization. *To be submitted.*

Lüdtke, F.L., Stahl, M.A., Zaia, B.G., Santos, V.S., Hashimoto, J.C., & Ribeiro, A.P.B. (2017). Evaluation of process parameters for obtaining nanostructured lipid carriers by high pressure homogenization.In: *17th AOCS LatinAmerican Congress and Exhibition on Fats, Oils, and Lipids*

Maiti, N. J., Dey, M., Barik, B., Malana, A., Dinda, A., & Patel, A. (2016). Effect of drug solubility and lipid carrier on drug release from nanostructured lipid carriers. *Biopharm Journal*, *03*, 87–97. www.biopharmj.com

Marangoni, A., & Rousseau, D. (2002). The Effects of Interesterification on the Physical Properties of Fats. In *Physical Properties of Lipids*. CRC Press. https://doi.org/10.1201/9780203909171.ch13

McClements, D. J. (2007). Critical review of techniques and methodologies for characterization of emulsion stability. *Critical Reviews in Food Science and Nutrition*, *47*(7), 611–649. https://doi.org/10.1080/10408390701289292

McClements, D. J. (2013). Utilizing food effects to overcome challenges in delivery of lipophilic bioactives: Structural design of medical and functional foods. *Expert Opinion on Drug Delivery, 10*(12), 1621–1632. https://doi.org/10.1517/17425247.2013.837448

McClements, D. J. (2015). *Food Emulsions: Principles, Practices and Techniques* (Taylor & Francis Group, Ed.; 3rd ed.).

McClements, D. J., Decker, E. A., & Weiss, J. (2007). Emulsion–based delivery systems for lipophilic bioactive components. *Journal of Food Science*, *72*(8). https://doi.org/10.1111/j.1750–3841.2007.00507.x

McClements, D. J., & Li, Y. (2010). Structured emulsion–based delivery systems: Controlling the digestion and release of lipophilic food components. *Advances in Colloid and Interface Science, 159*(2), 213–228. Elsevier B.V. https://doi.org/10.1016/j.cis.2010.06.010

McClements, J., & McClements, D. J. (2016). Standardization of Nanoparticle Characterization: Methods for Testing Properties, Stability, and Functionality of Edible Nanoparticles. *Critical Reviews in Food Science and Nutrition*, *56*(8), 1334–1362. https://doi.org/10.1080/10408398.2014.970267

Mengual, O., Meunier, G., Cayre, I., Puech, K., & Snabre, P. (1999). Characterisation of instability of concentrated dispersions by a new optical analyser: the TURBISCAN MA 1000. *Colloids and Surfaces A: Physicochemical and Engineering Aspects*, *152*(1–2). https://doi.org/10.1016/S0927–7757(98)00680–3

Miskandar, M. S., Che Man, Y. B., Rahman, A.R., Nor Aini, I., & Yusoff, M. S. A. (2006). Effects of emulsifiers on crystallization properties of low–melting blends of palm oil and olein. *Journal of Food Lipids*, *13*(1), 57–62. https://doi.org/10.1111/j.1745–4522.2006.00034.x

Mohammadi, M., Assadpour, E., & Jafari, S. M. (2019). Encapsulation of food ingredients by nanostructured lipid carriers (NLCs). In *Lipid–Based Nanostructures for Food Encapsulation Purposes* (pp. 217–270). Elsevier. https://doi.org/10.1016/b978–0–12–815673–5.00007–6

Nguyen, H. M., Hwang, I. C., Park, J. W., & Park, H. J. (2012). Enhanced payload and photo–protection for pesticides using nanostructured lipid carriers with corn oil as liquid lipid. *Journal of Microencapsulation*, *29*(6), 596–604. https://doi.org/10.3109/02652048.2012.668960

Okonogi, S., & Riangjanapatee, P. (2015). Physicochemical characterization of lycopene–loaded nanostructured lipid carrier formulations for topical administration. *International Journal of Pharmaceutics*, *478*(2), 726–735. https://doi.org/10.1016/j.ijpharm.2014.12.002

Oliveira, D. R. B., Michelon, M., de Figueiredo Furtado, G., Sinigaglia–Coimbra, R., & Cunha, R. L. (2016). β–Carotene–loaded nanostructured lipid carriers produced by solvent displacement method. *Food Research International*, *90*, 139–146. https://doi.org/10.1016/j.foodres.2016.10.038

Oliveira, G. M., Ribeiro, A. P. B., & Kieckbusch, T. G. (2015). Hard fats improve technological properties of palm oil for applications in fat–based products. *LWT – Food Science and Technology*, *63*(2), 1155–1162. https://doi.org/10.1016/j.lwt.2015.04.040

Pan, Y., Tikekar, R. v, & Nitin, N. (2016). Distribution of a Model Bioactive within Solid Lipid Nanoparticles and Nanostructured Lipid Carriers Influences its Loading Efficiency and Oxidative Stability. *International Journal of Pharmaceutics, 511*(1):322–330. https://doi.org/10.1016/j.ijpharm.2016.07.019

Park, S., Mun, S., & Kim, Y. R. (2018). Emulsifier Dependent in vitro Digestion and Bioaccessibility of β–Carotene Loaded in Oil–in–Water Emulsions. *Food Biophysics*, *13*(2), 147–154. https://doi.org/10.1007/s11483–018–9520–0

Pezeshki, A., Hamishehkar, H., Ghanbarzadeh, B., Fathollahy, I., Keivani Nahr, F., Khakbaz Heshmati, M., & Mohammadi, M. (2019). Nanostructured lipid carriers as a favorable delivery system for β–carotene. *Food Bioscience*, *27*, 11–17. https://doi.org/10.1016/j.fbio.2018.11.004

Pyo, S.–M., Müller, R. H., & Keck, C. M. (2017). Nanoencapsulation Technologies for the Food and Nutraceutical Industries Encapsulation by nanostructured lipid carriers. In *Nanoencapsulation Technologies for the Food and Nutraceutical Industries*. https://doi.org/10.1016/B978–0–12–809436–5/00004–5

Qian, C., Decker, E. A., Xiao, H., & McClements, D. J. (2012). Nanoemulsion delivery systems: Influence of carrier oil on β–carotene bioaccessibility. *Food Chemistry*, *135*(3). https://doi.org/10.1016/j.foodchem.2012.06.047

Qian, C., Decker, E. A., Xiao, H., & McClements, D. J. (2013). Impact of lipid nanoparticle physical state on particle aggregation and β–carotene degradation: Potential limitations of solid lipid nanoparticles. *Food Research International*, *52*(1), 342–349. https://doi.org/10.1016/j.foodres.2013.03.035

Queirós, M.S., Soares Viriato, R. L., Badan Ribeiro, A. P., & Gigante, M. L. (2021). Development of solid lipid nanoparticle and nanostructured lipid carrier with dairy ingredients. *International Dairy Journal*, 105186. https://doi.org/10.1016/j.idairyj.2021.105186

Rawal, S. U., & Patel, M. M. (2018). Lipid nanoparticulate systems: Modern versatile drug carriers. In *Lipid Nanocarriers for Drug Targeting* (pp. 49–138). Elsevier. https://doi.org/10.1016/B978–0–12–813687–4.00002–5

Ribeiro, A. P. B., Basso, R. C., & Kieckbusch, T. G. (2013). Effect of the addition of hardfats on the physical properties of cocoa butter. *European Journal of Lipid Science and Technology*, *115*(3), 301–312. https://doi.org/10.1002/ejlt.201200170

Rodrigo Campos. (2005). Experimental Methodology. In A. Marangoni (Ed.), *Fat Crystal Networks*.

Rohmah, M., Raharjo, S., Hidayat, C., & Martien, R. (2020). Application of Response Surface Methodology for the Optimization of β–Carotene–Loaded Nanostructured Lipid Carrier from Mixtures of Palm Stearin and Palm Olein. *JAOCS, Journal of the American Oil Chemists' Society*, *97*(2), 213–223. https://doi.org/10.1002/aocs.12310

Santos, P. P., Andrade, L. de A., Flôres, S. H., & Rios, A. de O. (2018). Nanoencapsulation of carotenoids: a focus on different delivery systems and evaluation parameters. *Journal of Food Science and Technology, 55*(10), 3851–3860. https://doi.org/10.1007/s13197–018–3316–6

Santos, V.S., Braz, B. B., Silva, A. Á., Cardoso, L. P., Ribeiro, A. P. B., & Santana, M. H. A. (2019). Nanostructured lipid carriers loaded with free phytosterols for food applications. *Food Chemistry*, *298*. https://doi.org/10.1016/j.foodchem.2019.125053

Sato, K. (2001). Crystallization behaviour of fats and lipids — a review. *Chemical Engineering Science*, *56*(7). https://doi.org/10.1016/S0009–2509(00)00458–9

Schaffazick, S. R., Guterres, S. S., Freitas, L. de L., & Pohlmann, A. R. (2003). Caracterização e estabilidade físico–química de sistemas poliméricos nanoparticulados para administração de fármacos. *Química Nova*, *26*(5). https://doi.org/10.1590/S0100–40422003000500017

Schenk, H., & Peschar, R. (2004). Understanding the structure of chocolate. *Radiation Physics and Chemistry*, *71*(3–4), 829–835. https://doi.org/10.1016/j.radphyschem.2004.04.105

Severino, P., Santana, M. H. A., & Souto, E. B. (2012). Optimizing SLN and NLC by 2 2 full factorial design: Effect of homogenization technique. *Materials Science and Engineering C*, *32*(6), 1375–1379. https://doi.org/10.1016/j.msec.2012.04.017

Shukat, R., Bourgaux, C., & Relkin, P. (2012). Crystallisation behaviour of palm oil nanoemulsions carrying vitamin E: DSC and synchrotron X–ray scattering studies. *Journal of Thermal Analysis and Calorimetry*, *108*(1), 153–161. https://doi.org/10.1007/s10973–011–1846–5

Silva, H. D., Cerqueira, M. Â., & Vicente, A. A. (2012). Nanoemulsions for Food Applications: Development and Characterization. *Food and Bioprocess Technology, 5*(3), 854–867. https://doi.org/10.1007/s11947–011–0683–7

Soleimanian, Y., Goli, S. A. H., Varshosaz, J., & Maestrelli, F. (2019). β–sitosterol Lipid Nano Carrier Based on Propolis Wax and Pomegranate Seed Oil: Effect of Thermal Processing, pH, and Ionic Strength on Stability and Structure. *European Journal of Lipid Science and Technology*, *121*(1). https://doi.org/10.1002/ejlt.201800347

Taiz, L., Zeiger Ian Max Møller, E., & Murphy, A. (2017). *Fisiologia e Desenvolvimento Vegetal – 6ª Edição*.

Tamjidi, F., Shahedi, M., Varshosaz, J., & Nasirpour, A. (2013). Nanostructured lipid carriers (NLC): A potential delivery system for bioactive food molecules. In *Innovative Food Science and Emerging Technologies*, *19*, 29–43. https://doi.org/10.1016/j.ifset.2013.03.002

Tamjidi, F., Shahedi, M., Varshosaz, J., & Nasirpour, A. (2014). Design and characterization of astaxanthin–loaded nanostructured lipid carriers. *Innovative Food Science and Emerging Technologies*, *26*, 366–374. https://doi.org/10.1016/j.ifset.2014.06.012

Valenzuela, A., Delplanque, B., & Tavella, M. (2011). Stearic acid: A possible substitute for trans fatty acids from industrial origin. *Grasas y Aceites*, *62*(2), 131–138. https://doi.org/10.3989/gya.033910

Wang, J. L., Dong, X. Y., Wei, F., Zhong, J., Liu, B., Yao, M. H., Yang, M., Zheng, C., Quek, S. Y., & Chen, H. (2014). Preparation and characterization of novel lipid carriers containing microalgae oil for food applications. *Journal of Food Science*, *79*(2), 169–177. https://doi.org/10.1111/1750–3841.12334

Yang, Y., Corona, A., Schubert, B., Reeder, R., & Henson, M. A. (2014). The effect of oil type on the aggregation stability of nanostructured lipid carriers. *Journal of Colloid and Interface Science*, *418*, 261–272. https://doi.org/10.1016/j.jcis.2013.12.024

Yi, J., Zhong, F., Zhang, Y., Yokoyama, W., & Zhao, L. (2015). Effects of Lipids on in Vitro Release and Cellular Uptake of β–Carotene in Nanoemulsion–Based Delivery Systems. *Journal of Agricultural and Food Chemistry*, *63*(50), 10831–10837. https://doi.org/10.1021/acs.jafc.5b04789

Zardini, A.A., Mohebbi, M., Farhoosh, R., & Bolurian, S. (2018). Production and characterization of nanostructured lipid carriers and solid lipid nanoparticles containing lycopene for food fortification. *Journal of Food Science and Technology*, *55*(1), 287–298. https://doi.org/10.1007/s13197–017–2937–5

Zhou, X., Wang, H., Wang, C., Zhao, C., Peng, Q., Zhang, T., & Zhao, C. (2018). Stability and in vitro digestibility of beta–carotene in nanoemulsions fabricated with different carrier oils. *Food Science and Nutrition*, *6*(8), 2537–2544. https://doi.org/10.1002/fsn3.862

CAPÍTULO VII

Fully hydrogenated soybean oil and high oleic sunflower oil β-carotene loaded nanostructured lipid carriers: cytotoxicity and bioaccessibility.

Submitted to Food & Function

7. Fully hydrogenated soybean oil and high oleic sunflower oil β-carotene loaded nanostructured lipid carriers: cytotoxicity and bioaccessibility

Fernanda Luisa Lüdtke[a], Jean-Michel Fernandes[b], Raquel Filipa Gonçalves[b], Joana Teresa Martins[b], Paulo Berni[b], Ana Paula Badan Ribeiro[a], Ana Cristina Pinheiro[b], Antonio Augusto Vicente[b]

[a]Department of Food Engineering and Technology, School of Food Engineering, State University of Campinas, 13083-862, Campinas, SP, Brazil.

[b]Centre of Biological Engineering, University of Minho, 4710-057 Braga, Portugal.

ABSTRACT

Nanotechnology offers great potential to significantly improve the solubility and bioavailability of many functional ingredients. The aim of this study was to evaluate fully hydrogenated soybean oil (FHSO) and high oleic sunflower oil (HOSO) β-carotene-loaded nanostructured lipid carriers (NLC) behavior during dynamic *in vitro* digestion, β-carotene bioaccessibility and potential cytotoxicity. The β-carotene loaded NLC were produced by high pressure homogenization (HPH) using two emulsifiers: enzymatically modified soy lecithin (NLC L_{β}) or Tween 80 (NLC T_{β}). The NLC T_{β} showed higher stability during the passage through the gastrointestinal tract (GIT) and provided higher β-carotene protection and delivery. The use of FHSO and HOSO as lipid matrix allowed to obtain a non-toxic and biocompatible NLC able to incorporate and protect β-carotene, with a feasible cost for application in foods.

Keywords: lipid nanoparticles; *in vitro* digestion; dynamic *in vitro* gastrointestinal system (DIVGIS); bioaccessibility; cell viability

7.1 Introduction

In recent years, significant efforts have been made on the development of new functional foods mainly due to the health benefits associated with their consumption (Fathi et al., 2013; Salvia-Trujillo et al., 2019; Zardini et al., 2018). In this regard, the incorporation of carotenoids as bioactive components into functional foods has been raising a great interest in food industry (Pezeshki et al., 2019; Salvia-Trujillo et al., 2013a; Zardini et al., 2018).

Carotenoids are a family of fat soluble pigments synthetized by plants, photosynthetic microorganisms, and some fungi, that have biological and chemical properties (Kopec & Failla, 2018; Namitha & Negi, 2010; Santos et al., 2018). Generally, carotenoids can be classified into two categories based on their functional group: xantophylls (which contain oxygen as functional group, like zeaxanthin and lutein) and carotenes (which are hydrocarbons, like β-carotene and lycopene) (Khalid et al., 2019).

Among carotenoids, β-carotene is considered the most nutritionally active (Hentschel et al., 2008), presenting a high provitamin A activity (Yuan et al., 2008). Additionally,

β-carotene possesses antioxidant activity which can block free radical-mediated reactions and reduce the risks of many disorders such as cancer and cardiovascular diseases (Rehman et al., 2020; Yuan et al., 2008). The same properties that make β-carotene present health beneficial functions, also create challenges in preventing their degradation once incorporated in food products (Boon et al., 2010). The use of carotenoids can be impaired by their oxidation, which can be accelerated by factors such as light, temperature, pH and presence of reactive oxygen forms (Davidov-Pardo et al., 2016; Yuan et al., 2008). Additionally, β-carotene presents low solubility in water (due to its hydrophobic character), high melting point and low bioavailability in crystalline form (Boon et al., 2010; Gutiérrez et al., 2013; Ribeiro & Cruz, 2005).

Usually, high β-carotene bioavailability requires high bioaccessibility which is greatly impacted by food matrix (van Loo-Bouwman et al., 2014). When a bioactive compound is orally consumed, it passes through various barriers, such as stomach and small intestine degradation conditions, until they are absorbed into the bloodstream (Jafari et al., 2017). Bioaccessibility describes the amount of the compound that is actually protected against these barriers, released from the food matrix and incorporated into mixed micelles for absorption in the GIT. Bioavailability describes the portion of the compound actually absorbed by the intestinal cell epithelium during the release of the food matrix in the GIT (Jafari et al., 2017; Kopec & Failla, 2018; McClements et al., 2015).

The entrapment of β-carotene in a lipid phase before digestion can considerably increase the compound's bioaccessibility as it facilitates the carotenoids' transfer to the micellar phase during digestion (Salvia-Trujillo et al., 2017). The oil phase can solubilize solid lipophilic bioactive compounds (crystalline form), increasing the molecular dispersion in the system. Lipids can also act as a barrier to the degradation of these compounds during their passage through the GIT, since most of the compounds that promote degradation are soluble in water (Zou et al., 2016). In addition, the presence of exogenous lipids in the small intestine stimulates the secretion of bile salts and lipases, which promote lipolysis. Lipolysis products, such as free fatty acids (FFA), can facilitate the formation of mixed micelles that increase nutrient bioaccessibility (Fu et al., 2019; Porter et al., 2007).

One mean of controlling the oral bioaccessibility of lipophilic bioactive ingredients, such as β-carotene, is to incorporate them in emulsion-based delivery systems (Das et al., 2020; McClements & Li, 2010). Due to the high instability of carotenoids, several strategies have been adopted to increase the stability and consequently, the bioaccessibility of these compounds. Nanostructured delivered systems could be an alternative to incorporate carotenoids, decreasing the degradation of these compounds (Boon et al., 2010). Lipid-based systems, such as nanoemulsions (NE) and lipid nanocarriers, can be used as an approach to

encapsulate β-carotene, improving their stability and bioaccessibility (Gomes et al., 2019; Salvia-Trujillo et al., 2017).

NLC composed by a binary mixture of a solid lipid and a spatially distinct liquid lipid, are created with a controlled nanostructure of lipids which do not form a perfect crystal (Shah et al., 2015). In this type of nanocarrier, the bioactive compounds are dissolved in the lipid phase with the lowest melting point, and combined are incorporated into the less organized structures of the lipid matrix with the highest melting point (solid) (Tamjidi et al., 2013). The oil incorporation in the solid matrix leads to the formation of an amorphous nanostructure with many imperfections in its matrix, which allows a greater space for bioactive compounds' incorporation (Fang et al., 2012; Pinto et al., 2014).

An efficacious application of nanocarriers depends on the choice of appropriate materials in terms of physiochemical properties for carotenoids' protection and targeted delivery (Rehman et al., 2020). Since the selection of the lipid matrix and the type of emulsifier have been shown to affect lipid nanoparticles (LN) susceptibility to lipolysis (Hur et al., 2009; Zhang et al., 2015), the choice of these materials is fundamental to obtain a NLC suitable for bioactive compounds delivery.

The type of lipid matrix used to obtain LN directly influences the bioavailability of the lipid-soluble bioactive compounds incorporated into the NLC structures (Tan & McClements, 2021). The lipid matrix influences the solubilization capacity of mixed micelles, usually long-chain fatty acids increase the size of the mixed micelles formed, thus being able to better accommodate the carotenoid molecules inside (Salvia-Trujillo et al., 2013a). The composition of the lipid matrix can also affect the oxidative stability of chemically labile bioactive compounds during food processing and storage, as well as during their passage through the GIT. Thus, the bioavailability of bioactive compounds can be significantly reduced if chemical transformations occur during these processes (Tan & McClements, 2021). Pure triacylglycerols (TAG) and their commercial blends can be successfully used to obtain NLC. However, the use of TAG in purified form is generally economically unfeasible when considering the scale and possible application in food. In this sense, the lipid matrices available in the oil and fat industry have high potential to be used to produce NLC. High oleic oils, as the HOSO, have demonstrably higher values of oxidative stability when compared to oils with high content of polyunsaturated fatty acids (O'Brien, 2009; Oliveira et al., 2016). So, the use of this lipid matrix to obtain NLC, can avoid chemical transformations, allowing higher protection and delivery of the β-carotene in GIT. Fully hydrogenated vegetable oils, like FHSO, can be used as a high melting point lipid matrix to obtain NLC, mainly due to the expressive levels of stearic acid (C18:0) which have a neutral atherogenic effect, with no adverse effect on the risk of cardiovascular diseases (Valenzuela et al., 2011).

It is well-known that the interfacial properties also influence the gastrointestinal fate of lipid particles: they influence the size of the particles obtained (surface area) and their aggregation status in the GIT; the adsorption of bile salts and lipases on their surface; the removal of products of lipid digestion, and mixed micelles formation and their properties (Singh et al., 2009). NLC can be stabilized by different types of emulsifiers, which can affect the properties of the LN obtained, as well as their behavior during digestion (Park et al., 2018). Therefore, the choice of the emulsifier is crucial, since it can directly affect the solubilization, diffusion, dissociation rate and thermodynamic activity of the bioactive compound incorporated into the structure (How et al., 2013).

At the nanoscale, the biological fate of delivery systems and bioactive compounds incorporated can be modified, influencing their absorption, distribution, metabolism, excretion and thus, their potential toxicity (McClements, 2013). Understanding the biological fate of nanostructures after passing through the GIT is necessary to predict and increase their functionality, the bioavailability of the bioactive compound and to assess its potential toxicity (Pinheiro et al., 2017).

Since the digestibility of NLC may affect the release of the bioactive compound encapsulated (Yang et al., 2017), the aim of this work was to evaluate the *in vitro* digestibility of β-carotene-loaded NLC (composed of HOSO and FHSO as a lipid matrix) using a dynamic gastrointestinal model. Also, the cytotoxicity of the developed nanostructures was assessed. The HPH process conditions, the emulsifiers and solid/liquid lipid ratio used to obtain and select the NLC for the study of *in vitro* digestibility were based on previous data (i.e., stability, physicochemical characterization, encapsulation efficiency and crystallization properties) obtained by our research group.

7.2 Materials and Methods

7.2.1 Materials

HOSO and FHSO were supplied by Cargill Foods (Brazil). β-Carotene (purity: 95 %) and Ethoxylated sorbitan monooleate (Tween 80) were purchased from Sigma-Aldrich (USA), and enzymatically modified soy lecithin (SL) SOLECTM AE IP was supplied by Solae (Brazil). Pepsin from porcine gastric mucosa, lipase and pancreatin (8 × USP) from porcine pancreas, bile extract porcine and other reagents of analytical grade were purchased from Sigma-Aldrich (St. Louis, USA). Caco-2 cell line (ATCC), obtained from human colon carcinoma, was kindly provided by the Department of Biology, University of Minho (Braga, Portugal). Dulbecco's modified Eagle's medium (DMEM), non-essential amino acids (NEAA) and phosphate-buffered saline (PBS) were obtained from Lonza (Basel, Switzerland).

Penicillin/streptomycin, trypsin-EDTA, 3-(4,5-dimethylthiazol-2-yl)-2,5-diphenyltetrazolium bromide (MTT) and dimethyl sulfoxide (DMSO) were purchased from Sigma-Aldrich (St. Louis, MO, USA); fetal bovine serum (FBS) was obtained from Merck (Darmstadt, Germany).

7.2.2 NLC production

The pre-emulsion was composed by FHSO and HOSO (60/40, w/w); aqueous phase (88 %) (ultrapure water) and emulsifier (2 %) (Tween 80 or SL). β-carotene (0.5 %) was mixed in the lipid melted phase and heated at 85 °C. On other hand, emulsifier and water were mixed together and then heated at 85 °C. Afterward, the oil phase and aqueous phase were mixed and homogenized at 10,000 rpm for 3 min by a high-speed Ultra-turrax homogenizer (T18, IKA Werke, Germany). Subsequently, the pre-emulsion passed through a high pressure homogenizer (NanoDeBee, Bee International, Massachusetts, USA) at 20,000 psi and 20 cycles of homogenization. The NE was cooled at 5 °C for 24 h and stored at 25 °C in covered glasses.

For the bioaccessibility tests, a control emulsion was prepared using the same composition of NLC, but not submitted to HPH. The phases were heated at 85 °C, mixed with high-speed Ultra-turrax homogenizer (T18, IKA Werke, Germany) at 5,000 rpm/5 min and immediately submitted to *in vitro* digestibility test.

7.2.3 *In vitro* digestion

The digestion process was based on the protocol proposed by Pinheiro et al. (2016) with some modifications based on the work of Mulet-Cabero et al. (2020). A dynamic *in vitro* gastrointestinal system (DIVGIS) was used in the digestion experiments (Fernandes et al., 2021). The DIVGIS consists of four compartments - stomach, duodenum, jejunum and ileum - that simulate the main conditions that occur during digestion in the human GIT. Each compartment is composed by two connected acrylic reactors with a flexible wall (stomacher bags) and connected by siliconetubes. The simulation of peristaltic movements was carried out by the alternate compression and relaxation of the flexible walls, through the passage of water (37 °C) in each reactor. Gastric and intestinal secretions were freshly prepared and secreted continuously inside the reactors by syringe pumps at pre-set flow rates. The jejunum and ileum compartments were connected to hollow fibers (Repligen Minikros ®, S02-S05U-05-P, Breda, The Netherlands) to simulate the absorption that occurs in the small intestine. These fibers divided the fluids into different fractions: jejunum filtrate, ileum filtrate and non-ileum filtrate (Pinheiro et al., 2017).

A volume of 100 mL of each sample (NLC L_β, NLC T_β, and a control sample obtained as described in 2.2) was used as the initialsample. The oral phase was carried out in a static

digestion bath at 37 °C, by the addition of the simulated salivary fluid (SSF) (KCl 15.1 mM, KH_2PO_4 3.7 mM, $NaHCO_3$ 13.6 mM, $MgCl_2(H_2O)_6$ 0.15 mM, $(NH_4)_2CO_3$ 0.06 mM, $CaCl_2(H_2O)_2$ 1.5 mM) and agitation at 120 rpm for 2 min. After the oral phase, the sample was introduced into the system through the gastric compartment, and the simulated gastric fluid (SGF) (KCl 6.9 mM, KH_2PO_4 0.9 mM, $NaHCO_3$ 25 mM, NaCl 47.2 mM, $MgCl_2(H_2O)_6$ 0.12 mM, $(NH_4)_2CO_3$ 0.5 mM, $CaCl_2(H_2O)_2$ 0.15 mM) and pepsin (3940 $U.mL^{-1}$) and lipase (65 $U.mL^{-1}$) solution were continuously secreted at the flow rate 0.4 mL min^{-1}. A constant volume was transferred to the duodenum compartment and then the simulated intestinal fluid (SIF) (KCl 6.8 mM, KH_2PO_4 0.8 mM, $NaHCO_3$ 85 mM, NaCl 38.4 mM, $MgCl_2(H_2O)_6$ 0.33 mM, $CaCl_2(H_2O)_2$ 0.6 mM), bile salts and pancreatin solution were continuously secreted at the flow rate 0.8 mL min^{-1}. At a predefined time, a constant volume of chyme was transferred to the subsequent compartment. The digestion experiments lasted approximately 4 h. During *in vitro* digestion, samples were collected directly from the lumen of the different compartments, from the jejunal and ileal filtrates and from the ileal delivery in order to determine the changes in the NLC structure during the digestion and the bioaccessibility of β-carotene entrapped in NLC.

Samples collected from the jejunum and ileum filtrates were used to determine particle size (PS), polydispersity index (PDI) and ζ-potential (ZP). These samples were also used to determine β-carotene bioaccessibility, and in this case, the samples were stored in falcon tubes wrapped in aluminum foil and subsequently frozen, remaining until the moment of analysis. The measurements of PS, PDI and ZP of samples collected after the oral phase, stomach, and duodenum in the time of ½ digestion, and of the filtered jejunum, ileum and unfiltered samples (collected at the end of digestion) were conducted immediately after the end of the *in vitro* digestibility test. We collect the sample in the time of ½ digestion for comparison purposes, as the dynamic nature of GI system fluids are always in and out. The simulation of digestions was done at least in triplicate.

7.2.4 Particle size, polydispersity index and ζ-potential

PS, PDI, and ZP of the NLC were measured at different stages of digestion by dynamic light scattering (DLS) (Zetasizer Nano ZS, MalvernInstruments, Worcestershire, UK). All samples were diluted at 1:100 with a buffer solution of the same pH of the samples.

7.2.5 β-Carotene bioaccessibility

β-carotene bioaccessibility at different stages of digestion was determined by liquid-liquid extraction and spectrophotometric analysis, based on the methodology described by Berni et al. (2020) with some modifications. Aliquots (5 mL) of each sample (i.e., jejunum and ileum filtrate) were vortexed with 10 mL of acetone with BHT (0.01 %) for 30 s; after 10 mL of

hexane were added and vortexed for 10 s. Distilled water was added until the final volume of 45 mL and then the solution was centrifuged (Allegra 64R, Beckman Coulter Inc., USA) at 10,000 rpm at 4 °C for 5 min. Upper phase containing β-carotene was collected and dried with N_2 flow, resuspended in hexane and analyzed by UV-VIS spectrophotometer (V-560, Jasco, USA) at 450 nm (absorbance peak). The concentration of β-carotene was determined from a previously prepared calibration curve of absorbance *versus* β-carotene concentration in hexane. The β-carotene bioaccessibility was calculated based on the following equation:

$$\boldsymbol{\beta - carotene\ bioaccessibility}\ (\%) = \frac{\mu g\ \beta - carotene\ filtrates \times 100}{\mu g\ \beta - carotene\ of\ initial\ sample}$$

where *β-carotene filtrates* is the total β-carotene in the jejunum and ileal filtrates (considering the total volume of sample collected in each filtrate).

7.2.6 Free fatty acids release

The amount of FFA released from the lipid digestion of NLC was determined by a pH-stat automatic method (Titrando 902, Metrohm, Switzerland). This method was also used to monitor the pH that was maintained at 7.0 *via* the titration of 0.05 N NaOH solution. The volume of NaOH added to the NLC was recorded, which was used to calculate the concentration of FFA released from the lipid phase during lipolysis.

NLC T_β, NLC L_β and a control sample were firstly submitted to oral and stomach phase in the DIVGIS. After 1 h 45 min of stomach phase, 20 mL of each sample was collected and placed into a glass reactor connected with a water bath at 37 °C. Intestinal fluids and bile were added to the sample under stirring and then the pH was adjusted to 7.0 using NaOH or HCl solutions. Pancreatin was added and the titration started.

Blanks experiments (without pancreatin) were performed to determine the volume of NaOH required to achieve the pH 7.0. The quantity of FFA released was calculated based on the following equation (Pinsirodom & Parkin, 2001):

$$\boldsymbol{FFA}\ (\boldsymbol{\mu mol}\ fatty\ acids/\ \boldsymbol{mL}\ of\ sample) = \frac{(Volume\ NaOH\ for\ sample - Volume\ NaOH\ for\ blank) \times C \times 1000}{Volume\ sample}$$

where *C* is the molar concentration of the NaOH titrant used (0.05 M).

7.2.7 Cytotoxicity assay

For the cellular viability assay, free β-carotene, β-carotene loaded NLC obtained

with Tween 80 and SL, and NLC obtained with Tween 80 and SL without β-carotene (free β-carotene NLC) samples were diluted to the following β-carotene concentrations: 1, 2.5, 5, 15 and 25 $\mu g.mL^{-1}$. The components used to produce NLC (i.e., HOSO, Tween 80 and SL emulsifiers) were also tested. FHSO was not tested due to its high melting point, which makes it difficult to dilute to perform the assay. β-carotene stock solution was preparedin pure ethanol (99.9 %), Tween 80 and SL stock solutions were prepared in ultrapure water. MTT assay was conducted according to Gonçalves et al. (2021a) with some modifications. Briefly, Caco-2 cells were cultured at 2×10^5 cells/well (in a 96-well microplate) in DMEM supplemented with 10 % (v/v) FBS, 1 % (v/v) NEAA, and 1 % (v/v) Penicillin/streptomycin. Cell culture was grown in a humidified 5 % CO_2 incubator at 37 °C during 48 h. After incubation, the cell culture medium was replaced by 200 μL of fresh culture medium containing tested samples. At least three replicates of each sample were analyzed. After 24 h of incubation, the samples were removed, and 100 μL of MTT solution (0.5 mg/mL in PBS) was added to the wells and incubated at 37 °C for 3 h. Then, formazan crystals generated were solubilized with 200 μL DMSO, followed by gentle stirring for 30 min on an orbital shake. Cell viability was assessed at 570 nm (reference wavelength set at 630 nm) and the results were expressed as cell viability (%) relative to the control (i.e., untreated cells in DMEM medium).

7.2.8 Statistical analysis

All experiments were carried out at least in triplicate. Experimental data were analyzed for significant differences using ANOVA. Means were compared using Tukey test by 0.05 % of significance using the OriginPro2018® Statistic Software (Origin Lab Corporation, Northampton, USA).

7.3 Results and discussion

7.3.1 Behavior of NLC under digestion

One of the most important applications of nanoparticles in food is as oral delivery systems for bioactive nutraceutical compounds. For this application, it is important to understand the behavior of nanoparticles as they pass through the human GIT (McClements, 2013). Since lipid digestion is highly correlated to the bioavailability of lipophilic bioactive compounds, the understanding of the digestibility process is essential. *In vitro* models are currently used as the main tool to understand the behavior of LN under GIT conditions, minimizing the negative implications associated with *in vivo* studies (ethical, economic, technical restrictions, among others) (Pinheiro et al., 2017). *In vitro* digestibility models can be divided into static or dynamic. Compared to static models, dynamic *in vitro* digestibility models are considered more suitable to provide a better prediction of the biological fate of delivery

systems due to a more effective simulation of the biochemical, biomechanical, and temporal *in vivo* attributes (Lin et al., 2018).

In this study, *in vitro* dynamic digestibility tests were performed with β-carotene loaded NLC obtained with different emulsifiers, to evaluate the behavior of these nanostructures during the passage through the GIT, as well as the β-carotene bioaccessibility. Two types of NLC were considered in this study: NLC L_β, obtained with SL, and NLC T_β, obtained with Tween 80.

7.3.2 Particle size, polydispersity index and ζ-potential

Several studies have shown that the LN properties' assessment, such as PS, surface ZP and LN response when subjected to different environmental conditions (pH, ionic strength, enzymatic activity) is necessary to control the release and absorption of compounds incorporated within these structures (Hou et al., 2014; Zhang et al., 2015). Thus, the evaluation of the PS, PDI and ZP of NLC subjected to an *in vitro* dynamic digestion was performed, considering the different digestion stages: initial sample (i.e., NLC before digestion), oral phase, gastric phase (time of ½ digestion), duodenum (time of ½ digestion), jejunum filtrate, ileum filtrate and final filtrate (unfiltered).

PS is one of the crucial factors to determine digestibility and bioaccessibility of lipophilic bioactive compounds incorporated in lipid structures (Hou et al., 2014; Salvia-Trujillo et al., 2013a), as it significantly influences lipid digestion kinetics, the subsequent mixed micelles formation and carotenoids entrapment into the micelles (Salvia-Trujillo et al., 2017). However, it is important to point out that it is unlikely that the PS will remain the same during the passage through the GIT, due to fragmentation, flocculation, and coalescence phenomena (Tan & McClements, 2021). Thus, this characteristic may increase, decrease, or remain stable under gastrointestinal conditions, depending on the initial PS and interfacial composition (Favé et al., 2004). Therefore, it is very important to understand how PS change during the GIT (Tan & McClements, 2021).

It is well-known that lipid particles coated with emulsifiers unstable in an acidic environment undergo strong aggregation and creaming in the stomach, often resulting in faster gastric emptying. On the other hand, particles coated with acid-stable emulsifiers tend to remain as individual particles during passage through the stomach (Tan & McClements, 2021; Wang et al., 2019). The nanostructures considered in this study showed different behavior during the passage through the GIT. The NLC T_β remained stable during the passage through the gastric compartment as can be seen in Figure 1, showing a PS similar to one observed in the oral phase, which indicates the absence of particle aggregation. Tween 80 is a non-ionic emulsifier that forms a compressed film around particle surfaces, stabilizing NLC formulations by creating steric (Souto et al., 2004). The NLC T_β stability under gastric conditions can be

explained by the steric repulsion presented by non-ionic emulsifiers, like Tween 80, in acidic medium (Golding & Wooster, 2010).

The results found in this study agree with previous studies, which reported that the size of particles coated by certain types of non-ionic emulsifiers, such as Tween 80, was not significantly altered under gastric conditions (Mun et al., 2007; Park et al., 2018; Salvia-Trujillo et al., 2013a; van Aken et al., 2011). Verkempinck et al. (2018) claimed that Tween 80 is not sensitive to pH changes in the gastric phase (pH 1 to 3), thus providing higher stability to emulsified delivery systems when compared to other emulsifiers. A study carried out by Salvia-Trujillo et al. (2017), reported that the use of Tween 80 as an emulsifier provided emulsions' stability under *in vitro* acidic conditions, even though these emulsions had different PS (15.1; 1.93 and 0.72 μm) before *in vitro* digestion, thus indicating that this emulsifier provides stability to particles with different dimensions.

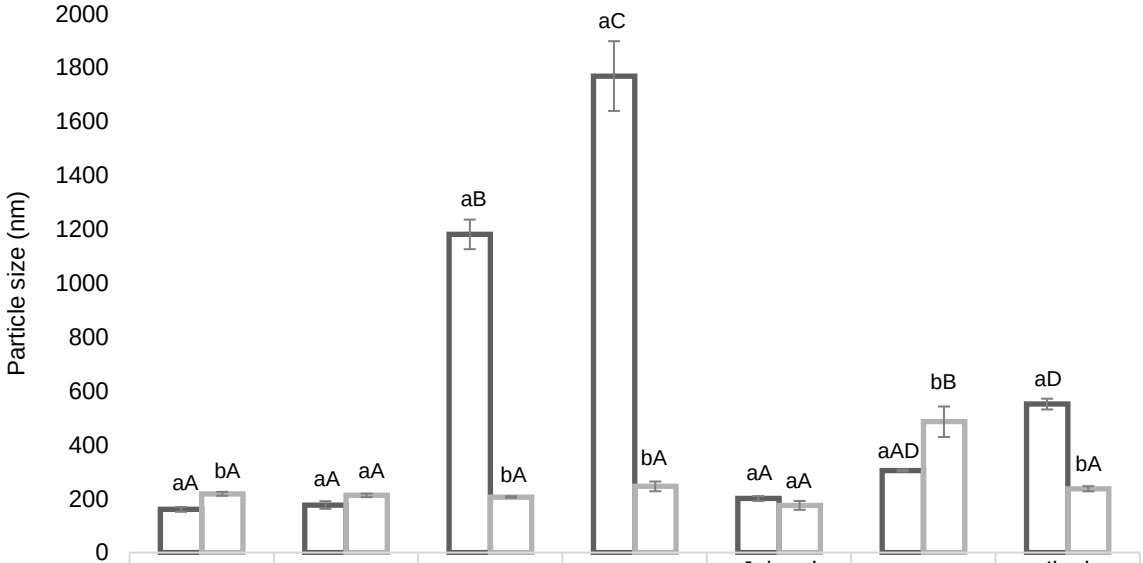

	Initial	Oral	Stomach	Duodenum	Jejunal filtrate	Ileal filtrate	Ileal delivery
NLC Lβ	160.17	176.62	1181.17	1769.00	200.61	304.43	551.27
NLC Tβ	218.18	212.37	206.16	245.68	175.13	485.67	236.93

Figure 1: Particle size of of β-carotene loaded NLC collected at different stages of *in vitro* digestion. Errors bars represent the standard deviation of n= 3 replicates. $^{A\text{-}D}$Different capital letters indicate significant difference between simulated gastrointestinal phases ($p< 0.05$) for the same NLC. $^{a\text{-}b}$ Different lower-case letters indicate significant difference between NLC in the same gastrointestinal phase ($p< 0.05$).

Regarding NLC L_β, their PS significantly increased ($p<0.05$) after being submitted to gastric conditions (Figure 1). This nanocarrier was produced using an enzymatically hydrolyzed lecithin, obtained by the hydroxylation of commercial SL. Several studies have shown that emulsified systems stabilized with SL have less stability under GIT conditions (Park et al., 2018; Verrijssen et al., 2015). A drastic droplets' destabilization under *in vitro* gastric

conditions has been previously reported in emulsions stabilized with phospholipids (Verrijssen et al., 2015) whereas in emulsions stabilized with non-ionic emulsifiers, the PS remained stable during the gastric phase (Salvia-Trujillo et al., 2013b, 2017). Similar results were reported by Park et al. (2018). These authors carried out an *in vitro* digestibility study using NE stabilized with different emulsifiers namely natural SL and Tween 20 (similar to those used in our study). The authors found that NE stabilized with Tween 20 was the only one stable (aggregation was not observed) in the gastric phase, indicating that the NE stabilized with SL were more apt to coalesce when subjected to gastric conditions. Therefore, the size increase observed in the present study during the passage through the GIT can be attributed to aggregation, coalescence, or flocculation due to the action of digestive enzymes and changes in pH and ionic strength (Pinheiro et al., 2013).

The measurement of the PS in the small intestine is important to determine the bioavailability of the bioactive compounds incorporated into the lipid phase (Tan et al., 2020). In this study, a significant increase in PS of NLC L_β from the gastric phase to the duodenum was observed (Figure 1), while NLC T_β maintained their PS in the duodenum and jejunum, showing an increase in PS only after passing through the ileum (the final small intestine compartment).

Most of the lipid digestion takes place in small intestine through the action of pancreatic lipase, which binds to the oil/water interface. In general, the size of the oil droplets together with the composition of the interfacial layer are fundamental for the activity of pancreatic lipase (McClements et al., 2009). The increase in NLC T_β PS can be attributed to reduced physical stability of these particles in the end of small intestine, which could be related to several physicochemical mechanisms that happened when the sample was exposed to small intestinal conditions. NLC T_β entered the duodenal compartment presenting a relatively high surface area for pancreatic lipase adsorption to particles surface. Thus, some molecules of the nonionic emulsifier (Tween 80) that originally covered the particle may have been displaced by lipase or other superficially active substances present in the intestinal environment from SIF (e.g., bile salts, phospholipids). The adsorption of these substances may have promoted a change in NLC composition, structure, and surface properties, reducing the physical stability of these particles and thus, allowing the digestion of lipids present in the NLC structure. Additionally, the digestion of TAG present in the NLC structure by lipase promotes the formation of FFA and monoacylglycerols (MAG), thus changing the structure's internal composition and surface properties, since FFA and MAG are also surface-active species (Qian et al., 2012). This result agrees to a study carried out by Abreu-Martins et al. (2020), who reported an increase in PS of solid LN and liquid LN at the end of the small intestine. Similar results were also obtained by Qian et al. (2012) that found a large increase in PS of NE

stabilized by a non-anionic emulsifier (Tween 20) after incubation in simulated small intestine fluids.

PDI is a parameter that indicates the size distribution and homogeneity of the analyzed particles. Homogeneous and dispersed particles indicate a PDI value in the range between 0.1 and 0.25; values higher than 0.5 represent high PDI and wide particle distribution (Lakshmi & Kumar, 2010). The PDI values found after the different digestion stages are shown in Figure 2. In general, it can be inferred that the PDI values confirmed NLC L_β destabilization in the gastric phase, because PDI values were higher than 0.9. This value is indicative of a very heterogeneous distribution, and it agrees with the PS found for this nanocarrier. On the other hand, the NLC T_β presented PDI values inferior than 0.5 in the oral and gastric phases and in the duodenal compartment, confirming the stability of the particles with Tween 80. Samples collected from the jejunum and ileum filtrate presented PDI values higher than 0.6 probably due to the presence of mixed micelles resulting from the lipid digestion process, which made the PS distribution heterogeneous.

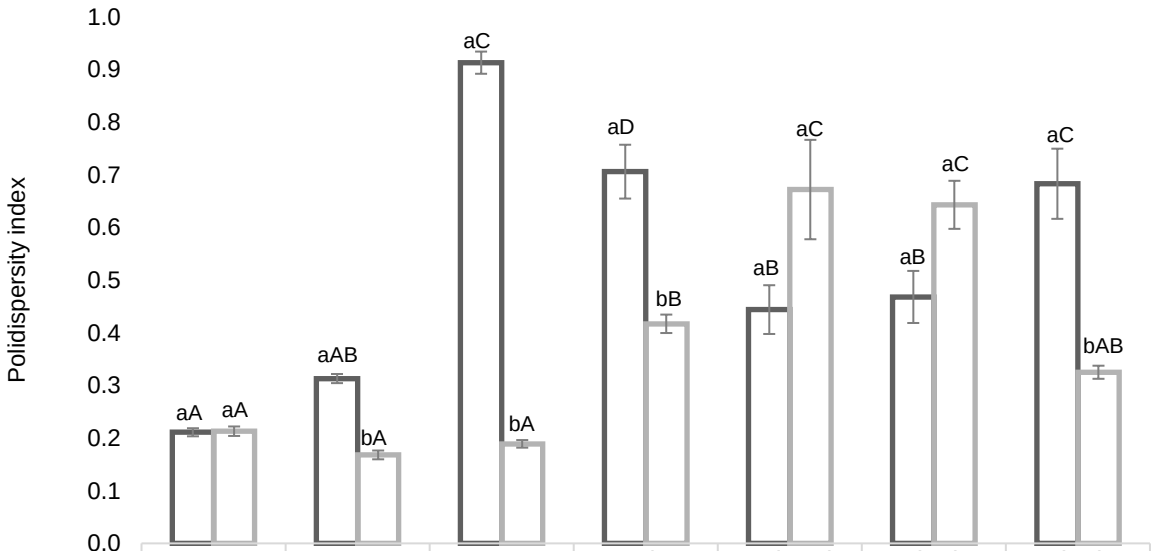

	Initial	Oral	Stomach	Duodenum	Jejunal filtrate	Ileal filtrate	Ileal delivery
NLC Lβ	0.211	0.313	0.913	0.706	0.444	0.468	0.683
NLC Tβ	0.213	0.168	0.189	0.417	0.672	0.643	0.325

Figure 2: Polydispersity index of samples of β-carotene loaded NLC collected at different stages of *in vitro* digestion. Errors bars represent the standard deviation of n= 3 replicates. $^{A\text{-}D}$Different capital letters indicate significant difference between simulated gastrointestinal phases ($p< 0.05$) for the same NLC. $^{a\text{-}b}$ Different lower-case letters indicate significant difference between NLC in the same gastrointestinal phase ($p< 0.05$).

The ZP is a very important characteristic since the electrical charge is responsible for the electrostatic interactions and subsequent stability of the emulsion-based system. In addition, electrical charge can also affect droplet/particle interactions within the intestinal

lumen and emulsion digestibility (Singh et al., 2009). This parameter provides relevant information about the electrical charge (mV) of the lipid particle surface depending on the species adsorbed at the oil-water interface (Salvia-Trujillo et al., 2017).

In this study, NLC presented differences in ZP values during the passage through the GIT as can be seen in Figure 3, probably due to the initial charge of these nanostructures. Park et al. (2018) reported that the electrical charge (ZP) and stability to aggregation of lipid droplets from NE submitted to *in vitro* digestibility tests changed according to the type of emulsifier used for NLC stabilization.

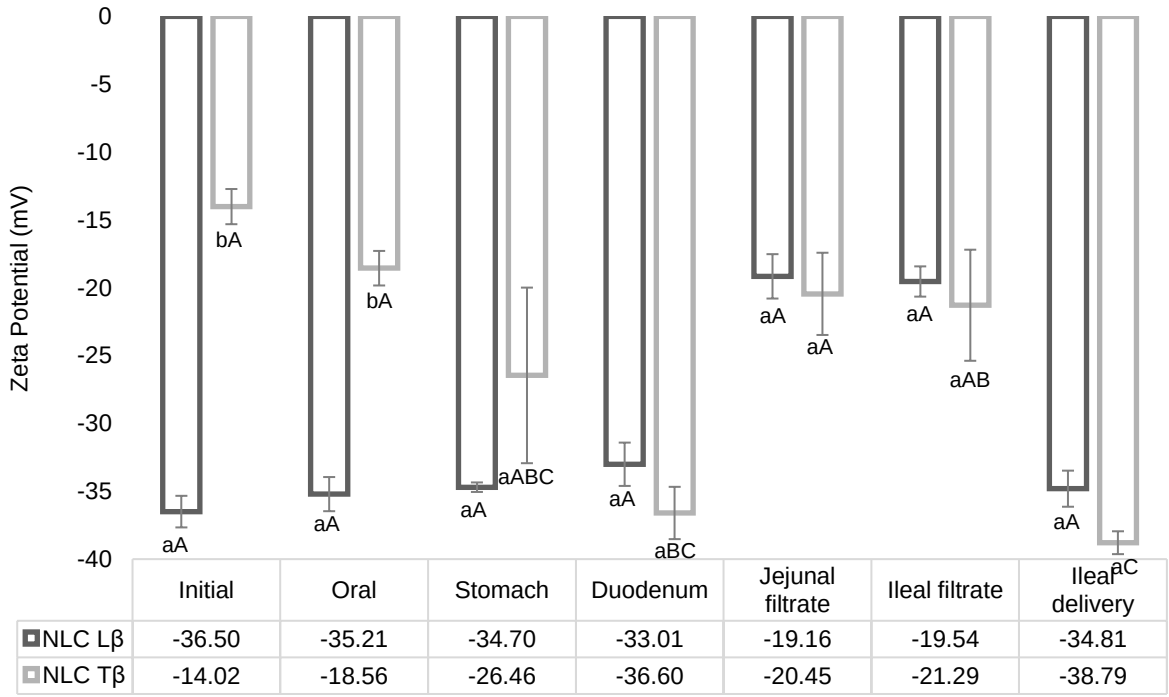

	Initial	Oral	Stomach	Duodenum	Jejunal filtrate	Ileal filtrate	Ileal delivery
NLC Lβ	-36.50	-35.21	-34.70	-33.01	-19.16	-19.54	-34.81
NLC Tβ	-14.02	-18.56	-26.46	-36.60	-20.45	-21.29	-38.79

Figure 3: ζ-Potential of samples of β-carotene loaded NLC collected at different stages of *in vitro* digestion. Errors bars represent the standard deviation of n= 3 replicates. $^{A\text{-}C}$Different capital letters indicate significant difference between simulated gastrointestinal phases ($p< 0.05$) for the same NLC. $^{a\text{-}b}$ Different lower-case letters indicate significant difference between NLC in the same gastrointestinal phase ($p< 0.05$).

The NLC T_β was produced using Tween 80, an emulsifier that, due to its non-ionic nature, stabilizes NLC formulations by creating steric hindrance resulting from the complex structure of this emulsifier (McClements & Rao, 2011; Souto et al., 2004). Thus, the particles stabilized with this emulsifier normally show neutral ZP values (McClements & Rao, 2011). This could explain the initial ZP value found in this study for NLC T_β, which was approximately -14 mV.

During the passage through the GIT, NLC T_β showed changes in the ZP value. Although not statistically significant, there was an increase (in modulus) in ZP value of NLC T_β after 2 h of passage through the gastric cavity, in contrast to some studies that reported a

decrease in the electrical charge of the particles when subjected to gastric conditions (Abreu-Martins et al., 2020). This increase was even more pronounced and, in this case significant, after 2 h of passage through the duodenum. Singh et al. (2009) reported that the negative charge of emulsified systems after the intestinal phase can be attributed to the presence of anionic FFA and other products of lipid digestion from lipolysis or complex colloidal structures formed from bile salts and phospholipids. Not only does the concentration of lipid species released at the end of the intestinal phase determine the electrical charge of emulsified systems subjected to digestion, but also the chain size of the FFA released in the process. Salvia-Trujillo et al. (2013a) reported that the negative charge of digested samples decreased with increasing chain length of released FFA.

Regarding NLC L_{β}, the ZP value remained stable and above -30 mV in the oral and gastric phases, and in the duodenal compartment, as shown in Figure 3. The ZP values of samples collected at the end of the intestinal phase (jejunum and ileum filtrates) showed a significant ($p<0.05$) reduction to values close to -20 mV. The results found for this NLC agree with the study carried out by Salvia-Trujillo *et al*. (2017) who reported a significant decrease in ZP value of carotenoid-enriched oil-in-water emulsions after the intestinal phase, thus suggesting a relationship between the electrical charge characteristics during *in vitro* digestibility and the degree of lipolysis.

7.3.2 Bioaccessibility

The most important factors that should be considered when designing a delivery system for application in food are the bioaccessibility and bioavailability of bioactive compounds (Jafari et al., 2017). The low bioavailability of bioactive compounds that have beneficial health effects can be overcome by incorporating these compounds into delivery systems such as NLC (Khare & Vasisht, 2014; Weiss et al., 2009), which can promote the entrapment and delivery of lipophilic bioactive compounds in their absorption sites in the GIT.

The type of emulsifier can affect the rate and extent of lipid digestion (Park et al., 2018); thus, the bioaccessibility of β-carotene incorporated into NLC obtained with SL and Tween 80 was evaluated to assess the effect of these emulsifiers in the β-carotene delivery for intestinal absorption. We also intended to verify if the lipid matrices considered in this study were able to promote the protection and delivery of bioactive compound in the GIT, since studies on the β-carotene bioaccessibility incorporated in NLC obtained using FHSO and/or HOSO were not reported to date.

The β-carotene bioaccessibility percentages in the jejunum and ileum were calculated in relation to the initial amount present in NLC L_{β} and T_{β}, and in the control sample. As some studies on β-carotene bioaccessibility use foods rich in carotenoids as a control, a

food that present the same materials and proportions as the NLC (but without undergoing the HPH process) has been chosen as the control sample. The bioaccessibility of β-carotene incorporated into NLC L_β and NLC T_β, and in the control sample is shown in Figure 4.

The total β-carotene bioaccessibility values found were 0.5 %, 0.23 % and 2.27 % for the control sample, NLC L_β and NLC T_β, respectively. In order to explain the low β-carotene bioaccessibility values obtained in this study, a combination of different hypothesis was proposed. Carotenoids bioavailability in foods is typically very low, mainly due to low chemical stability of these compounds, which partially elucidates the values found in the *in vitro* dynamic digestibility experiments carried out in the present study. Significant β-carotene loss has probably occurred as a result of its degradation (e.g., oxidation, isomerization) during the passage through the GIT due to enzymatic action, pH, oxygen, presence of pro-oxidants and photodegradation. Additionally, some intrinsic characteristics of the *in vitro* dynamic GI system used in this work promoted the adsorption of carotenoids in the plastic bags (used inside the reactors to allow the peristaltic movements), and in the hollow fiber membranes (used to simulate the intestinal absorption) (Berni et al., 2020). Therefore, even though this dynamic *in vitro* digestibility model allows a better simulation of the conditions found in the human GIT, we verified that it is not possible to state that the β-carotene bioaccessibility values found in this study will reflect the *in vivo* values, mainly due to β-carotene losses that occurred during the passage through the dynamic system.

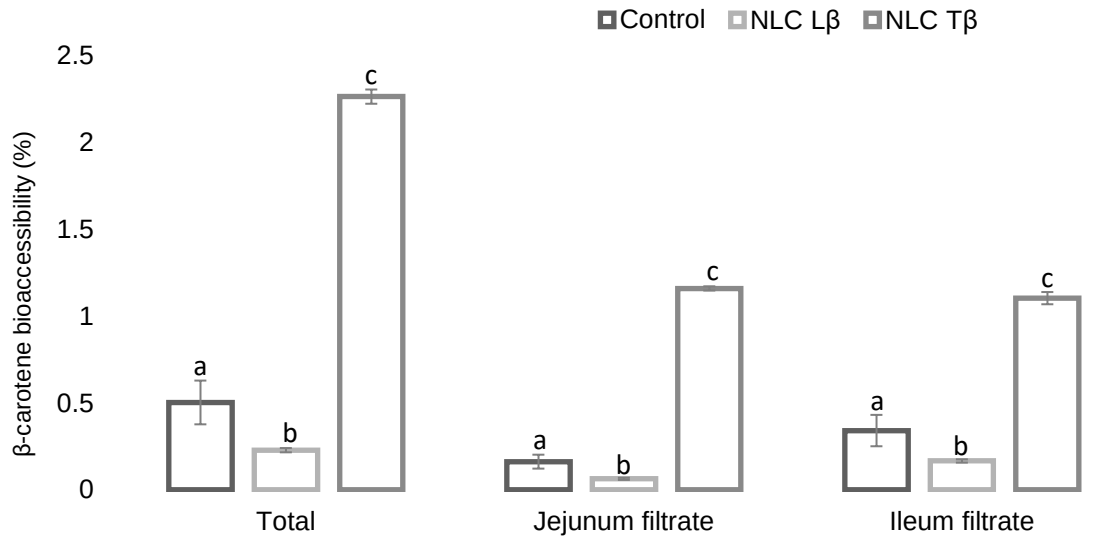

Figure 4: Bioaccessibility of β-carotene loaded NLC collected at different stages of *in vitro* digestion. Errors bars represent the standard deviation of n= 3 replicates. [a-c]Different letters indicate significant differences between the samples ($p< 0.05$).

Most of the studies carried out to assess β-carotene bioaccessibility used static *in vitro* digestibility systems. As *in vitro* static digestion models do not consider physical

processes that take place during the digestion, such as mixing, shear, changes in conditions over time or peristalsis (Lin et al., 2018) and normally, the particles remain in the same vessel throughout all the stages of digestion, the compounds' losses are not significant. Therefore, the β-carotene bioaccessibility found in studies that used static systems to evaluate the digestion behavior of lipid nanostructures usually obtain much higher than the values found in this study. For example, Salvia-Trujillo et al. (2013a) investigated the bioaccessibility of β-carotene incorporated in emulsions with different drop sizes (ranging from 0.2 to 23 μm) using a static digestibility system. The β-carotene bioaccessibility was around 59 % for the small size emulsion and 34 % for the large size emulsion. Han et al. (2019) studied the effect of the carrier oil, medium chain triglycerides (MCT) and long chain triglycerides (LCT), in the β-carotene bioaccessibility of emulsion-based delivery systems, using a static digestibility system. The β-carotene bioaccessibility found was 23.1 % and 65.5 % for the MCT and LCT emulsions, respectively. In another study, Yi et al. (2015) evaluated the bioaccessibility of β-carotene incorporated in NE (produced with different vegetable oils), using a two-stage *in vitro* digestion method. The authors found a β-carotene bioaccessibility close to 70 % in some NE delivery systems, positively correlated to the length of carrier oil. Abreu-Martins et al. (2020) studied the bioaccessibility of β-carotene incorporated in solid LN and liquid LN obtained from different lipid matrices (i.e., medium chain TAG, hydrogenated palm oil, glyceryl stearate) through a static digestibility method. The authors found that β-carotene bioaccessibility values ranged between 22.6 and 28.1%.

The differences in the bioaccessibility of β-carotene loaded NLC found using static and dynamic *in vitro* digestion systems was studied by Gomes et al. (2017). These authors prepared NLC with cupuacu butter and a mixture of two emulsifiers (Span 60 and Cremophor RH40). The β-carotene bioaccessibility in the static system was 92 % while in the dynamic system β-carotene bioaccessibility was nearly 20 %. These differences were attributed mainly to the more realistic digestion conditions simulated by the dynamic *in vitro* system and to β-carotene losses (11.8 %) along the process. The authors concluded that the dynamic system appeared to be more reliable to determine the bioaccessibility of bioactive compounds incorporated in the lipid nanoparticles. In another study, Gomes et al. (2019) evaluated the bioaccessibility of β-carotene loaded in NLC, produced with murumuru butter and a mixture of two non-ionic surfactants (Span 60 and Cremophor RH40) using a dynamic gastrointestinal system similar to the one used in our study. β-carotene bioaccessibility found in the dynamic system was about 42 %. β-carotene losses have also been reported in a study carried out by Berni et al. (2020) that used a similar dynamic gastrointestinal system equipment to assess the bioaccessibility of pitanga and buriti carotenoids (β-carotene and lycopene) loaded microemulsions. The β-carotene bioaccessibility values were approximately 2 % and 2.5 % for pitanga and buriti carotenoids loaded microemulsions, respectively. The authors attributed the

low β-carotene bioaccessibility values found to the carotenoid low stability and losses inside the dynamic gastrointestinal system.

One of the great advantages of nanoscale lipid-based delivery systems is the possibility of maintaining its large surface area until reaching the small intestine, thus promoting an increase in lipolysis rate. The smaller the lipid particle size, the greater the surface area available for lipase binding. Lipase has a globular shape of approximately 5 nm, so the smaller the size of the lipid particle/oil droplet, the greater the space covered by the lipase and, consequently, the greater the rate and extent of lipid digestibility (TAG conversion to FFA and MAG) (Salvia-Trujillo et al., 2017). The increase in lipolysis can generate more hydrolysis products (e.g., MAG and FFA), thereby, increasing mixed micelles production and the release and solubilization of bioactive compounds incorporated into the lipid phase; thus, making it more bioaccessible (Li & McClements, 2010; Salvia-Trujillo et al., 2017; Verrijssen et al., 2015). In our study, despite β-carotene losses observed throughout digestion, it was possible to verify β-carotene bioaccessibility differences between NLC L_β and NLC T_β. NLC L_β instability under gastric conditions was reflected in a lower bioaccessibility of β-carotene incorporated into these structures when compared to NLC T_β. As reported previously, the use of SL to stabilized NLC resulted in a drastic droplets destabilization under *in vitro* gastric conditions, promoting the PS increase from 176.2 (oral phase) to 1,181.17 nm (gastric phase). The PS, followed by the composition of the lipid matrix, are the factors that most affect the bioaccessibility of compounds incorporated into emulsion-based delivery systems (Zhou et al., 2018). This is mainly related to the surface area of lipid particles. In general, emulsifiers that lead to coalescence or flocculation of particles in the small intestine decrease the bioaccessibility of bioactive compounds incorporated into the particles (Tan et al., 2020).

Also, β-carotene bioaccessibility found for the NLC L_β was lower ($p<0.05$) compared to the value found for the control sample. As the use of Tween 80 has been shown to provide greater stability for the particles, the control sample was prepared using the same materials and the same proportions used to obtain the NLC T_β but without the HPH step. Through these results it was possible to verify that the use of SL to stabilize NLC did not promote the increase of the β-carotene bioaccessibility.

Moreover, the use of Tween 80 to stabilize NLC proved to be effective in increasing β-carotene bioaccessibility comparing to NLC L_β and to control sample, due the stability showed by these nanostructures under gastric conditions. Thus, NLC T_β surface area was maintained until reaching the small intestine, allowing larger area for lipase binding and consequently, increasing the release of β-carotene entrapped in the structure. A study carried out by Wang et al. (2012) demonstrated that the lower the PS, higher the inclusion efficiency of β-carotene in micelles. This fact reinforces our study results where NLC stabilized with

Tween 80 (NLC T_β) had a significantly higher bioaccessible fraction than NLC stabilized with SL (NLC L_β).

This study also demonstrated that the lipid matrices chosen to produce the NLC allowed to obtain NLC able to increase β-carotene bioaccessibility. FHSO, is obtained from the fully hydrogenation process of soybean oil. Fully hydrogenation was an alternative process found to be used for industrial plants previously used for the partial hydrogenation process, due to the need to adapt to zero trans fat legislation. Thus, from a widely available and inexpensive lipid matrix such as soybean oil, it is possible to obtain a lipid matrix with a high melting point composed of trisaturated TAG (stearic acid in this case) in a proportion similar to synthetic materials (Ribeiro et al., 2009, 2013; Wassell & Young, 2007). The genetic modification of conventional sunflower for the high oleic variety, through chemical mutagenesis and selective crossings, gave to HOSO ten times greater oxidative stability compared to soybean, canola and even sunflower oil of regular composition. So, this lipid matrix can be considered a premium raw material to obtain NLC at a much lower cost than oleic acid in its purified form (Gunstone, 2011; O'Brien, 2009). Thus, the results obtained in this study confirm that it is possible to increase β-carotene bioaccessibility using low cost lipid matrices available in the oil industry to obtain NLC, considering all the aspects discussed above.

7.3.3 Free fatty acids release

The pH-Stat method is an analytical tool with growing applications in the pharmaceutical and food fields for the characterization of lipid digestion under simulated small intestine conditions (Li & McClements, 2010). It is based on the amount of FFA released during the lipolysis process, by the addition of lipase at values close to neutrality (Li et al., 2011). During lipid digestion process, lipase acts by cleaving TAG ester bonds leading to the formation of two FFA and one MAG per TAG molecule. The formation of FFA in this process leads to a pH reduction of the medium. The pH drop is detected through electrodes that remain in contact with the sample throughout the analysis time. Upon detecting the drop, the equipment automatically adds NaOH so that the pH remains at predefined values. The volume of NaOH added to the samples is used to calculate the FFA generated by lipolysis.

In this study, the concentration of FFA released during the lipolysis process of NLC obtained with different emulsifiers was evaluated. Lipolysis assays were also performed on NLC without addition of pancreatic lipase, to demonstrate that the observed lipolysis occurred due to the action of the enzyme and not to particles autolysis (Jannin et al., 2015).

The lipolysis reaction occurred immediately after the onset of the intestinal phase (Figure 5). Up to 10 min of reaction, there was an exponential increase in FFA release. After this point, a stationary phase was reached, with a residual increase in FFA until the end of the

intestinal phase, which is in accordance with a study carried out by Abreu-Martins et al. (2020). The results obtained in our study suggest that the emulsifier molecules that originally covered the surface of the particle were rapidly displaced by bile salts and phospholipids present in the SIF, allowing the binding of lipase to lipid droplets' surface and consequently, FFA release (Qian et al., 2012).

The FFA concentration resulting from lipolysis is shown in the Figure 5. Results showed that Tween 80 used as an emulsifier to obtain NLC resulted in higher FFA release during the lipolysis process when compared to the use of SL. This high FFA production may be associated to the higher NLC T_{β} stability obtained with this emulsifier under gastric conditions. This is demonstrated through the PS value obtained after NLC passage through the GIT, which results in a higher surface area for of lipase and bile salts action (Pinheiro et al., 2013). Regarding NLC L_{β}, as previously discussed, there was a destabilization during gastric phase, leading to a significant increase in PS, which led to a reduction in the surface area for lipase binding and consequently, for lipolysis.

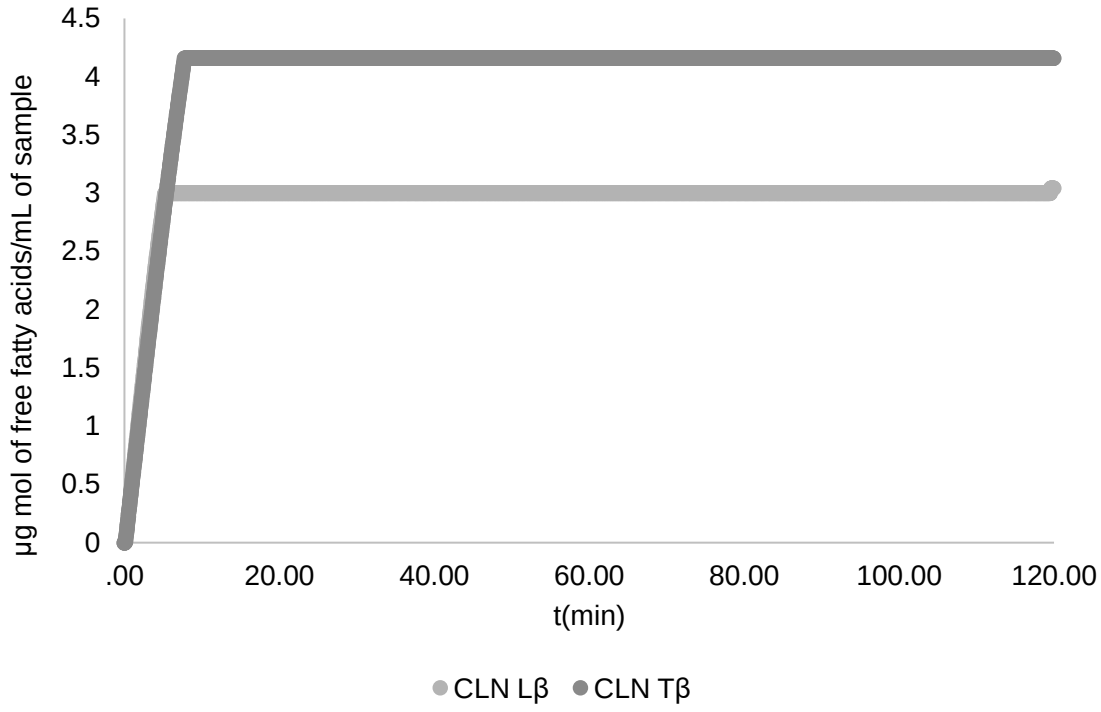

Figure 5: Free fatty acid release from β-carotene loaded NLC during *in vitro* digestion.

Similar behavior was observed in studies performed to evaluate the effect of different emulsifiers on the lipolysis rate of emulsion-based delivery systems. For example, Mun et al. (2007) investigated the influence of interfacial composition of corn oil-in-water emulsions coated by different emulsifiers (sodium caseinate, WPI, lecithin and Tween 20) on their *in vitro* digestion behavior. The authors found that the lipid droplets resistance to lipid

digestion decreased in the following order: non-ionic surfactant (Tween 20) > phospholipids (lecithin) > protein (caseinate or WPI). Pinheiro et al. (2013) studied the lipid digestion of curcumin-loaded NE prepared using corn oil and three different emulsifiers: Tween 20 (non-ionic), Sodium Dodecyl Sulphate (SDS, anionic) and DodecylTrimethylAmmonium Bromide (DTAB, cationic) through a pH-stat automatic titration unit. The Tween 20-stablized emulsion presented the highest total FFA produced, mainly due to the reduced emulsion droplet size throughout the simulated digestion. Park et al. (2018) evaluated the effect of emulsifiers, Tween 20 and soy lecithin, used to coat emulsions droplets containing β-carotene, on lipid digestion. Soy lecithin-stabilized emulsions showed the lowest rate and extent of lipid digestion compared to Tween 20-stabilized emulsions, which is in accordance to our work results. The authors attributed these results to the low emulsifying capacity presented by soy lecithin, showing coalescence of droplets after exposure to the gastric phase.

In general, the higher the FFA concentration released during lipid digestion, the higher the concentration of lipid species in the micellar fraction and, subsequently, the carotenoids micellarization capacity and bioaccessibility are higher (Salvia-Trujillo et al., 2017). However, the type of lipid species formed during digestion has also a strong influence on the solubilization capacity of mixed micelles and, consequently, on bioactive compound bioaccessibility. The presence of long-chain monounsaturated fatty acids, such as oleic acid, and long-chain monoacylglycerols in the micellar fraction, contribute to the increased β-carotene bioaccessibility (Abreu-Martins et al., 2020).

The results obtained in our study reinforce that the lipid digestion degree can be affected by the emulsifier used to stabilize NLC and highlight the direct relationship between bioaccessibility and the amount of FFA released during digestion. The NLC T_{β}, stabilized by a non-ionic emulsifier (Tween 80), presented the highest FFA release value during simulated lipolysis comparing to NLC L_{β}, which allowed a higher β-carotene delivery and superior amount of lipid products in mixed micelles. Thus, β-carotene bioaccessibility observed for NLC T_{β} was also higher than the one observed for the NLC L_{β}, due to a higher bioactive compound solubilization capacity (Lin et al., 2018; Wang et al., 2012), as discussed above.

7.3.4 Cytotoxicity

The reduced dimensions of the nanostructures provide a very large surface area, which can lead to some undesirable results after ingestion. Possible nanostructure-cell interactions can induce cytotoxicity and other consequences for the GIT (Martins et al., 2015). Typically, absorption occurs in epithelial cells of the inner walls of the small intestine and can be simulated using cell culture models (McClements & McClements, 2016). Thus, the knowledge related to toxicity and absorption of bioactive compounds and nanoparticles is important to establish delivery system effectiveness and safety (Mohammadi et al., 2019). The

NLC evaluated in this study were developed with the aim to be incorporated into foods, to produce effective functional foods through increased protection and delivery of bioactive compounds. Cellular viability studies are important to stablish the limiting amount of nanoparticles added to foods (Yu & Huang, 2013). So, we considered the digestive tract, especially the small intestine as the exposure route to NLC and β-carotene absorption. Caco-2 cell line was chosen in our study because it is a widely used line to study the cytotoxicity and absorption of bioactive compounds and nanoparticles (Jafari & McClements, 2017; Reboul et al., 2006).

The materials used to obtain NLC - free β-carotene, HOSO, Tween 80 and SL emulsifiers – were also tested to verify their possible individual cytotoxicity. FHSO was not tested due to its high melting point, which makes it difficult to dilute to perform the assay. It was observed that free β-carotene did not has a negative effect on cell viability (which was close to 100 %) at the concentrations tested (Figure 6a). Similar results were obtained by Yi et al. (2014), who demonstrated that β-carotene in its pure form at 0.1 % did not show cytotoxicity against Caco-2 cells. Han et al. (2019) also reported that pure β-carotene at concentration range of 0.1 - 0.005 $\mu g.ml^{-1}$ was not cytotoxic to Caco-2 cells. Also, the results showed that all materials used to produce NLC did not have a cytotoxic effect at the highest β-carotene concentration tested (25 µg/mL) (Figure 6b and 6c).

To investigate the effect of incorporating the bioactive compound into the NLC structure, we also evaluated the cytotoxicity of NLC obtained with Tween 80 and SL without β-carotene. Both free β-carotene NLC presented no cytotoxic effects at all the concentrations tested (Figure 6d and 6e), suggesting that these nanostructures did not show significant cytotoxicity to cells, even at the highest concentration tested (25 µg/mL). The interfacial NLC properties have an influence on their interactions with living cells and tissues. Thus, the emulsifier type used to stabilize NLC, its amount and interaction with the lipid core will have an effect on NLC performance in cells (Doktorovova et al., 2014). For example, Gomes et al. (2019) evaluated Caco-2 cells viability when in contact with β-carotene loaded NLC (produced using murumuru butter and a mixture of Span 60 and Cremophor RH40). The results indicated that NLC were toxic to the cells, probably due to the type of emulsifier used and to the extremely reduced particle size (ca. 35 nm). So, the authors concluded that a mixture of non-ionic surfactants and NLC with reduced average size can lead to a high level of cytotoxicity. In this sense, we verified that the emulsifiers used in this study to obtain NLC, SL and Tween 80, allowed the production of biocompatible and non-toxic particles. However, the entrapment of β-carotene in the NLC decreased cell viability for both NLC (Figure 6d and 6e). Regarding NLC $T_{\beta,}$ a significant ($p<0.05\%$) reduction in cell viability was observed with increasing of β-carotene concentration when compared to control, reaching values close to 86 % in higher concentration sample tested (25 µg/mL). A significant ($p<0.05\%$) reduction of cell viability was also observed

in the dilution of 25 μg/mL for NLC L_{β}, reaching values similar to those observed for NLC T_{β} at the same dilution (ca. 86 %). The effect of increased cytotoxicity in β-carotene loaded NLC can be explained by the better solubilization of the bioactive compound within the NLC structure being thus, available in higher concentration in the system (Doktorovova et al., 2014). Most authors who performed cell viability assays in LN consider that values above 70 % indicate that the particles do not present toxicity, and that the material can be considered safe (Doktorovova et al., 2014). In this context, although a reduction in cell viability (ca. 86 %) for β-carotene loaded NLC was observed, the values found indicate that these nanostructures are non-toxic and biocompatible. Also, Gonçalves et al. (2021b) found that different lipid-based nanostructures (NLC obtained with beewax as a solid lipid and MCT as a liquid lipid, lecithin and Tween 80 as emulsifiers) presented no cytotoxic effect at the highest concentration tested (40 μg/mL of curcumin).

The results obtained demonstrated that the lipid materials and emulsifiers tested in this study allow obtaining non-toxic, safe, and biocompatible NLC at the concentrations tested (1 - 25 μg/mL of β-carotene). However, the cell viability values obtained must be considered for the application of NLC in foods, and concentrations of β-carotene that allow a cell viability closer to 100 % must be chosen. Moreover, only by understanding the digestive fate of nanostructures/bioactive compounds is it possible to improve their performance and have conclusive information about the safety of nanostructures (Pinheiro et al., 2017).

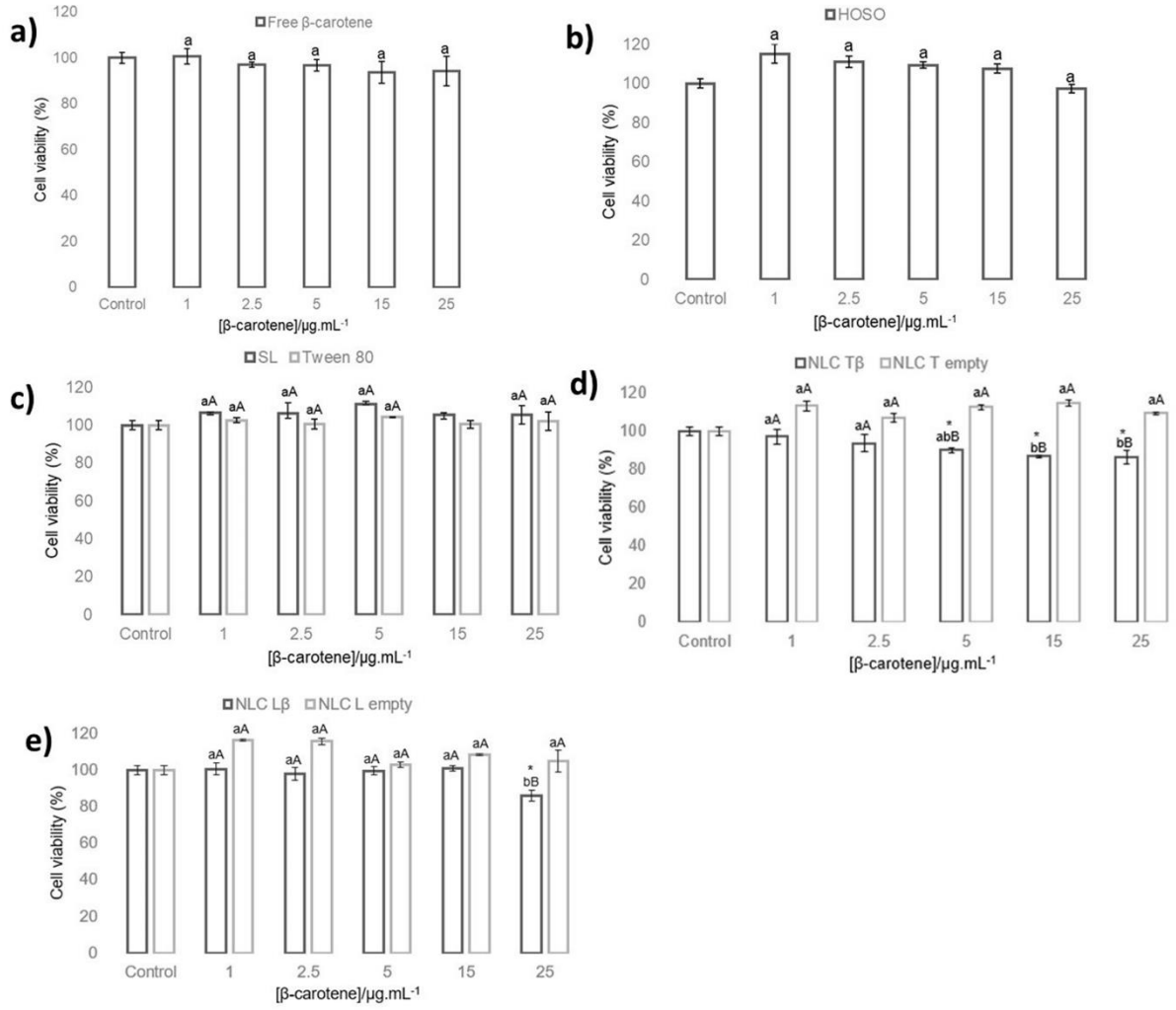

Figure 6: *In vitro* cell viability results for a) free β-carotene, b) high oleic sunflower oil (HOSO), c) emulsifiers (SL and Tween 80), d) NLC T_β and empty NLC T, and e) NLC L_β and empty NLC L measured by MTT assay. Errors bars represent the standard deviation (n= 3 replicates). $^{A\text{-}B}$ Different capital letters indicate significant differences between different samples tested at the same concentration ($p< 0.05$). $^{a\text{-}b}$ Different lower-case letters indicate significant differences between concentrations for the same sample ($p< 0.05$). *Asterisks indicate significant difference relative to the control group ($p< 0.05$).

7.4 Conclusions

The studies related to the *in vitro* digestibility and cytotoxicity of NLC provided relevant information about the behavior of these nanostructures in GIT, as well as their safety and biocompatibility. Presented results showed that the lipid digestion degree can be affected by the emulsifier used to stabilize NLC, since emulsifier directly influenced the stability of the particles under digestion. It was possible to verify that NLC obtained using Tween 80 (NLC T_β) as emulsifier showed better physical stability during the passage through an *in vitro* dynamic gastrointestinal system, compared to the other samples. Although the β-carotene losses in the dynamic gastrointestinal system were significantly high, the bioaccessible fraction found for

NLC T_β was relatively higher than the other samples tested, which is in line with the superior release of FFA observed for NLC T_β during the lipolysis process.

Both NLC developed and all the materials used for their production showed cell viabilities above 85 % at 25 µg/mL; thus, indicating the absence of cytotoxicity and the biocompatibility of the LN obtained.

The results obtained in this study are important for designing effective lipid-based nanodelivery systems, using conventional lipids derived from oil industry. In this context, the lipid materials considered, FHSO and HOSO, have great potential for obtaining non-toxic, biocompatible, and safe NLC, capable of promoting increased bioaccessibility of bioactive compounds, such as β-carotene.

7.5 Acknowledgments

Fernanda Luisa Ludtke acknowledges the Sao Paulo Research Foundation (FAPESP) for the financial support (grants #2018/03172-0, #2019/05176-6 and #2019/27354-3). Jean-Michel Fernandes and Raquel Gonçalves acknowledge the Foundation for Science and Technology (FCT) for their fellowship (SFRH/BD/147286/2019 and SFRH/BD/140182/2018, respectively). This study was supported by the Portuguese Foundation for Science and Technology (FCT) under the scope of the strategic funding of UIDB/04469/2020 unit.

7.6 References

Abreu-Martins, H. H., Artiga-Artigas, M., Hilsdorf Piccoli, R., Martín-Belloso, O., & Salvia-Trujillo, L. (2020). The lipid type affects the *in vitro* digestibility and β-carotene bioaccessibility of liquid or solid lipid nanoparticles. *Food Chemistry*, *311*, 126024. https://doi.org/10.1016/j.foodchem.2019.126024

Berni, P., Pinheiro, A. C., Bourbon, A. I., Guimarães, M., Canniatti-Brazaca, S. G., & Vicente, A. A. (2020). Characterization of the behavior of carotenoids from pitanga (*Eugenia uniflora*) and buriti (*Mauritia flexuosa*) during microemulsion production and in a dynamic gastrointestinal system. *Journal of Food Science and Technology*, *57*(2), 650–662. https://doi.org/10.1007/s13197-019-04097-7

Boon, C. S., McClements, D. J., Weiss, J., & Decker, E. A. (2010). Factors influencing the chemical stability of carotenoids in foods. *Critical Reviews in Food Science and Nutrition*, *50*(6), 515–532. https://doi.org/10.1080/10408390802565889

Das, N. M. A., Kobayashi, I., & Nakajima, M. (2020). Nanotechnology for bioactives delivery systems. *Journal of Food and Drug Analysis*, *20*(1), 184–188. https://doi.org/10.38212/2224-6614.2118

Davidov-Pardo, G., Gumus, C. E., & McClements, D. J. (2016). Lutein-enriched emulsion-based delivery systems: Influence of pH and temperature on physical and chemical stability. *Food Chemistry*, *196*, 821–827. https://doi.org/10.1016/j.foodchem.2015.10.018

Doktorovova, S., Souto, E. B., & Silva, A. M. (2014). Nanotoxicology applied to solid lipid nanoparticles and nanostructured lipid carriers - A systematic review of *in vitro* data. In *European Journal of Pharmaceutics and Biopharmaceutics,* 87(1), 1–18. https://doi.org/10.1016/j.ejpb.2014.02.005

Fang, C.-L., A. Al-Suwayeh, S., & Fang, J.-Y. (2012). Nanostructured Lipid Carriers (NLCs) for Drug Delivery and Targeting. *Recent Patents on Nanotechnology*, *7*(1), 41–55. https://doi.org/10.2174/18722105130105

Fathi, M., Varshosaz, J., Mohebbi, M., & Shahidi, F. (2013). Hesperetin-loaded solid lipid nanoparticles and nanostructure lipid carriers for food fortification: preparation, characterization, and modeling. *Food and Bioprocess Technology*, *6*(6), 1464–1475. https://doi.org/10.1007/s11947-012-0845-2

Favé, G., Coste, T.C., & Armand, M. (2004). Physicochemical properties of lipids: New strategies to manage fatty acid bioavailability. *Cellular and Molecular Biology*, 50 (7), 815-831.

Fernandes, J.M., Madalena, D.A., Vicente, A.A., & Pinheiro, A.C. (2021) Influence of the addition of different ingredients on the bioaccessibility of glucose released from rice during dynamic *in vitro* gastrointestinal digestion. *International Journal of Food Sciences and Nutrition*, 72 (1), 45-56. https://doi.org/10.1080/09637486.2020.1763926

Fu, D., Deng, S., McClements, D. J., Zhou, L., Zou, L., Yi, J., Liu, C., & Liu, W. (2019). Encapsulation of β-carotene in wheat gluten nanoparticle-xanthan gum-stabilized Pickering emulsions: Enhancement of carotenoid stability and bioaccessibility. *Food Hydrocolloids*, *89*, 80–89. https://doi.org/10.1016/j.foodhyd.2018.10.032

Golding, M., & Wooster, T. J. (2010). The influence of emulsion structure and stability on lipid digestion. In *Current Opinion in Colloid and Interface Science*, 15(1–2), 90–101. https://doi.org/10.1016/j.cocis.2009.11.006

Gomes, G. V. L., Sola, M. R., Marostegan, L. F. P., Jange, C. G., Cazado, C. P. S., Pinheiro, A. C., Vicente, A. A., & Pinho, S. C. (2017). Physico-chemical stability and *in vitro* digestibility of beta-carotene-loaded lipid nanoparticles of cupuacu butter (*Theobroma grandiflorum*) produced by the phase inversion temperature (PIT) method. *Journal of Food Engineering*, *192*, 93–102. https://doi.org/10.1016/j.jfoodeng.2016.08.001

Gomes, G. V. L., Sola, M. R., Rochetti, A. L., Fukumasu, H., Vicente, A. A., & Pinho, S. C. (2019). β-carotene and α-tocopherol coencapsulated in nanostructured lipid carriers of murumuru (*Astrocaryum murumuru*) butter produced by phase inversion temperature method: characterisation, dynamic *in vitro* digestion and cell viability study. *Journal of Microencapsulation*, *36*(1), 43–52. https://doi.org/10.1080/02652048.2019.1585982

Gonçalves, R. F. S., Martins, J. T., Abrunhosa, L., Baixinho, J., Matias, A. A., Vicente, A. A., & Pinheiro, A. C. (2021b). Lipid-based nanostructures as a strategy to enhance curcumin bioaccessibility: Behavior under digestion and cytotoxicity assessment. *Food Research International*, *143*, 110278. https://doi.org/10.1016/j.foodres.2021.110278

Gonçalves, R. F. S., Martins, J. T., Abrunhosa, L., Vicente, A. A., & Pinheiro, A. C. (2021a). nanoemulsions for enhancement of curcumin bioavailability and their safety evaluation: effect of emulsifier type. *Nanomaterials*, *11*(3), 815. https://doi.org/10.3390/nano11030815

Gunstone, F. D. (2011). Production and Trade of Vegetable Oils. In *Vegetable Oils in Food Technology*, F.D. Gunstone (Ed.). 6th edition, vol. 2. Wiley-Blackwell. https://doi.org/10.1002/9781444339925.ch1

Gutiérrez, F. J., Albillos, S. M., Casas-Sanz, E., Cruz, Z., García-Estrada, C., García-Guerra, A., García-Reverter, J., García-Suárez, M., Gatón, P., González-Ferrero, C., Olabarrieta, I., Olasagasti, M., Rainieri, S., Rivera-Patiño, D., Rojo, R., Romo-Hualde, A., Sáiz-Abajo, M. J., & Mussons, M. L. (2013). Methods for the nanoencapsulation of β-carotene in the food sector. *Trends in Food Science and Technology,* 32(2), 73–83. https://doi.org/10.1016/j.tifs.2013.05.007

Han, J.-R., Gu, L.-P., Zhang, R.-J., Shang, W.-H., Yan, J.-N., McClements, D. J., Wu, H.-T., Zhu, B.-W., & Xiao, H. (2019). Bioaccessibility and cellular uptake of β-carotene in emulsion-based delivery systems using scallop (*Patinopecten yessoensis*) gonad protein isolates: effects of carrier oil. *Food & Function*, *10*(1), 49-60. https://doi.org/10.1039/C8FO01390J

Hentschel, A., Gramdorf, S., Müller, R. H., & Kurz, T. (2008). β-Carotene-loaded nanostructured lipid carriers. *Journal of Food Science*, *73*(2), N1-N6. https://doi.org/10.1111/j.1750-3841.2007.00641.x

Hou, Z., Liu, Y., Lei, F., & Gao, Y. (2014). Investigation into the *in vitro* release properties of β-carotene in emulsions stabilized by different emulsifiers. *LWT - Food Science and Technology*, *59*(2P1), 867–873. https://doi.org/10.1016/j.lwt.2014.07.045

How, C. W., Rasedee, A., & Abbasalipourkabir, R. (2013). Characterization and cytotoxicity of nanostructured lipid carriers formulated with olive oil, hydrogenated palm oil, and polysorbate 80. *IEEE Transactions on Nanobioscience*, *12*(2), 72–78. https://doi.org/10.1109/TNB.2012.2232937

Hur, S. J., Decker, E. A., & McClements, D. J. (2009). Influence of initial emulsifier type on microstructural changes occurring in emulsified lipids during *in vitro* digestion. *Food Chemistry*, *114*(1), 253–262. https://doi.org/10.1016/j.foodchem.2008.09.069

Jafari, S. M., & McClements, D. J. (2017). Nanotechnology approaches for increasing nutrient bioavailability. *Advances in Food and Nutrition Research,* 81, 1–30. https://doi.org/10.1016/bs.afnr.2016.12.008

Jafari, S. M., Paximada, P., Mandala, I., Assadpour, E., & Mehrnia, M. A. (2017). Nanoencapsulation Technologies for the Food and Nutraceutical Industries Encapsulation by nanoemulsions. In *Nanoencapsulation Technologies for the Food and Nutraceutical Industries*. https://doi.org/10.1016/B978-0-12-809436-5/00002-1

Jannin, V., Dellera, E., Chevrier, S., Chavant, Y., Voutsinas, C., Bonferoni, C., & Demarne, F. (2015). *In vitro* lipolysis tests on lipid nanoparticles: Comparison between lipase/co-lipase and pancreatic extract. *Drug Development and Industrial Pharmacy*, *41*(10), 1582–1588. https://doi.org/10.3109/03639045.2014.972412

Khalid, M., Saeed-ur-Rahman, Bilal, M., Iqbal, H. M. N., & Huang, D. (2019). Biosynthesis and biomedical perspectives of carotenoids with special reference to human health-related applications. *Biocatalysis and Agricultural Biotechnology,* 17, 399–407. https://doi.org/10.1016/j.bcab.2018.11.027

Khare, A. R., & Vasisht, N. (2014). Nanoencapsulation in the Food Industry: Technology of the Future. In *Microencapsulation in the Food Industry*, Editor(s): A. G. Gaonkar, N. Vasisht, A. R. Khare, R. Sobel (Eds.), Microencapsulation, pp. 151–155. *Academic Press*. https://doi.org/10.1016/b978-0-12-404568-2.00014-5

Kopec, R. E., & Failla, M. L. (2018). Recent advances in the bioaccessibility and bioavailability of carotenoids and effects of other dietary lipophiles. *Journal of Food Composition and Analysis,* 68, 16–30. https://doi.org/10.1016/j.jfca.2017.06.008

Lakshmi, P., & Kumar, G. A. (2010). Nano-suspension technology: A review. *International Journal of Pharmacy and Pharmaceutical Sciences*, *4*, 35–40.

Li, Y., Hu, M., & McClements, D. J. (2011). Factors affecting lipase digestibility of emulsified lipids using an *in vitro* digestion model: Proposal for a standardised pH-stat method. *Food Chemistry*, *126*(2), 498–505. https://doi.org/10.1016/j.foodchem.2010.11.027

Li, Y., & McClements, D. J. (2010). New mathematical model for interpreting pH-stat digestion profiles: Impact of lipid droplet characteristics on *in vitro* digestibility. *Journal of Agricultural and Food Chemistry*, *58*(13), 8085–8092. https://doi.org/10.1021/jf101325m

Lin, Q., Liang, R., Williams, P. A., & Zhong, F. (2018). Factors affecting the bioaccessibility of β-carotene in lipid-based microcapsules: Digestive conditions, the composition, structure and physical state of microcapsules. *Food Hydrocolloids,* 77, 187–203. https://doi.org/10.1016/j.foodhyd.2017.09.034

Martins, J. T., Ramos, Ó. L., Pinheiro, A. C., Bourbon, A. I., Silva, H. D., Rivera, M. C., Cerqueira, M. A., Pastrana, L., Malcata, F. X., González-Fernández, Á., & Vicente, A. A. (2015). Edible bio-based nanostructures: delivery, absorption and potential toxicity. In *Food Engineering Reviews,* 7(4), 491–513. https://doi.org/10.1007/s12393-015-9116-0

McClements, D. J. (2013). Utilizing food effects to overcome challenges in delivery of lipophilic bioactives: Structural design of medical and functional foods. *Expert Opinion on Drug Delivery,* 10(12), 1621–1632. https://doi.org/10.1517/17425247.2013.837448

McClements, D. J., Decker, E. A., Park, Y., & Weiss, J. (2009). Structural design principles for delivery of bioactive components in nutraceuticals and functional foods. *Critical Reviews in Food Science and Nutrition*, *49*(6), 577–606. https://doi.org/10.1080/10408390902841529

McClements, D. J., Li, F., & Xiao, H. (2015). The nutraceutical bioavailability classification scheme: Classifying nutraceuticals according to factors limiting their oral bioavailability. *Annual Review of Food Science and Technology,* 6, 299–327. https://doi.org/10.1146/annurev-food-032814-014043

McClements, D. J., & Li, Y. (2010). Structured emulsion-based delivery systems: Controlling the digestion and release of lipophilic food components. *Advances in Colloid and Interface Science,* 159(2), 213–228. https://doi.org/10.1016/j.cis.2010.06.010

McClements, D. J., & Rao, J. (2011). Food-Grade nanoemulsions: formulation, fabrication, properties, performance, biological fate, and potential toxicity. *Critical Reviews in Food Science and Nutrition*. 51(4), 285–330. https://doi.org/10.1080/10408398.2011.559558

McClements, J., & McClements, D. J. (2016). Standardization of nanoparticle characterization: methods for testing properties, stability, and functionality of edible nanoparticles. *Critical Reviews in Food Science and Nutrition*, *56*(8), 1334–1362. https://doi.org/10.1080/10408398.2014.970267

Mohammadi, M., Assadpour, E., & Jafari, S. M. (2019). Encapsulation of food ingredients by nanostructured lipid carriers (NLCs). In *Nanoencapsulation in the Food Industry, Lipid-Based Nanostructures for Food Encapsulation Purposes.* S. M. Jafari (Ed.), Academic Press, 2, 217–270. Academic Press. https://doi.org/10.1016/b978-0-12-815673-5.00007-6

Mulet-Cabero, A.-I., Egger, L., Portmann, R., Ménard, O., Marze, S., Minekus, M., le Feunteun, S., Sarkar, A., Grundy, M. M.-L., Carrière, F., Golding, M., Dupont, D., Recio, I., Brodkorb, A., & Mackie, A. (2020). A standardised semi-dynamic *in vitro* digestion method suitable for food – an international consensus. *Food & Function*, *11*(2), 1702–1720. https://doi.org/10.1039/C9FO01293A

Mun, S., Decker, E. A., & McClements, D. J. (2007). Influence of emulsifier type on *in vitro* digestibility of lipid droplets by pancreatic lipase. *Food Research International*, *40*(6), 770-781. https://doi.org/10.1016/j.foodres.2007.01.007

Namitha, K. K., & Negi, P. S. (2010). Chemistry and biotechnology of carotenoids. *Critical Reviews in Food Science and Nutrition*, *50*(8), 728–760. https://doi.org/10.1080/10408398.2010.499811

O'Brien, R. D. (2009). Fats and Oils: Formulating and Processing for Applications, R. D. O'Brien (Ed.), 3rd edition. CRC Press. https://doi.org/10.1201/9781420061673

Oliveira, D. R. B., Michelon, M., de Figueiredo Furtado, G., Sinigaglia-Coimbra, R., & Cunha, R. L. (2016). β-Carotene-loaded nanostructured lipid carriers produced by solvent displacement method. *Food Research International*, *90*, 139–146. https://doi.org/10.1016/j.foodres.2016.10.038

Park, S., Mun, S., & Kim, Y. R. (2018). Emulsifier Dependent *in vitro* Digestion and Bioaccessibility of β-Carotene Loaded in Oil-in-Water Emulsions. *Food Biophysics*, *13*(2), 147–154. https://doi.org/10.1007/s11483-018-9520-0

Pezeshki, A., Hamishehkar, H., Ghanbarzadeh, B., Fathollahy, I., Keivani Nahr, F., Khakbaz Heshmati, M., & Mohammadi, M. (2019). Nanostructured lipid carriers as a favorable delivery system for β-carotene. *Food Bioscience*, *27*, 11–17. https://doi.org/10.1016/j.fbio.2018.11.004

Pinheiro, A. C., Coimbra, M. A., & Vicente, A. A. (2016). *In vitro* behaviour of curcumin nanoemulsions stabilized by biopolymer emulsifiers – Effect of interfacial composition. *Food Hydrocolloids*, *52*, 460-467. https://doi.org/10.1016/j.foodhyd.2015.07.025

Pinheiro, A. C., Gonçalves, R. F., Madalena, D. A., & Vicente, A. A. (2017). Towards the understanding of the behavior of bio-based nanostructures during *in vitro* digestion. *Current Opinion in Food Science,* 15, 79–86. https://doi.org/10.1016/j.cofs.2017.06.005

Pinheiro, A. C., Lad, M., Silva, H. D., Coimbra, M. A., Boland, M., & Vicente, A. A. (2013). Unravelling the behaviour of curcumin nanoemulsions during *in vitro* digestion: Effect of the surface charge. *Soft Matter*, *9*(11), 3147–3154. https://doi.org/10.1039/c3sm27527b

Pinsirodom, P., & Parkin, K. L. (2001). Lipase Assays. *Current Protocols in Food Analytical Chemistry*, 00: C3.1.1-C3.1.13. https://doi.org/10.1002/0471142913.fac0301s00

Pinto, M. F., Moura, C. C., Nunes, C., Segundo, M. A., Costa Lima, S. A., & Reis, S. (2014). A new topical formulation for psoriasis: Development of methotrexate-loaded nanostructured lipid carriers. *International Journal of Pharmaceutics*, *477*(1–2), 519–526. https://doi.org/10.1016/j.ijpharm.2014.10.067

Porter, C. J. H., Trevaskis, N. L., & Charman, W. N. (2007). Lipids and lipid-based formulations: Optimizing the oral delivery of lipophilic drugs. *Nature Reviews Drug Discovery,* 6(3), 231–248. https://doi.org/10.1038/nrd2197

Qian, C., Decker, E. A., Xiao, H., & McClements, D. J. (2012). Nanoemulsion delivery systems: Influence of carrier oil on β-carotene bioaccessibility. *Food Chemistry*, *135*(3). https://doi.org/10.1016/j.foodchem.2012.06.047

Reboul, E., Klein, A., Bietrix, F., Gleize, B., Malezet-Desmoulins, C., Schneider, M., Margotat, A., Lagrost, L., Collet, X., & Borel, P. (2006). Scavenger Receptor Class B Type I (SR-BI) Is Involved in Vitamin E Transport across the Enterocyte. *Journal of Biological Chemistry*, *281*(8). https://doi.org/10.1074/jbc.M509042200

Rehman, A., Tong, Q., Jafari, S. M., Assadpour, E., Shehzad, Q., Aadil, R. M., Iqbal, M. W., Rashed, M. M. A., Mushtaq, B. S., & Ashraf, W. (2020). Carotenoid-loaded nanocarriers: A comprehensive review. *Advances in Colloid and Interface Science*, 275, 102048. https://doi.org/10.1016/j.cis.2019.102048

Ribeiro, A. P. B., Basso, R. C., Grimaldi, R., Gioielli, L. A., dos Santos, A. O., Cardoso, L. P., & Guaraldo Gonçalves, L. A. (2009). Influence of chemical interesterification on thermal behavior, microstructure, polymorphism and crystallization properties of canola oil and fully hydrogenated cottonseed oil blends. *Food Research International*, *42*(8), 1153–1162. https://doi.org/10.1016/j.foodres.2009.05.016

Ribeiro, A. P. B., Basso, R. C., & Kieckbusch, T. G. (2013). Effect of the addition of hardfats on the physical properties of cocoa butter. *European Journal of Lipid Science and Technology*, *115*, 301-312. https://doi.org/10.1002/ejlt.201200170

Ribeiro, H. S., & Cruz, R. C. D. (2005). Biliquid foams containing carotenoids. *Engineering in Life Sciences*, *5*(1), 84–88. https://doi.org/10.1002/elsc.200403367

Salvia-Trujillo, L., Qian, C., Martín-Belloso, O., & McClements, D. J. (2013a). Influence of particle size on lipid digestion and β-carotene bioaccessibility in emulsions and nanoemulsions. *Food Chemistry*, *141*(2), 1472–1480. https://doi.org/10.1016/j.foodchem.2013.03.050

Salvia-Trujillo, L., Qian, C., Martín-Belloso, O., & McClements, D. J. (2013b). Modulating β-carotene bioaccessibility by controlling oil composition and concentration in edible nanoemulsions. *Food Chemistry*, *139*(1–4), 878–884. https://doi.org/10.1016/j.foodchem.2013.02.024

Salvia-Trujillo, L., Verkempinck, S. H. E., Sun, L., van Loey, A. M., Grauwet, T., & Hendrickx, M. E. (2017). Lipid digestion, micelle formation and carotenoid bioaccessibility kinetics: Influence of emulsion droplet size. *Food Chemistry*, *229*, 653–662. https://doi.org/10.1016/j.foodchem.2017.02.146

Salvia-Trujillo, L., Verkempinck, S. H. E., Zhang, X., van Loey, A. M., Grauwet, T., & Hendrickx, M. E. (2019). Comparative study on lipid digestion and carotenoid bioaccessibility of emulsions, nanoemulsions and vegetable-based in situ emulsions. *Food Hydrocolloids*, *87*, 119–128. https://doi.org/10.1016/j.foodhyd.2018.05.053

Santos, P. P., Andrade, L. de A., Flôres, S. H., & Rios, A. de O. (2018). Nanoencapsulation of carotenoids: a focus on different delivery systems and evaluation parameters. *Journal of Food Science and Technology,* 55(10), 3851–3860. https://doi.org/10.1007/s13197-018-3316-6

Shah, R., Eldridge, D., Palombo, E., & Harding, I. (2015). Lipid nanoparticles: production, characterization and stability. In *SpringerBriefs in Pharmaceutical Science & Drug Development,* IX, 97. Springer International Publishing. 10.1007/978-3-319-10711-0 .

Singh, H., Ye, A., & Horne, D. (2009). Structuring food emulsions in the gastrointestinal tract to modify lipid digestion. *Progress in Lipid Research,* 48(2), 92–100. https://doi.org/10.1016/j.plipres.2008.12.001

Souto, E. B., Wissing, S. A., Barbosa, C. M., & Müller, R. H. (2004). Evaluation of the physical stability of SLN and NLC before and after incorporation into hydrogel formulations. *European Journal of Pharmaceutics and Biopharmaceutics*, *58*(1), 83–90. https://doi.org/10.1016/j.ejpb.2004.02.015

Tamjidi, F., Shahedi, M., Varshosaz, J., & Nasirpour, A. (2013). Nanostructured lipid carriers (NLC): A potential delivery system for bioactive food molecules. *Innovative Food Science and Emerging Technologies,* 19, 29–43. https://doi.org/10.1016/j.ifset.2013.03.002

Tan, Y., & McClements, D. J. (2021). Improving the bioavailability of oil-soluble vitamins by optimizing food matrix effects: A review. *Food Chemistry*, *348*. https://doi.org/10.1016/j.foodchem.2021.129148

Tan, Y., Zhang, Z., Zhou, H., Xiao, H., & McClements, D. J. (2020). Factors impacting lipid digestion and ß-carotene bioaccessibility assessed by standardized gastrointestinal model (INFOGEST): Oil droplet concentration. *Food and Function*, *11*(8), 7126–7137. https://doi.org/10.1039/d0fo01506g

Valenzuela, A., Delplanque, B., & Tavella, M. (2011). Stearic acid: A possible substitute for trans fatty acids from industrial origin. *Grasas y Aceites*, *62*(2), 131–138. https://doi.org/10.3989/gya.033910

van Aken, G. A., Bomhof, E., Zoet, F. D., Verbeek, M., & Oosterveld, A. (2011). Differences in *in vitro* gastric behaviour between homogenized milk and emulsions stabilised by Tween 80, whey protein, or whey protein and caseinate. *Food Hydrocolloids*, *25*(4), 781-788. https://doi.org/10.1016/j.foodhyd.2010.09.016

van Loo-Bouwman, C. A., Naber, T. H. J., Minekus, M., van Breemen, R. B., Hulshof, P. J. M., & Schaafsma, G. (2014). Food matrix effects on bioaccessibility of β-carotene can be measured in an *in vitro* gastrointestinal model. *Journal of Agricultural and Food Chemistry*, *62*(4), 950–955. https://doi.org/10.1021/jf403312v

Verkempinck, S. H. E., Salvia-Trujillo, L., Moens, L. G., Charleer, L., van Loey, A. M., Hendrickx, M. E., & Grauwet, T. (2018). Emulsion stability during gastrointestinal conditions effects lipid digestion kinetics. *Food Chemistry*, *246*, 179–191. https://doi.org/10.1016/j.foodchem.2017.11.001

Verrijssen, T. A. J., Smeets, K. H. G., Christiaens, S., Palmers, S., van Loey, A. M., & Hendrickx, M. E. (2015). Relation between *in vitro* lipid digestion and β-carotene bioaccessibility in β-carotene-enriched emulsions with different concentrations of l-α-phosphatidylcholine. *Food Research International*, *67*, 60–66. https://doi.org/10.1016/j.foodres.2014.10.024

Wang, P., Liu, H. J., Mei, X. Y., Nakajima, M., & Yin, L. J. (2012). Preliminary study into the factors modulating β-carotene micelle formation in dispersions using an *in vitro* digestion model. *Food Hydrocolloids*, *26*(2), 427–433. https://doi.org/10.1016/j.foodhyd.2010.11.018

Wang, X., Lin, Q., Ye, A., Han, J., & Singh, H. (2019). Flocculation of oil-in-water emulsions stabilised by milk protein ingredients under gastric conditions: Impact on *in vitro* intestinal lipid digestion. *Food Hydrocolloids*, *88*, 272–282. https://doi.org/10.1016/j.foodhyd.2018.10.001

Wassell, P., & Young, N. W. G. (2007). Food applications of trans fatty acid substitutes. *International Journal of Food Science & Technology*, *42,* 503-517. https://doi.org/10.1111/j.1365-2621.2007.01571.x

Weiss, J., Gaysinsky, S., Davidson, M., & McClements, J. (2009). Nanostructured Encapsulation Systems: Food Antimicrobials. In *Global Issues in Food Science and Technology,* G. Barbosa-Cánovas, A. Mortimer, D. Lineback, W. Spiess, K. Buckle, P. Colonna (Eds), 425–479. Academic Press. https://doi.org/10.1016/B978-0-12-374124-0.00024-7

Yang, T. S., Liu, T. T., & Liu, H. I. (2017). Effects of aroma compounds and lipid composition on release of functional substances encapsulated in nanostructured lipid carriers lipolyzed by lipase. *Food Hydrocolloids*, *62*, 280–287. https://doi.org/10.1016/j.foodhyd.2016.08.019

Yi, J., Lam, T. I., Yokoyama, W., Cheng, L. W., & Zhong, F. (2014). Controlled release of β-carotene in β-lactoglobulin-dextran- conjugated nanoparticles" *in vitro* digestion and transport with caco-2 monolayers. *Journal of Agricultural and Food Chemistry*, *62*(35), 8900–8907. https://doi.org/10.1021/jf502639k

Yi, J., Zhong, F., Zhang, Y., Yokoyama, W., & Zhao, L. (2015). Effects of lipids on *in vitro* release and cellular uptake of β-carotene in nanoemulsion-based delivery systems. *Journal of Agricultural and Food Chemistry*, *63*(50), 10831–10837. https://doi.org/10.1021/acs.jafc.5b04789

Yu, H., & Huang, Q. (2013). Investigation of the cytotoxicity of food-grade nanoemulsions in Caco-2 cell monolayers and HepG2 cells. *Food Chemistry*, *141*(1), 29–33. https://doi.org/10.1016/j.foodchem.2013.03.009

Yuan, Y., Gao, Y., Zhao, J., & Mao, L. (2008). Characterization and stability evaluation of β-carotene nanoemulsions prepared by high pressure homogenization under various emulsifying conditions. *Food Research International*, *41*(1), 61–68. https://doi.org/10.1016/j.foodres.2007.09.006

Zardini, A. A., Mohebbi, M., Farhoosh, R., & Bolurian, S. (2018). Production and characterization of nanostructured lipid carriers and solid lipid nanoparticles containing lycopene for food fortification. *Journal of Food Science and Technology*, *55*(1), 287–298. https://doi.org/10.1007/s13197-017-2937-5

Zhang, R., Zhang, Z., Zou, L., Xiao, H., Zhang, G., Decker, E. A., & McClements, D. J. (2015). Enhancing nutraceutical bioavailability from raw and cooked vegetables using excipient emulsions: influence of lipid type on carotenoid bioaccessibility from carrots. *Journal of Agricultural and Food Chemistry*, *63*(48), 10508–10517. https://doi.org/10.1021/acs.jafc.5b04691

Zhou, X., Wang, H., Wang, C., Zhao, C., Peng, Q., Zhang, T., & Zhao, C. (2018). Stability and *in vitro* digestibility of beta-carotene in nanoemulsions fabricated with different carrier oils. *Food Science and Nutrition*, *6*(8), 2537–2544. https://doi.org/10.1002/fsn3.862

Zou, L., Zheng, B., Zhang, R., Zhang, Z., Liu, W., Xiao, H., & McClements, D. J. (2016). Enhancing the bioaccessibility of hydrophobic bioactive agents using mixed colloidal dispersions: curcumin-loaded zein nanoparticles plus digestible lipid nanoparticles, *Food Research International*, *81*, 74-82. https://doi.org/10.1016/j.foodres.2015.12.035

CAPÍTULO VIII

DISCUSSÃO GERAL

8. DISCUSSÃO GERAL

O desenvolvimento das pesquisas em nanotecnologia demonstra que sistemas de liberação em nanoescala exibem funcionalidade superior quando comparados aos sistemas convencionais de encapsulação, justificando o grande interesse por nano-sistemas carreadores, que se caracterizam pela alta estabilidade cinética e termodinâmica. Neste contexto, nanopartículas desenvolvidas à base de lipídios estão entre as tecnologias de incorporação e entrega de compostos bioativos mais promissoras no campo da nanotecnologia. O grande potencial de aplicação de sistemas lipídicos em nanoescala, a exemplo dos carreadores lipídicos nanoestruturados (CLN), encontra-se bem estabelecido na indústria farmacêutica, e consiste em um foco atual das pesquisas no campo da ciência de alimentos. Como uma das principais tendências no desenvolvimento destas estruturas, destaca-se o uso de óleos e gorduras comestíveis e/ou comercialmente disponíveis no âmbito da indústria de alimentos, em substituição às matrizes lipídicas sintéticas, que se mostram pouco viáveis para aplicações alimentícias, em termos de custo e de aspectos regulatórios.

Em virtude da importância da abordagem nanotecnológica associada à área de óleos e gorduras, no que se refere à aplicação de materiais lipídicos diversos e ao conhecimento de suas propriedades de cristalização, este trabalho teve como objetivo a obtenção de CLN com incorporação de β-caroteno utilizando matérias-primas convencionais na indústria de alimentos. A escolha dos materias lipídicos utilizados neste estudo (OSTH e OGAO) foi realizada com base nas seguintes premissas: emprego de frações lipídicas biocompatíveis, representadas por gorduras naturais ou resultantes de processos usuais de modificação lipídica; e utilização de sistemas lipídicos com características de composição química e propriedades de cristalização adequadas ao desenvolvimento de nanoestruturas. Para atender os objetivos propostos, o projeto foi dividido em quatro etapas que, sequencialmente, trouxeram informações pertinentes acerca da obtenção de nanopartículas lípidicas.

A mudança de escala altera as propriedades dos materiais lipídicos utilizados para a obtenção de CLN, em consequência do aumento da área superficial e da mudança nas forças físicas que atuam sobre essas partículas (SIEGRIST *et al*., 2008). Assim sendo, o conhecimento das propriedades físicas e de cristalização das matrizes lipídicas utilizadas para obtenção dos CLN é importante para otimizar sua formação, estabilidade e atuação funcional (KHARAT; MCCLEMENTS, 2019). Nesse sentido, avaliamos a composição, as propriedades físicas e de cristalização de sistemas lipídicos compostos por OSTH e OGAO, com o intuito de obter CLN com características de cristalinidade adequadas para a incorporação de compostos bioativos.

Os sistemas lipídicos foram compostos por OSTH:OGAO (m/m) nas proporções 90:10, 80:20, 70:30, 60:40, 50:50, 40:60, 30:70, 20:80 e 10:90 e caracterizados quanto a composição química, cristalinidade e propriedades físicas gerais para a obtenção de nanopartículas lipídicas. Consideramos, para a avaliação microscópica e do hábito polimórfico, a estabilização das amostras através de dois métodos: o primeiro (MI) correspondendo ao método recomendado pela metodologia oficial (AOCS, 2009), e o segundo (MII) ao protocolo usualmente empregado para recristalização da fase lipídica dispersa de CLN.

Uma vez que a composição química da fase lipídica utilizada em sua obtenção impacta fortemente tanto as características dos CLN, como a bioacessibilidade do composto bioativo incorporado à estrutura, verificamos que a composição em ácidos graxos dos sistemas lipídicos expressou o potencial do OSTH e OGAO para o desenvolvimento de CLN. O OSTH apresentou conteúdo expressivo de ácido esteárico, AG que além de possibilitar a obtenção de CLN biocompatíveis, devido a seu maior ponto de fusão contribui para a proteção e entrega do composto bioativo incorporado à estrutura. O OGAO apresentou conteúdo expressivo de ácido oleico, o que representa, além da possibilidade de obtenção de CLN com propriedades físico-químicas adequadas para a incorporação de compostos bioativos, a possibilidade de solubilização, proteção e entrega dos compostos no local de absorção no TGI humano.

De forma geral o aumento de OGAO nos sistemas lipídicos OSTH:OGAO modificou as propriedades térmicas, a cristalinidade e composição em TAG e AG da base lipídica totalmente saturada (OSTH). O aumento na proporção de OGAO nos sistemas lipídicos OSTH:OGAO promoveu a redução no conteúdo de gordura sólida e no ponto de fusão, a diminuição da temperatura inicial de cristalização e da temperatura final de fusão, a redução do percentual de área cristalizada e do diâmetro médio dos cristais, devido ao incremento de TAG triinsaturados provenientes dessa fonte lipídica.

Tanto o hábito polimórfico, avaliado por difração de Raios-X, quanto à formação da rede cristalina, avaliada por microscopia de luz polarizada, foram influenciados pelo método de estabilização. Nesse sentido, quando avaliados através do método que considera o protocolo usualmente empregado para recristalização da fase lipídica dispersa dos CLN (MII), os sistemas lipídicos OSTH:OGAO apresentaram estabilização na forma polimórfica mais estável (β) precocemente ao método sugerido nos protocolos oficiais (MI). Para a maior parte dos sistemas lipídicos o percentual de área cristalizada foi inferior e o diâmetro médio dos cristais foi superior para o MII quando comparado ao MI, reforçando a importância da recristalização da fase lipídica utilizada para obtenção de CLN a baixas temperaturas, após o rompimento das partículas em escala nanométrica.

Todos os sistemas lipídicos OSTH:OGAO (m/m) avaliados apresentaram compatibilidade total e ao menos um evento de fusão próximo ou acima de 37°C, indicando resistência térmica a temperatura corporal. Através dos resultados obtidos com a caracterização dos sistemas lipídicos pode-se direcioná-los de acordo com as suas propriedades físico-químicas e de cristalização para a obtenção de CLN com finalidades específicas. Assim sendo, os sistemas lipídicos OSTH:OGAO (m/m) 90:10, 80:20 e 70:30 representam sistemas com elevada cristalinidade; os sistemas lipídicos 60:40, 50:50 e 40:60 apresentam cristalinidade intermediária; enquanto os sistemas 30:70 e 20:80 representam sistemas lipídicos de baixa cristalinidade. O sistema lipídico 10:90 OSTH:OGAO (m/m) não apresentou propriedades físicas e de cristalização adequadas para obtenção de CLN.

A redução de escala de macro para nano teve início na Etapa I, que correspondeu a uma abordagem exploratória inicial da avaliação de emulsificantes, com diferentes características funcionais e estruturais, e das condições de processo de homogeneização a alta pressão para obtenção de CLN. Para isto, realizou-se a obtenção de CLN a partir de triestearina (TS) e trioleína (TO), matrizes lipídicas purificadas e amplamente empregadas na produção de nanopartículas pela indústria farmacêutica, porém de elevado custo. A escolha dessas matrizes lipídicas correspondeu a um sistema lipídico modelo, composto por materiais cuja eficiencia para a obtenção de nanopartículas estáveis foi amplamente comprovada e estudada nos últimos anos. O sistema lipídico utilizado para composição de CLN, correspondeu a proporção TS:TO (m/m) de 40:60, representativa da composição equivalente entre ácidos graxos saturados e insaturados.

Há alguns desafios a serem transpostos para a aplicação de CLN em produtos alimentícios, dentre eles a seleção do emulsificante adequado para a obtenção das partículas, uma vez que o número de emulsificantes aprovados para uso alimentar é limitado. Baseado nesta premissa, consideramos a investigação da efetividade de cinco emulsificantes com características químicas e estruturais distintas, com ampla faixa de valores de balanço hidrofílico lipofílico (BHL) e capacidade emulsificante, visando o maior entendimento sobre o desempenho dos emulsificantes em processos de HAP na obtenção de CLN de composição lipídica regular. Dessa forma, avaliamos o efeito de emulsificantes naturais (Lecitina de soja modificada enzimaticamente, isolado proteico do soro de leite e de soja) e sintéticos (Tween 80 e Span 60) na obtenção de CLN através da HAP.

As condições de processo da HAP foram definidas através de um planejamento fatorial completo 2^2 com três repetições no ponto central, que considerou pressões de homogeneização (PH) variando de 700 a 900 bar, e o número de 1 a 3 ciclos (NC), como variáveis independentes. Considerando as configurações mais típicas dos equipamentos HAP, optamos por este planejamento devido principalmente a sensibilidade das condições de

processo consideradas como variáveis independentes, que poderiam representar condições difíceis de serem executadas na prática caso optássemos por outro planejamento.

As condições operacionais otimizadas para obtenção dos CLN foram definidas a partir da avaliação da distribuição de tamanho de partículas das amostras de NL, avaliadas a 24hs e 15 dias após a obtenção, considerando-se o Tamanho de Partícula (TP), Índice de Polidispersidade (IP) e o Potencial Zeta (PZ) como as variáveis dependentes do planejamento experimental. Cinco planejamentos fatoriais foram realizados, um para cada emulsificante, com o intuito de avaliar individualmente o efeito de cada emulsificante sobre as características dos CLN. Neste estudo, as condições de processo PH e NC afetaram significativamente algumas das variáveis dependentes consideradas, indicando assim, através das superfícies de resposta, curvas de contorno e modelos lineares, as condições ótimas para cada variável e cada emulsificante específico. A efetividade dos emulsificantes considerados neste estudo foi afetada de acordo com suas características físico-químicas e estruturais.

Verificamos que as variáveis independentes consideradas no planejamento fatorial afetaram a obtenção de CLN de distintos modos: a PH foi responsável pelo rompimento das gotículas de óleo, e o NC pela formação de novas interfaces e o recobrimento das gotículas formadas. De forma geral, os modelos lineares obtidos após a ANOVA indicaram que as dimensões dos CLN obtidos utilizando emulsificantes não-iônicos, Tween 80 e Span 60, foram afetadas apenas pelo NC aplicados durante a HAP, o que sugere que o maior NC proporciona o maior recobrimento das partículas por estes emulsificantes, promovendo assim, a redução do TP e IP. O uso de LS para a estabilização de CLN resultou na obtenção de modelos lineares que indicam que as variáveis dependentes (TP, IP e PZ) foram afetadas por todas as variáveis independentes (PH e NC). A efetividade da LS para a obtenção de CLN pode ser explicada pela similaridade da estrutura química deste emulsificante com a fase lipídica e seu peso molecular intermediário dentre os emulsificantes considerados, resultando em efetiva interação com os componentes lipídicos e efetiva taxa de recobrimento das partículas obtidas. No caso de proteínas, devido à instabilidade física apresentada pela dispersão contendo os CLN estabilizados com SPI, foi impossível inferir como cada variável (PH e NC) afetou a obtenção de nanoestruturas com este emulsificante. Já as dimensões dos CLN obtidos com WPI foram afetadas apenas pela PH aplicada, indicando que para emulsificantes que apresentam maior peso e tamanho molecular, foi necessário a aplicação de maior pressão para a redução da tensão superficial e, assim, a obtenção de CLN de menores dimensões.

Observamos, dessa forma, que a obtenção tecnológica de CLN utilizando Span 60 e SPI foi inviabilizada, principalmente por características estruturais destes emulsificantes, incompatíveis com a velocidade necessária para recobrimento da partícula e a interação entre a molécula emulsificante e a fase lipídica dispersa. Os demais emulsificantes (Tween 80, LS

e WPI) foram considerados efetivos para a obtenção de CLN. Embora as condições de processo ótimas tenham sido indicadas para cada variável e para cada emulsificante específico, partindo de um sistema lipídico padrão, neste estudo representado por um sistema modelo contendo teores equivalentes de ácidos graxos saturados e insaturados, recomendamos as condições do ponto central (PH=700bar e NC=2) para a obtenção de CLN, por serem satisfatórias e por representarem, na prática, condições de processo intermediárias em termos da prevenção do desgaste do homogeneizador a alta pressão.

Considerando os resultados obtidos a partir da caracterização dos sistemas lipídicos OSTH:OGAO (m/m), selecionou-se os sistemas 80:20, 60:40, 40:60 e 20:80 como representativos das faixas de cristalinidade (baixa, intermediária e alta) para compor os CLN na Etapa II, a fim de verificar a influência da composição lipídica sob as propriedades físicas e de cristalização destas nanoestruturas. LS, Tween 80 e WPI foram utilizados individualmente como emulsificantes, resultando na obtenção de 12 nanoestruturas distintas. As condições de processo empregadas foram a pressão de 700bar e 2 ciclos de homogeneização, conforme definido na Etapa I. Os CLN foram avaliados segundo os parâmetros: TP, IP e PZ; Comportamento térmico na fusão; Conteúdo de gordura sólida; Polimorfismo; Morfologia e Estabilidade física via *Turbiscan* após 48hs, 7, 15, 30, e 60 dias de estabilização a 25°C.

Os resultados obtidos neste estudo demonstraram que os emulsificantes considerados para a obtenção de CLN (LS, Tween 80 e WPI) influenciaram mais as características físico-químicas dos nanocarreadores do que as propriedades térmicas e de cristalização. Todos os emulsificantes considerados proporcionaram a obtenção de CLN em escala nanométrica para todos os sistemas lipídicos. No entanto, as características estruturais destes emulsificantes e a interação com a fase lipídica, resultaram na obtenção de CLN com características distintas de acordo com o grau de saturação/insaturação do sistema lipídico. Devido à facilidade de associação tanto TAG/TAG, quanto TAG/emulsificante verificou-se a diminuição nas dimensões dos CLN obtidos com LS com o aumento do teor de AGS no sistema lipídico, sendo que, para este emulsificante, as menores dimensões foram observadas para os CLN obtidos com o sistema lipídico 80:20 (OSTH:OGAO) (TP<226,33 nm).

De maneira geral, quanto maior a habilidade de um emulsificante em reduzir a tensão superficial, menores serão os tamanhos das partículas obtidas (HAKANSSON *et al*., 2013). Assim sendo, nesta etapa, o uso de Tween 80 promoveu a obtenção de CLN com menores dimensões (TP 160,07- 223,00nm) durante os 60 dias de armazenamento. Devido às suas características estruturais e seu baixo peso molecular, este emulsificante se adsorve rapidamente a interface óleo/água, promovendo a obtenção de CLN com menores dimensões (LEE *et al*., 2013). No caso deste emulsificante, verificou-se o aumento no TP com aumento

do grau de insaturação do sistema lipídico, porém, apenas até a proporção 40:60 (OSTH:OGAO m/m). Os CLN obtidos a partir do sistema lipídico com maior grau de insaturação (20:80 OSTH:OGAO m/m) apresentaram dimensões inferiores ao CLN obtido com o sistema lipídico 40:60 OSTH:OGAO (m/m), indicando que devido ao fato do Tween 80 apresentar em sua estrutura um ácido graxo monoinsaturado, ocorreu uma maior interação entre o emulsificante e o alto teor de ácido oleico presente no sistema lipídico 20:80 (OSTH:OGAO) promovendo, assim, a obtenção de partículas com menores dimensões (PINTO; DE BARROS; FONSECA, 2018).

No caso do WPI, não foi possível estabelecer uma relação linear entre o aumento/diminuição do grau de insaturação do sistema lipídico com a redução/aumento do TP. As menores dimensões foram encontradas para o CLN W60:40, sendo inferiores a 260 nm durante os 60 dias de armazenamento. O uso deste emulsificante resultou na obtenção de CLN com maiores dimensões (256,33 a 360,67nm) durante os 60 dias de armazenamento, devido principalmente à sua estrutura globular e heterogênea, o que promove a difusão de forma mais lenta para a interface, resultando assim, na obtenção de partículas com maiores dimensões.

O grau de insaturação do sistema lipídico não afetou parâmetros como PZ e IP quando obtidos a partir do mesmo emulsificante; entretanto diferenças foram observadas quando os CLN foram obtidos a partir de emulsificantes distintos, indicando que o tipo de emulsificante utilizado para obtenção de CLN tem influência direta sobre o PZ e o IP destas nanoestruturas. Em relação ao IP, os CLN obtidos utilizando WPI como emulsificante apresentaram menores valores de IP (1,56-1,81). Porém os demais CLN (obtidos com LS e Tween 80) apresentaram valores de IP inferiores a 2,5 indicando partículas homogêneas e com distribuição granulométrica estreita do sistema (SCHAFFAZICK *et al*., 2003).

Todos os CLN apresentaram |PZ| > 20 mV, indicando boa estabilidade física ao longo dos 60 dias, devido à repulsão eletrostática entre as partículas, minimizando possível tendência ao fenômeno de agregação. Uma das maneiras de confirmar a estabilidade física é pela análise de Turbidimetria através do *Turbiscan*. A determinação da estabilidade física via *Turbiscan* demonstrou que quanto maior o grau de insaturação do sistema lipídico, maior a instabilidade física verificada para os CLN, associada a alterações no retroespalhamento da luz durante o período de armazenamento. Esta avaliação representou fator determinante para escolha do sistema lipídico a ser utilizado para incorporação de β-caroteno.

Verificamos que o comportamento térmico, o polimorfismo e o SFC foram governados pela composição dos sistemas lipídicos. Diferenças no grau de instauração do sistema lipídico promoveram a obtenção de CLN com diferentes comportamentos térmicos, sendo que, quanto maior o grau do insaturação do sistema lipídico, menor temperatura de pico e entalpia de fusão foram observadas. Não foi possível verificar pico de fusão para todos

os CLN obtidos com o sistema lipídico 20:80 OSTH:OGAO (m/m), indicando que a utilização desse sistema para a obtenção de CLN com incorporação de compostos bioativos poderia comprometer tanto a estrutura, quanto a estabilidade dos compostos incorporados. As curvas de fusão dos CLN obtidos para os demais sistemas lipídicos mostraram um único evento endotérmico por volta de 60 °C, temperatura correspondente à fusão da matriz lipídica sólida nas nanopartículas (OSTH). A faixa de fusão observada para os CLN encontrou-se entre 62,54 e 67,15°C, indicando a resistência dessas nanoestruturas a temperatura corporal (37°C) e a possibilidade de aplicação dessas estruturas em alimentos submetidos a processamentos térmicos.

Observou-se a redução no conteúdo de gordura sólida (SFC) com o aumento do grau de insaturação do sistema lipídico, sendo que os CLN obtidos com o sistema lipídico 20:80 OSTH:OGAO (m/m) apresentaram os menores valores durante todo o período de armazenamento. O aumento no grau de insaturação, entretanto, não alterou a forma polimórfica dos CLN obtidos. Todos os CLN apresentaram estabilização na forma β desde as 48 hs após a obtenção, devido principalmente a grande homogeneidade da composição em ácidos graxos e triacilgliceróis do OSTH e OGAO, matérias-primas lipídicas que apresentam a tendência a estabilização dos cristais na forma polimórfica β.

A redução de escala de macro para nano promoveu alterações significativas nas propriedades térmicas, no grau de cristalinidade e no hábito polimórfico das matrizes lipídicas utilizadas neste estudo. Os CLN apresentaram maior SFC e estabilização polimórfica na forma mais estável (β) desde as 48hs, indicando ausência de transições polimórficas tardias que ocorreram nos sistemas lipídicos em macroescala, conforme discutido anteriormente. Estes resultados sugerem que, embora a caracterização em macroescala forneça importantes informações acerca do comportamento de sistemas lipídicos, é substancial caracterizá-los em nanoescala em termos de propriedades térmicas e de cristalização.

Dentre os sistemas lipídicos considerados, os sistemas 80:20, 60:40 e 40:60 OSTH:OGAO (m/m) proporcionaram a obtenção de partículas estáveis e com características de cristalinidade adequadas para obtenção de CLN, uma vez que as propriedades térmicas, o SFC e as propriedades de cristalização foram mantidas durante os 60 dias de armazenamento. Tanto as transições polimórficas, quanto as propriedades térmicas não foram influenciadas pelo tempo de avaliação, devido principalmente ao fato das matérias primas de alto e baixo ponto de fusão utilizadas para a obtenção de CLN formarem sistemas muito compatíveis, que podem ser considerados sistemas robustos de cristalização.

A incorporação de uma fase lipídica de menor ponto de fusão em sistemas lipídicos para obtenção de CLN proporciona maior espaço para acomodação de compostos bioativos, resultando assim em uma maior capacidade de carga (MOHAMMADI; ASSADPOUR; JAFARI, 2019). Assim sendo, embora os demais sistemas lipídicos tenham

sido eficazes na obtenção de CLN, verificamos que o sistema lipídico 60:40 OSTH:OGAO (m/m) proporcionou a obtenção de CLN estáveis fisicamente (|PZ| > 20 mV), com tamanho de partícula em escala nanométrica (TP<260,67 nm), com boa estabilidade física via *Turbiscan*, temperatura de fusão (entre 56,93 e 63,00°C) adequada para aplicação em alimentos, sendo, portanto, selecionado como matriz lipídica para obtenção de CLN com incorporação de β-caroteno.

A Etapa III teve como intuito avaliar o potencial das estruturas CLN para a incorporação de compostos bioativos lipossolúveis. Nesse sentido, foram obtidos CLN com incorporação de β-caroteno, utilizando três distintos emulsificantes: LS (CLN L_β), Tween 80 (CLN T_β) e WPI (CLN W_β) para estabilização. A escolha pelo β-caroteno ocorreu em virtude de este ser um composto modelo para a avaliação de nanoestruturas como sistemas de entrega e liberação controlada em alimentos. Os CLN foram avaliados quanto à eficiência de incorporação e capacidade de carga do composto bioativo, bem como a avaliação da estabilidade cristalina e polimórfica das nanoestruturas com incorporação de β-caroteno, conforme a etapa anterior (II). Devido à instabilidade química apresentada pelo β-caroteno, nesta etapa a avaliação destes parâmetros ocorreu em um intervalo menor, incluindo, neste caso, a avaliação após 45 dias de obtenção.

A incorporação do β-caroteno às estruturas CLN promoveu o aumento signitificativo do TP observado para os CLN L_β e W_β, enquanto o CLN T_β manteve dimensões similares à nanoestrutura sem incorporação do composto bioativo, obtidos na Etapa II. Embora tenha se observado um aumento no TP para o CLN L_β, o TP observado durante o período considerado neste estudo esteve na faixa de 208,67-266,67nm. No caso do CLN W_β, a incorporação do β-caroteno à estrutura promoveu um aumento de aproximadamente 90 nm no TP, que apresentaram dimensões superiores a 340nm. Em contrapartida, quando obtidos com as mesmas condições, porém sem incorporação do bioativo na etapa anterior, os CLN apresentaram TP de aproximadamente 260nm durante os 60 dias de armazenamento. Esse aumento no TP com a incorporação do β-caroteno à estrutura pode ter ocorrido devido ao aumento da tensão interfacial e da viscosidade da fase lipídica dispersa com a solubilização do bioativo, dificultando a redução de tamanho durante a homogeneização (TAMJIDI *et al*., 2014).

Embora o uso de distintos emulsificantes tenha resultado na obtenção de partículas com cargas distintas, devido a composição e conformação estrutural das moléculas emulsificantes, todos os CLN obtidos apresentaram PZ superiores a |20mV|. O tipo de emulsificante utilizado para estabilização de CLN com incorporação de β-caroteno afetou a estabilidade física destas nanoestruturas em dispersão. A diferença na instabilidade física observada através dos perfis de retroespalhamento para os CLN pode ser explicada pelas diferentes características estruturais apresentadas entre eles. Dentre os emulsificantes

considerados neste estudo, o uso de Tween 80 proporcionou a obtenção de dispersões de CLN mais estáveis durante os 60 dias de armazenamento. Os demais emulsificantes considerados neste estudo proporcionaram a obtenção de dispersões de CLN menos estáveis, sendo que o uso de WPI para estabilização resultou na desestabilização precoce quando comparado aos demais CLN.

Tanto a redução de escala, quanto a incorporação do composto bioativo, não representaram a diminuição da cristalinidade do sistema, de forma contrária a incorporação do β-caroteno à estrutura, resultou em aumento na cristalinidade do sistema, que foi significativamente superior em comparação aos CLN obtidos sem incorporação do composto. Dentre os emulsificantes considerados neste estudo, o Tween 80 proporcionou a obtenção de CLN com maiores valores de SFC a 25°C, sendo superiores a 85%. A redução no SFC observada para os CLN L_β e W_β foi acompanhada da redução da estabilidade física via turbiscan com o passar do período de armazenamento.

Os diferentes emulsificantes considerados nesta etapa não afetaram a resistência térmica, tampouco o hábito polimórfico dos CLN obtidos, uma vez que não foram observadas diferenças significativas entre os CLN L_β, T_β e W_β. O comportamento térmico observado para os carreadores indicou a incorporação e solubilização completa do β-caroteno nas matrizes lipídicas que o compõem, uma vez que apenas um pico de fusão foi observado. As curvas de fusão dos CLN obtidos apresentaram um único evento endotérmico por volta de 60 °C, temperatura correspondente à fusão do OSTH, indicando que o comportamento térmico na fusão foi governado pela matriz lipídica de maior ponto de fusão utilizada para obtenção das nanoestruturas. De forma geral a incorporação de β-caroteno à estrutura CLN não afetou a temperatura inicial, final e de pico da fusão avaliados por DSC, quando comparados aos CLN sem incorporação do bioativo. No entanto, verificou-se um aumento na energia necessária para a fusão (ΔH J/g) nos CLN com incorporação de β-caroteno, o que pode estar relacionado a cristalinidade intrínseca deste composto.

A incorporação β-caroteno à estrutura promoveu, ainda, a alteração no hábito polimórfico dos CLN que se estabilizaram nas formas polimórficas β e β', enquanto as estruturas sem incorporação de β-caroteno se estabilizam na forma β desde as 48hs após a obtenção. Durante o processo de obtenção, o β-caroteno foi solubilizado na fase lipídica dos CLN, o que pode ter promovido uma associação com os TAG, e ainda com os emulsificantes utilizados para a obtenção das partículas, modificando, portanto, a forma em que os TAG se arranjaram e recristalizaram durante o resfriamento. O tempo de estabilização não teve efeito sobre o polimorfismo, indicando que os CLN não apresentaram transição polimórfica tardia, o que é desejável do ponto de vista de incorporação de compostos bioativos, pois neste caso, alterações polimórficas poderiam vir acompanhadas de alterações no formato da partícula e, consequentemente, resultar na expulsão do composto incorporado à estrutura.

Nesta etapa, avaliamos a separação dos CLN da dispersão através de dois métodos. No primeiro método, consideramos uma metodologia baseada em Oliveira *et al*. (2016), que consistiu na extração líquido-líquido do β-caroteno incorporado aos CLN. Já no segundo método consideramos a quantificação direta do β-caroteno incorporado através da separação dos CLN da dispersão aquosa por ultracentrifugação. Os valores encontrados para a capacidade de carga (CC) e para a eficiência de incorporação (EI) para o mesmo CLN foram muito distintos, e variaram conforme o método utilizado para extração do β-caroteno. Os valores encontrados após a extração pelo Método I indicam que este método não se mostrou adequado para a separação do β-caroteno incorporado nos CLN do β-caroteno livre. Através deste método, a CC e EI encontrada para os CLN L_{β}, T_{β} e W_{β} apresentou valores muito baixos que variaram durante o período de armazenamento, indicando que este método não refletiu as mudanças das dispersões e dos CLN que ocorreram com o tempo. Já os valores de CC e EI encontrados através do Método II, demonstraram que, neste estudo, a separação dos CLN das dispersões por ultracentrifugação mostrou-se mais adequada para o isolamento do β-caroteno incorporado nos CLN do β-caroteno livre. Por meio dos valores obtidos após a separação dos CLN da dispersão aquosa pelo Método II, verificou-se que o uso de Tween 80 proporcionou a obtenção de CLN com valores superiores de CC e EI de β-caroteno durante os 60 dias de armazenamento.

Apesar de todo seu potencial como sistemas de entrega de compostos bioativos, nanoestruturas para aplicações em alimentos estão associadas a algumas preocupações sobre a possível toxicidade. Somente através da compreensão do destino digestivo das nanoestruturas/compostos bioativos é possível melhorar seu desempenho e ter informações conclusivas sobre a segurança das nanoestruturas (PINHEIRO *et al*., 2017). Uma vez que a digestão lipídica está altamente correlacionada à biodisponibilidade de compostos bioativos lipossolúveis, pois os compostos precisam ser liberados da matriz lipídica e incorporados em micelas mistas formadas pelos produtos da digestão lipídica (TAN; MCCLEMENTS, 2021), a compreensão do processo de digestibilidade é fundamental para a determinação da bioacessibilidade destes compostos. Dessa forma, selecionou-se, em razão do conjunto de resultados obtidos na Etapa III, os CLN com incorporação de β-caroteno obtidos com LS (CLN L_{β}) e Tween 80 (CLN T_{β}) para o estudo da digestibilidade *in vitro* e citotoxicidade.

Para os experimentos de digestibilidade *in vitro* foi utilizado um modelo dinâmico, cuja montagem experimental é baseada no sistema TIM-1 (TNO intestinal model) e encontra-se no LIP, Centro de Engenharia Biológica/UMinho. Durante os ensaios, amostras foram coletadas e avaliadas quanto ao TP, IP e PZ com o intuito de avaliar o comportamento das nanoestruturas durante a passagem pelo TGI. Ao final do ensaio, amostras foram coletadas dos filtrados do jejuno e do íleo para determinação da bioacessibilidade do β-caroteno incorporado às estruturas CLN.

Uma das grandes vantagens dos CLN é o seu tamanho reduzido, o que reflete em uma área superficial maior para a ação das enzimas durante o processo digestivo. No entanto, para que essa vantagem potencial seja explorada, é preciso garantir que a partícula chegue ao intestino delgado com dimensões nanométricas, para assim facilitar a adsorção da lipase pancreática. As nanoestruturas consideradas neste estudo apresentaram comportamentos distintos durante a passagem pelo TGI. Os CLN T_{β} permaneceram estáveis durante a passagem pelo compartimento gástrico em contraste aos CLN L_{β} que apresentaram desestabilização sob condições gástricas, resultando em um aumento drástico no TP e IP dessas estruturas após a passagem pelo compartimento do estômago. A desestabilização encontrada para o CLN L_{β} refletiu em menor liberação de ácidos graxos e, consequentemente, em menor bioacessibilidade do β-caroteno incorporado à estrutura, conforme descrito a seguir.

Perdas significativas de β-caroteno ocorrem em consequência da degradação do composto (oxidação, isomerização, por exemplo) durante a passagem pelo TGI devido à ação enzimática, pH, oxigênio e presença de pró-oxidantes e pela fotodegradação. Aliado a isto, características do sistema de digestibilidade *in vitro* utilizado nos ensaios, promoveram a adsorção de carotenoides nos sacos *stomacher*, entre as peças de acrílico dos reatores e nas membranas de fibra ótica, acentuando ainda mais estas perdas (BERNI *et al*., 2020). A perda quantitativa média de β-caroteno no sistema encontrada neste estudo (superior a 62%) evidencia a necessidade de avaliações complementares relacionadas aos materiais utilizados para compor o sistema de digestibilidade *in vitro*, focados principalmente na redução de adsorção do composto.

Embora as perdas quantitativas de β-caroteno no sistema tenham sido significativamente elevadas, foi possível verificar diferenças entre as amostras consideradas. A fração bioacessível encontrada para o CLN T_{β} foi relativamente superior as demais amostras testadas nesse estudo, o que pode ser explicada pela maior estabilidade frente as condições do TGI conferida pelo Tween 80 aos CLN. A utilização de Tween 80 como emulsificante resultou ainda em maior liberação de ácidos graxos durante o processo de lipólise quando comparado ao uso de LS. Essa maior produção também pode estar associada à maior estabilidade das nanoestruturas, que permaneceram com TP em nanoescala após a passagem pelo compartimento gástrico, resultando assim, em uma maior área superficial disponível para ação da lipase.

Realizou-se ainda um estudo exploratório e inicial sobre a possível citotoxicidade das nanoestruturas e dos componentes utilizados para sua obtenção, com o intuito de determinar a quantidade limite a ser adicionada em sistemas alimentícios sem que haja danos celulares. Para tal, foram realizados ensaios de citotoxicidade considerando os materiais utilizados para a obtenção dos CLN (com exceção do OSTH), as estruturas CLN vazias, o

composto bioativo em sua forma livre e as estruturas CLN com incorporação do composto. O estudo foi realizado através da linhagem celular de adenocarcinoma do cólon humano - Caco-2 que fornece dados importantes relacionados principalmente à dose limite a ser ingerida, e corresponde a um dos principais modelos de absorção intestinal utilizados para o estudo das características de transporte e permeabilidade de compostos bioativos. Dessa forma, a determinação da viabilidade celular permitiu o estudo mais completo desde o momento da ingestão até a absorção intestinal dos CLN com incorporação de β-caroteno.

Mesmo quando testadas na diluição mais concentrada, as amostras consideradas neste estudo apresentaram viabilidade celular superior a 85%, indicando que tanto o material utilizado para obtenção, quanto os CLN obtidos são atóxicos e biocompatíveis. Assim sendo, deve-se considerar a concentração (µg de β-caroteno/ml) mais próxima a 100% de nanopartículas para a aplicação em alimentos sem que haja danos celulares. Cabe ressaltar que o material que estará em contato com as células não serão as partículas e, sim, as estruturas formadas a partir da digestão destas. Dessa forma, a ingestão deste tipo de nanoestrutura formada por estes materiais será provavelmente menos acentuada.

Esse estudo teve o intuito de realizar uma abordagem exploratória que englobasse desde as características moleculares das matrizes lipídicas até a absorção das nanoestruturas e dos compostos bioativos incorporados a estas no TGI humano. Em virtude do conjunto de dados obtidos e compilados, foi possível verificar o potencial de OSTH e OGAO, para a obtenção de CLN com incorporação de compostos bioativos. Isso representa, na prática, novas possibilidades de aplicações para matérias-primas disponíveis comercialmente e já utilizadas pela indústria de óleos e gorduras, bem como a redução no custo de obtenção de nanoestruturas lipídicas, que normalmente são obtidas com materiais lipídicos purificados. O uso de matrizes lipídicas disponíveis na indústria de óleos e gorduras representa a redução do custo de obtenção em aproximadamente 95%, tendo em conta os valores praticados no Brasil. Assim sendo, o OSTH e OGAO, apresentam elevado potencial como fontes lipídicas de ácidos graxos de alto e baixo ponto de fusão, respectivamente, proporcionando a obtenção de CLN com características de fusão adequada para incorporação de compostos bioativos em alimentos, como o β-caroteno avaliado neste estudo. A redução de escala modificou o comportamento das matrizes lipídicas consideradas neste estudo, ampliando, assim, a possibilidade de uso destas matérias-primas na indústria de alimentos.

Uma das maiores preocupações do uso de nanoestruturas na área de alimentos é a falta de conhecimento sobre como as propriedades físico-químicas em nanoescala podem alterar o destino biológico de nanoestruturas e a biodisponibilidade dos compostos bioativos incorporados a elas. Dessa forma, os ensaios de digestibilidade *in vitro* dinâmica e citotoxicidade de CLN com incorporação de β-caroteno trouxeram informações relevantes relacionadas à aplicação de nanoestruturas lipídicas em alimentos, indicando que tanto as

matérias-primas, quanto os CLN desenvolvidos, foram consideradas atóxicas e biocompatíveis. Assim, verificamos através deste estudo a possibilidade de modular a formulação das frações lipídicas utilizadas para obtenção de CLN, para uma digestibilidade lipídica direcionada para alcançar a bioacessibilidade ideal de compostos bioativos lipofílicos.

CAPÍTULO IX

CONCLUSÃO GERAL

9. CONCLUSÃO GERAL

Os resultados obtidos demonstraram que as matérias-primas lipídicas propostas neste estudo, possibilitaram a obtenção de CLN em escala nanométrica e com elevada estabilidade físico-química, para incorporação de compostos bioativos como o β-caroteno.

A técnica de homogeneização a alta pressão proporcionou a obtenção de CLN estáveis e em nanoescala, sendo que as condições do ponto central do planejamento experimental (pressão de 700 bar e 2 ciclos de homogeneização) foram consideradas como ideais para obtenção de CLN estáveis.

As propriedades físico-químicas dos CLN obtidos nas diferentes etapas do estudo foram influenciadas pela composição da fase lipídica (proporção OSTH:OGAO) e pelo emulsificante utilizado para este fim. De forma geral, à medida que a proporção de ácidos graxos saturados no sistema lipídico diminuiu, as partículas apresentaram maior tamanho, maior instabilidade física e menor temperatura de pico e entalpia de fusão. O aumento no grau de insaturação, entretanto, não alterou a forma polimórfica dos CLN obtidos.

No que se refere à efetividade dos emulsificantes verificou-se que, dentre os emulsificantes considerados neste estudo, o monooleato de sorbitana etoxilado, Tween 80, proporcionou a obtenção de CLN estáveis, com menores tamanhos de partícula, maior capacidade de incorporação do β-caroteno e maior estabilidade frente as condições gástricas. A adição dos emulsificantes não promoveu alteração na forma polimórfica dos CLN obtidos.

Os CLN obtidos, com e sem incorporação de β-caroteno, apresentaram elevada estabilidade cristalina, resistência à temperatura corporal e faixa de fusão adequada para incorporação em alimentos.

Através dos ensaios de digestibilidade *in vitro* dinâmica, foi possível verificar que os CLN obtidos utilizando Tween 80 como emulsificante apresentaram maior estabilidade física durante a passagem pelo TGI. Embora as perdas quantitativas de β-caroteno no sistema tenham sido significativamente elevadas, a fração bioacessível encontrada para essa nanoestrutura lipídica (CLN T_{β}) foi relativamente superior as demais amostras testadas, o que está de acordo com a maior liberação de ácidos graxos durante o processo de lipólise.

A realização de estudos relacionados a digestibilidade *in vitro* dinâmica e citotoxicidade de CLN forneceram informações pertinentes relativas à aplicação de nanoestruturas lipídicas em alimentos. Nesse sentido, constatou-se que o óleo de soja totalmente hidrogenado e o óleo de girassol alto oleico são consideradas matérias-primas

aptas para a obtenção de nanopartículas lipídicas seguras, com perfil toxicológico aceitável e biocompatíveis.

CAPÍTULO X

SUGESTÕES PARA TRABALHOS FUTUROS

10. SUGESTÕES PARA TRABALHOS FUTUROS

- Incorporação dos CLN produzidos em sistemas alimentícios e avaliação em termos de estabilidade do β-caroteno, digestibilidade *in vitro*;

- Determinar a bioacessibilidade do β-caroteno a partir de ensaios de digestibilidade utilizados modelos estáticos;

- Incorporação de outros compostos bioativos lipossolúveis às nanoestruturas desenvolvidas neste estudo;

- Verificar a influência do ponto de fusão de CLN com sob a bioacessibilidade do composto bioativo;

- Estudo da linhagem das células Caco-2 integradas com amostras recolhidas após os ensaios de digestibilidade *in vitro,* com o intuito de avaliar a citotoxicidade dos efluxos da digestão e verificar o efeito das mudanças causadas pela passagem no TGI sobre a absorção de compostos bioativos;

- Estudo da citotoxicidade *in vivo* com intuito de correlacionar com os dados obtidos após os ensaios *in vitro*;

- Estudo da composição em ácidos graxos liberados após os ensaios de digestibilidade, tanto nos efluxos recolhidos, quanto no método de titulação automática, a fim de verificar qual ácido graxo é liberado preferencialmente de acordo com as matérias primas;

- Realizar estudos contemplando diferentes concentrações de óleos vegetais para compor a fase lipídica e assim verificar a influência do conteúdo lipídico (%) na bioacessibilidade de compostos bioativos.

- Estudo amplo com fontes lipídicas com composição em ácidos graxos o mais variada possível, a fim de verificar o comportamento e a influência da composição da matriz lipídica no processo digestivo.

- Estudo da estabilidade de CLN durante e após o processamento de alimentos, como pasteurização, esterilização, desidratação, tratamentos térmicos.

- Estudo da estabilidade de CLN submetidos a condições extremas de pH, força iônica, temperatura e umidade.

MEMÓRIA DO PERÍODO DE DOUTORADO

MEMÓRIA DO PERÍODO DE DOUTORADO

A doutoranda Fernanda Luisa Lüdtke ingressou no programa de pós-graduação em Tecnologia de Alimentos do Departamento de Tecnologia de Alimentos/FEA/Unicamp em fevereiro de 2016. Durante o período de doutorado foram obtidos 33 créditos nas disciplinas que seguem: TP240–Tecnologia de Café e Cacau, TP242–Lípides em Alimentos e Implicações Nutricionais, TP188–Tópicos Especiais sobre Lipídios, TP199–Seminários, TP357–Microencapsulação Aplicada a Alimentos e Nutrientes, TP121–Tópicos em Engenharia de Alimentos, AP200–Técnicas de Comunicações nas Apresentações em Público, TP256–Análise Instrumental Aplicada a Lipídios, TP333–Planejamento Experimental e Otimização de Processos.

Além das disciplinas cursadas, a doutoranda atuou no Programa de Estágio Docente (PED) com atividades de apoio parcial junto à docência da disciplina TA221–Característica e Pré–Processamento de Grãos por dois períodos, durante dois períodos (como voluntária no período de março a julho de 2017 e como bolsista no período de março a julho de 2018), agregando mais 4 créditos.

A doutoranda usufruiu por 29 meses (março de 2016 a julho de 2018) de auxílio financeiro da Capes. Tendo aprovada a bolsa de Doutorado Regular junto à FAPESP (Processo 2018/03172–0), passou a usufruir do auxílio no mês de agosto de 2018 que se estendeu até fevereiro de 2021. Além do auxílio de Doutorado Regular, a doutoranda usufruiu de auxílio na modalidade de Bolsa de Estágio e Pesquisa no Exterior (BEPE) (Processo 2019/05176–6) durante o período de julho de 2019 a outubro de 2020, considerando um período adicional de 4 meses no exterior devido aos inconvenientes da pandemia.

A doutoranda participou em 2016 da organização do Fórum de Debates "Mitos e Verdades sobre o Óleo de Coco", realizado na Unicamp e do Fórum de Debates II: "Mitos e Verdades sobre o Óleo de Canola", realizado na Unicamp/Limeira. No mesmo ano, participou ainda do Workshop técnicas instrumentais avançadas na avaliação da cristalização de óleos e gorduras: teoria e prática, organizado pelo Laboratório de óleos e gorduras/FEA/Unicamp. Em 2017 participou do Workshop de Azeite de Oliva, organizado pelo Laboratório de óleos e gorduras/FEA/Unicamp e do congresso internacional 17th AOCS Latin American Congress and Exhibition on Fats, Oils and Lipids, realizado em Cancún, México. No mesmo ano, participou da equipe organizadora do 12º Simpósio Latino Americano de Ciência de Alimentos, realizado em Campinas. No ano de 2018, a doutoranda participou da 2ª Reunião de Usuários de Criomicroscopia Eletrônica, organizada pelo Centro Nacional de Pesquisa em Energia e Materiais–CNPEMM. Em 2019, participou da organização do Simpósio Internacional "OILS and FATS for the future: the next decade", evento organizado pelo Laboratório de óleos e gorduras/FEA/Unicamp. Ainda no mesmo ano participou do III Workshop: Bioproducts and

Fuels, realizado pela FEA/Unicamp; do Workshop Novas Soluções para Análises Rápidas de Gordura e Proteína, realizado no DEB/UMinho/Portugal; e do congresso internacional “17th Euro Fed Lipid Congress And Expo” realizado em Sevilha, Espanha.

Em 2020, a doutoranda participou de uma série de eventos organizados pela FEA/Unicamp denominados Conexão FEA– Mesa Redonda Online, correspondendo aos seguintes temas: Digestão *in vitro* e Bioacessibilidade: Avanços e Desafios, e Enzimas: uma relação dinâmica e versátil com a pesquisa e a indústria. Participou, no mesmo ano, da organização do Webinar Tópicos em óleos e gorduras que correspondeu a quatro módulos: Módulo I – Cristalização e técnicas instrumentais em óleos e gorduras, Módulo II – Legislação e reformulação de produtos de base lipídica, Módulo III – Refino e Modificação de Óleos e Gorduras e Módulo IV – Biotecnologia aplicada a área de óleos e gorduras. No ano de 2021 participou dos eventos Conexão FEA – Mesa Redonda Online denominados Impressão 3D – aplicações em alimentos e biomedicina; Alimentos Funcionais; e Emulsões na Indústria de Alimentos.

As pesquisas referentes ao projeto de Doutorado resultaram até o momento em 1 artigo experimental que será submetido ao periódico *Journal of Food Engineering*; 2 artigos experimentais que serão submetidos ao periódico *Journal of Food Structure*; 1 artigo experimental que será submetido ao periódico *Food Research International* e 1 artigo experimental que será submetido ao periódico *Food & Function,* e em 7 trabalhos publicados em anais de eventos (*17th AOCS Latin American Congress and Exhibition on Fats, Oils and Lipids*, *18th Latin American Congress and Exhibition on Fats, Oils and Lipids* e *17th Euro Fed Lipid Congress And Expo*).

Artigos submetidos a periódicos

LÜDTKE, F.L.; STAHL, M.A.; GRIMALDI, R.; FORTE, M.B.S.; GIGANTE, M.L.; RIBEIRO, A.P.B. Performance of natural and synthetic emulsifiers in the optimization of high pressure homogenization conditions to produce nanostructured lipid carriers. *Journal of Food Engineering*.

LÜDTKE, F.L.; GRIMALDI, R.; CARDOSO, L.P., RIBEIRO, A.P.B Lipid systems based on fully hydrogenated soybean oil and high oleic sunflower oil to obtain nanostructured lipid carriers: composition, physical properties, and crystallization parameters. *Food Structure*.

LÜDTKE, F.L.; STAHL, M.A.; GRIMALDI, R.; CARDOSO, L.P.; GIGANTE, M.L.; RIBEIRO, A.P.B. High oleic sunflower oil and fully hydrogenated soybean oil nanostructured lipid carriers: development and characterization. *Food Structure*.

LÜDTKE, F.L.; GRIMALDI, R.; CARDOSO, L.P.; GIGANTE, M.L.; VICENTE, A.A.; RIBEIRO, A.P.B. Development and characterization of β–carotene–loaded nanostructured lipid carriers produced with fully hydrogenated soybean oil and high oleic sunflower oil. *Food Research International*.

LÜDTKE, F.L.; FERNANDES, J.M.; GONÇALVES, R.F.; MARTINS, J.T.; BERNI, P.; RIBEIRO, A.P.B.; PINHEIRO, A.C.; VICENTE, A.A. Fully hydrogenated soybean oil and high oleic sunflower oil β–carotene loaded nanostructured lipid carriers: cytotoxicity and bioaccessibility. *Food & Function.*

Artigos publicados em revistas científicas

SILVA, T. J.; GRIMALDI, L. M.; **LÜDTKE, F. L**.; SILVA, M. G.; GODOI, K. R. R.; GRIMALDI, R.; RIBEIRO, A. P. B. Açai oil: Physicochemical properties and aplication potential. INFORM magazine – American Oil Chemists' Society. INFORM magazine – American Oil Chemists' Society, p. 22 – 24, 2021.

GRIMALDI, L. M.; GODOI, K. R. R.; **LÜDTKE, F. L.**; SILVA, T. J.; SILVA, M. G.; GRIMALDI, R.; RIBEIRO, A.P. B. Lauric fats from the Brazilian Amazon: babassu and murumuru. IInform (Champaign): International News on Fats, Oils and Related Materials, p. 18 – 20, 2021.

SILVA, M. G.; GRIMALDI, L. M.; GODOI, K. R. R.; **LÜDTKE, F. L.**; SILVA, T. J.; GRIMALDI, R.; RIBEIRO, A.P. B. Physicochemical and thermal behavior of tucumã oil and butter. IInform (Champaign): International News on Fats, Oils and Related Materials, p. 24 – 27, 2021.

LÜDTKE, F.L.; GRIMALDI, L. M.; SILVA, T. J.; GODOI, K. R. R.; SILVA, M. G.; GRIMALDI, R. RIBEIRO, A.P. B. Physicochemical properties of Andiroba (Carapa guianensis) and Pracaxi (Pentaclethra macroloba) oils. IInform (Champaign): International News on Fats, Oils and Related Materials, p. 30 – 33, 2021.

GRIMALDI, L. M.; **LÜDTKE, F.L.**; SILVA, T. J.; GODOI, K. R. R.; SILVA, M. G.; GRIMALDI, R.; RIBEIRO, A.P. B. Crystallization profile of bacuri (Platonia insigns) and cupuacu (*Theobrama grandiflorum*) fats from the Brazilian Amazon Rainforest. International News on Fats, Oils and Related Materials, v. 31, p. 18–23, 2020.

GODOI, K. R. R.; GRIMALDI, L. M.; **LÜDTKE, F.L.**; SILVA, T. J.; SILVA, M. G.; GRIMALDI, R.; RIBEIRO, A.P. B. Chemical composition and thermal behavior of Brazil nut (*Bertholletia excelsa*) oil. International News on Fats, Oils and Related Materials, v. 31, p. 23–25, 2020.

Trabalhos publicados em anais de congressos

STAHL, M. A.; **LÜDTKE, F. L**.; GRIMALDI, R.; GIGANTE, M. L.; HASHIMOTO, J. C.; RIBEIRO, A. P. B. Lipid nanoparticles formulated with conventional vegetable oils and fats: physical properties and stability. In: 18th Latin American Congress and Exhibition on Fats, Oils and Lipids– AOCS, 2019, Foz do Iguaçu. 18th Latin American Congress and Exhibition on Fats, Oils and Lipids– AOCS, 2019.

LÜDTKE, F. L.; STAHL, M. A.; GRIMALDI, R.; RIBEIRO, A. P. B. Nanostructured lipid carriers using high oleic sunflower oil and fully hydrogenated soybean oil: evaluation of emulsifiers. In: 17th Euro Fed Lipid Congress and Expo Seville, 2019, Sevilha.17th Euro Fed Lipid Congress and Expo Seville, 2019.

LÜDTKE, F. L.; STAHL, M. A.; SILVA, A. A.; CARDOSO, L. P.; RIBEIRO, A. P. B. Crystallization properties of nanostructured lipid carriers obtained with high oleic sunflower oil and fully hydrogenated soybean oil. In: 17th Euro Fed Lipid Congress and Expo Seville, 2019, Sevilha. 17th Euro Fed Lipid Congress and Expo Seville, 2019.

LÜDTKE, F. L.; GRIMALDI, L. M.; SILVA, M. G.; SILVA, T. J.; RIBEIRO, A. P. B.; GRIMALDI, R. Chemical characterization of Bacuri (*Platonia insigns*) fat. In: Simpósio Internacional "OILS and FATS for the future: the next decade", Campinas, 2019.

SILVA, T. J.; SILVA, M. G.; **LÜDTKE, F. L.**; GRIMALDI, L. M.; GRIMALDI, R.; RIBEIRO, A. P. B. Cupuacu butter: physicaland chemical characterization and its potential application. In: Simpósio Internacional "OILS and FATS for the future: the next decade", Campinas, 2019.

GRIMALDI, L. M.; **LÜDTKE, F. L.**; SILVA, M. G.; SILVA, T. J.; GRIMALDI, R.; RIBEIRO, A. P. B. Physical–chemical characterization and thermal properties of tucuma pulp oil.In: Simpósio Internacional "OILS and FATS for the future: the next decade", Campinas, 2019.

LÜDTKE, F.L.; STAHL, M. A.; ZAIA, B. G.; SANTOS, V. S.; HASHIMOTO, J. C.; RIBEIRO, A. P. B. Evaluation of process parameters for obtaining nanostructured lipid carriers by high pressure homogenization. In: 17th AOCS LatinAmerican Congress and Exhibition on Fats, Oils, and Lipids, 2017, Cancún. 17th AOCS Latin American Congress and Exhibitionon Fats, Oils, and Lipids, 2017.

LÜDTKE, F. L.; STAHL, M. A.; ZAIA, B. G.; RIBEIRO, A. P. B. Characterization of lipid matrices for obtaining Nanostructured Lipid Carriers. In: 17th AOCS Latin American Congress and Exhibition on Fats, Oils, and Lipids, 2017, Cancún. 17th AOCS LatinAmerican Congress and Exhibition on Fats, Oils, and Lipids, 2017.

STAHL, M. A.; **LÜDTKE, F. L.**; HASHIMOTO, J. C.; RIBEIRO, A. P. B. Effect of Emulsifiers Ethoxylated Sorbitan Monooleateand Sorbitan Monostearate on the Characteristics of Solid Lipid Nanoparticles. In: 17th AOCS Latin American Congress andExhibition on Fats, Oils, and Lipids, 2017, Cancún. 17th AOCS Latin American Congress and Exhibition on Fats, Oils, and Lipids,2017.

STAHL, M. A.; **LÜDTKE, F. L.**; SANTOS, V. S.; HASHIMOTO, J. C.; RIBEIRO, A. P. B. Evaluation of Parameters of the High Pressure Homogenization for Obtaining Solid Lipid Nanoparticles. In: 17th AOCS Latin American Congress and Exhibition onFats, Oils, and Lipids, 2017, Cancún. 17th AOCS Latin American Congress and Exhibition on Fats, Oils, and Lipids, 2017.

GRIMALDI, R.; **LÜDTKE, F.L**. Estudio del degomado no convencional del aceite de salvado de arroz. In: 17thAOCS Latin American Congress and Exhibition on Fats, Oils, and Lipids, 2017, Cancún. 17th AOCS Latin American Congress and Exhibition on Fats, Oils, and Lipids, 2017.

CAPÍTULO XI

REFERÊNCIAS BIBLIOGRÁFICAS

11. REFERÊNCIAS BIBLIOGRÁFICAS

AOCS. American Oil Chemists' Society**. Official methods and recommended practices of the American Oil Chemists' Society**. 6ed, Champaign, 2009.

ATTAMA, A.A.; MOMOH, M.A.; BUILDERS, P.F. Lipid Nanoparticulate Drug Delivery Systems: A Revolution in Dosage Form Design and Development. In: Sezer, Ali Demir (Ed). **Recent Advances in Novel Drug Carrier Systems**, 107-140, 2012. Intech.

BERNI, P. *et al*. Characterization of the behavior of carotenoids from pitanga (*Eugenia uniflora*) and buriti (*Mauritia flexuosa*) during microemulsion production and in a dynamic gastrointestinal system. **Journal of Food Science and Technology**, v.57, p.650-662, 2020.

CARBONELL-CAPELLA, J.M.; BUNIOWSKA, M.; BARBA, F.J.; ESTEVE, M.J.; FRÍGOLA, A. Analytical Methods for Determining Bioavailability and Bioaccessibility of Bioactive Compounds from Fruits and Vegetables: A Review. **Comprehensive Reviews in Food Science and Food Safety**, v. 13, p. 155-171, 2014.

CARRIÈRE, F. Impact of gastrointestinal lipolysis on oral lipid-based formulations and bioavailability of lipophilic drugs. **Biochimie**, v.125, p.297-305, 2016.

DONHOWE, E.G.; KONG, F. Beta-carotene: Digestion, Microencapsulation, and *In vitro* Bioavailability. **Food Bioprocess and Technology**, v.7, p. 338-354, 2014.

GOMES, G. V. L.; SOLA, M. R.; ROCHETTI, A. L.; FUKUMASU, H.; VICENTE, A. A.; PINHO, S. C. β-carotene and α-tocopherol coencapsulated in nanostructured lipid carriers of murumuru (*Astrocaryum murumuru*) butter produced by phase inversion temperature method: characterisation, dynamic *in vitro* digestion and cell viability study. **Journal of Microencapsulation**, v.36, p. 43-52, 2019.

GONÇALVES, R. F.S.; MARTINS, J.T.; DUARTE, C.M.M.; VICENTE, A.A.; PINHEIRO, A.C. Advances in nutraceutical delivery systems: From formulation design for bioavailability enhancement to efficacy and safety evaluation. **Trends in Food Science & Technology**, v. 78, p. 270-291, 2018.

HAKANSSON, A.; INNINGS, F.; TRAGARDH, C.; BERGENSTAHL, B. A high-pressure homogenization emulsification model—Improved emulsifier transport and hydrodynamic coupling. **Chemical Engineering Science**, v. 91, p. 44-53, 2013.

HUANG, Q.; YU, H.; RU, Q. Bioavailability and delivery of nutraceuticals using nanotechnology. **Journal of Food Science**, v.75, p.50-57, 2010.

JAFARI, S.M.; MCCLEMENTS, D.J. Nanotechnology Approaches for Increasing Nutrient Bioavailability. **Advances in Food and Nutrition Research**, v.81, p.1-30, 2017.

KATOUZIAN, I.; ESFANJANI, A.F.; JAFARI, S.M.; AKHAVAN, S. Formulation and application of a new generation of lipid nano-carriers for the food bioactive ingredients. **Trends in Food Science & Technology**, v.68, p. 14-25, 2017.

KHARAT, M.; MCCLEMENTS, D.J. Fabrication and characterization of nanostructured lipid carriers (NLC) using a plant-based emulsifier: Quillaja saponin. **Food Research International**, v.26, p. 1-11, 2019.

LEE, L.L.; NIKNAFS, N.; HANCOCKS, R.D.; NORTON, I.T. Emulsification: Mechanistic understanding. **Trends in Food Science & Technology**, v. 31, p. 72-79, 2013.

LIN, Q.; LIANG, R.; WILLIAMS, P.A.; ZHONG, F. Factors affecting the bioaccessibility of β-carotene in lipid-based microcapsules: Digestive conditions, the composition, structure and physical state of microcapsules. **Food Hydrocolloids**, v.77, p. 187-203, 2018.

MCCLEMENTS, D.J.; XIAO, H. Excipient foods: designing food matrices that improve the oral bioavailability of pharmaceuticals and nutraceuticals. **Food & Function**, v.5.; p. 1320-1333, 2014.

MCCLEMENTS, D.J.; LI, F.; XIAO, H. The Nutraceutical Bioavailability Classification Scheme: Classifying Nutraceuticals According to Factors Limiting their Oral Bioavailability. **Annual Review of Food Science and Technology**, v.6, p. 13.1-13.29, 2015.

MOHAMMADI, M.; ASSADPOUR, E.; JAFARI, S.M. Encapsulation of food ingredientes by nanostructured lipid carriers (NLCs). In: **Lipid-Based Nanostructures for Food Encapsulation Purposes**, v.2, p.217-270, 2019.

OLIVEIRA *et al*. β-Carotene-loaded nanostructured lipid carriers produced by solvent displacement method. **Food Research International**, v. 90, p. 139-146, 2016.

PASCOVICHE, D.M.; GOLDSTEIN, N.; FISHMAN, A.; LESMES, U. Impact of fatty acids unsaturation on stability and intestinal lipolysis of bioactive lipid droplets. **Colloids and Surfaces A**, 561, p. 70‑78, 2019.

PEZESHKI, A.; HAMISHEHKAR, H.; GHANBARZADEH, B.; FATHOLLAHYD, I.; NAHR, F.K.; HESHMATI, M.K.; MOHAMMADI, M. Nanostructured lipid carriers as a favorable delivery system for β-carotene. **Food Bioscience**, v.27, p.11-17, 2019.

PINHEIRO, A.C.; GONÇALVES, R.F.S.; MADALENA, D.A.; VICENTE, A. A. Towards the understanding of the behavior of bio-based nanostructures during *in vitro* digestion. **Current Opinion in Food Science**, v. 15, p. 79-86, 2017.

PINTO, M.F.; MOURA, C.C.; NUNES, C.; SEGUNDO, M.A.; LIMA, S.A.C.; REIS, S. A new topical formulation for psoriasis: Development of methotrexate-loaded nanostructured lipid carriers. **International Journal of Pharmaceutics**, v.477, p. 519-526, 2014.

PINTO, F.; BARROS, D.P.C.; FONSECA, L.P. Design of multifunctional nanostructured lipid carriers enriched with α-tocopherol using vegetable oils. **Industrial Crops & Products**, v. 118, p. 149-159, 2018.

PYO, S.M.; MÜLLER, R.H.; KECK, C.M. Encapsulation by nanostructured lipid carriers. In book: **Nanoencapsulation Technologies for the Food and Nutraceutical Industries**, p.114-137, 2017.

REZAEI, A.; FATHI, M.; JAFARI, S.M. Nanoencapsulation of hydrophobic and low-soluble food bioactive compounds within different nanocarriers. **Food Hydrocolloids**, v.88, p.146-162, 2019.

SALVIA-TRUJILLO, L., QIAN, C., MARTÍN-BELLOSO, O., MCCLEMENTS, D.J. Influence of Particle Size on Lipid Digestion and β-carotene Bioaccessibility in Emulsions and Nanoemulsions, **Food Chemistry**¸v.141, p.1472-1480, 2013.

SALVIA-TRUJILLO, L.; VERKEMPINCK, S.H.E.; SUN, L.; VAN LOEY, A.M.; GRAUWET, T.; HENDRICKX, M.E. Lipid digestion, micelle formation and carotenoid bioaccessibility kinetics: Influence of emulsion droplet size. **Food Chemistry**, v. 229, p.653-662, 2017.

SCHAFFAZICK, S.R.; GUTERRES, S.S.; FREITAS, L.L.; POHLMANN, A.R. Caracterização e estabilidade físico-química de sistemas poliméricos nanoparticulados para administração de fármacos. **Quimica Nova**, v. 26, n. 5, p. 726-737, 2003.

SIEGRIST, M.; STAMPFLI, N.; KASTENHOLZ, H.; KELLER, C. Perceived risks and perceived benefits of different nanotechnology foods and nanotechnology food packaging. **Appetite**, v.51, p. 283-290, 2008.

SOLEIMANIAN, Y.; GOLI, S.A.H.; VARSHOSAZ, J.; MAESTRELLI, F. β-sitosterol lipid nano carrier based on propolis wax and pomegranate seed oil: Effect of thermal processing, pH and ionic strength on stability and structure. **European Journal of Lipid Science and Technology**, v.121, p. 1-31, 2018.

TAMJIDI, F; SHADEDI, M.; VARSHOSAZ, J.; NASIRPOUR, J. Nanostructured lipid carriers (NLC): A potential delivery system for bioactive food molecules. **Innovative Food Science and Emerging Technologies**, v. 19, p. 29-43, 2013.

TAMJIDI, F; SHADEDI, M.; VARSHOSAZ, J.; NASIRPOUR, J. Design and characterization of astaxanthin-loaded nanostructured lipid carriers. **Innovative Food Science and Emerging Technologies**, v. 26, p. 366-374, 2014.

TAN, Y.; MCCLEMENTS, D.J. Improving the bioavailability of oil-soluble vitamins by optimizing food matrix effects: A review. **Food Chemistry**, v.348, 2021.

WILDE, P.J.; CHU, B.S. Interfacial & colloidal aspects of lipid digestion**. Advances in Colloid and Interface Science**, v.165, p.14-22, 2011.

ZHENG, K. *et al*. The effect of polymer–surfactant emulsifying agent on the formation and stability of α-lipoic acid loaded nanostructured lipid carriers (NLC). **Food Hydrocolloids**, v. 32, p.72-78, 2013.

CAPÍTULO XII

ANEXOS

12. ANEXOS

Figura 4: Sistema gastrointestinal dinâmico (DIVGIS) utilizado para os ensaios de digestibilidade *in vitro*.

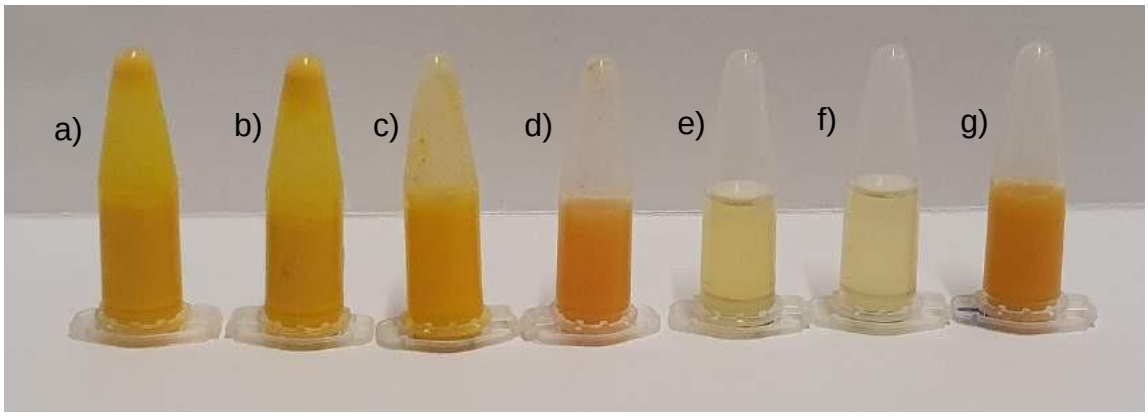

Figura 5: Amostras recolhidas em diferentes fases dos ensaios de digestibilidade *in vitro* dinâmica dos carreadores lipídicos nanoestruturados com incorporação de β-caroteno obtidos com lecitina de soja (CLN L_{β}). a) CLN; b) fase oral; c) compartimento gástrico; d) compartimento do duodeno; e) filtrado do jejuno; f) filtrado do íleo e g) filtrado final.

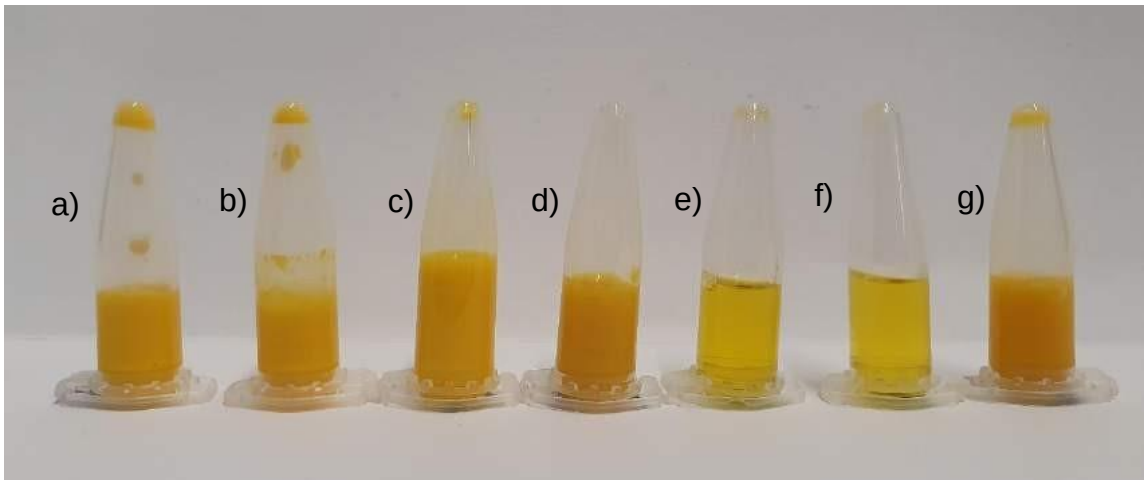

Figura 6: Amostras recolhidas em diferentes fases dos ensaios de digestibilidade *in vitro* dinâmica dos carreadores lipídicos nanoestruturados com incorporação de β-caroteno obtidos com Tween 80 (CLN T_{β}). a) CLN; b) fase oral; c) compartimento gástrico; d) compartimento do duodeno; e) filtrado do jejuno; f) filtrado do íleo e g) filtrado final.

Universidade do Minho
Escola de Engenharia

Braga, 30 de novembro de 2020.

Parecer do Supervisor

No âmbito da bolsa de estágio e pesquisa no exterior - BEPE (Processo FAPESP 2019/05176-6) a aluna Fernanda Luisa Lüdtke, realizou parte de sua investigação de doutoramento no Laboratório de Indústria e Processos (LIP) do Centro de Engenharia Biológica(CEB) da Universidade do Minho (UMinho), no período de 01 de julho de 2019 à 31 de outubro de 2020, sob minha orientação. Durante este período, a aluna desenvolveu atividades previstas em seu plano de trabalho intitulado "Avaliação da digestibilidade *in vitro* de carreadores lipídicos nanoestruturados com incorporação de β-caroteno" utilizando o modelo *in vitro* dinâmico instalado em nosso laboratório, cuja montagem experimental é baseada no sistema TIM-1 (*TNO intestinal model*).

Devido a avaria do homogeneizador a alta pressão, equipamento utilizado para obtenção das nanoestruturas, o cronograma previsto para o projeto teve seu início postergado. Além disso, devido as consequencias da pandemia do Covid-19 decretada pela OMS, o acesso ao laboratório ocorreu de forma restrita e controlada, respeitando as normativas da universidade. Apesar destes contratempos, os objetivos principais propostos no projeto foram cumpridos, como o estudo da digestibilidade *in vitro* dos nanocarreadores, a determinação da bioacessibilidade do β-caroteno incorporado às nanoestruturas, o perfil de liberação de ácidos graxos e o estudo da citotoxicidade. Porém, algumas atividades previstas, como o estudo da permeabilidade, o acompanhamento de alterações estruturais durante a digestibilidade através de abordagens microscópicas e a realização de ensaios de citotoxicidade em amostras recolhidas após os ensaios de digestibilidade *in vitro*, tiveram sua execução inviabilizada.

Os resultados obtidos a partir do desenvolvimento deste projeto são promissores e trazem informações relevantes acerca do impacto do uso de distintos emulsificantes na digestibilidade de nanopartículas, da bioacessibilidade de compostos bioativos, do perfil de liberação de ácidos graxos de nanopartículas obtidas utilizando matérias-primas lipídicas convencionais e da citotoxicidade de nanoestruturas e componentes utilizados em sua obtenção. Neste sentido, também foi possível verificar alguns ajustes a serem executados no sistema digestivo *in vitro*, isto é, determinar e ajustar metodologias para extração e quantificação de β-caroteno e o perfil de liberação de ácidos graxos partindo de um processo de digestibilidade *in vitro* dinâmica. A obtenção destes dados e os resultados alcançados implicará na publicação de um artigo científico em revista internacional.

A bolseira evidenciou inúmeras qualidades pessoais e profissionais, das quais se destaca a sua perseverança, espírito crítico, iniciativa e boa capacidade de trabalho, que permitiram desempenhar com sucesso este projeto, apesar de todas as contrariedades.

Pelo acima referido, o parecer é de total satisfação pelo trabalho desenvolvido pela doutoranda Fernanda Luisa Lüdtke.

Prof. Dr. António Augusto Martins de Oliveira Soares Vicente
Supervisor